FINNISH ROAD ADMINISTRATION

S12 Solutions to improve main roads

Capacity and Level of Service at Finnish Unsignalized Intersections

Finnra Reports1/2004

S 12 Solutions to improve main roads

R. Tapio Luttinen

Capacity and Level of Service at Finnish Unsignalized Intersections

Finnra Reports

1/2004

Finnish Road Administration

Helsinki 2004

Finnra Reports 1/2004
ISBN 951-803-180-0
ISSN 1457-9871
TIEH 3200849E

PDF version (www.tiehallinto.fi/julkaisut)
ISBN 951-803-181-9
ISSN 1459-1553
TIEH 3200849E-v

Edita Prima Oy
Helsinki 2004

The publication is sold by
Email: asiakaspalvelut.prima@edita.fi
Tel. Int. +358 20 450 011
Telefax Int. +358 20 450 2470

YMPÄRISTÖMERKKI
MILJÖMÄRKT
441 057
Painotuote

Finnish Road Administration
Traffic Engineering
Opastinsilta 12 A
P.O. Box 33
00521 HELSINKI
FINLAND
Telephone: Int. +358 204 2211

R. TAPIO LUTTINEN: Capacity and Level of Service at Finnish Unsignalized Intersections. Helsinki 2004, Finnish Road Administration, Finnra Reports 1/2004, ISBN 951-803-180-0, ISSN 1457-9871, TIEH 3200849E.

Keywords: capacity, level of service, unsignalized intersections

ABSTRACT

Since late 70's capacity and delay at unsignalized intersections have been estimated following the Swedish method adjusted for Finnish conditions. During the past 25 years the performance of both drivers and vehicles has changed, and new calculation methods have been developed. It has become necessary to update the analysis methodology of Finnish unsignalized intersections.

Major attention has been given to capacity analysis methodology, because capacity estimates have a central role in the estimation of other performance measures, such as delays and queue lengths. In addition, delay estimates are very sensitive to inaccuracies in capacity estimates, especially at high degrees of saturation.

Capacity at an unsignalized intersection has been described as a conditional expectation, from which the capacity equations for the most common headway distributions are easily obtained. For Rank 3 and Rank 4 capacity analysis a new theoretical approach has been developed. The movement capacity of Rank 3 streams is adjusted both for Rank 2 queues and for the modified headway distribution and lower flow rates during the free-departure periods of Rank 2 streams. The Rank 4 stream adjustment factors are shown to be multiplicative even across streams of different ranks.

The report presents the theoretical background required to manually perform operational analysis of unsignalized intersections and to understand and evaluate published methodologies and capacity analysis software. The methods can be used both for simple calculations with a calculator or a spreadsheet and for advanced analytical procedures.

The theoretical results and the results of three international methodologies—HCM2000, Swedish Capcal 2, and Danish DanKap—have been compared with simulated capacities and delays. HCM2000 gives higher potential capacities than the simulation results. Movement capacities of Rank 3 and Rank 4 streams are, however, slightly too low. The potential capacities of Capcal 2 are very similar to the simulated capacities. Rank 3 movement capacities are similar as in HCM2000, but Rank 4 capacities are too low. DanKap follow the methodology of HCM2000.

Based on theoretical results and simulation experiments new capacity and delay estimation methods have been presented for ordinary unsignalized intersections and for roundabouts. The new estimators have a more solid theoretical foundation and are in better agreement with simulation results than the other methodologies evaluated.

R. TAPIO LUTTINEN: Capacity and Level of Service at Finnish Unsignalized Intersections [Valo-ohjauksettomien liittymien välityskyky ja palvelutaso Suomessa]. Helsinki 2004, Tiehallinto, Finnra Reports 1/2004, ISBN 951-803-180-0, ISSN 1457-9871, TIEH 3200849E.

Asiasanat: välityskyky, palvelutaso, valo-ohjaukseton liittymä

TIIVISTELMÄ

Valo-ohjauksettomien liittymien välityskyvyn ja viipeiden arviointi Suomessa perustuu 70-luvun lopussa kehitettyyn ruotsalaiseen menetelmään. Kuluneiden runsaan 25 vuoden aikana sekä ajoneuvokanta, liikenekulttuuri että analyysitekniikat ovat kehittyneet. Myös suomalaisten laskentamenetelmien uudistaminen on tullut ajankohtaiseksi.

Välityskykyestimaateilla on suuri vaikutus liikennevirran laadullisten mittareiden, kuten viipeiden ja jonojen pituuksien estimaatteihin. Välityskyvyn laskentamenetelmillä on siten toimivuustarkasteluissa keskeinen rooli.

Valo-ohjauksettoman liittymän välityskyky voidaan ilmaista ehdollisten todennäköisyyksien avulla, jolloin lauseke saa helposti ymmärrettävän muodon ja välityskykylausekkeet pääsuunnan liikenteen eri aikavälijakaumille voidaan johtaa helposti. Kolmannen ja neljännen tason virtojen välityskyvyn analyysiin on esitetty uusi teoreettinen lähestymistapa, jossa välityskykyä korjataan ottaen huomioon toisen tason virtojen jonot sekä aikavälijakauman muuttuminen ja saapuvien ajoneuvojen alhaisempi määrä vapaan liikennevirran aikana. Neljännen tason korjauskertoimet osoittautuivat, vastoin odotuksia, multiplikatiivisiksi.

Esitetty teoria tarjoaa tarvittavat taustatiedot toimivuustarkastelujen suorittamiselle sekä julkaistujen laskentamenetelmien ja -ohjelmien arvioimiselle. Esitettyjä menetelmiä voidaan käyttää sekä yksinkertaisiin laskelmiin että vaativiin analyyseihin.

Teoreettisia tuloksia sekä kolmea laskentamenetelmää – HCM2000 (USA), Capcal 2 (Ruotsi) ja DanKap (Tanska) – on verrattu HUTSIM-simulointiohjelmalla arvioituihin välityskykyihin ja viipeisiin. HCM2000:n välityskykyarviot perustuvat oletukseen satunnaisesta liikennevirrasta, joka johtaa suurempiin välityskykyihin kuin sekä simulointitulokset että Capcal 2 osoittavat. Kolmannen tason virtojen välityskyvyn arviointimenetelmä on samanlainen sekä HCM2000:ssa että Capcal 2:ssa. Välityskykyarviot ovat simulointituloksia alhaisempia. Neljännen tason virtojen välityskykyarviot ovat Capcal 2:ssa selvästi liian alhaisia. HCM2000:ssa on korjaustermi, joka selvästi parantaa tuloksia. DanKapin laskentamenetelmä on saman kaltainen kuin HCM2000:ssa.

Teoreettisten tulosten ja simulointikokeiden perusteella on esitetty uudet välityskyvyn ja viipeiden laskentamenetelmät sekä tavanomaisille valo-ohjauksettomille liittymille että kiertoliittymille. Uusien laskentamenetelmien tuottamat välityskyvyn ja viipeiden estimaatit ovat lähempänä simulointituloksia kuin vertailumenetelmien arvot. Esitetyillä menetelmillä on myös vankka teoreettinen perusta, jonka johdosta ne eivät tarvitse ylimääräisiä korjaustermejä.

PREFACE

Most of the intersections in Finland are unsignalized. The vast majority of them have yield signs on minor-road approaches. Other unsignalized intersections are either stop controlled, uncontrolled (observing the "right before left" principle), or roundabouts. The operational analysis of unsignalized intersections is of great significance both to highway authorities and to road users. This report presents a theoretical overview and suggests a new methodology for capacity analysis of unsignalized intersections.

The description of an unsignalized intersection in terms of gap acceptance and queuing models is rather detailed. It was considered necessary to define the concepts carefully, because the literature contains numerous different and mutually incompatible modeling approaches.

A rather extensive evaluation of theoretical models was considered necessary in order to highlight the strengths and limitations of existing analysis methodologies. Some new methods are presented, especially for capacity estimation. Minor modifications are presented for the delay-estimation method.

The basic ideas necessary to understand capacity and delay models have been presented. Although the text contains a considerable number of equations, mathematics has been kept at a level accessible to anyone familiar with the basics of calculus and probability theory. Some effort has been made to describe theories and formulas to a reader, who is not an expert in the field. As far as possible, the text is self contained. The style is similar as in the reports on two-lane highways (Luttinen 2001) and signalized intersections (Luttinen & Nevala 2002) published earlier.

The bibliographic references have been selected, as far as possible, to credit the original sources of the ideas under discussion. Some references to recent overviews and text-books have been presented when considered appropriate. In many cases the models are based on other systems having some analogies with unsignalized intersections. In fact, observation of analogies between very different systems is in the core of mathematical modeling. The reader is pointed to some of these analogies.

The report was written by Dr. R. Tapio Luttinen from TL Consulting Engineers Ltd, and currently from the Helsinki University of Technology. The simulation experiments were conducted with HUTSIM software with help from Jouni Ojala and Nina Koivisto at the Helsinki University of Technology. The Laboratory of Transportation Engineering at the Helsinki University of Technology also collected and analyzed the gap acceptance measurements. Dr. Iisakki Kosonen provided valuable information about some details of the HUTSIM model.

Discussions with professors Urho Pulkkinen (VTT Industrial Systems), Rod Troutbeck (Queensland University of Technology), and Werner Brilon (Ruhr University Bochum) are thankfully acknowledged. Professor Troutbeck also provided a spreadsheet containing an implementation of the maximum likelihood method for the estimation of critical gaps.

Under the name NORDKAP (NORDiskt KAPacitetssamarbete, Nordic capacity co-operation) there has been considerable exchange of information and joint research between Denmark, Finland, Norway, and Sweden. Because traffic conditions in these countries have many similarities, the experiences and research results obtained in one country are of particular interest to the other countries. For this research the results of Dr. Ola Hagring (University of Lund, Sweden) have been very valuable.

This report is part of the Finnra strategic project S12 (Solutions to improve main roads). The work has been coordinated by deputy director Pauli Velhonoja at Finnra Traffic Engineering. Some discussion on the capacity theory presented here has been published prior to this final report (Luttinen 2003, Luttinen 2004*b*, Luttinen 2004*a*).

Helsinki, 3rd July 2004

Finnish Road Administration

Traffic Engineering

Contents

GLOSSARY

The terminology of the *Highway Capacity Manual* (Transportation Research Board 2000), and American terminology in general, has been followed. Most of the definitions below have been taken from the Highway Capacity Manual, possibly with slight modifications. A major exception is the definition of a gap, which is similar to the definition presented by (Drew 1968). The term "critical gap" has been used, as in HCM2000, although it may be replaced with a more consistent "critical headway" in the future. See discussion on page 30.

Acceleration delay: Time lost due to the limited acceleration capability of a vehicle.

Adjustment factor: A multiplicative factor that adjusts a capacity or service flow rate from one representing an ideal or base condition to one representing a prevailing condition.

Analysis period: A single time period during which a capacity analysis is performed.

Approach: A set of lanes at an intersection that accommodates all left-turn, through and right-turn movements from a given direction.

Base conditions: Characteristics for a given type of facility that are assumed to be the best possible from the point of view of capacity; that is, characteristics if further improved would not result in increased capacity. (Ideal conditions.)

Base saturation flow rate: The maximum steady flow rate at which previously stopped passenger cars can cross the stop or yield line under base conditions and in the absence of conflicting higher priority vehicles.

Calibration: The process of adjusting model parameters in order to minimize the difference between model results and measurements.

Capacity: The maximum hourly rate at which persons or vehicles can reasonably be expected to traverse a point or uniform section of a lane or a roadway during a given time period under prevailing roadway, traffic, and control conditions.

Conflicting movements: Traffic streams in conflict at an intersection.

Control condition: The traffic controls and regulations in effect for a segment of street or highway, including the type, phasing, and timing of traffic signals; stop signs; lane use and turn controls; and similar measures during the analysis period.

Control delay: The component of delay that results when a control causes vehicles on a lane or a lane group to reduce speed or to stop; it is measured by comparison with the uncontrolled condition.

Counting process: A continuous-time process that represents the number of occurrences of some event, such as arrival of vehicles, during a time period.

Critical gap: The minimum major-stream headway during which a typical minor-stream vehicle can make a maneuver. (Critical headway)

Deceleration delay: Time lost due to deceleration.

Degree of saturation: Same as demand-to-capacity ratio.

Delay: The additional travel time experienced by a driver, passenger or pedestrian.

Demand flow rate: The flow rate expected to desire service past a point or segment of the highway system at some future time, or the traffic currently arriving or desiring service past such a point.

Demand-to-capacity ratio: The ratio of demand flow rate to capacity at a traffic facility. (D/C ratio)

Design application: Using capacity analysis procedures to assess a traffic facility for a specified level of service.

Deterministic model: A mathematical model that is not subject to randomness.

Equilibrium condition: The expected state of a system that may have cyclic fluctuations, but otherwise is time independent. (Steady state condition)

Exclusive turn lane: A designated lane used only by vehicles making a left or right turn.

Flow rate: The expected rate at which vehicles pass a given point at a given time or during a time interval. (Rate of flow)

Flow ratio: The ratio of the demand flow rate to the saturation flow rate for a lane group at an intersection.

Follow-up time: Time between the departure of one minor-stream vehicle and the departure of the next vehicle using the same gap under a condition of continuous queuing.

Gap: A time interval between two consecutive major-stream vehicles evaluated by a minor-stream driver for a crossing or merging operation.

Gap acceptance: The process by which a minor-stream vehicle accepts an available gap to maneuver.

Geometric delay: The component of delay that results when geometric features cause vehicles to reduce their speed in negotiating a facility.

Headway: Time between two vehicles passing a point measured from front bumper to front bumper. (Interarrival time)

Heavy vehicle: Any vehicle with more than four wheels touching the pavement during normal operation.

Ideal conditions: Base conditions.

Impedance: The reduction in the capacity of a minor stream, caused by congestion in major streams.

Initial queue: The unmet demand from previous periods at the beginning of an analysis period.

Lag: Time interval between a random event, such as the arrival of a minor-stream vehicle, and the passage of the next priority-stream vehicle. (Forward waiting time)

Lane group: A set of lanes established at an intersection approach for separate capacity and level-of-service analysis.

Lane-group delay: The control delay for a given lane group.

Level of service: A qualitative measure describing operational conditions within a traffic stream, generally described in terms of such factors as speed and travel time, freedom to maneuver, traffic interruptions, comforts and convenience, and safety.

Major road: The roadway of a higher importance in an intersection.

Major stream: A traffic stream or a set of traffic streams to which the subject stream must give right of way.

Markov chain: A stochastic process in which the future state of the system depends on its present state but not on its past history.

Measure of effectiveness: A quantitative parameter describing the performance of a transportation facility or service.

Minor road: The road of lower importance at an unsignalized intersection, controlled by yield or stop signs.

Minor stream: A traffic stream which must give right of way to a higher priority stream.

Movement capacity: The capacity of a specific movement at an unsignalized intersection approach, assuming that the traffic has exclusive use of a separate lane.

Operational application: A use of capacity analysis to determine the level of service on an existing or projected facility, with known or projected traffic, roadway, and control conditions

Opposing flow rate: The flow rate at the direction of travel opposite to the direction under analysis.

Overflow period: Time period during which demand exceeds capacity.

Passenger-car equivalent: The number of passenger cars having the same impedance effect as a single heavy vehicle of a given type, under prevailing roadway, traffic, and control conditions. (PCE)

Peak period: Time period during which arrival flow rate exceeds capacity.

Performance measure: A quantitative or qualitative characteristic describing the quality of service provided by a transportation facility or service.

Planning application: A use of capacity analysis to estimate the level of service, the volume than can be accommodated, or the number of lanes required, using estimates, HCM default values, and local default values as input.

Platoon: A group of vehicles or pedestrians traveling together as a group, either voluntarily or involuntarily because of signal control or other factors.

Potential capacity: The capacity of a specific movement at an unsignalized intersection approach, assuming that it is unimpeded by other movements and has exclusive use of a separate lane.

Prevailing condition: The geometric, traffic, and control conditions during the analysis period.

Priority stream: A traffic stream to which the subject stream must give right of way.

Quality of service: The capability of a transportation facility or system under given conditions to meet the needs of its users.

Queue: A line of vehicles, bicycles or persons waiting to be served by a system.

Rank: A level of priority in the hierarchy of traffic streams at an unsignalized intersection.

Recreational vehicle: A heavy vehicle, generally operated by a private motorist, engaged in the transportation of recreational equipment or facilities; examples include campers, boat trailers, and motorcycle trailers.

Renewal process: A counting process for which the interarrival times (headways) are independent and identically distributed non-negative random variables.

Safety lag: Time interval at a conflict area from the departure of a minor-stream vehicle to the arrival of a major-stream vehicle.

Saturation flow rate: The hourly rate at which previously queued passenger cars can traverse an intersection approach under prevailing conditions in the absence of conflicting higher priority vehicles.

Service flow rate: The maximum hourly rate at which persons or vehicles can reasonably be expected to traverse a point or uniform section of a lane or roadway during a given time period under prevailing roadway, traffic, and control conditions while maintaining a designated level of service.

Service measure: A specific performance measure used to assign a level of service.

Service time: The time period that a customer spends in a service facility. At unsignalized intersections the time period during which a vehicle not blocked by vehicles ahead blocks the vehicle behind from reaching the stop/yield line.

Simulation model: A computer program that uses mathematical models to conduct experiments with traffic events on a transportation facility or system over extended periods of time.

Spacing: The distance between two successive vehicles in a traffic lane measured from front bumper to front bumper.

Stationary conditions: Conditions not changing during the analysis period.

Steady state conditions: The expected state of the system may have cyclic fluctuations, but otherwise it is time independent. (Equilibrium conditions)

Stochastic model: A mathematical model that employs random variables for at least one input parameter.

Stochastic process: A series of random variables indexed over time or space. In a discrete time stochastic process the index set consists of discrete units of time. In a continuous time stochastic process the index set is a subset of nonnegative real numbers.

Stop line: A line behind which vehicles should stop as directed by a stop sign or a traffic signal.

Stop time: A portion of control delay when vehicles are at complete stop. Also "stop delay".

Stream: A distinguishable element of the total traffic flow traversing an intersection—for example, that performing a particular movement (OECD Road Research Group 1974)

Time-in-queue delay: Time spent in a queue; from stopping at the end of queue to passing the stop line.

Through vehicles: All vehicles passing directly through an intersection.

Traffic condition: A characteristic of traffic flow, including distribution of vehicle types in the traffic stream, directional distribution of traffic, lane use distribution of traffic, and type of driver population on a given facility during the analysis period.

Transient conditions: The system is not in equilibrium, but its state depends on time. (Time-dependent conditions)

Transition probability: The probability that a system at a given state at one time will be at a certain state at a later time.

Truck: A heavy vehicle engaged primarily in the transport of goods and materials or in the delivery of services other than public transport.

Undersaturation: A traffic condition in which the arrival flow rate is lower than the capacity.

Utilization factor: The fraction of time that a server in a queuing system is busy or a traffic facility is occupied.

Validation: Determining whether the selected model is appropriate for the given conditions and for the given task. It compares model prediction with measurements or observations.

Volume: The number of persons or vehicles passing a point on a lane, roadway, or other trafficway during some time interval.

Waiting time in queue: Time spent in a queue waiting for service.

Waiting time in system: Time spent in queue and in service.

Yield line: A line of triangles at an unsignalized intersection to intensify the effect of a yield sign. At a yield controlled approach the stop line is replaced by a yield line.

SYMBOLS AND ABBREVIATIONS

a	Acceleration or deceleration rate
A_i	Number of arrivals between departures i and $i-1$
$A(\tau)$	Number of arrivals during $(0, \tau]$
$A(\tau_1, \tau_2)$	Number of arrivals during $(\tau_1, \tau_2]$
ACF	Additive Conflict Flows methodology
$B(\tau)$	Backward waiting time at time τ
b	Current duration of headway
C	Capacity
C_i	Capacity of stream i
$C_{\mathrm{a},i}$	Potential capacity of stream i during unimpeded periods
$C_{\mathrm{L},i}$	Potential capacity of minor stream i under limited priority
$C_{\mathrm{m},i}$	Movement capacity of minor stream i
$C_{\mathrm{p},i}$	Potential capacity of minor stream i
c	Cycle length $(t_\mathrm{a} + t_\mathrm{b})$
$D(\tau)$	Number of departures during $(0, \tau]$
$D(\tau_1, \tau_2)$	Number of departures during $(\tau_1, \tau_2]$
d	Central island diameter in a roundabout
D/C	Demand-to-capacity ratio
E_B	Equivalency factor for buses
E_HV	Equivalency factor for heavy vehicles
E_R	Equivalency factor for recreational vehicles
E_T	Equivalency factor for trucks
$\mathbb{E}[X]$	Expected value of random variable X
$\mathbb{E}[\,X \mid Y\,]$	Expected value of random variable X under condition Y
$f(\cdot)$	Probability density function
$f_\mathrm{e}(\cdot)$	Probability density function of service times for isolated vehicles
$f_\mathrm{q}(\cdot)$	Probability density function of service times for queuing vehicles
$f_S(\cdot)$	Probability density function of service times
$f_\Upsilon(\cdot)$	Probability density function of lags
$F(\cdot)$	Cumulative distribution function (see $f(\cdot)$ for subscripts)
$f_{\mathrm{a},i}$	Fraction of time available for gap acceptance in stream i
f_e	Adjustment factor for exiting traffic
f_i	Impedance factor of a Rank 2 stream i
f_L	Adjustment factor for limited priority merge
f_q	Adjustment factor for impedance effects in average service time
Finnra	Finnish Road Administration
$G(z)$	Probability-generating function
$\bar{h}$	Average departure headway
$h_{i,k}$	Departure headway of vehicle k in stream i
$\bar{h}_j$	Average departure headway of stream j
HBS	*Handbuch für die Bemessung von Straßenverkehrsanlagen*
HCM	*Highway Capacity Manual*
HUT	Helsinki University of Technology
I_k	The set of priority streams for minor stream k
i.i.d.	Independent and identically distributed
L_a	Queue length exceeded a percent of time
$L(\tau)$	Number of customers in a queue at time τ
l_f	Effective entry flare length
l_v	Vehicle length

l_w	Length of weaving section
LOS	Level of service
MOE	Measure of effectiveness
$N(\tau)$	Number of customers in a system at time τ
n_g	Average number of pedestrians in a group
$\mathbf{P}$	One-step transition probability matrix
P_B	Proportion or percentage of buses in traffic flow
P_{HV}	Proportion or percentage of heavy vehicles in traffic flow
P_R	Proportion or percentage of recreational vehicles in traffic flow
P_T	Proportion or percentage of trucks in traffic flow
$\mathbb{P}\{A\}$	Probability of event A
$\mathbb{P}\{ A \mid Y \}$	Probability of event A under condition Y
p_0	Probability of a lag being accepted
$p_{0,i}$	Probability of empty system in stream i
p_e	Proportion of arriving flow exiting (turning right) before subject entry
p_g	Probability that a gap is rejected
p_i	Proportion of stream i in a set of streams
p_{ij}	One-step transition probability from state i to state j
$p_{k,j}$	Fraction of pedestrians in stream j given priority by vehicle stream k
p_l	Probability that a lag is rejected
p_n	Probability of rejecting n consecutive gaps, or lag and $n-1$ gaps
$p_{z,i}$	Probability of empty system in streams 1, 4, and i
pc	Passenger car
PCE	passenger-car equivalent
pcu	Passenger car unit
q	Flow rate, traffic volume (veh/h)
$q_{a,i}$	Average stream i flow rate (veh/h) during free-flow periods
q_c	Circulating flow at a roundabout
q_e	Rate of flow exiting (turning right) before subject entry
q_g	Hourly arrival rate of pedestrian groups
q_{II}	Flow rate of a Rank 2 movement
q_{III}	Flow rate of a Rank 3 movement
q_i	Flow rate of movement i
q_M	Major-stream flow rate
$q_{M,i}$	Major-stream flow rate for movement i
q_P	Peak flow rate
q_p	Hourly arrival rate of pedestrians
$q(\tau)$	Flow rate at time τ
R^2	Coefficient of determination
$R(\cdot)$	Survivor function (see $f(\cdot)$ for subscripts)
r_c	Inscribed circle radius of a roundabout
r_e	Entry radius at a roundabout
S	Service time
$\bar{S}$	Average service time
S_e	Service time for vehicles arriving to an empty system
S_q	Service time for queuing vehicles
$\bar{S}_i$	Average service time of stream i
$S^{(i)}$	Service time of vehicle i
s_i	Saturation flow rate of stream i
T	Headway (stochastic variable)

T_i	Time interval between major-stream departures $i-1$ and i
$T(\mathrm{A}, \mathrm{B})$	Time interval between events A and B
$T(\tau)$	Current headway at time τ
$T_{\mathrm{bc},i}$	Busy cycle in stream i
$T_{\mathrm{bp},i}$	Busy period in stream i
$T_{\mathrm{ip},i}$	Idle period in stream i
t	Length of a headway
t_0	Queue accumulation and discharge time
t_a	Antiblock length
t_b	Block length
t_c	Critical gap
t_f	Follow-up time
$t_\mathrm{f}^{(i)}$	Follow-up time after vehicle i
t_i	Length of the i^{th} headway
t_o	Shortest acceptable major stream headway in a flow-analogy model
t_p	Intraplatoon headway
t_pb	Time interval of pedestrian blockage
v/c	Volume-to-capacity ratio
v_a	Approach cruise speed
v_e	Exit cruise speed
v_n	Negotiation speed
v_p	Pedestrian walking speed
W	Control delay
$\bar{W}$	Average control delay
$W^{(i)}$	Control delay of vehicle i
$W(\tau)$	Cumulative delay during $(0, \tau]$
$\bar{W}_2$	Average delay according to Tanner (1962)
W_a	Acceleration delay
W_e	Waiting time of an isolated minor stream vehicle
$\bar{W}_\mathrm{D}$	Average waiting time in an M/D/1 queuing system
W_d	Deceleration delay
$\bar{W}_\mathrm{G}$	Average waiting time in an M/G/1 queuing system
W_g	Geometric delay
W_ga	Acceleration component of geometric delay
W_gd	Deceleration component of geometric delay
$\bar{W}_\mathrm{M}$	Average waiting time in an M/M/1 queuing system
W_m	Queue move-up time
W_n	Delay due to low negotiation speed
W_o	Overflow delay
W_Q	Waiting time in queue
W_q	Waiting time at yield/stop line for queuing vehicles
W_S	Waiting time in system
W_s	Stop delay
W_T	Waiting time in system under transient conditions
W_t	Total delay
w_a	Approach width
w_e	Entry width
w_l	Lane width
w_w	Width of a weaving section
$\alpha(t)$	Gap acceptance function; maximum number of departures in headway t

α_k	Probability of k arrivals during the service time of a queuing vehicle
β	Unit extension interval
β_k	Probability of k arrivals during the service time of an isolated vehicle
γ	Scale parameter of Cowan's M3 distribution
δ_i	Service departure time of vehicle i
$\delta(x-a)$	Unit impulse (Dirac delta) function
$\epsilon(x)$	Unit step (Heaviside) function
ε_i	Time of entry of minor stream vehicle i
θ	Scale parameter of shifted exponential distribution
κ	Randomness constant of service times
κ_i	Reserve capacity of stream i
λ_i	Flow rate (veh/s) of stream i
$\lambda_{\mathrm{a},i}$	Average stream i flow rate (veh/s) during free-flow periods
ϕ_i	Proportion of free headways in stream i
ρ_{e}	Service quotient for isolated (non-queuing) vehicles
ρ_i	Utilization factor, demand-to-capacity ratio of stream i
ρ_i'	Demand-to-capacity ratio of stream i
ρ_{P}	Peak demand-to-capacity ratio
ρ_{q}	Service quotient for queuing vehicles
σ^2	Variance
σ_{e}^2	Variance of service times for vehicles arriving to an empty system
σ_{q}^2	Variance of service times for queuing vehicles
τ	Time
τ_i	Arrival time of vehicle i
τ_{o}	Length of overflow period
τ_{P}	Length of peak period
$\Upsilon(\tau)$	Lag (forward waiting time) at time τ
υ	Length of lag
υ_{s}	Safety lag
χ	Probability of major stream antiblock and minor stream follow-up time
$\stackrel{\mathrm{d}}{=}$	Equal in distribution
$(a, b]$	Time interval $a < \tau \leq b$
$i \vee j$	Stream i or j
$i \wedge j$	Streams i and j
$\lfloor x \rfloor$	Floor function (greatest integer not larger than x)
$\langle x \rangle$	Nearest integer of x
x_+	Positive part of x; i.e., $x_+ = (x + \lvert x \rvert)/2$

1 INTRODUCTION

1.1 Methodological approaches

The majority of intersections in Finland are unsignalized. The vast majority of these have yield signs on minor road approaches. Other unsignalized intersections are either stop controlled, uncontrolled, observing the "right before left" principle, or roundabouts, which are becoming increasingly popular.

At an unsignalized intersection each driver must find a safe moment for the movement observing current traffic, traffic signs (stop or yield) and pertinent regulations ("right before left"). Accordingly, modeling of operations at an unsignalized intersection is about the interactions between vehicles under the geometric conditions of the intersection. The most important modeling approaches have been stochastic (gap acceptance theory) and statistical (regression analysis).

In Britain the capacity analysis of unsignalized intersections has been based on *statistical models* (Kimber & Coombe 1980, Kimber 1980, Semmens 1988, O'Flaherty 1997). Regression analysis has been used to find the parameters and to estimate the values of the coefficients which give a good fit between estimated and measured capacity. This method is not sensitive to the headway distribution models, it gives a clear method to estimate the effect of intersection geometry, and can model heavily congested conditions under which the process of simple gap-acceptance gives way to a more interactive one, in which major road vehicles adjust their headways to allow minor road vehicles to enter, as well as situations, such as multi-lane roundabouts, where the assumed vehicle interaction rules become very arbitrary (Kimber & Coombe 1980, Kimber 1989). Some other examples of statistical capacity models have been presented by Louah (1988), Simon (1991), Hakkert, Mahalel & Asante (1991), and Aakre (1998). When capacity has been estimated, queuing theory can be used to estimate queue lengths and delays (Kimber & Hollis 1979), although regression analysis has also been used in delay estimation (e.g., Kyte, Zegeer & Lall 1991).

Most of the analysis procedures of unsignalized intersections are, however, based on stochastic models; i.e., *gap acceptance theory*. It is assumed that a minor stream vehicle can enter an intersection, when the time interval to the next arriving higher priority vehicle is larger than a critical gap, and a safe time interval (follow-up time) has passed since the departure of the preceding minor stream vehicle. Capacity and delay are functions of follow-up times and the availability of headways larger than critical gaps in higher priority streams. Statistical methods are applied to estimate the parameters that describe "microscopic" properties of the process, such as critical gaps and follow-up times of minors stream vehicles as well as headway distributions of major streams. Whereas statistical models estimate the effects of intersection geometry on capacity directly, in stochastic models gap acceptance parameters are adjusted for the local conditions (Kimber 1980).

Gap acceptance theory has been developed especially in Germany by Grabe (1954), Harders (1968), and Siegloch (1973), without forgetting the theoretical foundation laid by Anglo-Saxon scientists, such as Major & Buckley (1962) and Tanner (1962). Roundabouts are usually analyzed as series of intersections or short merging zones. Gap acceptance theory can be adjusted for conditions, where an approaching major-stream vehicle slows down to give way to a merging minor-stream vehicle. This type of operation is called "limited priority merge" (Troutbeck & Kako 1999, Troutbeck 1999).

Priority stream headways are usually assumed to follow exponential distribution. This approach has been used in many capacity manuals, such as in Germany (Brilon,

Großmann & Blanke 1994, FGSV 2001) and in the U.S. (Transportation Research Board 2000). A bunched exponential headway model used originally by Tanner (1962) has received much attention later in a generalized form (Troutbeck 1986, Akçelik & Chung 1994, Hagring 1998*b*). The Swedish method (Statens vägverk 1977, Hanson 1978, Bergh 1991) uses four different headway distributions, based on number of lanes, distance from traffic signals, and type of movement.

Gap acceptance can also be described in terms of traffic signal analogy, as suggested by Winsten (in Beckmann, McGuire & Winsten 1956), and recently developed by Akçelik (1994*a*). Time periods blocked by higher priority vehicles are considered as red intervals and time periods available for minor stream vehicles are considered as green periods. Siegloch (1973) and McDonald & Armitage (1978) associated a lost time with each major stream vehicle and assumed that at other time intervals minor stream vehicles enter an intersection (roundabout) at constant saturation flow rate.

A *third approach* is to apply a model structure based on gap acceptance theory, but to use regression analysis to fit the model to measured capacity values. Parameters, such as critical gap and follow-up time, loose their behavioral (microscopic) meaning, and become coefficients of a statistical (macroscopic) model. Examples of this approach have been presented by Stuwe (1991), Brilon & Stuwe (1993), Guichet (1997), and Aagaard (1995), among others.

The Additive Conflict Flows (ACF) procedure (Brilon & Wu 2001, Brilon & Wu 2002, Brilon & Miltner 2002) combines traffic signal analogy with a statistical framework. The D/C ratio of a major flow is the sum of the D/C ratios of component major flows, and during the remaining fraction of time the minor stream can discharge at saturation flow rate. Parameters are estimated using statistical procedures based on goodness of fit between observed and estimated capacities. The ACF method was developed to simplify the analysis of the hierarchy of priorities as well as the pedestrian and cyclist movements at unsignalized intersections. The new draft chapter for unsignalized intersections in the forthcoming German capacity manual follows the ACF procedure.

1.2 State of the art in Finland

In early 70's the capacity analysis of Finnish unsignalized intersections (Häkli 1971, Syyrakki, Lyly & Granberg 1975) was an implementation of the methodology of Harders (1968) as presented by Jessen (1968)—see also Siegloch (1973), appendix 17. Since late 70's capacity and delay at unsignalized intersections have been estimated following the Swedish method adjusted for Finnish conditions (Tiensuunnittelutoimisto 1978). These adjustments have also been implemented in the Finnish version of the Swedish Capcal software (Tiensuunnittelutoimisto 1987, Kehittämiskeskus 1991). — Pursula & Peltola (1997, 1998) have presented an overview of the capacity analysis and design practice of Finnish unsignalized intersections.

The new intersection design manual (Tie- ja liikennetekniikka 2001) presents a set of charts for capacity estimation in planning applications. The level-of-service classification follows the 1985 HCM (Transportation Research Board 1985, Lyly 1988). Roundabouts are analyzed as series of T-intersections (Tie- ja liikennetekniikka 2001). For the operational analysis of unsignalized intersections the old manual method (Tiensuunnittelutoimisto 1978) and Capcal are still used. The old critical gaps have not been updated, even though new measurements have suggested lower values (Uusiheimala 1995, Niittymäki & Uusiheimala 1996).

The Swedish Capcal has been updated to Capcal 2 and further to Capcal 3. Capcal 2[1] updated the calculation procedures, particularly for the vehicle-operating and emission costs (SNRA 1995*b*, Hagring 1997). Small changes were also made to critical gaps and to estimation of service times (SNRA 1995*b*). Capcal 3 is a Windows version reproducing the methodology of Capcal 2. A new version is under development.

1.3 Research objectives

After the development of the current Finnish capacity estimation procedure in the 1970's the performance of both drivers and vehicles has changed, and new calculation methods have been developed. It has become necessary to update the analysis methodology of Finnish unsignalized intersections.

The methodological basis in this research is gap acceptance theory. It is widely used worldwide. The most important advantage of the model is, however, in the parameter estimation. Statistical capacity models require observations from congested intersections.[2] Such data are difficult to obtain and were not available for this research. The same problem has been reported in Denmark (Vejdirektoratet 1999*a*) and in Sweden (Hagring 1996*b*). Parameters of stochastic (gap acceptance) models can be estimated under uncongested conditions also, although there is always an element of error, when results from one traffic condition are applied to another.

As Brilon, Wu & Bondzio (1997) have remarked, one cannot be sure that linear regression models apply also in the areas of a capacity-flow diagram where only a few measurement points have been observed. The structure of a gap acceptance model is informative, and parameters have a physical meaning. This gives credibility to the model even in those areas of the diagram where empirical evidence is scarce. It is easier to transfer a gap-acceptance model to conditions different from a regression model.

The present report gives updated critical gap values and suggests a performance analysis procedure for Finnish unsignalized intersections. New field measurements have been made to update the methodology. The theoretical results and the results of three international methodologies—HCM2000 (Transportation Research Board 2000), Capcal 2 (SNRA 1995*b*), and Danish DanKap (Vejdirektoratet 1999*b*)—have been compared with the capacities and delays simulated by HUTSIM (Kosonen 1996, Kosonen 1999). Based on these results a recommendation is made for a new analysis methodology.

Major attention has been given to capacity analysis methodology, because capacity estimates have a central role in the estimation of other performance measures, such as delays and queue lengths. In addition, delay estimates are very sensitive to capacity estimates, especially at high degrees of saturation (Hagring 1998*b*). The report includes some new theoretical results, especially for the capacity analysis of Rank 3 and Rank 4 streams. These results were made available in a preliminary report (Luttinen 2003), and are presented here with some modifications.

[1] The version referred to in this document is Capcal Dos 2.10.

[2] Akçelik (1998) has, however, suggested the estimation of capacity based on measuring departure flow rates during queued portions of gap-acceptance cycles.

2 GAP ACCEPTANCE THEORY

2.1 Relative priority of traffic streams

Unsignalized intersections can be either uncontrolled, yield-sign controlled, stop-sign controlled, or roundabouts. *Uncontrolled intersections* follow the right-before-left rule. The priority is implicit, given in the rules of the Highway Code only (OECD Road Research Group 1974). Each vehicle must give way to vehicles approaching from the right. Left turning vehicles must give way to opposing traffic.

At *yield-sign controlled intersections* the yielding approaches are referred to as minor-road approaches. The approaches that are not controlled by yield signs are referred to as major-road approaches. All minor-road vehicles yield the right-of-way to major-road vehicles. Left-turning vehicles in all approaches yield right-of-way to opposing through and right turning vehicles.

At *stop-sign controlled intersections*[1] the minor-road approaches are controlled by stop signs. The principles of operation are otherwise similar to yield controlled intersections, but minor road vehicles must stop at the stop line before proceeding.

Roundabouts have a circulating roadway around a central island. All vehicles entering a roundabout must yield to circulating vehicles. All vehicles entering or exiting a roundabout make a right turn.

The theory describing the operations at an unsignalized intersection is called *gap acceptance theory*. It includes four basic elements (cf. Transportation Research Board 2000):

1. Relative priority of traffic streams
2. Distribution (availability) of gaps in higher priority streams
3. Usefulness of gaps to yielding vehicles (gap acceptance)
4. Queue discharge

The availability of gaps is described by a probability distribution of headways in higher priority streams. A gap acceptance function describes the usefulness of headways as well as queue discharge. The relative priority of traffic streams will be discussed next.

In an uncontrolled intersection of two one-way roads displayed in Figure 2.1 the south-bound traffic (q_{11}) must yield to east-bound traffic (q_2). The intersection operates in the same way, if the northern approach has a yield sign. (In Finland a yield sign is not used in this case, because it is not necessary.) If there is a stop sign, vehicles must stop before passing the sign. An intersection of two one-way roads is the simplest case to analyze, and it is used in the derivation of potential capacity and delay equations.

The traffic steams at a four-leg intersection are presented in Figure 2.2. The numbering follows HCM2000 (Transportation Research Board 2000). Streams 13–16 are pedestrians crossing the road.

The operation is more complicated than in the simple case of Figure 2.1. All minor road vehicles yield the right-of-way to major road vehicles. Left-turning vehicles in all approaches yield right-of-way to opposing through and right-turning vehicles. There is a hierarchy of priorities. Through and right-turning movements on the major road

[1] HCM2000 (Transportation Research Board 2000) calls this type of intersection two-way stop-controlled (TWSC). All-way stop-controlled (AWSC) intersections,widely used in the U.S., are not used in Finland.

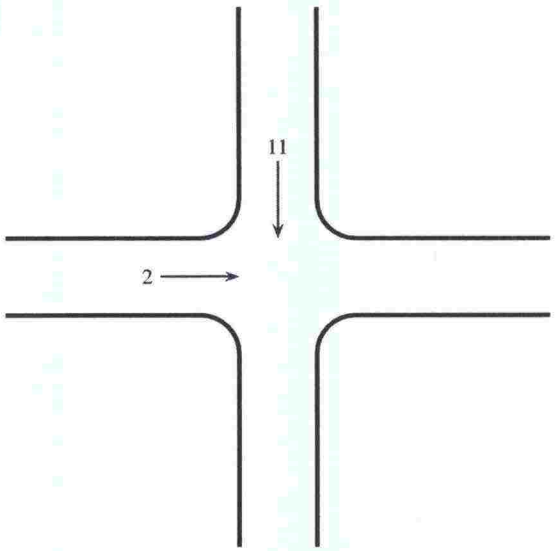

Figure 2.1: An intersection of two one-way roads

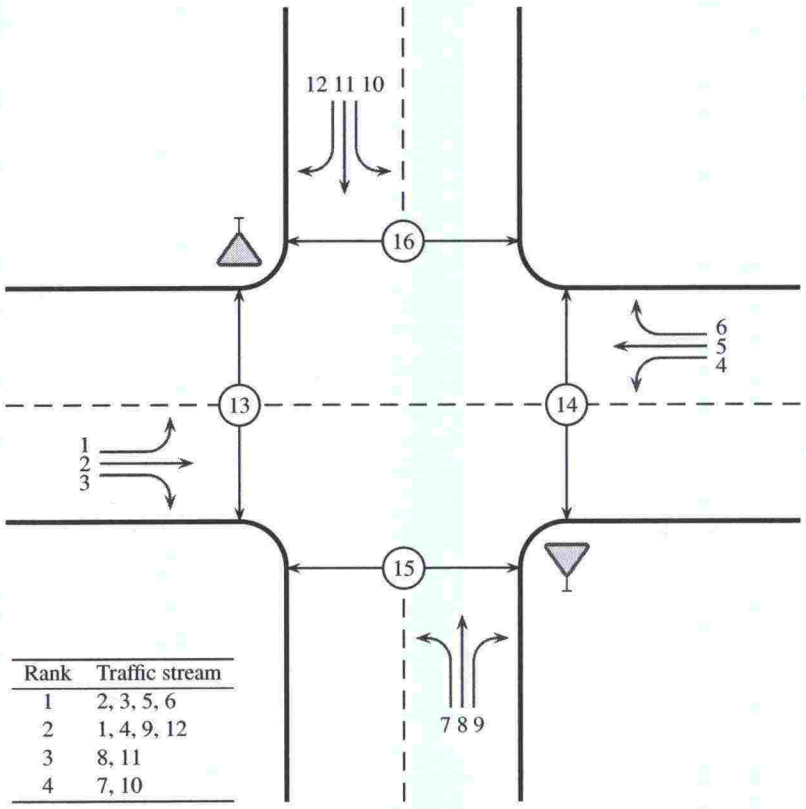

Rank	Traffic stream
1	2, 3, 5, 6
2	1, 4, 9, 12
3	8, 11
4	7, 10

Figure 2.2: Traffic streams at a four-leg intersection

(2, 3, 5, and 6) have absolute priority. This group of movements is called Rank 1. Left turning traffic from the major road (1, 4) and right turning traffic from the minor road (9, 12) have Rank 2. They must give priority to Rank 1 movements. Through traffic on the minor road (8, 11) has Rank 3. It must give priority to all movements on the major road (Ranks 1 and 2). Finally, left turning traffic from the minor road (7, 10) is subordinate to all other streams, and it has Rank 4.

All yielding vehicles, which do not find an acceptable lag at arrival must decelerate and/or stop to wait for the next safe gap. There may, however, also be vehicles or pedestrians of higher rank waiting for an acceptable gap. Accordingly, a vehicle must find an acceptable gap or lag *after* all waiting higher rank vehicles and pedestrians have passed the conflict area.

Right turning stream 3 does not have a conflict with minor road streams 7, 8 and, 9. It is, however, possible that minor road drivers are not confident that a major street vehicle will turn right, until they see a clear indication of its intentions. Accordingly, a stream may have an effect on the performance of another stream, even though no conflict exists between the two streams.

The traffic streams at a T-intersection are presented in Figure 2.3. There are only three hierarchical levels of priorities (ranks). Consequently, there are less possible conflicts between streams, so that it is easier for a driver to observe the safe gaps in priority streams.

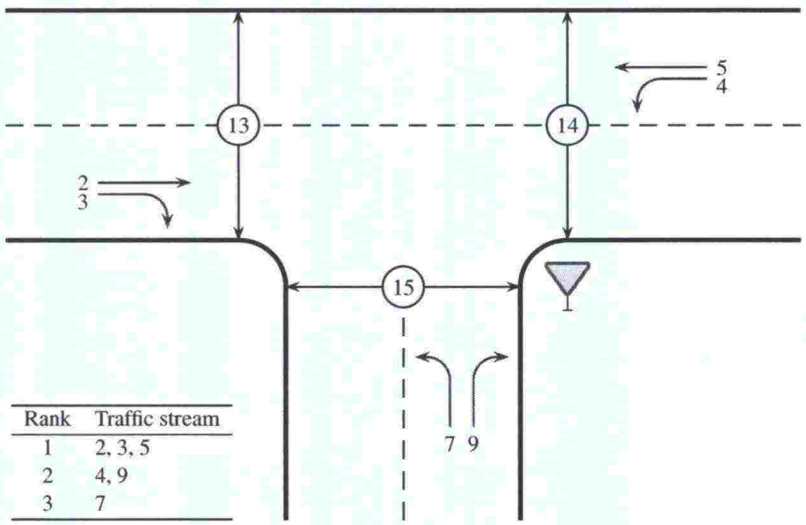

Figure 2.3: Traffic streams at a T-intersection

If the major road has a wide central island, one or more minor-road vehicles can be stored between the two directions of major-road traffic streams. In this case minor road through or left-turn vehicles may operate in two stages, if there is storage space available (Brilon, Wu & Lemke 1996, Brilon & Wu 1999, Luttinen 1998)

In HCM2000 (Transportation Research Board 2000) pedestrian flows (15, 16) across the minor road have Rank 1 and pedestrian flows across the major road (13, 14) have Rank 2. HCM2000, however, states that the priority of pedestrian movements with respect to vehicular movements may be a policy issue varying by jurisdiction. In the Finnish guidelines (Tiensuunnittelutoimisto 1978) minor street movements are considered subordinate to pedestrian flows across the minor road. Pedestrian flows across the major road are ignored.—The capacity and level of service of pedestrian facilities

is discussed e.g. in Chapter 18 of HCM2000 (Transportation Research Board 2000).

Current Finnish highway code states that vehicles must give priority to a pedestrian who is on a crosswalk or is about to set foot on the crosswalk. A vehicle may not pass without stopping another vehicle that has stopped in front of a crosswalk. A turning vehicle must give priority to pedestrians crossing the road, where the driver is turning to. However, the priorities between pedestrians and vehicles observed in reality cannot be described with clear rules. Because pedestrians have a "higher" priority over turning vehicles than over through vehicles, pedestrian flow 15 has a higher priority over movement 3 (Rank 1) than over movement 8 (Rank 3). This breaks the hierarchical structure of priorities. In addition, these rules are often not observed by or even known to pedestrians and vehicle drivers (see also Brilon & Wu 2001, Brilon & Wu 2002). Consequently, the Rank of pedestrian flows is not defined in Figure 2.2. The effect of pedestrians should, however, be considered in the capacity calculations.

According to the hierarchy in Figures 2.2 and 2.3 the major street through vehicles have absolute priority. They may, however, experience delays due to three reasons:

1. If major road through vehicles cannot pass queuing left-turn vehicles, they have to wait for the clearance of the queue (Kimber & Coombe 1980, Bonneson & Fitts 1997, Bonneson & Fitts 1999).

2. Even without queues a through vehicles may have to decelerate, if it follows a vehicle decelerating for a turning maneuver.

3. At high traffic volumes major-road vehicles may be slightly delayed to accommodate minor-road vehicles (Troutbeck 1990, Troutbeck & Kako 1997, Troutbeck & Kako 1999).

Wang (2000) has found that major and minor-stream traffic volumes do not have a significant effect on critical gaps. However, if major-stream vehicles adjust their speeds to accommodate minor-stream vehicles, the result can be observed also in the availability of gaps (headway distribution), not only in the gap acceptance behavior (see Troutbeck 1997*b*, Troutbeck & Kako 1999).

At *uncontrolled intersections* all vehicles obey the right-before-left rule. It is possible to have a situation where priorities are unspecified. Such a situation occurs, when vehicles of streams 2, 4, and 7 simultaneously wait for an opportunity to proceed. Each vehicle must yield to another vehicle, none has priority over all others. The methods described in this report cannot be applied to uncontrolled intersections. The German manual (FGSV 2001) suggests 600–800 pc/h as the sum of maximum flow rates of all four approaches at an uncontrolled intersection.

At *roundabouts* (Fig. 2.4) vehicle circle counterclockwise. Approaching flows (q_a) give priority to circulating flows (q_c). This ensures an uninterrupted flow in the circulating roadway. Circulating and approaching flows merge immediately at the entrance to the circulating roadway. Each vehicle must make two right turns. All other movements are eliminated. As a subordinate vehicle enters the circulating roadway it becomes a priority vehicle.

In Finland the geometric features of most roundabouts are designed so that speeds are reduced to 20–40 km/h. Safety is the most important factor in the design, even if it increases delays. Low speed of circulating traffic makes it easy and safe for approaching vehicles to enter the roundabout.

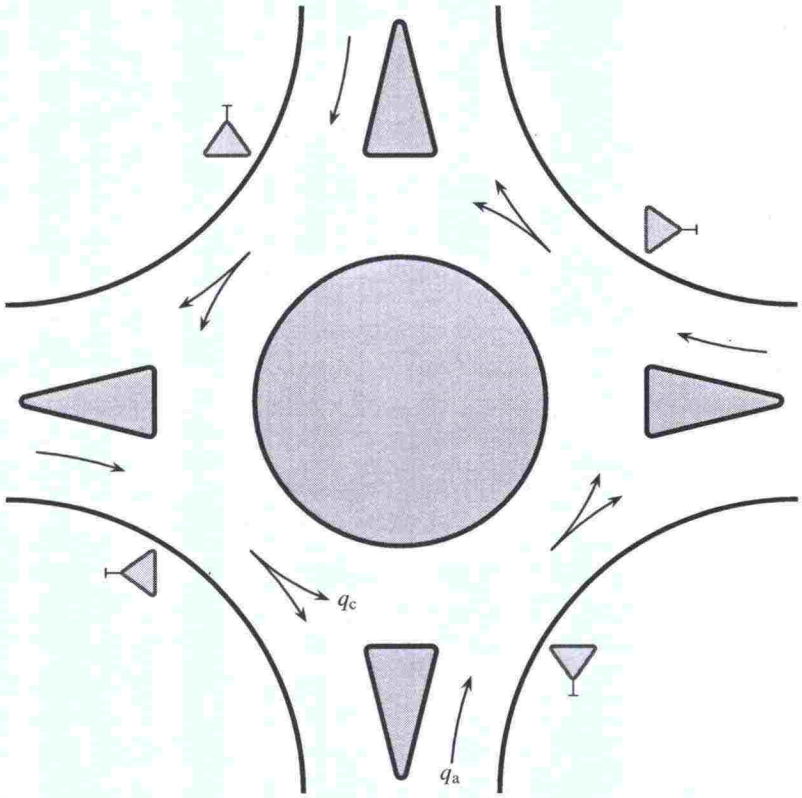

Figure 2.4: Traffic streams at a roundabout

Because vehicles entering a roundabout make a right turn, the operation can be assumed to be similar with the operation of right turning streams at yield (or stop) controlled intersections. The intersection angle is, however, usually smaller in roundabouts, which makes the operation similar to a (very) short merge area. If a roundabout is analyzed as a series of unsignalized T-intersections, the roundabout must be so large that the merges can be considered independent. According to the German manual (FGSV 2001), this approach can be used for roundabouts having an inscribed circle diameter larger than 26 meters. For other cases Troutbeck (1991) suggests that this approach can be used in an iterative manner, which quickly converges to solutions.

If pedestrian volumes are high, pedestrian crossings at roundabouts should be grade separated. If this is not the case, crosswalks should be located so that exiting vehicles stopped in front of a crosswalk do not disturb the circulating flow.

2.2 Definition of priority streams

A vehicle, whose driving path crosses or merges with a higher priority movement, cannot enter an intersection, until these higher priority movements provide a safe gap. For a minor stream k the set I_k includes all conflicting streams that have a higher priority than stream k. For example, at a four-leg intersection (Fig. 2.2) the set of conflicting priority streams for minor stream 8 includes streams 1, 2, 4, 5, and 6; i.e., $\{1, 2, 4, 5, 6\} \in I_8$. It is, however, necessary to take a closer look at the definition of priority streams.

In the discussion above, it was observed that pedestrian flows do not conform to the hierarchy of priorities of vehicular flows. It was not possible to assign a Rank to ped-

estrian flows. In section 3.8 the effect of pedestrian flows on vehicular capacities is estimated using the fraction of pedestrians that have priority over the subject minor stream. This fraction must be estimated for each location on the basis of field measurements or knowledge of local conditions. *Pedestrians are not included in the major flow of a gap acceptance process.*

So far it has been assumed that drivers know which higher priority vehicles are arriving to the conflict area, and which are using a nonconflicting lane or are turning into another direction. Special questions arise with major road right turning vehicles, through vehicles on multi-lane highways, and circling vehicles on multi-lane roundabouts as well as exiting vehicles on roundabouts.

Not all right turning vehicles display a turning sign. Some of those that do so, do so very late. Even when the turning sign is displayed, minor-road drivers may be hesitant and wait until there are also other indications that the major-road vehicle is indeed turning. Accordingly, some part of the major road right-turn stream could be included in the major flow, if it approaches the intersection on a lane sharing a through movement in conflict with the subject movement. In many current methods half of the right-turn streams (3 or 6) is included in the major stream. This principle is followed in HCM2000 (Transportation Research Board 2000) and HBS 2001 (FGSV 2001), and in the Norwegian manual (Statens Vegvesen 1985). On the other hand, Capcal 2 (SNRA 1995*b*) follows the old Swedish method (Statens vägverk 1977) and includes in the major flow only those streams which are in actual conflict with the subject movement. The same principle is followed in DanKap (Vejdirektoratet 1999*b*).

At roundabouts exiting vehicles have a similar role as major-road right turning vehicles at three and four-leg intersections. According to HCM2000 at most well-designed roundabouts the effect of vehicles exiting into the road, where subject vehicles are entering, can be ignored. Exiting flows are also ignored in HBS 2001, Capcal 2, DanKap and in the Norwegian manual. According to Hagring (1998*b*) most research reports have not found any significant effect due to exiting flows. This was also his own conclusion.

If a minor stream merges with a multi-lane stream, only that part of the higher priority stream should be counted, which are in conflict with the subject stream. Traffic flows on other lanes may have an impact on minor-stream drivers, but it is usually ignored. This principle is followed in HCM2000, HBS 2001, Capcal 2, and DanKap.

If a major-road right turning movement (3 or 6) is separated by a triangular island and face a stop or yield sign, priority is reversed. In this case major-road right turning vehicles no longer have Rank 1, but they should be analyzed as a Rank 2 movement at a T-intersection.

2.3 Gap availability

2.3.1 Gaps, lags, and headways

The time distance from front bumper to front bumper between two consecutive vehicles passing an observation point is called a *headway*. It is the sum of the time used by a vehicle to pass the observation point (occupancy time) and the time interval (gap) to the arrival of the next vehicle (Luttinen 1996). At unsignalized intersections the minor-road drivers consider gaps (unoccupied time intervals) as possible opportunities for their crossing or merging maneuvers. However, it is easier to describe traffic flow

in terms of headways than in terms of gaps and occupancy times.[2] In this discussion *gap* is the headway between two consecutive major stream vehicles evaluated by a minor-stream driver for the purpose of crossing or merging. The availability of gaps is described by headway distributions of higher priority streams; i.e., gaps are considered to be equal to headways (Troutbeck & Brilon 1997). It is assumed that the differences in major stream vehicle lengths and speeds (i.e., occupancy times) can be ignored.

Mathematically the arrival of vehicles is described as a point process, where each arrival is a point in the time axis (Fig. 2.5). Because vehicle length is ignored, gaps and headways are equal. Headway (gap) t_n is the time interval between vehicles $n-1$ and n. Each headway is connected to the vehicle which terminates the time interval. From the point of view of a minor-road driver it is thus possible to consider traffic flow on a major road as a succession of moving gaps (Raff 1950, Buckley 1962).

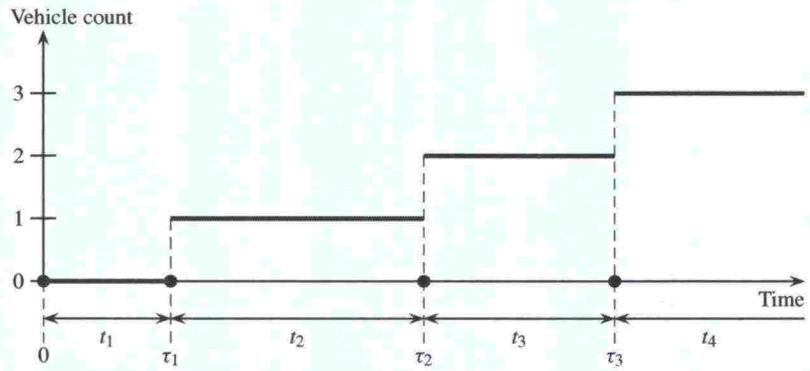

Figure 2.5: Vehicle arrivals as a point process (Luttinen 1990)

Let us assume that a vehicle enters a stop line or a yield line at time τ, the preceding priority vehicle has passed the conflict point at time τ_i, and the next priority vehicle will pass at time τ_{i+1} (Fig. 2.6). The time from the passage of the previous priority vehicle, $B(\tau) = \tau - \tau_i$, is called *backward waiting time* or current life (Karlin & Taylor 1975). The time to the passage of the next priority vehicle, $\Upsilon(\tau) = \tau_{i+1} - \tau$, is called *forward waiting time* or excess life in the theory of stochastic processes and *lag* in traffic flow theory. The current headway at time τ is the headway of priority stream vehicle $i+1$; i.e., $T(\tau) = T_{i+1} = \tau_{i+1} - \tau_i = B(\tau) + \Upsilon(\tau)$.

Some of the major road gaps are not accepted by minor road vehicles, some gaps are accepted by one vehicle, and some gaps allow the entry of several vehicles. Consequently, more detailed information than a *deterministic headway model* ($\forall i : t_i = \bar{t}$) is required (see Watson 1933, Clayton 1941, Catchpole & Plank 1986). For realistic estimation of capacity and delays it is necessary to have a realistic model of the frequency of gaps of different lengths. In mathematical models the availability of gaps is described by a *probability distribution* of vehicle headways (see Luttinen 1996).

A *cumulative distribution function* gives the probability that a randomly[3] selected head-

[2]Headway can be considered as the inverse individual flow rate of each vehicle (Dawson & Chimini 1968). The sum of headways $\tau_n = \sum_{i=1}^{n} t_i$ is the time interval between the arrivals of vehicles 0 and n, so that the number of headways (vehicles) divided by the sum of headways gives a proper estimate of flow rate ($\tilde{\lambda} = n\tau_n^{-1}$).

[3]It should be emphasized that the headway that occurs for a randomly arriving vehicle or pedestrian is not randomly selected. It is more probable that a random observer arrives during a long headway than during a short headway. This length-biased sampling is the reason for the well-known waiting time

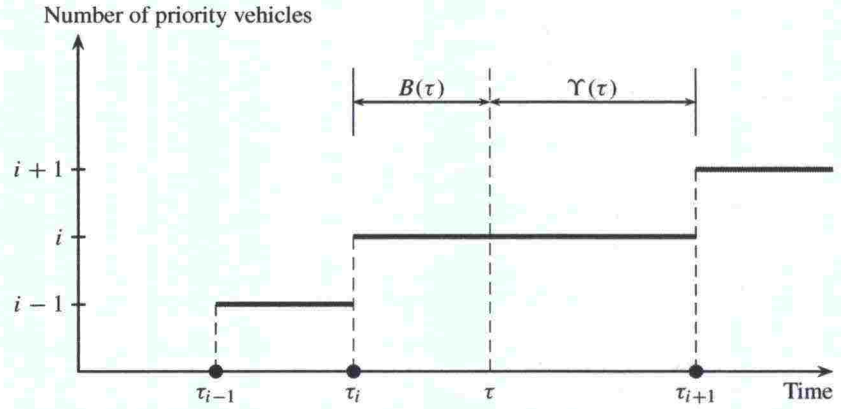

Figure 2.6: Backward waiting time $B(\tau)$ and lag $\Upsilon(\tau)$ (Luttinen 1990)

way is not larger than a given value

$$F(t) = \mathbb{P}\{T < t\} = \int_0^t f(u)\ \mathrm{d}(u) \tag{2.1a}$$

$$F(\infty) = \mathbb{P}\{T < \infty\} = \int_0^\infty f(u)\ \mathrm{d}(u) = 1, \tag{2.1b}$$

where $f(t)$ is the *probability density function*. Because headways cannot have negative length, the lower limit of integration is zero. In conventional probability analysis $F(t)$ is defined as $\mathbb{P}\{T \leq t\}$. The definition given above is more useful in gap acceptance theory. For distributions continuous at t, both definitions give identical numerical results.

The probability that a randomly selected headway is larger than a given value is called *survivor function*

$$R(t) = \mathbb{P}\{T \geq t\} = \int_t^\infty f(u)\ \mathrm{d}(u) = 1 - F(t)\,. \tag{2.2}$$

In reliability and life data analysis this function gives the probability that an object survives or operates reliably for a given time (see e.g. Nelson 1982, Crowder, Kimber, Smith & Sweeting 1991).

The expectation $\mathbb{E}[T]$ is the average headway from the distribution:

$$\mathbb{E}[T] = \bar{t} = \int_0^\infty t f(t)\ \mathrm{d}t. \tag{2.3}$$

Because $f(t) = 0$ when $t < 0$, expectation can also be expressed in terms of the

paradox (Feller 1966, Daganzo 1997).

survivor function (Grimmett & Stirzaker 2001):[4]

$$\mathbb{E}[T] = \bar{t} = \int_0^\infty [1 - F(t)]\,\mathrm{d}t = \int_0^\infty R(t)\ \mathrm{d}t. \tag{2.4}$$

If we count n consecutive headways, the expected duration of the count is $\mathbb{E}[\tau_n] = n\bar{t}$. Flow rate ($\lambda = q/3600$) is the inverse of average headway: $\lambda = n(\mathbb{E}[\tau_n])^{-1} = \bar{t}^{-1}$. This is an unconventional definition of flow rate, but it helps to demonstrate the relationship between flow rate and average headway. For a more detailed analysis of this relationship the reader is referred to the discussions by Haight (1963) on synchronous and asynchronous counting and by Luttinen (2001) on doubly synchronous counting, as well as to a discussion on renewal processes in any standard textbook on stochastic processes (e.g., Ross 1996).

The *lags* experienced by randomly arriving vehicles have a different distribution than headways. If $R(\upsilon) = \mathbb{P}\{T > \upsilon\}$ is the survivor function of the headway distribution and $\mathbb{E}[T]$ is the expected headway, the probability density function of lags can be expressed using the *Palm-Khintchine equation* (Palm 1943, Khintchine 1960, Cox & Isham 1980):

$$f_\Upsilon(\upsilon) = \frac{R(\upsilon)}{\mathbb{E}[T]} = \lambda R(\upsilon)\,. \tag{2.5}$$

Cox & Miller (1965) have presented an application of this equation for the estimation of delays at unsignalized intersections.

The survivor function of lags is obtained directly from equation (2.5) as

$$R_\Upsilon(\upsilon) = \lambda \int_\upsilon^\infty R(y)\,\mathrm{d}y. \tag{2.6}$$

The expected value of a lag can be expressed in terms of the moments of the headway distribution:

$$\begin{aligned}
\mathbb{E}[\Upsilon] &= \int_0^\infty \upsilon f_\Upsilon(\upsilon)\ \mathrm{d}\upsilon \\
&= \frac{1}{\mathbb{E}[T]} \int_0^\infty \upsilon R(\upsilon)\ \mathrm{d}\upsilon \\
&= \frac{1}{\mathbb{E}[T]} \int_0^\infty \upsilon \int_\upsilon^\infty f(y)\ \mathrm{d}y\,\mathrm{d}\upsilon \\
&= \frac{1}{\mathbb{E}[T]} \int_0^\infty \left(\int_0^y \upsilon\,\mathrm{d}\upsilon \right) f(y)\ \mathrm{d}y \\
&= \frac{1}{\mathbb{E}[T]} \int_0^\infty \frac{y^2}{2} f(y)\ \mathrm{d}y \\
&= \frac{\mathbb{E}[T^2]}{2\,\mathbb{E}[T]} = \frac{\bar{t}}{2} + \frac{\sigma_T^2}{2\bar{t}}.
\end{aligned} \tag{2.7}$$

See Kleinrock (1975) for a different approach.

[4]This equation can be proved by integration with change of order (Ross 2002)

$$\begin{aligned}
\int_0^\infty R(t)\ \mathrm{d}t &= \int_0^\infty \int_t^\infty f(u)\,\mathrm{d}u\,\mathrm{d}t \\
&= \int_0^\infty \left(\int_0^u \mathrm{d}t \right) f(u)\,\mathrm{d}u \\
&= \int_0^\infty u f(u)\,\mathrm{d}u.
\end{aligned}$$

For a geometric interpretation see Gnedenko (1962).

2.3.2 Geometric distribution

Winsten (in Beckmann et al. 1956) has estimated the delay at an unsignalized intersection considering time in finite sized steps. If the probability of an arrival during a time interval of unit length is p, the probability of a headway of k time units is $(1-p)^{k-1}p$. During one time unit, the number of arrivals can be 0 or 1. The probability p of an arrival can be interpreted as the flow rate; i.e., number of arrivals per time unit. The arrival process is binomial, and headways follow the *geometric distribution*, which has density, distribution, and survivor functions as follows:

$$f(k) = \mathbb{P}\{K = k\} = (1-p)^{k-1}p \tag{2.8a}$$

$$F(k) = \mathbb{P}\{K \leq k\} = p\sum_{i=1}^{k}(1-p)^{i-1} = p\sum_{i=0}^{k-1}(1-p)^{i} = 1-(1-p)^{k} \tag{2.8b}$$

$$R(k) = \mathbb{P}\{K > k\} = 1 - F(k) = (1-p)^{k}, \tag{2.8c}$$

where p is the probability of arrival during the minimum time interval, and K is the headway (measured in discrete time intervals). The expected length of a headway is (Matloff 1988)

$$\begin{aligned}
\mathbb{E}[K] &= p\sum_{i=1}^{\infty} iq^{i-1} \\
&= p\frac{\mathrm{d}}{\mathrm{d}q}\sum_{i=1}^{\infty} q^{i} \\
&= p\frac{\mathrm{d}}{\mathrm{d}q}\left[\frac{1}{1-q} - 1\right] \\
&= p\frac{1}{(1-q)^{2}} \\
&= \frac{1}{p},
\end{aligned} \tag{2.9}$$

where $q = 1 - p$. Average headway is the reciprocal of the flow rate, as expected.

If headways are i.i.d. and a randomly selected headway is less than t with probability $p = F(t)$, the probability of k consecutive headways $T < t$ follows geometric distribution:

$$p_k = p^{k}(1-p) = [F(t)]^{k}R(t)\,. \tag{2.10}$$

The expected number of consecutive headways $T < t$ is

$$\begin{aligned}
\mathbb{E}[K] &= (1-p)\sum_{i=1}^{\infty} ip^{i} \\
&= (1-p)p\sum_{i=1}^{\infty} ip^{i-1} \\
&= (1-p)p\frac{1}{(1-p)^{2}} \\
&= \frac{p}{1-p} \\
&= \frac{F(t)}{R(t)}.
\end{aligned} \tag{2.11}$$

Geometric distribution is a discrete-time headway model. Modern microscopic traffic models are, however, based on continuous-time headway distributions, the most important of which will be discussed below. Even in continuous-time models geometric distribution can be used to estimate probabilities and expectations of i.i.d. events, as shown above.

2.3.3 Negative exponential distribution

If vehicles are assumed to move at their desired speeds and independently of each other, traffic volumes follow Poisson distribution, and headways are *exponentially distributed*. The probability density, cumulative distribution, and survivor functions are

$$f(t) = \lambda \mathrm{e}^{-\lambda t} \tag{2.12a}$$

$$F(t) = 1 - \mathrm{e}^{-\lambda t} \tag{2.12b}$$

$$R(t) = 1 - F(t) = \mathrm{e}^{-\lambda t}, \tag{2.12c}$$

where λ is the scale parameter (see Fig. 2.7). The expected headway is equal to the inverse scale parameter:

$$\mathbb{E}[T] = \int_0^\infty R(t)\,\mathrm{d}t = \int_0^\infty \mathrm{e}^{-\lambda t}\mathrm{d}t = \frac{1}{\lambda}. \tag{2.13}$$

This indicates that the scale parameter is equal to the flow rate expressed in veh/s; i.e., $\lambda = q/3600$.

Negative exponential distribution is the interarrival time distribution of totally random arrivals. The counting process follows the Poisson distribution. At low flow rates the negative exponential density function is highest, and distribution function (Fig. 2.7) rises steeply. For long headways the density approaches asymptotically zero and the distribution function unity. This indicates both a substantially high probability of very short headways, even at low flow rates, and the possibility of very long headways, even at high flow rates.

Several authors (e.g., Weiss & Herman 1962, Breiman 1963, Thedéen 1964) have demonstrated that under rather weak assumptions (no vehicle interaction, identically and independently distributed speeds) the number of vehicles in an arbitrary time interval will be asymptotically Poisson distributed as time tends to infinity. Thus, headways will asymptotically follow the exponential distribution. If the combined headways of several independent streams passing a reference point are considered, the limitations of the Poisson assumption become less severe.

Exponential distribution has the Markov ("lack of memory") property (Luttinen 1990):

$$\begin{aligned} \mathbb{P}\{\, T > b + v \,|\, T > b \,\} &= \frac{\mathrm{e}^{-\lambda(b+v)}}{\mathrm{e}^{-\lambda b}} \\ &= \mathrm{e}^{-\lambda v} \\ &= \mathbb{P}\{T > v\}, \end{aligned} \tag{2.14}$$

where b is the current duration of headway (backward waiting time) and v is the lag (Fig. 2.6). This indicates that lags have the same distribution as headways:

$$f_\Upsilon(v) = \frac{R_T(v)}{\mathbb{E}[T]} = \lambda \mathrm{e}^{-\lambda v}. \tag{2.15}$$

In fact, exponential distribution is the only continuous-time distribution that has the Markov property (Feller 1957).

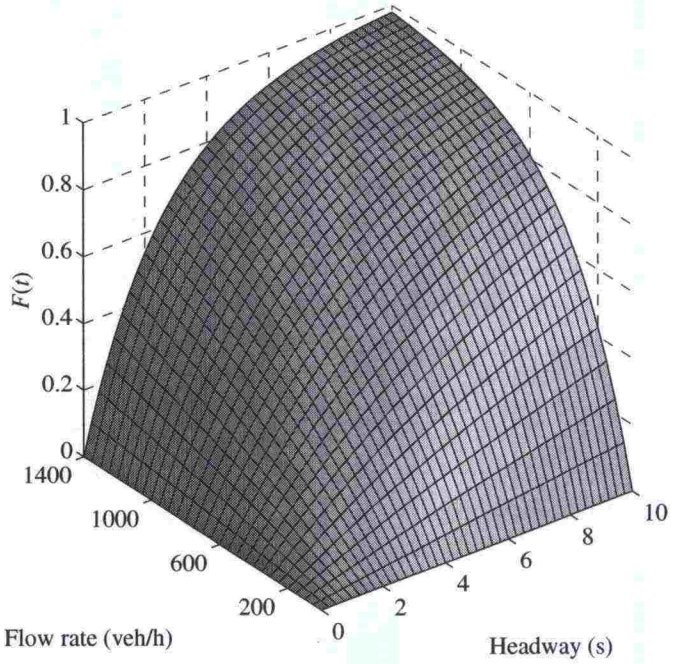

Figure 2.7: Negative exponential cumulative distribution function for vehicle headways

Because of the Markov property it is not necessary to keep track of the time elapsed since the last arrival. This makes the Poisson process mathematically tractable (Tijms 2003). Therefore, the negative exponential distribution is often preferred over other, more realistic but also more complex headway distributions. In many cases explicit solutions can only be found when the arrival process is assumed Poisson. Since Adams (1936) the negative exponential distribution has played a central role in traffic flow theory.

If the arrival process is Poisson and the number of arrivals during a given time interval $(0, \tau]$ is n, the distribution of the arrival times is similar as the distribution of n uniformly distributed events in time interval $(0, \tau]$ (Karlin & Taylor 1981, Tijms 2003). This indicates that Poisson arrivals are completely random in time. An important consequence of this is the PASTA (Poisson Arrivals See Time Averages) property (Wolff 1989). When the arrival process is Poisson, the average state of a system during arrival times is equal to the time average state of the system.

The exponential model has two major limitations: The model allows unrealistically short headways, and it does not describe platooning. The model gets more distorted as flow rates increase. Consequently, the exponential distribution can be considered as a realistic headway model under very low-flow conditions only, approximately $q <$ 150 veh/h (Luttinen 1996).

The exponential distribution can also be used to describe the headways of free vehicles, which are not driving in platoons. This indicates that empirical headway distributions have an "exponential tail" (Luttinen 1996). Because very short headways are not likely to be "free", the exponential distribution should be modified.

2.3.4 Shifted exponential distribution

If headways have a minimum length of t_p, and headways larger than t_p are exponentially distributed, the resulting model is called *shifted exponential distribution.* It has probability density

$$f(t) = \begin{cases} 0, & \text{if } t < t_p \\ \theta e^{-\theta(t-t_p)}, & \text{if } t \geq t_p, \end{cases} \tag{2.16}$$

where θ is the scale parameter and t_p is the location parameter. The distribution function (Fig. 2.8) is

$$F(t) = \begin{cases} 0, & \text{if } t < t_p \\ 1 - e^{-\theta(t-t_p)}, & \text{if } t \geq t_p, \end{cases} \tag{2.17}$$

and the survivor function is

$$R(t) = \begin{cases} 1, & \text{if } t < t_p \\ e^{-\theta(t-t_p)}, & \text{if } t \geq t_p. \end{cases} \tag{2.18}$$

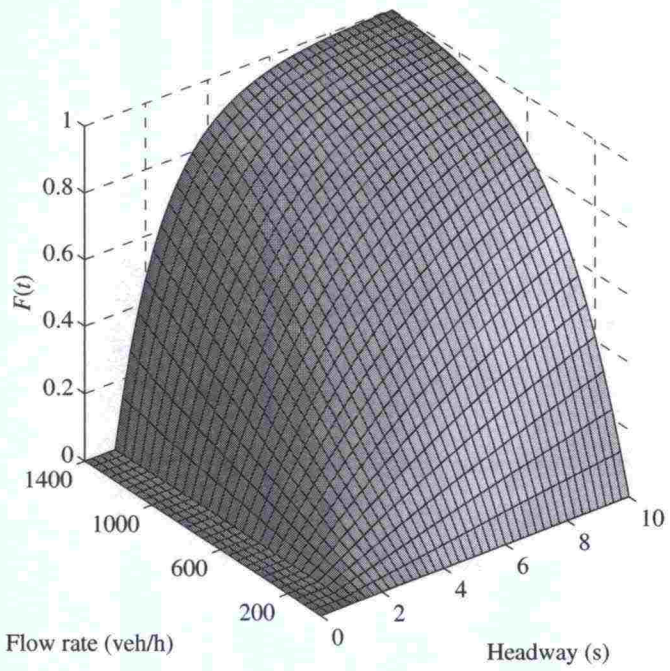

Figure 2.8: Shifted exponential cumulative distribution function with minimum headway $t_p = 1\,s$

Shifted exponential distribution is the conditional distribution of exponential headways larger than t_p:

$$\mathbb{P}\{\, T > t \,|\, T > t_p \,\} = \frac{\mathbb{P}\{T > t\}}{\mathbb{P}\{T > t_p\}} = \frac{e^{-\lambda t}}{e^{-\lambda t_p}} = e^{-\lambda(t-t_p)}, \qquad t_p \leq t. \tag{2.19}$$

This distribution avoids the problem of extremely short headways, but does not model platooning.

The shape of the distribution function is similar to the negative exponential distribution (Fig. 2.7), but the probability of headways smaller than the minimum headway (t_p) is null. After the minimum headway the distribution function rises even steeper than the negative exponential distribution function, and approaches asymptotically unity. The model does not include platooning, but the density is highest at headways just larger than the minimum headway.

The expected headway is

$$\mathbb{E}[T] = \int_0^\infty R(t)\,\mathrm{d}t = \int_0^{t_p} 1\,\mathrm{d}t + \int_{t_p}^\infty \mathrm{e}^{-\theta(t-t_p)}\,\mathrm{d}t = t_p + \frac{1}{\theta}. \tag{2.20}$$

Scale parameter θ can now be expressed in terms of flow rate as

$$\theta = \frac{1}{\mathbb{E}[T] - t_p} = \frac{\lambda}{1 - \lambda t_p} = \frac{q}{3600 - q t_p}. \tag{2.21}$$

Thus, the average flow rate of an arrival process with shifted exponential time headways is

$$\lambda = \frac{1}{\mathbb{E}[T]} = \frac{\theta}{1 + \theta t_p}. \tag{2.22}$$

Oliver (1961) has derived the explicit counting distribution.

The probability density function of the lag distribution is

$$f_\Upsilon(\upsilon) = \frac{R(\upsilon)}{\mathbb{E}[T]} = \frac{\theta R(\upsilon)}{1 + \theta t_p} = \begin{cases} \dfrac{\theta}{1 + \theta t_p}, & \text{if } \upsilon < t_p \\ \dfrac{\theta \mathrm{e}^{-\theta(\upsilon - t_p)}}{1 + \theta t_p}, & \text{if } \upsilon \geq t_p. \end{cases} \tag{2.23}$$

The survivor function of the lag distribution can be obtained by integrating the density function. When $\upsilon < t_p$, the survivor function is

$$\begin{aligned} R_\Upsilon(\upsilon) &= \frac{\theta}{1 + \theta t_p} \int_\upsilon^{t_p} \mathrm{d}y + \frac{1}{1 + \theta t_p} \int_{t_p}^\infty \theta \mathrm{e}^{-\theta(\upsilon - t_p)}\,\mathrm{d}y \\ &= \frac{\theta(t_p - \upsilon)}{1 + \theta t_p} + \frac{1}{1 + \theta t_p} \\ &= 1 - \frac{\theta \upsilon}{1 + \theta t_p}, \qquad \upsilon < t_p. \end{aligned} \tag{2.24}$$

When $\upsilon \geq t_p$, the survivor function is

$$\begin{aligned} R_\Upsilon(\upsilon) &= \frac{1}{1 + \theta t_p} \int_\upsilon^\infty \theta \mathrm{e}^{-\theta(\upsilon - t_p)}\,\mathrm{d}y \\ &= \frac{\mathrm{e}^{-\theta(\upsilon - t_p)}}{1 + \theta t_p}, \qquad \upsilon \geq t_p. \end{aligned} \tag{2.25}$$

Consequently, the survivor function is

$$R_\Upsilon(\upsilon) = \begin{cases} 1 - \dfrac{\theta \upsilon}{1 + \theta t_p}, & \text{if } \upsilon < t_p \\ \dfrac{\mathrm{e}^{-\theta(\upsilon - t_p)}}{1 + \theta t_p}, & \text{if } \upsilon \geq t_p. \end{cases} \tag{2.26}$$

When the location parameter (minimum headway) is zero, we obtain the survivor function of negative exponential distribution, as expected.

Once the survivor function of the lag distribution is known, the expected lag is obtained as

$$\begin{aligned}\mathbb{E}[\Upsilon] &= \int_0^\infty R_\Upsilon(\upsilon)\,\mathrm{d}\upsilon \\ &= \int_0^{t_\mathrm{p}} \left(1 - \frac{\theta\upsilon}{1+\theta t_\mathrm{p}}\right)\mathrm{d}\upsilon + \frac{1}{1+\theta t_\mathrm{p}} \int_{t_\mathrm{p}}^\infty \mathrm{e}^{-\theta(\upsilon - t_\mathrm{p})}\,\mathrm{d}u \\ &= t_\mathrm{p} - \frac{\theta t_\mathrm{p}^2}{2(1+\theta t_\mathrm{p})} + \frac{1}{\theta(1+\theta t_\mathrm{p})} \\ &= \frac{1}{2\theta}\left((1+\theta t_\mathrm{p}) + \frac{1}{(1+\theta t_\mathrm{p})}\right).\end{aligned} \tag{2.27}$$

Equation (2.7) gives naturally the same result, when the substitutions for mean $\bar{t} = t_\mathrm{p} + \theta^{-1}$ and variance $\sigma_T^2 = \theta^{-2}$ of the shifted exponential headway distribution are made. When $t_\mathrm{p} = 0$, the result is equal to the expectation of negative exponential distribution (θ^{-1}).

2.3.5 Erlang distribution

Another simple model used in the analysis of unsignalized intersections is the *Erlang distribution* (Erlang 1917*a*, Erlang 1917*b*), which is a special case of the *gamma distribution*. It is easily tractable in mathematical analysis, but not as easy as the exponential distribution, and not particularly good as a headway model (Luttinen 1991, Luttinen 1996). The Erlang distribution has not been used in this research, but it has been applied in the old Swedish method (Nordqvist, Bång & Hansson 1973, Statens vägverk 1977). See also Yeo (1962), Voigt (1973), and Prevedouros (1988).

2.3.6 Cowan's M3 distribution

A headway distribution can also be described as a mixture of follower and free-vehicle headways. If headways in platoons are assumed to be constant (t_p) and free-vehicle headways follow shifted exponential distribution, the cumulative distribution function is obtained as (Cowan 1975)

$$F(t) = \begin{cases} 0, & \text{if } t < t_\mathrm{p} \\ 1 - \phi \mathrm{e}^{-\gamma(t-t_\mathrm{p})}, & \text{if } t \geq t_\mathrm{p}, \end{cases} \tag{2.28}$$

where ϕ is the proportion of free-vehicle headways, and γ is the scale parameter. Buckley (1962) called this a regular-random distribution, but nowadays it is most often known as Cowan's M3 distribution according to (Cowan 1975). The survivor function is

$$R(t) = \begin{cases} 1, & \text{if } t < t_\mathrm{p} \\ \phi \mathrm{e}^{-\gamma(t-t_\mathrm{p})}, & \text{if } t \geq t_\mathrm{p}, \end{cases} \tag{2.29}$$

The expectation is

$$\mathbb{E}[T] = \int_0^\infty R(t)\,\mathrm{d}t = \int_0^{t_\mathrm{p}} 1\,\mathrm{d}t + \phi \int_{t_\mathrm{p}}^\infty \mathrm{e}^{-\gamma(t-t_\mathrm{p})}\,\mathrm{d}t = t_\mathrm{p} + \frac{\phi}{\gamma}. \tag{2.30}$$

Maximum flow rate $q_\mathrm{max} = 3600\,(\min \mathbb{E}[T])^{-1} = 3600 t_\mathrm{p}^{-1}$ is attained when all vehicles move in platoons ($\phi = 0$). The method-of-moments estimator for the scale parameter is obtained as

$$\tilde{\gamma} = \frac{\phi}{\mathbb{E}[T] - t_\mathrm{p}} = \frac{\phi q}{3600 - q t_\mathrm{p}}. \tag{2.31}$$

Because the proportion $1 - \phi$ of vehicles are followers and have a headway of size t_p, the density function has a mass of $1 - \phi$ at t_p. This point mass can be described using a unit impulse (Dirac delta) function (Spanier & Oldham 1987)

$$\delta(t - t_p) = \begin{cases} \infty & \text{if } t = t_p \\ 0 & \text{otherwise} \end{cases} \quad \text{and} \quad \int_0^\infty \delta(t - t_p)\,dt = 1, \tag{2.32}$$

which gives the probability density function (Plank 1982, Luttinen 1999)

$$f(t) = \begin{cases} 0, & \text{if } t < t_p \\ (1 - \phi)\delta(t - t_p) - \phi\gamma e^{-\gamma(t - t_p)}, & \text{if } t \geq t_p. \end{cases} \tag{2.33}$$

Figure 2.9 displays the coefficient of variation

$$C(T) = \frac{\sqrt{\text{var}(T)}}{\mathbb{E}[T]} = \frac{\sqrt{\phi(2 - \phi)}}{\gamma t_p + \phi} \tag{2.34}$$

of Cowan's M3 distribution. It is zero for deterministic headways ($\phi = 0$), reaches the maximum $[\gamma t_p(2 + \gamma t_p)]^{-1/2}$ at $\phi = \gamma t_p(1 + \gamma t_p)^{-1}$, and decreases to $(1 + \gamma t_p)^{-1}$ as ϕ reaches unity and the distribution becomes shifted exponential (Luttinen 1999). At low values of γ the peak rises above unity, but it stays below unity when γ is large. Although M3 gives a very crude approximation of short headways, it can produce moment characteristics very similar to real headway distributions (Luttinen 1999).

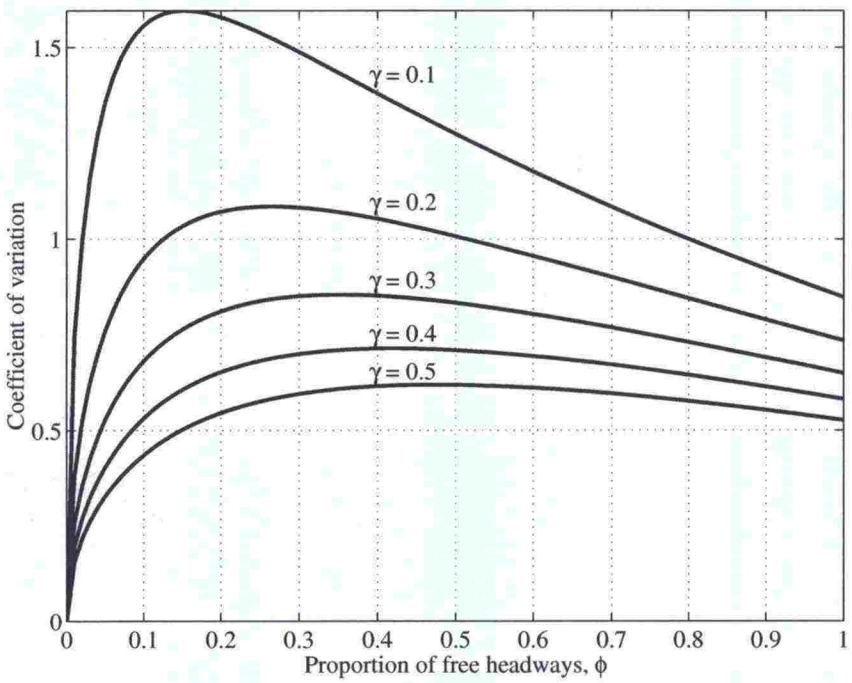

Figure 2.9: Coefficient of variation of Cowan's M3 distribution with $t_p = 1.8$ s (Luttinen 1999)

The density function of the lag distribution is

$$f_\Upsilon(v) = \frac{R(v)}{\mathbb{E}[T]} = \frac{\gamma R(v)}{\phi + \gamma t_p} = \begin{cases} \dfrac{\gamma}{\phi + \gamma t_p}, & \text{if } v < t_p \\ \dfrac{\phi\gamma e^{-\gamma(v - t_p)}}{\phi + \gamma t_p}, & \text{if } v \geq t_p. \end{cases} \tag{2.35}$$

The survivor function of the lag distribution can be obtained by integrating the density function. When $\upsilon < t_p$, the survivor function is[5]

$$\begin{aligned} R_\Upsilon(\upsilon) &= \frac{\gamma}{\phi + \gamma t_p} \int_\upsilon^{t_p} \mathrm{d}y + \frac{\phi}{\phi + \gamma t_p} \int_{t_p}^{\infty} \gamma \mathrm{e}^{-\gamma(\upsilon - t_p)}\, \mathrm{d}y \\ &= \frac{\gamma(t_p - \upsilon) + \phi}{\phi + \gamma t_p} \\ &= 1 - \frac{\gamma \upsilon}{\phi + \gamma t_p}, \qquad \upsilon < t_p. \end{aligned} \tag{2.36}$$

When $\upsilon \geq t_p$, the survivor function is

$$\begin{aligned} R_\Upsilon(\upsilon) &= \frac{\phi}{\phi + \gamma t_p} \int_\upsilon^{\infty} \gamma \mathrm{e}^{-\gamma(\upsilon - t_p)}\, \mathrm{d}y \\ &= \frac{\phi \mathrm{e}^{-\gamma(\upsilon - t_p)}}{\phi + \gamma t_p}, \qquad \upsilon \geq t_p. \end{aligned} \tag{2.37}$$

The survivor function can now be expressed as

$$R_\Upsilon(\upsilon) = \begin{cases} 1 - \dfrac{\gamma \upsilon}{\phi + \gamma t_p}, & \text{if } \upsilon < t_p \\ \dfrac{\phi \mathrm{e}^{-\gamma(\upsilon - t_p)}}{\phi + \gamma t_p}, & \text{if } \upsilon \geq t_p. \end{cases} \tag{2.38}$$

When the proportion (ϕ) of free headways is unity, we obtain the survivor function of shifted exponential distribution.

Because the flow rate λ (veh/s) is the inverse of the expected headway $\mathbb{E}[T]$, the lag density can be expressed as (Hagring 1998*a*):

$$f_\Upsilon(\upsilon) = \lambda R(\upsilon) = \begin{cases} \lambda, & \text{if } \upsilon < t_p \\ \lambda \phi \mathrm{e}^{-\gamma(\upsilon - t_p)}, & \text{if } \upsilon \geq t_p. \end{cases} \tag{2.39}$$

The survivor function of the lag distribution can likewise be expressed as (see Hagring 1998*a*)

$$R_\Upsilon(\upsilon) = \begin{cases} 1 - \lambda \upsilon, & \text{if } \upsilon < t_p \\ \dfrac{\lambda}{\gamma} \phi \mathrm{e}^{-\gamma(\upsilon - t_p)}, & \text{if } \upsilon \geq t_p. \end{cases} \tag{2.40}$$

A model similar to Cowan's M3 was presented earlier by Tanner (1953, 1961*a*, 1967) and (Miller 1961). Tanner modeled traffic flow as departures from an M/D/1 queuing system (exponential interarrival times and one server with constant service times). Because the arrival process is Poisson (Khintchine 1960), the proportion of constant (t_p) headways is equal to the utilization factor of the server (Luttinen 1990)

$$1 - \phi = \mathbb{P}\{T = t_p\} = \lambda t_p = \frac{q t_p}{3600}. \tag{2.41}$$

[5]The survivor function can be obtained more easily as follows:

$$R_\Upsilon(\upsilon) = 1 - F_\Upsilon(\upsilon) = 1 - \frac{\gamma}{\phi + \gamma t_p} \int_0^{\upsilon} \mathrm{d}y = 1 - \frac{\gamma \upsilon}{\phi + \gamma t_p}, \qquad \upsilon < t_p.$$

Using equations (2.30) and (2.41) parameters ϕ and γ can be expressed as

$$\phi = 1 - \lambda t_p = 1 - \frac{q t_p}{3600} \tag{2.42}$$

$$\gamma = \frac{\phi}{\frac{1}{\lambda} - t_p} = \lambda = \frac{q}{3600}. \tag{2.43}$$

The last result indicates that the scale parameter γ of the shifted exponential distribution of free headways is equal to the scale parameter λ of the negative exponential interarrival time distribution of the underlying M/D/1 queuing process. The distribution function is

$$F(t) = \begin{cases} 0, & \text{if } t < t_p \\ 1 - (1 - \lambda t_p)e^{-\lambda(t - t_p)}, & \text{if } t \geq t_p. \end{cases} \tag{2.44}$$

The headways are no longer independent; i.e., platoon lengths do not follow geometric distribution, as in the M3 model, but the Borel-Tanner distribution (Tanner 1953, Tanner 1961*a*, Tanner 1961*b*, Haight & Breuer 1960, Prabhu 1965). The autocorrelation of headways does not have any influence on capacity estimates, but delays are sensitive to the order of headways (Kyte, Tian, Mir, Hameedmansoor, Kittelson, Vandehey, Robinson, Brilon, Bondzio, Wu & Troutbeck 1996).

Figure 2.10 displays the cumulative distribution function of headways from an M/D/1 queuing process with service time (i.e., headway in platoon) $t_p = 2$ s. There is a discontinuity at $T = t_p$. The probability of shorter headways is null. The proportion of follower headways increases linearly with increasing flow rate, as indicated by equation (2.42). When headways are larger than t_p, the cumulative distribution function approaches asymptotically unity. Maximum flow rate is $\lambda = t_p^{-1}$ or $q = 3600 t_p^{-1}$, when all vehicles are followers ($\phi = 0$).

M3 distribution is a good headway model, if there is no need for accurate modeling of short gaps. Such is the case in the analysis of unsignalized intersections. M3 can reproduce data with moment characteristics very similar to real headway distributions, and it gives good results in capacity analysis for unsignalized intersections (Luttinen 1999). Properties of the M3 distribution and the estimation of its parameters have been discussed by several authors (see Brilon 1988*a*, Akçelik & Chung 1994, Sullivan & Troutbeck 1994, Hagring 1996*b*, Troutbeck 1997*b*, Luttinen 1999, Tanyel & Yayla 2003).

The M3 distribution has been widely used in the capacity and delay analysis of unsignalized intersections and roundabouts (Akçelik 1994*a*, Hagring 1996*b*, Hagring 1998*b*, Luttinen 1999, Sullivan & Troutbeck 1994, Troutbeck 1986, Troutbeck 1991, Troutbeck & Kako 1997), especially in Australia. The headway distribution for a two-lane case; i.e., a superposition of two M3 distributions, has been derived by Troutbeck (1986) and Hagring (1998*b*). See also section 3.3.

More advanced mixed distributions, such as the *semi-Poisson distribution* (Buckley 1962, Buckley 1968, Luttinen 1994) and the *generalized queuing model* (Cowan 1975, Branston 1976), use a specific distribution for headways in platoons and exponential distribution for free-vehicle headways. These models are more realistic, but they are also more difficult to use in mathematical analysis (Luttinen 1996).

Most of the current unsignalized intersection models use either negative exponential distribution or Cowan's M3 distribution for major stream headways. For a more detailed description of headway distributions the reader is referred to Luttinen (1996).

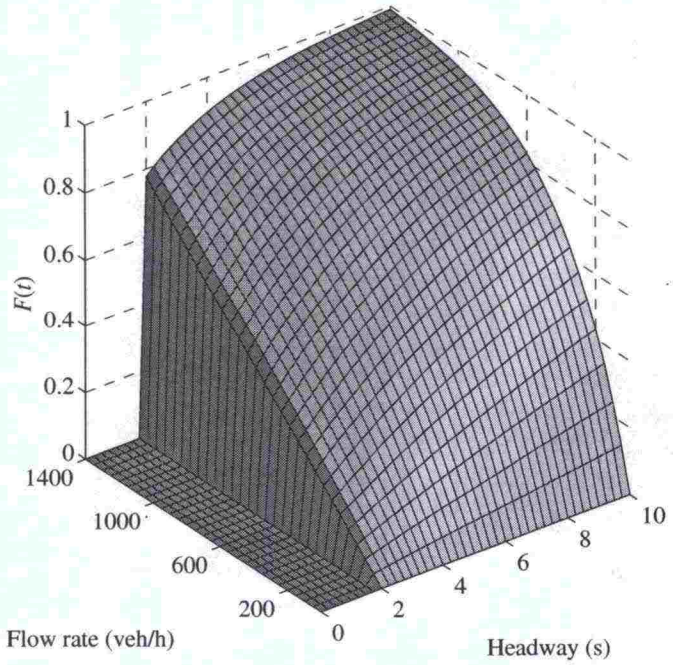

Figure 2.10: Cumulative distribution function of headways from an M/D/1 queuing process with service time $t_p = 2\,s$

2.4 Gap acceptance and queue discharge

The arrivals and departures at an unsignalized intersection can be described by a queuing model demonstrated in Figure 2.11. When a minor-stream vehicle enters the stop line or yield line (first position in a queue, time 0 in Figure 2.11) the driver must evaluate whether the lag in priority streams is safe for entry. If the driver considers the lag unsafe, the vehicle waits for a safe headway. The minimum acceptable major-stream headway is assumed to be equal for all vehicles, and it is called the critical acceptance gap, or simply the *critical gap* (t_c).

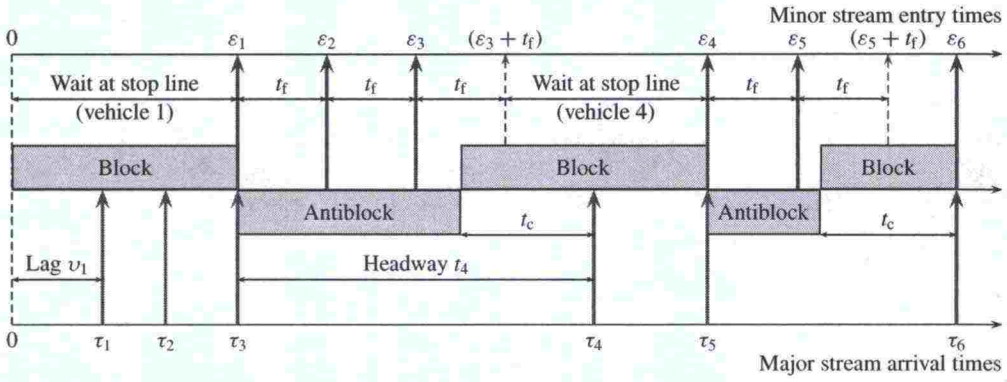

Figure 2.11: Queue discharge at an unsignalized intersection

A minor stream driver attempts to maximize her/his utility by accepting a major stream headway having a safety risk lower than the value of the expected delay resulting from

headway rejection. Critical gap can be regarded as a compromise between the demand for safe entry to an intersection and for minimizing delay (Hagring 1998*b*). Gap acceptance theory is a microscopic (stochastic) theory, which describes the behavior of individual drivers, as opposed to macroscopic (statistical) models describing traffic flow at an aggregate level.

Each major-stream vehicle blocks minor-stream vehicles from entering the intersection. The *block*, as Raff (1950) called this time interval, starts t_c seconds before the major-stream vehicle arrives and lasts until the beginning of the next major-stream headway $t_i \geq t_c$ (Fig. 2.11). The time interval between two blocks is called an *antiblock*. An antiblock starts when a headway $t_i \geq t_c$ starts and ends t_c before the arrival of the next major-stream vehicle. Minor-stream vehicles can enter the intersection during antiblocks. A minor-stream vehicle is assumed to enter the intersection immediately at the beginning of an antiblock or immediately after having reached the stop line during an antiblock (Weiss & Maradudin 1962).—Assuming a traffic signal analogy, suggested first by Winsten (in Beckmann et al. 1956), blocks can be considered red intervals and antiblocks green intervals.

When a minor stream vehicle enters the intersection, it takes some time before the next vehicle can take its position at the head of the queue. After this the process is repeated. The minimum headway between two minor stream vehicles entering the same major stream gap is called *follow-up time* (t_f). During an antiblock vehicles from a minor stream queue enter the intersection separated by follow-up times.[6] An interval t_f after the queue has discharged, minor stream vehicles can proceed without delay until the next block starts. At a yield controlled intersection a vehicle approaching an intersection or discharging from a queue can proceed without stopping, if the lag is long enough.

The operation can be described as a *single server queuing system* with deterministic (t_f) service times. The service is, however, occasionally interrupted, because customers can enter service during antiblock intervals only. A more comprehensive description of several conflicting streams would be a single server system with *priority queues*. Each customer type (rank) has a separate queue. The first customer in the highest rank queue is always served first. Switching from one queue to another requires a "reorientation time" $t_c - t_f$ (Jaiswal 1968). The hierarchy of conflicts in an entire unsignalized intersection is, however, too complicated to be described by a single queuing system. For example, in a four-legged intersection (Fig. 2.2) streams 4 and 8 have a conflict, as do streams 3 and 4, but stream 3 and 8 vehicles can enter the intersection simultaneously. Queuing models are limited, but nevertheless useful tools in the analysis of unsignalized intersections.

It is assumed that service starts as a vehicle crosses stop line. Service time is equal to the follow-up time. When service ends, the next vehicle can enter service (cross stop line).

[6] According to Akçelik (1994*a*) the first minor stream vehicle enters an intersection t_f after the beginning of an antiblock. Consequently, the last vehicle can enter the intersection $t_c - t_f$ before the arrival of the next major stream arrival. See also Kyte et al. (1996).

According to Tanner (1962) and Yeo & Weesakul (1964) a minor stream vehicle can depart t_c after the last vehicle in a block, and the next block starts when the next major stream vehicle arrives. Mathematically the model is unchanged if the block starts a constant time $u < t_c$ before the first vehicle and terminates $t_c - u$ after the last vehicle (Tanner 1962). By setting $u = t_c - t_f$, we obtain the model of Akçelik (1994*a*). The model in Figure 2.11 was suggested by Weiss & Maradudin (1962), and it is obtained by setting $u = t_c$.

In terms of a queuing process, entry time is the time of departure from service. In Figure 2.11 major stream arrival times can be interpreted as service departure times, while minor stream entry times should be considered as service entry times. See Figure 3.16 on page 79 for more details.

The reference point of a priority stream is the conflict point between the priority and minor streams. However, in the gap acceptance process no service times are usually assumed for priority streams. The entry of minor-stream vehicles is blocked by critical gaps and follow-up times only.

In Figure 2.11 the first vehicle enters the intersection at the same time as the major stream vehicle arrives ($\varepsilon_1 = \tau_3$ and $\varepsilon_4 = \tau_5$); i.e., passes the conflict point. When the "service is completed", the minor stream vehicle passes the conflict point. Thus, t_f is also the minimum time interval between a major stream vehicle and a merged minor stream vehicle. This is, however, an extension of the basic queuing model.

The service of a minor stream vehicle may overlap the critical gap. In Figure 2.11 vehicle 3 departs at $\varepsilon_3 + t_f$, when major stream vehicle 4 has already blocked the entry of minor stream vehicle 4. The minimum headway between a minor stream vehicle and a major stream vehicle is $t_c - t_f$.

This discussion raises three issues concerning time intervals between vehicles.

1. Critical gap (t_c) cannot be shorter than the follow-up time (t_f). Otherwise the arrival time of the next major stream vehicle (such as τ_6 in Figure 2.11) might take place before a minor stream vehicle has departed from service ($\varepsilon_5 + t_f$). This is an important condition for capacity models, which assume a constant queue of minor stream vehicles. The condition $t_f \leq t_c$ ensures that there is always a minor stream vehicle waiting at the stop line when an antiblock starts (Plank & Catchpole 1984).

2. Even if $t_c > t_f$, the headway between the merged vehicle and the next major stream vehicle ($\tau_6 - \varepsilon_5 - t_f$) may become too short, in which case the major stream vehicle has to decelerate in order to delay its arrival and to keep the headway safe. Because the priority of major stream vehicles is limited, this type of operation is called "limited priority merge" (see Troutbeck 2002). Major stream priority becomes limited, if $t_c < t_f + t_p$, where t_p is the follower headway between major stream vehicles.—To make the argument simpler, follower headway (headway between vehicles in a platoon) has been assumed constant.

3. The minor stream follow-up time (t_f) cannot be shorter than the major stream follower headway (t_p). Otherwise the minor stream queue discharge rate would be higher than the major stream capacity. The major stream cannot receive merging vehicles at this rate.

Because drivers and vehicles differ, the minimum gaps and lags accepted by drivers and the headways between discharging vehicles differ from vehicle to vehicle. Driver behavior is heterogeneous. In addition, even under similar conditions a driver may behave differently at different times. A driver may accept a gap that is shorter than a gap rejected by the same driver earlier. This kind of behavior is called inconsistent. It is apparent that inconsistency is related to real inconsistency in driver behavior, but it is possible that most of the observed "inconsistent" behavior can be explained by situation-specific factors, such as waiting time and variation in speed and type of major stream vehicles (Hagring 1998*b*).

In mathematical models driver behavior is usually assumed to be both consistent and homogeneous. A *consistent* driver behaves in the same way every time at similar situations. An inconsistent driver may approve a gap that is shorter than a gap that the same driver had rejected earlier. An inconsistent driver determines a new critical gap for

each major stream headway (Ashworth 1969, Plank & Catchpole 1984), or assigns to each gap a probability of crossing (Weiss & Maradudin 1962, Hawkes 1968). Typically the acceptable headway decreases as the number of rejected gaps increases. Such a driver is called impatient. (If critical gap increases as the number of rejected gaps increases, the behavior is not inconsistent according to the definition.) Accordingly, inconsistency increases capacity.

If drivers are *homogeneous*, there is no difference in behavior among different drivers under similar conditions. Homogeneous but inconsistent drivers have the same way of selecting a critical gap for each individual headway. In the case of heterogeneous and consistent drivers, each driver (or vehicle type) has an individual critical gap sampled from a common distribution. This critical gap is applied consistently to all major stream headways. Vehicles with large critical gaps are more likely to be found at the head of the queue (Catchpole & Plank 1986), which leads to a decrease in capacity (Wegmann 1991).

When a minor stream consists of heterogeneous and inconsistent drivers each driver has an individual way to sample critical gaps for each individual headway or lag. Because inconsistency increases capacity and heterogeneity decreases it, the overall effect of the assumption of consistent and homogeneous drivers has been considered to be minimal compared to the case of heterogeneous and inconsistent drivers (Catchpole & Plank 1986, Troutbeck 1988, Transportation Research Board 1997, Hagring, Rouphail & Sørensen 2003).

In summary, the major assumptions in basic gap acceptance models are

1. Similar (consistent) behavior of each driver under similar conditions
2. Similar (homogeneous) behavior among all drivers
3. Minor stream vehicles have similar critical gaps in all priority streams and between vehicles of different priority streams
4. Gap acceptance is similar to lag acceptance.
5. Gaps of all independent priority streams are superimposed into a single stream of gaps
6. The availability of priority-stream gaps is described by a statistical headway distribution model
7. Minor-road vehicles arrive randomly
8. Priority stream vehicles do not adjust their behavior to accommodate an entering vehicle; i.e., gap-acceptance behavior is similar at all traffic volumes
9. Minor stream vehicles can distinguish priority vehicles from vehicles exiting before the conflict area

It is also assumed that follow-up time is shorter than critical gap. This assures that under a continuous queue there is always a vehicle waiting for entry as a new gap begins. If critical gap was shorter than follow-up time, the mathematical models would allow the possibility of queue discharge headways shorter that follow-up times.

Several models have relaxed one or more of these assumptions. Herman & Weiss (1961) and Weiss & Maradudin (1962) introduced a gap acceptance probability; i.e., the probability that a waiting driver accepts a headway of given length. Ashworth (1969) and

Plank & Catchpole (1984) have developed a capacity formula for heterogeneous and consistent drivers. Catchpole & Plank (1986) and Madanat, Cassidy & Wang (1994) have analyzed the operation of unsignalized intersections for heterogeneous and inconsistent drivers; thus relaxing assumptions 1 and 2. Troutbeck has relaxed assumption 8 and studied gap acceptance under "limited priority merge" (Bunker & Troutbeck 1994*a*, Bunker & Troutbeck 1994*b*, Troutbeck 1995, Troutbeck 1997*b*, Troutbeck & Kako 1999, Troutbeck 1999).

Tanner (1967) was the first to relax assumption 5. He estimated minor-stream capacity assuming two or more independent priority streams with different flow rates. See also Troutbeck (1986). Gazis, Newell, Warren & Weiss (1967), Fisk (1989) and Hagring (1998*b*) have extended the model to include the case where different lanes (priority streams) have different critical gaps (assumption 3).—Only streams without mutual conflicts can be considered independent. When priority streams are from more than one rank, special analysis methods are required.

The effect of nonpriority vehicles, such as major-road right turners, can be taken into a model by adding a proportion of this stream to a priority stream.

In advanced methodologies many of these assumptions have been relaxed, but in the core of these methods is usually a potential capacity or delay formula with most of these assumptions. Some adjustments are then presented to make the method more general.

The nature of a problem becomes often clearer when it is compared with other, but similar problems. In a mathematical sense the following traffic engineering problems have many similarities with the unsignalized intersection case:[7]

Pedestrians crossing a road also face a gap acceptance problem. Haight (1963) refers to the items delayed as vehicles or pedestrians "according as they do or do not form queues". Early studies of the pedestrian-crossing problem have been presented by Adams (1936), Tanner (1951), and Mayne (1954). Cowan (1984) has generalized Adams' result for the M3 headway distribution. See also section 4.2.3.

If all waiting pedestrians can cross the road when a headway larger than the critical gap starts, the follow-up time is zero. This makes the analysis simpler. However, if all waiting pedestrians can cross the road during a headway larger than the critical gap, the capacity of a pedestrian crossing is either infinite or zero. Such a model makes more sense in delay studies than in capacity studies.—Detailed information of pedestrian gap acceptance and vehicle headway distributions can also be used to evaluate the accident risk of pedestrians (Cohen, Dearnaley & Hansel 1955, Song, Dunne & Black 1993, Pasanen 1991).

Tanner (1951) remarked the similarity between the pedestrian crossing problem and the operation of vehicle-actuated *traffic signals*, as described by Garwood (1940). Beckmann et al. (1956) presented the operation of a stop-controlled intersection in terms of red (block) and green (antiblock) interval sequences generated by the priority stream gaps. A minor stream has "green" when conflicting major streams have no "green demand". The generation and extension of blocks (Fig. 2.11) is mathematically very similar to the operation of vehicle detectors (Fig. 2.12). In the theory of stochastic processes this type of operation is known as a Type II counter (Parzen 1962). Akçelik (1994*a*) has described a traffic-signal analogy in modeling gap-acceptance at unsignalized intersections.

[7] It is also worth mentioning that queuing theory was first developed in the context of telephone traffic (Erlang 1909, Erlang 1917*a*, Erlang 1917*b*).

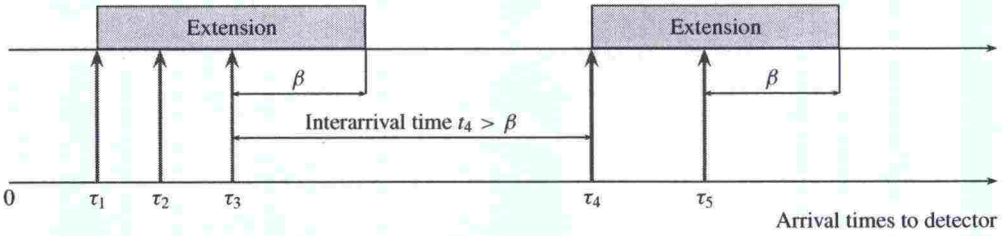

Figure 2.12: Extension principle of vehicle detectors

Another model similar to the unsignalized intersection is the operation of *merging zones* (see Haight, Bisbee & Wojcik 1962, Haight 1963, Drew 1967). Unlike the minor road drivers at unsignalized intersections, merging drivers can change the gap acceptance criterion by changing their speeds, and they have a limited opportunity to determine the location of the merge. In more advanced models the effect of turbulence on priority streams should be considered (Transportation Research Board 2000).

Passing on two-lane highways is a gap-acceptance process, where a passing vehicle moves in the opposite direction to the "priority stream". Drivers can determine the time and location of passing considering gap availability and sight restrictions. The order in which vehicles pass each others is not fixed, and several vehicles on a road segment may pass simultaneously. Consequently, this problem is usually described at a macroscopic level. Tanner (1953) presented an early description of the problem stating also the similarities with unsignalized intersection and pedestrian crossing problems. For an overview of these models see McLean (1989) and Luttinen (2001). Miller & Pretty (1968) have discussed the gap-acceptance of inconsistent drivers.

2.5 Fluid-analogy model

The number of customers in a system at time τ is the initial number of customers in system plus the difference between arrivals and departures: $N(\tau) = N(0) + A(\tau) - D(\tau)$. When $A(\tau)$, or $D(\tau)$, is large, the law of large numbers indicates that with probability one

$$\lim_{\tau\to\infty} \frac{A(\tau) - \mathbb{E}[A(\tau)]}{\mathbb{E}[A(\tau)]} = 0. \tag{2.45}$$

This suggests that the arrival and departure processes can be approximated by their time-related average values:

$$\mathbb{E}[N(\tau)] = \mathbb{E}[N(0)] + \mathbb{E}[A(\tau)] - \mathbb{E}[D(\tau)]\,. \tag{2.46}$$

In a fluid-analogy model a discontinuous stochastic process is replaced by a continuous deterministic process (see Kleinrock 1976, Newell 1982, Wolff 1989).

A *fluid-analogy model* is useful especially in capacity estimation and in the estimation of delays at oversaturated conditions. Once a queue has grown so large that its vanishing probability is negligible, a fluid approximation will give a reliable estimate of the future growth of the expected queue (Newell 1971).

According to the central limit theorem the change in queue length approaches normal distribution. This suggests a *diffusion approximation* (Glynn 1990, Newell 1982) for cases where the stochastic process becomes mathematically intractable or too complicated and the random variation cannot be ignored. The delay estimation methods of unsignalized intersections use both stochastic and fluid-analogy approaches. The dif-

fusion approach has found some applications in the analysis of signalized intersections (e.g. Newell 1965), but little or none in the analysis of unsignalized intersections.

The basic characteristics of a fluid-analogy model and its use in capacity estimation will be discussed next. A fluid analogy model for the analysis of oversaturated conditions will be presented in section 4.4.2.

Let us assume that vehicles arrive at an intersection at arrival rate $q(t)$. The cumulative number of arrivals is

$$A(\tau) = \int_0^\tau q(u)\,\mathrm{d}u. \tag{2.47}$$

If the arrival rate is constant, the cumulative arrival curve is linear: $A(\tau) = q\tau$ (Fig. 2.13). Cumulative demand is the number of arrivals plus the initial queue[8] at the beginning of the observation period (Gazis & Potts 1965):

$$A'(\tau) = L(0) + A(\tau). \tag{2.48}$$

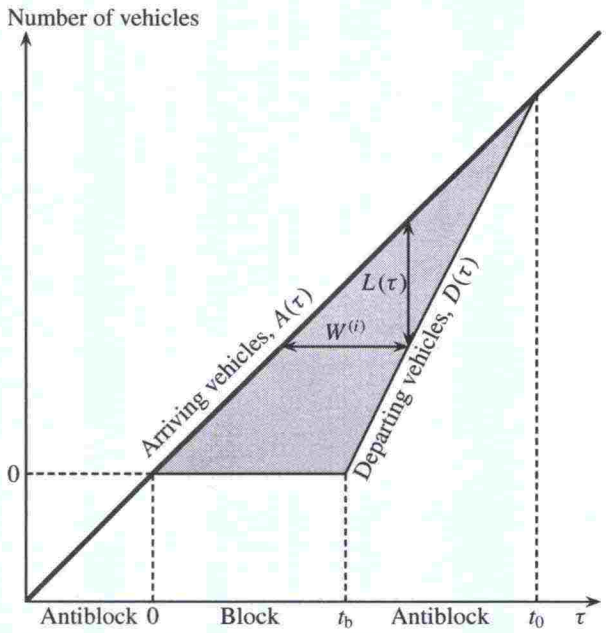

Figure 2.13: Fluid analogy model for a minor stream

The cumulative number of departures is

$$D(\tau) = \int_0^\tau d(u)\,\mathrm{d}u, \tag{2.49}$$

where $d(\tau)$ is the departure rate. During a block of length t_b no vehicles depart the intersection; that is

$$\begin{aligned} d(\tau) &= 0, \qquad 0 < \tau \leq t_b \\ D(\tau) &= 0, \qquad 0 < \tau \leq t_b. \end{aligned} \tag{2.50}$$

[8]Fluid analogy models do not consider individual vehicles. So, no distinction can be made between vehicles in queue an vehicles in service.

When an antiblock starts at $\tau = t_b$, the queue starts to discharge at saturation flow rate $s = t_f^{-1}$:

$$\begin{aligned} d(\tau) &= s, && t_b < \tau \leq t_0 \\ D(\tau) &= \int_{t_b}^{\tau} s \, du = s(\tau - t_b), && t_b < \tau \leq t_0, \end{aligned} \tag{2.51}$$

where t_0 is the time when the queue has discharged. After t_0 the discharge rate is equal to the arrival rate:

$$\begin{aligned} d(\tau) &= q(\tau), && t_0 < \tau \leq c \\ D(\tau) &= A(\tau), && t_0 < \tau \leq c, \end{aligned} \tag{2.52}$$

assuming that $t_0 < c$ and $q(\tau) \leq s$, and the cycle time c is the sum of the block (t_b) and antiblock (t_a) periods.

The length of a queue (in vehicles) is the initial queue $L(0)$ at $\tau = 0$ plus the difference between cumulative arrivals and departures. Graphically it is the vertical difference between cumulative arrival and departure curves. The queue has discharged at time t_0, when the number of arrivals is equal to the number of departures (Newell 1965)

$$L(t_0) = L(0) + A(t_0) - D(t_0) = L(0) + qt_0 - s(t_0 - t_b) = 0. \tag{2.53}$$

During a differential time interval $(t, t + dt]$ the delay experienced is $L(t)\,dt$. The cumulative delay during the cycle length c is equal to the area of the triangle in Figure 2.13 and can be obtained by a method analogous to the uniform delay in traffic signal control (Newell 1965)

$$\begin{aligned} W(t_c) &= \int_0^c L(u)\,du = \int_0^{t_0} qu\,du - \int_{t_b}^{t_0} s(u - t_b)\,du \\ &= \frac{qst_b^2}{2(s-q)} = \frac{t_b^2}{2\left(\frac{1}{q} - \frac{1}{s}\right)}, \qquad q \leq \frac{st_a}{c}. \end{aligned} \tag{2.54}$$

The average delay per vehicle can be obtained by dividing the cumulative delay by the number of arriving (and departing) vehicles during an average cycle (Newell 1965):

$$W = \frac{\int_0^{t_c} L(u)\,du}{\int_0^{t_c} q(u)\,du} = \frac{W(t_c)}{qt_c} = \frac{t_b^2}{2t_c\left(1 - \frac{q}{s}\right)}, \qquad q \leq \frac{st_a}{t_c}. \tag{2.55}$$

The horizontal distance between the arrival and departure curves gives the waiting time of a "vehicle".

Capacity is reached when the number of arrivals during an average cycle (sum of the average block length t_b and the average antiblock length t_a) is equal to the number of vehicles discharging during an average antiblock t_b:

$$\begin{aligned} C_p c &= \frac{t_a}{t_f} \\ C_p &= \frac{t_a}{t_f c}, \end{aligned} \tag{2.56}$$

where the proportion of average antiblock (t_a) from the average cycle time (c) is the probability of a lag larger than or equal to a minimum acceptable lag t_o. Accordingly, the potential capacity is

$$C_p = \frac{R_\Upsilon(t_o)}{t_f} = sR_\Upsilon(t_o), \tag{2.57}$$

where $s = t_f^{-1}$ is the saturation flow rate. If Figure 2.13 describes average conditions, capacity is reached when the time (t_0) required for queue build-up and discharge is equal to the cycle time. When $q \leq C_p$, the deterministic system is in equilibrium. A more detailed discussion on capacity will be presented next.

3 CAPACITY AT UNSIGNALIZED INTERSECTIONS

3.1 Definition of capacity

According to HCM2000 (Transportation Research Board 2000) capacity is

> the maximum sustainable flow rate at which vehicles or persons reasonably can be expected to traverse a point or uniform segment of a lane or roadway during a specified time period under given roadway, geometric, traffic, environmental, and control conditions; usually expressed as vehicles per hour, passenger per hour, or persons per hour.

Thus, capacity has three basic elements:

1. Capacity is a location specific measure.
2. Capacity is a maximum flow rate.
3. Capacity describes steady-state conditions.

According to gap acceptance theory the capacity of a minor stream (k) is limited by its saturation flow rate ($s_k = t_{f,k}^{-1}$) and the availability of antiblocks at conflict areas. A movement may have several conflict areas. It is, however, assumed that a vehicle waits at a stop line or yield line until an antiblock is available at all conflict areas. If a median supplies storage spaces for vehicles, so that a movement can be performed in two stages, capacity of that movement is measured at the median stop or yield line considering the bottleneck effect of first stage gap acceptance and the limited number of storage spaces in the median. Accordingly, the capacity at an unsignalized intersection is defined as the *stop-line capacity*.

Besides interactions between a minor stream and higher priority movements capacity can be limited by interactions between movements in the same approach. When a lane is shared by several movements and/or one movement occupies several lanes, it is most informative to use as a unit of analysis the group of lanes which are occupied by the interacting traffic streams in the approach. From this analysis it is also possible to obtain lane-specific performance measures.

Roundabouts may have additional bottlenecks (see Hagring 1998*b*): *i*) In narrow weaving areas heavy vehicles may have operational difficulties or they may prevent the simultaneous use of an adjacent lane. *ii*) Pedestrians may limit the capacity of exiting vehicles.

The maximum flow rate is attained, when there is a continuous queue of subject movement vehicles arriving to the intersection. Because of possible downstream bottlenecks due to short lanes or two-stage gap acceptance there may be periods of empty queues at some lanes of a lane group.

Capacity is estimated for one minor stream or a group of movements in one approach. The flow rates of higher priority streams are given, and the minor stream capacity is estimated under these higher priority flow rates. A capacity of an entire intersection is not defined, unless it is defined as the sum of arrival flow rates, which gives D/C ratio $\rho_i = 1$ at the most saturated lane group (see OECD Road Research Group 1974). This requires that the proportions of arrival flow rates for each movement can be estimated under the conditions when capacity is reached (Nordqvist et al. 1973).

At roundabouts the circulating flow is generated by merging processes at each entry point. Thus, the flow rate at subject approach has an effect on merging processes and capacities at other approaches, and eventually on the major flow of the subject approach itself (see Akçelik 1998). The procedures below assume that the properties of major flow do not depend on the flow rate in the subject approach. The capacity of an approach is estimated assuming that all other traffic flows and driver behaviour attributes remain the same. This assumption gives capacity estimates suitable for the estimation of degrees of saturation, and eventually of delays and queues under prevailing conditions (Troutbeck 1997*b*).

Capacity is the reasonably *expected* maximum *sustainable* flow rate under *given conditions*. Capacity does not describe maximum observed flow rate during some short period of time. It describes the average (expected) maximum flow rate that can be sustained over long time periods under given conditions. Mathematically the capacity of a minor stream k can be defined as (Plank & Catchpole 1984, Catchpole & Plank 1986, Wegmann 1991)

$$C_k = \lim_{\tau \to \infty} \frac{\mathbb{E}[D_k(\tau)]}{\tau}, \tag{3.1}$$

where $D_k(\tau)$ is the number of stream k vehicles crossing a stop line during time interval $(0, \tau]$ assuming a continuous queue. When the process has been going on for a long time, the system has reached a *steady state* and the effect of initial state can be neglected. During the analysis period $(0, \tau]$ traffic and roadway conditions are assumed to stay unchanged.

The expected number of departures during a long time interval $(0, \tau]$ is[1]

$$\mathbb{E}[D_k(\tau)] = \mathbb{E}[A_M(\tau)]\,\mathbb{E}[\alpha]\,, \tag{3.2}$$

where $A_M(\tau)$ is the number of major stream vehicles (gaps) during time interval $(0, \tau]$ and $\mathbb{E}[\alpha]$ is the expected number of stream k departures during a randomly selected major stream headway. Capacity can now be expressed as (Plank & Catchpole 1984)

$$C_k = \lim_{\tau \to \infty} \frac{\mathbb{E}[A_M(\tau)]}{\tau}\,\mathbb{E}[\alpha] = q_M\,\mathbb{E}[\alpha]\,, \tag{3.3}$$

where q_M is the major stream flow rate.

Because in real world traffic conditions change frequently, analysis must be based on short time intervals, which may not be in a steady state. In HCM2000 (Transportation Research Board 2000) the analysis interval is 15 minutes. This is a compromise between considerations on short term fluctuations and stability of macroscopic traffic flow measures. Shorter time interval would allow better adjustment for short traffic fluctuations. The generalization of the results to stable flow conditions would, however, be problematic. Longer interval length would describe stable conditions better, but nonstationarity of traffic flow within the time interval could cause bias to the results. When steady state analyses are applied to finite time intervals, the performance of the facility during these periods will have considerable stochastic variation around the estimated performance

[1] Let the length of a time period be the sum of n headways ($\tau = t_1 + t_2 + \cdots + t_n$) and let the expected number of minor stream departures during a randomly selected major stream headway t_i be $\mathbb{E}\big[D_k(t_i)\big] = \mathbb{E}[\alpha]$. The expected number of departures during a time interval $(0, \tau]$ is $\mathbb{E}\big[D_k(\tau)\big] = \sum \mathbb{E}\big[D_k(t_i)\big] = n\,\mathbb{E}[\alpha]$. For a long time interval $\lim_{\tau \to \infty} \mathbb{E}[N(\tau)] = \tau / \mathbb{E}[t] = n$.

measures. Also a bias due to initial conditions, such as long or short initial queues[2] on major streams, cannot be excluded.

Following HCM2000 two further capacity concepts are defined:

Potential capacity (C_p) is the capacity of a specific movement at an unsignalized intersection approach, assuming that it is unimpeded by other movements and has exclusive use of a separate lane or lanes.

Movement capacity (C_m) is the capacity of a specific movement at an unsignalized intersection approach, assuming that the traffic has exclusive use of a separate lane or lanes.

Capacity estimation proceeds in four stages:

1. Critical gaps and follow-up times are estimated under prevailing conditions.
2. Potential capacity is estimated for each movement assuming that they have exclusive use of separate lanes and there is no queuing in higher priority streams.
3. Movement capacity is estimated taking into account the impedance effects of higher priority queues.
4. Capacity of the movements on a lane group is estimated considering also the effects of shared and short lanes.

Stages 2–4 are described below. Stage 1 is described in chapter 7.

For an overview of unsignalized intersection and roundabout capacity analysis theory and methods the reader is referred to Brown (1995), Kyte et al. (1996), Transportation Research Board (1997), Troutbeck & Brilon (1997), and Louah (1986). The discussion below follows the report of Luttinen (2003).

3.2 Potential capacity under one priority stream

3.2.1 Definition of potential capacity

The theoretical foundation for capacity analysis of unsignalized intersections was laid in the 1960's especially by Tanner (1962), Major & Buckley (1962), and Harders (1968). Consequently, the first edition of HCM (Bureau of Public Roads 1950) did not discuss unsignalized intersections. Even the second edition (Highway Research Board 1965) did not present any analysis methodology for unsignalized intersections. Two tables were presented as examples of capacities of "four-way stop intersections". By the time of the third edition (Transportation Research Board 1985) theoretical models and empirical field data were at such a level that enabled the presentation of specific analysis procedures. The HCM methodology was adopted from German guidelines (FGS 1972), which were based on the research by Harders (1968). See Baass (1987), Brilon (1988*a*), and Kyte et al. (1991).

Capacity is the expected hourly rate at which vehicles can enter an intersection under prevailing conditions. Capacity is estimated for streams of ranks lower than 1. The

[2]Steady state capacity estimates should be adjusted for finite analysis periods with *longer* or *shorter* than expected initial major stream queues; i.e., expected queues under equilibrium conditions. Longer (shorter) initial queues indicate impedance effects higher (lower) than under steady state conditions. If all initial major stream queues are considered as excess flows, minor stream capacity will be underestimated.

methods described below cannot be applied to uncontrolled intersections or Rank 1 flows. The German manual (FGSV 2001) suggests 1,800 pc/h as a maximum flow rate for Rank 1 through streams. At uncontrolled intersections the manual estimates the maximum number of vehicles entering the intersection from all four approaches to be in the range 600–800 pc/h. In the Norwegian guidelines (Statens Vegvesen 1985) the capacity estimates for uncontrolled intersections are much higher (Table 3.1).

Table 3.1: Capacity (veh/h) of uncontrolled intersections in the Norwegian guidelines (Statens Vegvesen 1985) as a function of minimum and maximum flow rates in the intersection approaches

Percent left turns	q_{min}/q_{max} 1.0	0.8	0.6	0.4	0.2	0.0
0	1,700	1,650	1,600	1,600	1,650	2,000
< 10	1,600	1,550	1,550	1,500	1,500	1,750
< 20	1,500	1,500	1,500	1,450	1,450	1,600

This section describes the basic theoretical formulas used to estimate the *potential capacity* of unsignalized intersections. Only a simple crossing operation, as in Figure 2.1, or a simple merge operation, as in a roundabout entry (Fig. 2.4), is discussed. It is assumed that merging operations between the legs of a roundabout can be ignored. The road and traffic conditions are assumed optimal. Unless stated otherwise, the models follow the assumptions presented above (page 46).

Potential capacity describes the capacity of a minor stream under ideal conditions assuming that it is unimpeded by other movements and has exclusive use of a separate lane (Transportation Research Board 2000). When the impedance effects (queuing in higher priority streams) are considered, HCM2000 calls the capacity estimate a *movement capacity*. Because Rank 2 vehicles do not face any impedance effects due to queuing at higher priority streams, the movement capacity of a Rank 2 stream is equal to the potential capacity:

$$\boxed{C_{m,k} = C_{p,k}, \qquad k \in \{1, 4, 9, 12\}.} \tag{3.4}$$

It is assumed that there is a continuous queue of minor stream vehicles (stream 11 in Fig. 2.1) waiting to enter the intersection. The expected number of vehicles departing from a queue during a headway t is given by a *gap acceptance function*

$$\alpha(t) = \sum_{i=1}^{\infty} i p_i(t) \tag{3.5}$$

where $p_i(t)$ is the probability of i departures during headway t.

The expected number of departing vehicles during a randomly selected headway is obtained by integration

$$\mathbb{E}[\alpha] = \int_0^{\infty} \alpha(t) f(t)\, \mathrm{d}t, \tag{3.6}$$

where $f(t)$ is the probability density function of major stream headways. Potential capacity is obtained by multiplying $\mathbb{E}[\alpha]$ by the number (q_M) of major stream headways per time unit (Siegloch 1973)

$$C_p = q_M\, \mathbb{E}[\alpha] = q_M \int_0^{\infty} \alpha(t) f(t)\, \mathrm{d}t. \tag{3.7}$$

Accordingly, capacity is expressed in terms of traffic flow rate, gap-acceptance function $\alpha(t)$, and the headway distribution.

3.2.2 Stepwise gap acceptance function

A minor stream vehicle enters the intersection, if there is a headway or lag larger or equal to the critical gap t_c in the priority stream 2. Critical lag is assumed to be equal to the critical gap. Vehicles entering the intersection during the same priority stream headway have discharge headways equal to the follow-up time t_f.

During a headway of $0 < t < t_c$ no vehicles can enter the intersection. One vehicle can enter during a headway of $t_c \leq t < t_c + t_f$. Two vehicles can enter during a headway $t_c + t_f \leq t < t_c + 2t_f$. Accordingly

$$p_i(t) = \begin{cases} 1, & \text{if } t_c + (i-1)t_f \leq t < t_c + it_f \\ 0, & \text{otherwise.} \end{cases} \tag{3.8}$$

Gap acceptance function is a step function

$$\alpha(t) = \left\lfloor \frac{t - t_c + t_f}{t_f} \right\rfloor_+ = \begin{cases} 0, & \text{if } t < t_c \\ \left\lfloor \frac{t-t_c+t_f}{t_f} \right\rfloor, & \text{if } t \geq t_c, \end{cases} \tag{3.9}$$

where $\lfloor X \rfloor$ is the floor function; i.e., greatest integer not larger than X (Spanier & Oldham 1987).

The probability of i arrivals during a randomly selected headway is the probability that the headway has an appropriate length:

$$\begin{aligned} \mathbb{P}\{\alpha = i\} &= \mathbb{P}\{t_c + (i-1)t_f \leq t < t_c + it_f\} \\ &= \int_{t_c+(i-1)t_f}^{t_c+it_f} f(u)\,\mathrm{d}u \\ &= F(t_c + it_f) - F(t_c + (i-1)t_f) \\ &= R(t_c + (i-1)t_f) - R(t_c + it_f)\,, \end{aligned} \tag{3.10}$$

where $f(t)$ is the probability density function, $F(t)$ is the cumulative distribution function, and $R(t) = 1 - F(t)$ is the survivor function of the major road headway distribution.

Capacity (maximum number of entering vehicles per time unit) is obtained by multiplying the expected number of minor road vehicles entering during a major road headway by the expected number of major road headways (vehicles) per time unit:

$$\begin{aligned} C_p &= q_M \sum_{i=0}^{\infty} i\, \mathbb{P}\{t_c + (i-1)t_f \leq t < t_c + it_f\} \\ &= q_M \sum_{i=0}^{\infty} i \int_{t_c+(i-1)t_f}^{t_c+it_f} f(u)\,\mathrm{d}u \\ &= q_M \sum_{i=0}^{\infty} i\, [R(t_c + (i-1)t_f) - R(t_c + it_f)] \\ &= q_M \sum_{i=0}^{\infty} R(t_c + it_f) \qquad \text{(veh/h).} \end{aligned} \tag{3.11}$$

Capacity is high, if the frequency of large headways is high. Consequently, capacity increases as the coefficient of variation of priority stream headways increases (Luttinen 1990). If priority stream flow rate is zero, the minor road queue discharges at headways t_f, and the capacity is t_f^{-1} veh/s or $3600 t_f^{-1}$ veh/h.

If major stream headways follow the *negative exponential distribution*, the minor stream capacity is (Major & Buckley 1962, Drew 1968, Harders 1968)[3]

$$\begin{aligned} C_{\mathrm{p}} &= q_{\mathrm{M}} \sum_{i=0}^{\infty} R(t_{\mathrm{c}} + i t_{\mathrm{f}}) \\ &= q_{\mathrm{M}} \sum_{i=0}^{\infty} \mathrm{e}^{-\lambda(t_{\mathrm{c}} + i t_{\mathrm{f}})} \\ &= q_{\mathrm{M}} \mathrm{e}^{-\lambda t_{\mathrm{c}}} \sum_{i=0}^{\infty} \mathrm{e}^{-i\lambda t_{\mathrm{f}}} \\ &= \frac{q_{\mathrm{M}} \mathrm{e}^{-\lambda t_{\mathrm{c}}}}{1 - \mathrm{e}^{-\lambda t_{\mathrm{f}}}} \\ &= \boxed{\frac{q_{\mathrm{M}} \mathrm{e}^{-q_{\mathrm{M}} t_{\mathrm{c}}/3600}}{1 - \mathrm{e}^{-q_{\mathrm{M}} t_{\mathrm{f}}/3600}},} \qquad 0 \le t_{\mathrm{f}} \le t_{\mathrm{c}}. \end{aligned} \tag{3.12}$$

See Figure 3.1. The result was obtained using the convergence property of a geometric series; i.e.,

$$\sum_{i=0}^{\infty} a^i = \frac{1}{1-a}, \qquad a < 1. \tag{3.13}$$

If follow-up time is zero, the entire queue can discharge simultaneously, and the capacity is infinite. This is the capacity of a simple pedestrian crossing model.

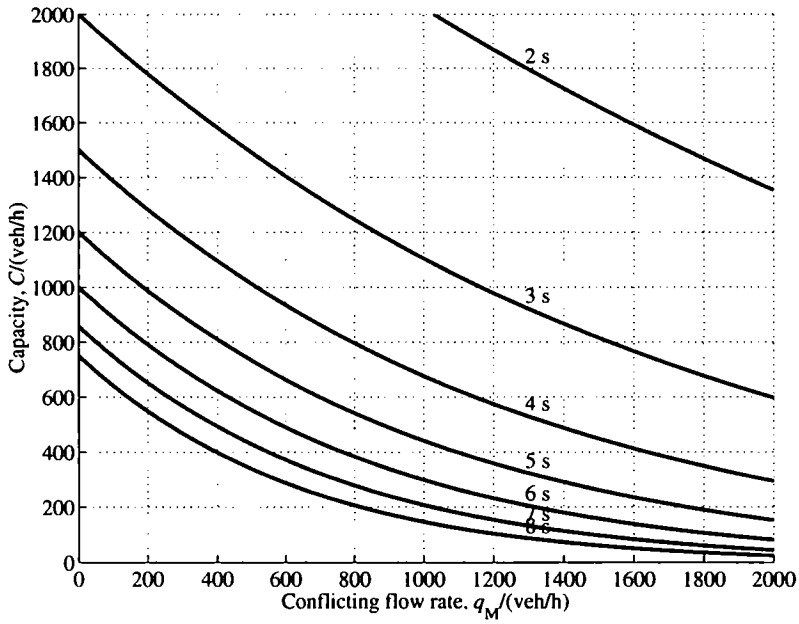

Figure 3.1: Minor-stream potential capacity with different critical gaps, $t_{\mathrm{f}} = 0.6 t_{\mathrm{c}}$, and major-stream headways following the negative exponential distribution

Equation (3.12) is used in HCM 1985 (Transportation Research Board 1985, Baass 1987), HCM2000 (Transportation Research Board 2000), DanKap (Vejdirektoratet

[3]According to Major & Buckley (1962) this equation was first obtained by Fisher (1960). However, the equation was presented already by Nordqvist (1958). For a different kind of proof see Heidemann (1991).

1999*b*) and in the Norwegian guidelines (Statens Vegvesen 1985, Aakre 1998). Capcal 2 uses this equation for minor through and left turn movements, and when the priority streams occupy at least four lanes (SNRA 1995*b*, Hagring 1997).

This approach can be used to generalize the potential capacity equation for headway distributions having an *exponential tail*; i.e., the distribution of headways larger than t_c is exponential. Because exponential distribution has independent increments, that is $R(a+b) = R(a)\,R(b)$, equation (3.11) can be expressed as

$$\begin{aligned} C_p &= q_M \sum_{i=0}^{\infty} R(t_c + i t_f) \\ &= q_M R(t_c) \sum_{i=0}^{\infty} e^{-i\xi t_f} \\ &= \boxed{\frac{q_M R(t_c)}{1 - e^{-\xi t_f}},} \end{aligned} \tag{3.14}$$

where ξ is the scale parameter of the exponential tail distribution. The expected number of departing vehicles during a randomly selected headway, $\mathbb{E}[\alpha]$, is the expected number of departures (α) during a headway larger than the critical gap multiplied by the probability of a headway larger than the critical gap. Accordingly, equation (3.14) gives capacity as

$$\boxed{C_p = q_M\,\mathbb{E}[\alpha] = q_M\,\mathbb{E}[\,\alpha \mid T \geq t_c\,]\,\mathbb{P}\{T \geq t_c\}\,.} \tag{3.15}$$

This expression is valid for any headway distribution. When headways $T \geq t_c$ are exponentially distributed,

$$\mathbb{E}[\,\alpha \mid T \geq t_c\,] = \frac{1}{1 - e^{-\xi t_f}} \tag{3.16}$$

is obtained as the expectation (2.9) of a geometric distribution. For an approach to derive capacity as the inverse of average service time for queuing vehicles see section 4.2.2.

For priority stream headways following the *shifted exponential distribution* the minor stream potential capacity can be obtained as (Gipps 1982, Luttinen 1990)

$$\begin{aligned} C_p &= q_M \sum_{i=0}^{\infty} R(t_c + i t_f) \\ &= q_M \sum_{i=0}^{\infty} e^{-\theta(t_c + i t_f - t_p)} \\ &= q_M e^{-\theta(t_c - t_p)} \sum_{i=0}^{\infty} e^{-i\theta t_f} \\ &= \frac{q_M e^{-\theta(t_c - t_p)}}{1 - e^{-\theta t_f}}, \qquad 0 \leq t_p \leq t_c,\, 0 \leq t_f \leq t_c. \end{aligned} \tag{3.17}$$

If $t_p = 0$, the equation gives the potential capacity for exponential headways (3.12). When substitution (2.21) for θ is made, capacity can be expressed as

$$\boxed{C_p = \frac{q_M \exp\left(\frac{-q_M(t_c - t_p)}{3600 - q_M t_p}\right)}{1 - \exp\left(\frac{-q_M t_f}{3600 - q_M t_p}\right)}} \quad \text{(veh/h)}. \tag{3.18}$$

As Figure 3.2 displays, the minor-stream potential capacity decreases as the major stream minimum headway (t_p) increases and variance decreases (see Luttinen 1990, Luttinen 1996). The loss in capacity is largest at high major stream flow rates.

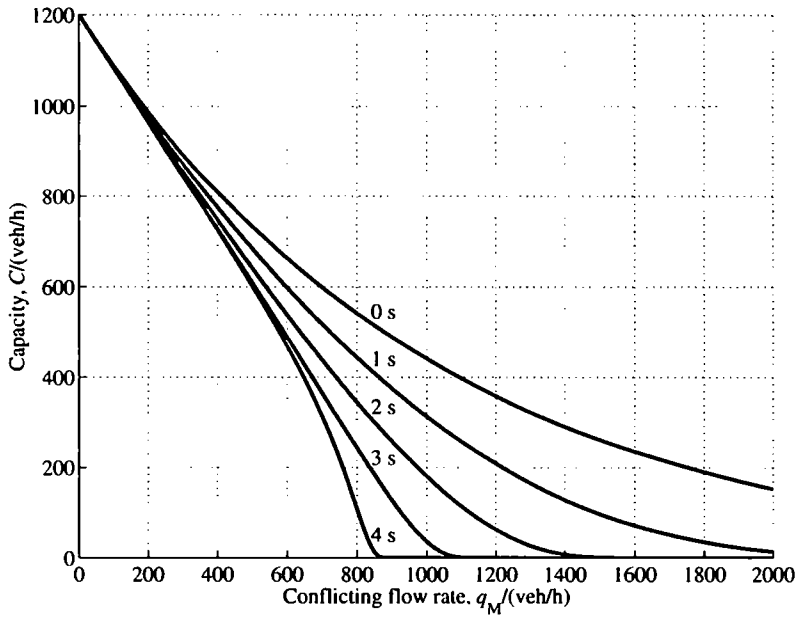

Figure 3.2: Minor stream potential capacity when critical gap is 5 s, follow-up time 3 s, and major stream headways follow shifted exponential distribution with minimum headway (location parameter) ranging from zero to four seconds

The survivor function (2.29) of *Cowan's M3 distribution* differs from the shifted exponential survivor function (2.18) by the factor ϕ. Thus, the potential capacity is (Plank 1982):

$$\begin{aligned} C_p &= q_M \sum_{i=0}^{\infty} R(t_c + i t_f) \\ &= q_M \phi \sum_{i=0}^{\infty} e^{-\gamma(t_c + i t_f - t_p)} \\ &= \boxed{\frac{q_M \phi e^{-\gamma(t_c - t_p)}}{1 - e^{-\gamma t_f}}}, \qquad 0 \le t_p \le t_c, 0 \le t_f \le t_c, 0 \le \phi \le 1. \end{aligned} \tag{3.19}$$

It can be interpreted as minor stream capacity across a stream, where the proportion ϕ of headways are available for gap acceptance and these headways follow the shifted exponential distribution. This is a special case of the capacity equation of Tanner (1967). If $\phi = 1$, we get the capacity for shifted exponential headways (3.17). For exponential headways (3.12) we set $\phi = 1$ and $t_p = 0$.

In the Australian roundabout capacity guideline (Austroads 1993) parameter γ has been defined by the method of moments (2.31) as

$$\gamma = \frac{\phi q_M}{3600 - q_M t_p}, \tag{3.20}$$

where $q_M = q_c$ is the circulating flow rate at the entry. The proportion of free headways is lower than predicted by Tanner's M/D/1 model (Akçelik & Troutbeck 1991):

$$\phi = 0.75(1 - \lambda t_p) = 0.75\left(1 - \frac{q_M t_p}{3600}\right). \tag{3.21}$$

See also Troutbeck (1993) and Troutbeck & Kako (1997).

Troutbeck & Kako (1997) have modified capacity equation (3.19) for "limited priority merge". It describes the reduced capacity due to major stream vehicles slowing down in order to allow enough space for a merging minor-stream vehicle. The delay of a major-stream vehicle reduces the next gap. On the other hand, shorter critical gaps (t_c) during limited priority operation increase capacity.

Some major-stream vehicles have to slow down, if critical gap t_c is less than $t_f + t_p$. These vehicles have to delay their entry in order to keep the headway to a merged vehicle at t_p (see Figure 2.11 and related discussion above). The capacity of limited priority merge is

$$C_L = \frac{q_M f_L \phi e^{-\gamma(t_c - t_p)}}{1 - e^{-\gamma t_f}}, \qquad t_p < t_c < t_f + t_p, \tag{3.22}$$

where

$$f_L = \frac{1 - e^{-\gamma t_f}}{1 - e^{-\gamma(t_c - t_p)} - \gamma\left(t_c - t_p - t_f\right) e^{-\gamma(t_c - t_p)}} \tag{3.23}$$

is the adjustment factor for limited priority merge (Fig. 3.3). Parameter γ is estimated as in equation (3.20). If $t_c > t_f + t_p$, major stream vehicles have absolute priority and f_L should be set to 1. See also Bunker & Troutbeck (1994*a*), Bunker & Troutbeck (1994*b*), Troutbeck (1995), Troutbeck (1997*b*), and Troutbeck & Kako (1999).

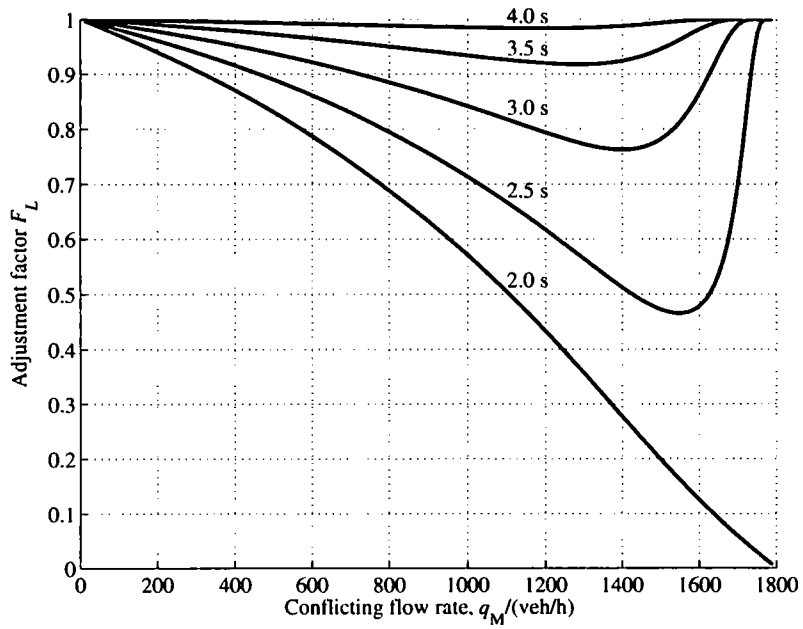

Figure 3.3: Adjustment factor f_L with $t_f = 2.5\,s$, $\phi = 0.8$, and $t_p = 2\,s$ (Troutbeck 1995)

If the traffic flow is considered as departures from an M/D/1 queuing system, substitutions (2.42) and (2.43) are made, and we obtain the capacity formula presented by

Tanner (1962)

$$C_p = \frac{q_M (1 - \lambda t_p) e^{-\lambda(t_c - t_p)}}{1 - e^{-\lambda t_f}}, \tag{3.24}$$

where $\lambda = q_M/3600$ veh/s.[4] If the minimum headway condition is removed ($t_p = 0$), equation 3.24 is equivalent to the capacity equation (3.12) for exponential headways.

Tanner's formula has been used in numerous manuals (e.g. Road Research Laboratory 1965, Hobbs 1974, Austroads 1988). Capcal 2 uses this model for major road left turns and minor road right turns when the major flow occupies one lane only (SNRA 1995*b*, Hagring 1997).

Figure 3.4 displays minor stream capacity according to Tanner (1962) with different critical gaps and $t_f = 0.6t_c$. The follower headway in a platoon is $t_p = 1.8$ s, as in Capcal 2 (SNRA 1995*b*, Hagring 1997). The platooning model decreases the frequency of large headways at high flow rates more steeply than the exponential headway model (Fig. 3.1). When all vehicles travel in platoons, $q_M = 3600/1.8 = 2000$ veh/h, and there is no capacity left to a minor stream.

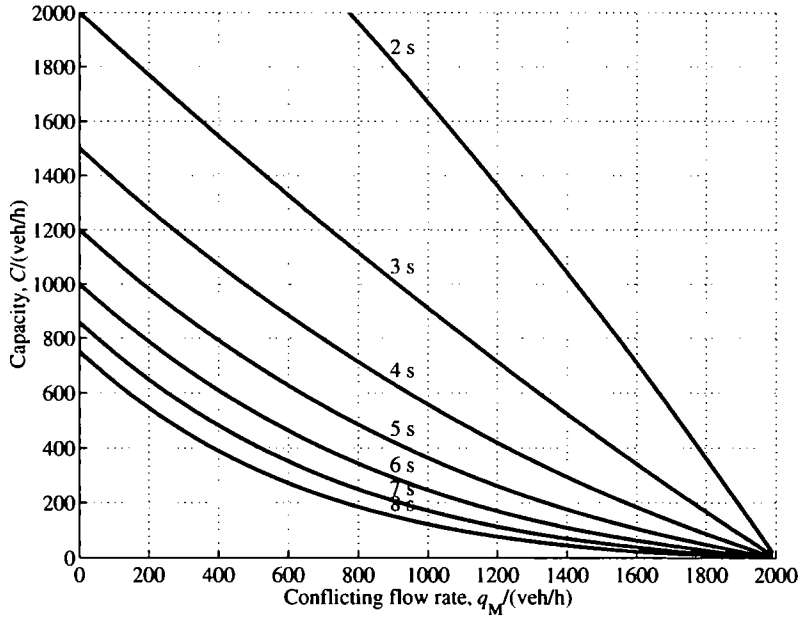

Figure 3.4: Capacity according to Tanner with different critical gaps, $t_f = 0.6t_c$, and platoon headways $t_p = 1.8s$

Figure 3.5 shows the effect of major stream bunching on minor stream capacity. As bunching increases (ϕ decreases) the proportion of short intra-bunch headways increases, and so does also the average length of free headways. This improves capacity. If $\phi = 1.0$, there is no bunching, and the major stream headways follow the shifted exponential distribution. Shifted exponential distribution has a lower coefficient of variance than the negative exponential distribution and gives lower capacity for minor stream vehicles. This is, however, just a feature of the M3 model, and it cannot be taken as an evidence of capacity reduction at low platoon percentages. By more extensive

[4]Tanner obtained the equation as a limiting case when delay approached infinity. Brennan & Fitzgerald (1979) presented a direct derivation of the capacity equation (3.24).

comparisons Siegloch (1973) concluded that slight disturbances (bunching) reduce capacity, medium disturbances increase capacity slightly, and severe disturbances increase capacity significantly (Brilon 1988*a*).

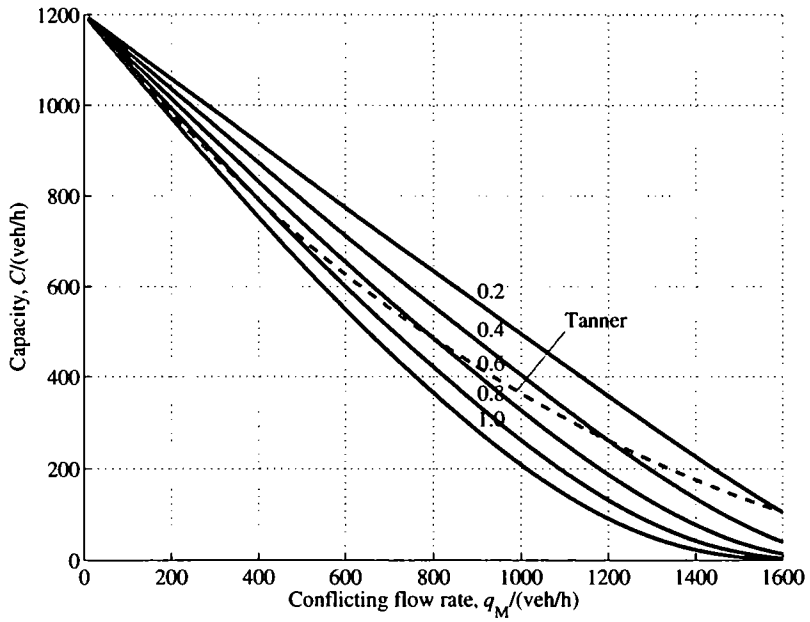

Figure 3.5: Capacity with different proportions of free vehicles, critical gap $t_c = 5\,s$, follow-up time $t_f = 3\,s$, and intra-platoon headway $t_p = 1.8\,s$ compared with the Tanner model (dashed curve)

A comparison of figures 3.1 and 3.4 indicates that at high major road flow rates, when the variation of headways decreases, the minor stream capacity (3.19) decreases below the capacity of the exponential model (3.12). This could be expected by the shape of the coefficient of variation curve (Fig. 2.9). Absolute priority is assumed.

Figure 3.6 displays the capacity of a minor stream under limited priority conditions based on Tanner's headway distribution (M/D/1 output) with flow-dependent critical gaps ($t_c = 5.0 - 6.0\lambda$) and follow-up times ($t_f = 0.6t_c$) and constant ($t_p = 1.8\,s$) follower headway in platoons. It is compared with Tanner's capacity formula (absolute priority) with the same critical gaps, follow-up times, and follower headways. The parameters are not necessarily realistic and they may produce excess curvature, but they highlight the difference between the two models. Under flow-dependent gap acceptance the capacity curve has steepest slopes at low and high flow rates. This can be inferred from Tanner's capacity formula (Fig. 3.4) by assuming large (5 s) critical gaps at low flow rates and small (2 s) critical gaps at high flow rates. If critical gaps decrease with increasing flow rate the capacity curve becomes more linear, especially under limited priority. This gives some theoretical support for the British linear regression models (Kimber & Coombe 1980), as suggested by (Troutbeck 2002).

3.2.3 Linear gap acceptance function

In a *fluid analogy model* gap acceptance function is continuous for headways larger than the shortest acceptable headway t_0 (see section 2.5). A *linear gap acceptance*

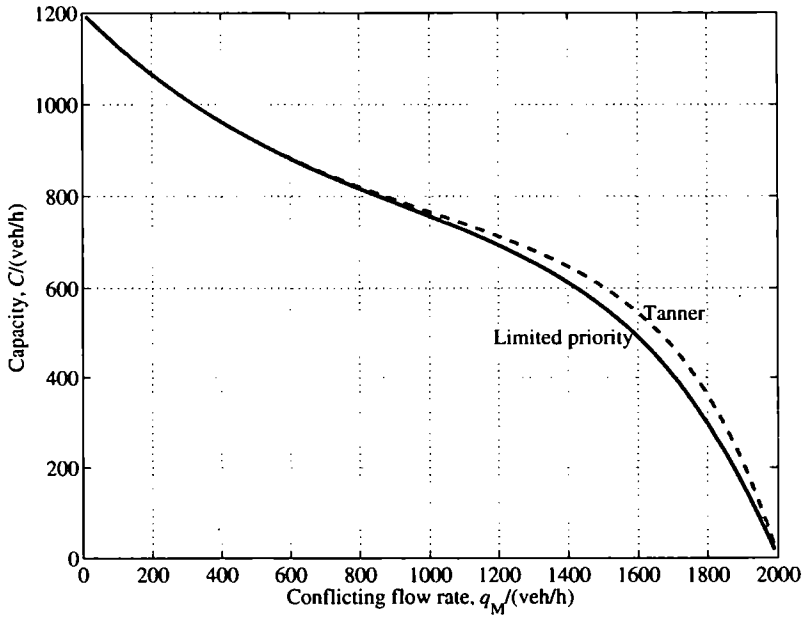

Figure 3.6: An example of minor stream capacity under flow-dependent gap acceptance and major stream arrivals from an M/D/1 queuing system with limited (solid curve) or absolute (dashed curve) priority

function has been suggested by Siegloch (1973) as

$$\alpha(t) = \left(\frac{t - t_o}{t_f}\right)_+ = \left(\frac{t - t_c + \frac{t_f}{2}}{t_f}\right)_+, \tag{3.25}$$

where $t_o = t_c - t_f/2$ is the shortest acceptable headway. The minor-stream departure process is considered as a fluid flowing into the headways of the priority stream. As long as the lag is larger than t_o the minor stream departure flow rate is t_f^{-1}.

As Figure 3.7 indicates, equation (3.25) is a linear approximation of the step function (3.9). Linear gap acceptance function can be interpreted as a simplified means to describe the average gap acceptance behaviour of heterogeneous drivers. The potential capacity is obtained as

$$\begin{aligned} C_p &= q_M \int_0^\infty \alpha(t) f(t)\,dt \\ &= \frac{q_M}{t_f} \int_{t_o}^\infty (t - t_o) f(t)\,dt \\ &= \frac{q_M}{t_f} \left[\int_{t_o}^\infty t f(t)\,dt - t_o R(t_o)\right]. \end{aligned} \tag{3.26}$$

For negative exponential priority stream headways and linear gap acceptance function

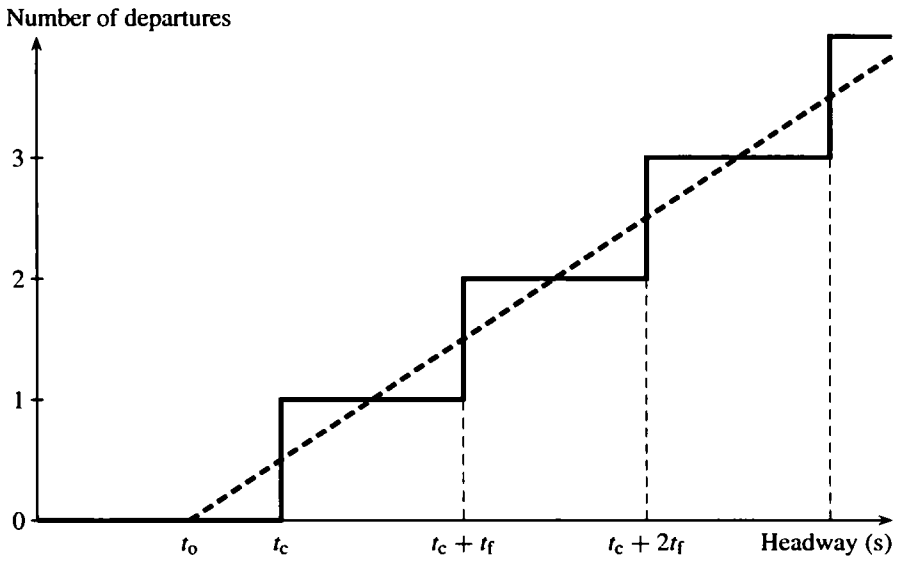

Figure 3.7: Step function and a linear model for gap acceptance

the potential capacity is obtained as (Siegloch 1973, Schnabel & Lohse 1997)

$$\begin{aligned} C_p &= \frac{q_M}{t_f} \int_{t_0}^{\infty} (t - t_0)\, \lambda e^{-\lambda t}\, dt \\ &= \frac{\lambda q_M}{t_f} \left[\int_{t_0}^{\infty} t e^{-\lambda t}\, dt - t_0 \int_{t_0}^{\infty} e^{-\lambda t}\, dt \right] \\ &= \frac{q_M}{t_f} \left[\left(\lambda^{-1} - t - t_0\right) e^{-\lambda t} \right]_{t=t_0}^{\infty} \\ &= \frac{q_M}{\lambda t_f} e^{-\lambda t_0} \\ &= \boxed{\frac{3600}{t_f} e^{-q_M t_0/3600}.} \end{aligned} \tag{3.27}$$

Because t_f is the minimum headway and the exponential part is the probability (proportion of time) of a lag larger than t_0, the equation can be expressed as

$$\boxed{C_p = s\, \mathbb{P}\{\Upsilon > t_0\} = s R_\Upsilon(t_0)\,,} \tag{3.28}$$

where s is the maximum flow rate of the minor stream in the case of no higher priority flow; i.e., saturation flow rate. $\mathbb{P}\{\Upsilon > t_0\}$ is the proportion of time that minor stream vehicles find an acceptable lag. During this time minor stream vehicles can discharge at maximum rate. For a fluid analogy model, capacity can be expressed as the *product of minor stream saturation flow rate* (s) *and the probability of a lag larger than the minimum acceptable gap* (t_0) (Akçelik 1998). The same result (2.57) was obtained in section 2.5 by a heuristic method.

In the German guidelines (Brilon et al. 1994, FGSV 2001) equation (3.27) has been used, but the difference between equations (3.27) and (3.12) has been considered insignificant (see Brilon 1991). The comparison of Figures 3.1 and 3.8 demonstrates that the capacities of equations (3.12) and (3.27) are virtually identical (see also Troutbeck & Brilon 1997). According to Brilon & Stuwe (1993) Siegloch's equation (3.27) with parameters estimated by regression analysis was slightly better as a capacity estimate for German roundabouts than a linear regression equation. — HCM has applied equation (3.27) in the 1994 update (Transportation Research Board 1994).

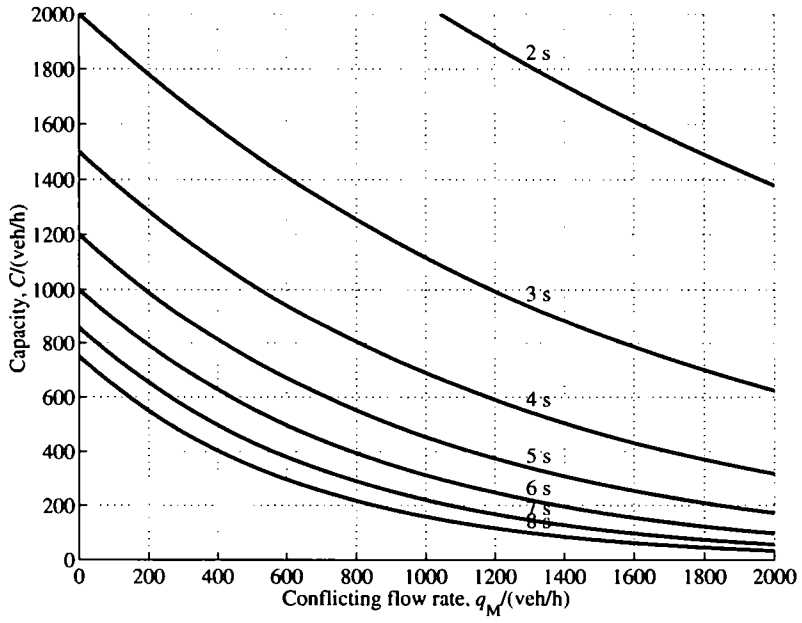

Figure 3.8: Minor-stream capacity with different critical gaps, $t_f = 0.6t_c$, linear gap acceptance function and major stream headways following the negative exponential distribution

Equation (3.27) has a simpler form than equation (3.12). Because it can be transformed into a linear equation by taking a logarithm, it is easy to apply in linear regression analysis (Guichet 1997, Aagaard 1995). The model also has a simple logic: During the time available for gap acceptance minor stream discharges at maximum rate. The operation of individual vehicles can be ignored.

For shifted exponential headways the potential capacity is

$$\begin{aligned} C_p &= \frac{q_M}{t_f}\left[\int_{t_o}^{\infty} t\theta e^{-\theta(t-t_p}\,dt - t_o R(t_o)\right] \\ &= \frac{q_M}{t_f}\left[\left(t_o + \frac{1}{\theta}\right)e^{-\theta(t_o-t_p)} - t_o e^{-\theta(t_o-t_p)}\right] \\ &= \frac{q_M}{\theta t_f} e^{-\theta(t_o-t_p)}, \qquad t_o > t_p. \end{aligned} \tag{3.29}$$

The application of equation (2.21) gives (Brilon 1988*a*)

$$C_p = \frac{3600 - q_M t_p}{t_f} e^{-\theta(t_o-t_p)}, \qquad t_o > t_p. \tag{3.30}$$

The equation can also be expressed in the familiar form

$$C_p = \frac{3600 e^{-\theta(t_o-t_p)}}{t_f(1+\theta t_p)} = s\,\mathbb{P}\{\Upsilon > t_o\}, \qquad t_o > t_p. \tag{3.31}$$

Because the smallest acceptable headway should be larger than the follower headway in a platoon ($t_o > t_p$), in Cowan's M3 distribution only the exponential tail of the distribution has an effect on the capacity. It differs from the shifted exponential distribution by

factor ϕ, thus giving the following potential capacity equation (Troutbeck 1997*a*, Troutbeck & Brilon 1997)

$$\begin{aligned} C_p &= \frac{q_M}{t_f}\left[\phi\gamma\int_{t_o}^{\infty} t e^{-\gamma(t-t_p)}\,dt - t_o R(t_o)\right] \\ &= \frac{\phi q_M}{\gamma t_f} e^{-\gamma(t_o-t_p)}, \qquad t_o > t_p. \end{aligned} \tag{3.32}$$

Equation (2.43) indicates that for an M/D/1 departure process $\phi\gamma^{-1} = \bar{t} - t_p = \lambda^{-1} - t_p$. When this substitution and the substitution for $q_M = 3600\lambda$ are made, the modification of Tanner's capacity model (3.24) is obtained as (Brilon 1988*a*):

$$C_p = \frac{3600(1-\lambda t_p)}{t_f} e^{-\lambda(t_o-t_p)}, \qquad t_o > t_p, \tag{3.33}$$

where parameter $\lambda = q_M/3600$ veh/s (Brilon 1988*a*, Transportation Research Board 1997). This equation can also be presented as

$$C_p = \frac{3600\phi e^{-\gamma(t_o-t_p)}}{t_f(\phi+\gamma t_p)} = s\,\mathbb{P}\{\Upsilon > t_o\}, \qquad t_o > t_p. \tag{3.34}$$

The results are virtually identical with the original Tanner model (3.24) as displayed in Figure 3.4. McDonald & Armitage (1978) have used equation (3.33) as a capacity model for a roundabout entry. Following the terminology of signalized intersections they interpreted t_f^{-1} as saturation flow rate and t_o as a "lost time" associated with each circulating vehicle and blocking the entry of minor-stream vehicles.

3.3 Potential capacity under multiple priority streams

The potential capacity models described above assume a single conflicting priority (major) stream on one lane. In most cases a minor stream faces many priority streams, some of which may share lanes with other streams or occupy several lanes. This section discusses the effect of multiple *independent* priority streams. Sections 3.5 and 3.6 discuss the capacity under dependent priority streams. The effect of shared lanes is discussed in section 3.7.

Let us consider a T-intersection (Fig. 2.3 on page 27) with an exclusive left-turn lane in the major road. The major road through movements (2 and 5) can be considered as two independent priority streams for the minor road left turn stream (7). The set of independent priority streams for minor stream 7 is $I_7 = \{2, 5\}$. Stream 4 (major road left turn) is not independent, because it must give way to streams 2 and 3.

On multi-lane highways (Fig. 3.9) traffic flows on adjacent through and right turn lanes can be considered independent. Minor road right turning vehicles (stream 9) must give way to traffic flow on one major road lane; i.e., $I_9 = \{2a\}$. Minor road left-turn vehicles (7) must give way to other major road through streams, but they can ignore stream 5a; i.e., $I_7 = \{2a, 2b, 5b\}$.

If the independent priority streams are described as point processes, the combined priority stream is a *superposition* of the component point processes.[5] As Figure 3.10 indicates, the superimposed process does not have the minimum headway restrictions that the component processes may have.

[5]In reliability theory a superimposed process is a system having several components in series. When a component fails, it is immediately replaced with a new component of the same type. (Thompson 1988, Høyland & Rausand 1994)

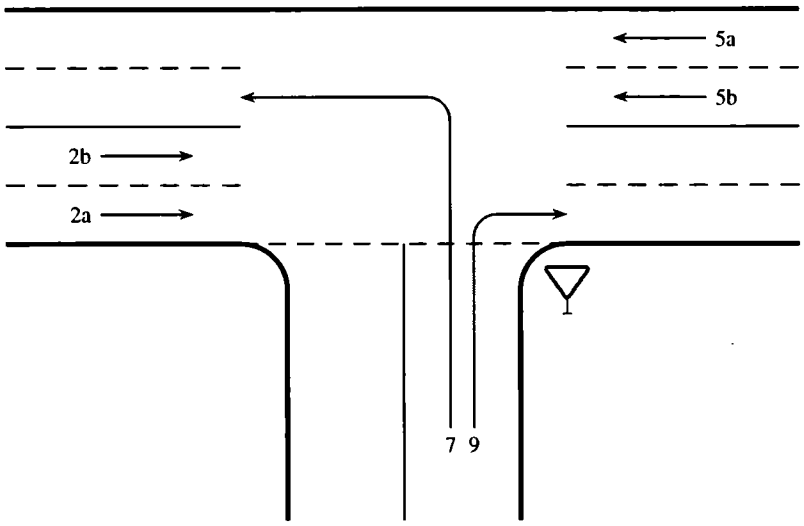

Figure 3.9: T-intersection of a four-lane major road

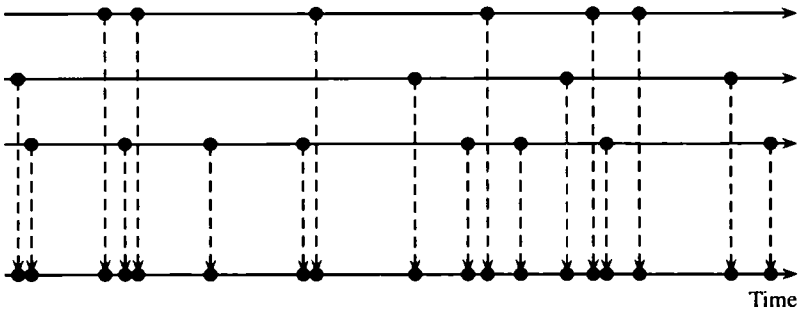

Figure 3.10: Superposition of three independent point processes (cf. Cox & Smith 1954)

A superimposed process is more like a Poisson process than the component processes (Cox & Isham 1980). Palm (1943) proposed that the superposition of a large number of independent sparse point processes leads to a Poisson process in the limit. This first limit theorem of point processes was proved by Khintchine (1960). See also Gnedenko (1967), Çinlar (1972), and Cox & Isham (1980). The theorem explains the central role of Poisson processes in traffic flow theory. If the arrivals of each vehicle are considered as a separate process, the arrival process of all vehicles at a given location is a superposition of thousands of component processes, which can be approximated as a Poisson process. However, physical lengths and safety intervals of vehicles as well as limited passing opportunities make the component processes dependent on each others, which dependency the Poisson approximation ignores.

Another important result in the theory of point processes is that a superposition of two independent renewal processes is a renewal process if and only if the components are Poisson processes (Çinlar 1972, Cox & Isham 1980). As we shall see below, this superimposed process is also a Poisson process. Memoryless component processes produce a memoryless superimposed process. If component processes are renewal processes, but their future depends on history (such as a minimum headway condition), all points in the superimposed process are no longer renewal points.

The number of points in a superimposed process during a (long) time interval is the

sum of points in the component processes during the same time interval. Thus, the flow rate of a superimposed process is the sum of the component flow rates

$$q_{M,k} = \sum_{i \in I_k} q_i, \tag{3.35}$$

where I_k is the set of independent priority streams for minor stream k.

Let us assume a major road with multiple lanes ($i \in I_k$) of independent traffic streams, which a minor stream k must give way to. When a minor stream vehicle reaches the first position in the queue at time τ, the lag is the time interval to the arrival of the first vehicle in any component process $i \in I_k$. The survivor function of a lag distribution in a superimposed process is (Thompson 1988)

$$\begin{aligned} R_{\Upsilon,I_k}(\upsilon) &= \mathbb{P}\{\Upsilon_{I_k}(\tau) > \upsilon\} \\ &= \prod_{i \in I_k} \mathbb{P}\{\Upsilon_i(\tau) > \upsilon\} \\ &= \prod_{i \in I_k} R_{\Upsilon,i}(\upsilon), \end{aligned} \tag{3.36}$$

where $\Upsilon_i(\tau)$ is the lag in component process i starting from time τ, and $\Upsilon_{I_k}(\tau)$ is the lag in the superimposed process. The calculation of probability $\mathbb{P}\{\Upsilon_i(\tau) > \upsilon\}$ may require information about arrivals preceding time τ on lane (component process) i.

If τ is the time of last arrival in a superimposed process, the headway over all lanes is larger than t, if the headway on lane j (the lane of last arrival) and lags on other lanes are all larger than t (Cox & Smith 1954):

$$\begin{aligned} R_{I_k,j}(t) &= \mathbb{P}\{T_j > t\} \prod_{\substack{i \in I_k \\ i \neq j}} \mathbb{P}\{\Upsilon_i(\tau) > t\} \\ &= R_j(t) \prod_{\substack{i \in I_k \\ i \neq j}} R_{\Upsilon,i}(t), \qquad j \in I_k. \end{aligned} \tag{3.37}$$

The probability that a random point is from a component process $j \in I_k$ is the expected proportion of process j points in the superimposed process (Weiss & Maradudin 1962):

$$p_j = \frac{q_j}{\sum_{i \in I_k} q_i} = \frac{q_j}{q_{M,k}}. \tag{3.38}$$

The survivor function of headways in a superimposed process can now be presented as

$$\begin{aligned} R_{I_k}(t) &= \sum_{j \in I_k} p_j \, \mathbb{P}\{T_j > t\} \prod_{\substack{i \in I_k \\ i \neq j}} \mathbb{P}\{\Upsilon_i(\tau) > t\} \\ &= \sum_{j \in I_k} p_j R_j(t) \prod_{\substack{i \in I_k \\ i \neq j}} R_{\Upsilon,i}(t) \\ &= q_{M,k}^{-1} \sum_{j \in I_k} q_j R_j(t) \prod_{\substack{i \in I_k \\ i \neq j}} R_{\Upsilon,i}(t). \end{aligned} \tag{3.39}$$

For the probability density function of superimposed headways on a multi-lane highway, the reader is referred to Weiss & Maradudin (1962).

If stream k has a stepwise gap acceptance function (3.9), the potential capacity is obtained following equation (3.11):

$$\begin{aligned} C_{\mathrm{p},k} &= q_{\mathrm{M},k} \sum_{l=0}^{\infty} R_{l_k}(t_{\mathrm{c},k} + l t_{\mathrm{f},k}) \\ &= \boxed{\sum_{l=0}^{\infty} \sum_{j \in l_k} \left[q_j R_j(t_{\mathrm{c},k} + l t_{\mathrm{f},k}) \prod_{\substack{i \in l_k \\ i \neq j}} R_{\Upsilon,i}(t_{\mathrm{c},k} + l t_{\mathrm{f},k}) \right].} \end{aligned} \tag{3.40}$$

It is assumed that there is no serial correlation between consecutive headways (see Luttinen 1996). Then the history of headways on lane j preceding time τ does not affect the probability $\mathbb{P}\{T_j > t\}$. It is also assumed that the history of other processes in l_k can be ignored, which is not always a realistic assumption.

In a Poisson process headways follow *negative exponential distribution*, and the Markov property simplifies equations considerably. Lag distributions on each lane are identical with headway distributions and they do not depend on previous history of the process:

$$\begin{aligned} \mathbb{P}\{\Upsilon_i(\tau) > \upsilon\} &= \mathbb{P}\{\Upsilon_i > \upsilon\} \\ &= \mathbb{P}\{T_i > \upsilon\} \\ &= \mathrm{e}^{-\lambda_i \upsilon}. \end{aligned} \tag{3.41}$$

The survivor function of headways in a superimposed process is

$$R_{l_k}(\upsilon) = \prod_{i \in l_k} \mathrm{e}^{-\lambda_i t} = \mathrm{e}^{-t \sum_{i \in l_k} \lambda_i}. \tag{3.42}$$

Because this is the negative exponential distribution with parameter $\lambda = \sum_{i \in l_k} \lambda_i = q_{\mathrm{M},k}/3600$, the capacity of stream k can be calculated using equation (3.12) as follows:

$$C_{\mathrm{p},k} = \frac{q_{\mathrm{M},k} \mathrm{e}^{-t_{\mathrm{c}} q_{\mathrm{M},k}/3600}}{1 - \mathrm{e}^{-t_{\mathrm{f}} q_{\mathrm{M},k}/3600}}. \tag{3.43}$$

The allocation of major flow among component streams has no effect on capacity, unless these streams have different critical gaps (Hagring 1998*b*).

The theory of superimposed point processes gives credibility to Poisson process (exponential headways) as a gap availability model under multiple independent priority streams. The results also indicate that under Poisson assumption the superimposed process is mathematically no more complicated than the component processes. A superposition of Poisson processes is a Poisson process having as a parameter the sum of component-process parameters.

If headways follow *shifted exponential distribution* the survivor functions of headways and lags in the component processes are

$$R_i(t) = \mathrm{e}^{-\theta_i (t - t_{\mathrm{p},i})}, \qquad t_{\mathrm{p},i} < t \tag{3.44}$$

$$R_{\Upsilon,i}(\upsilon) = \frac{\mathrm{e}^{-\theta_i (\upsilon - t_{\mathrm{p},i})}}{1 + \theta_i t_{\mathrm{p},i}}, \qquad t_{\mathrm{p},i} < \upsilon. \tag{3.45}$$

The capacity of a minor stream yielding to several independent major streams having

shifted exponential headway distributions can now be expressed as

$$\begin{aligned}
C_{\mathrm{p},k} &= \sum_{l=0}^{\infty} \sum_{j \in I_k} \left[q_j R_j\left(t_{\mathrm{c},k} + l t_{\mathrm{f},k}\right) \prod_{\substack{i \in I_k \\ i \neq j}} R_{\Upsilon,i}\left(t_{\mathrm{c},k} + l t_{\mathrm{f},k}\right) \right] \\
&= \sum_{l=0}^{\infty} \sum_{j \in I_k} \left(q_j \mathrm{e}^{-\theta_j (t_{\mathrm{c},k} + l t_{\mathrm{f},k} - t_{\mathrm{p},j})} \prod_{\substack{i \in I_k \\ i \neq j}} \frac{\mathrm{e}^{-\theta_i (t_{\mathrm{c},k} + l t_{\mathrm{f},k} - t_{\mathrm{p},i})}}{1 + \theta_i t_{\mathrm{p},i}} \right) \\
&= \sum_{l=0}^{\infty} \frac{\mathrm{e}^{-\sum_{i \in I_k} \theta_i (t_{\mathrm{c},k} + l t_{\mathrm{f},k} - t_{\mathrm{p},i})}}{\prod_{i \in I_k} (1 + \theta_i t_{\mathrm{p},i})} \sum_{j \in I_k} q_j (1 + \theta_j t_{\mathrm{p},j}) \\
&= \frac{\mathrm{e}^{-\sum_{i \in I_k} \theta_i (t_{\mathrm{c},k} - t_{\mathrm{p},i})}}{\prod_{i \in I_k} (1 + \theta_i t_{\mathrm{p},i})} \left(\sum_{l=0}^{\infty} \mathrm{e}^{-l t_{\mathrm{f},k} \sum_{i \in I_k} \theta_i} \right) \sum_{j \in I_k} q_j (1 + \theta_j t_{\mathrm{p},j}) \\
&= \frac{\mathrm{e}^{-\sum_{i \in I_k} \theta_i (t_{\mathrm{c},k} - t_{\mathrm{p},i})} \sum_{i \in I_k} q_i (1 + \theta_i t_{\mathrm{p},i})}{\left(1 - \mathrm{e}^{-t_{\mathrm{f},k} \sum_{i \in I_k} \theta_i}\right) \prod_{i \in I_k} (1 + \theta_i t_{\mathrm{p},i})}, \qquad \forall i : t_{\mathrm{p},i} < t_{\mathrm{c},k}.
\end{aligned} \tag{3.46}$$

Because the flow rate of a shifted exponential headway process can be expressed as

$$q_i = 3600 \lambda_i = \frac{3600\, \theta_i}{1 + \theta_i t_{\mathrm{p},i}}, \tag{3.47}$$

the capacity of minor stream k is

$$\begin{aligned}
C_{\mathrm{p},k} &= \frac{3600\, \mathrm{e}^{-\sum_{i \in I_k} \theta_i (t_{\mathrm{c},k} - t_{\mathrm{p},i})} \sum_{i \in I_k} \theta_i}{\left(1 - \mathrm{e}^{-t_{\mathrm{f},k} \sum_{i \in I_k} \theta_i}\right) \prod_{i \in I_k} (1 + \theta_i t_{\mathrm{p},i})} \\
&= \frac{3600\, \theta \prod_{i \in I_k} R_{\Upsilon,i}\left(t_{\mathrm{c},k}\right)}{1 - \mathrm{e}^{-\theta t_{\mathrm{f},k}}}, \qquad \forall i : t_{\mathrm{p},i} < t_{\mathrm{c},k} \\
&= \frac{3600\, \theta R_{\Upsilon,I_k}\left(t_{\mathrm{c},k}\right)}{1 - \mathrm{e}^{-\theta t_{\mathrm{f},k}}},
\end{aligned} \tag{3.48}$$

where $\theta = \sum_{i \in I_k} \theta_i$, and the lag distribution of a superimposed process is

$$R_{\Upsilon,I_k}(\upsilon) = \frac{\mathrm{e}^{-\sum_{i \in I_k} \theta_i (\upsilon - t_{\mathrm{p},i})}}{\prod_{i \in I_k} (1 + \theta_i t_{\mathrm{p},i})}. \tag{3.49}$$

If all minimum headways ($t_{\mathrm{p},i}$) are zero, the result is equal to a capacity across random (Poisson) traffic streams.

Tanner (1967), Troutbeck (1986), Fisk (1989), and Hagring (1998*b*) have derived the capacity of a minor stream crossing or merging independent major streams each having a *Cowan's M3 headway distribution.* They assumed that minimum headways in all streams are identical. With the help of equation (3.40) the potential capacity can be

obtained directly as:

$$
\begin{aligned}
C_{\mathrm{p},k} &= \sum_{l=0}^{\infty}\sum_{j\in I_k}\left(q_j R_j\left(t_{\mathrm{c},k}+lt_{\mathrm{f},k}\right)\prod_{\substack{i\in I_k\\ i\neq j}} R_{\Upsilon,i}\left(t_{\mathrm{c},k}+lt_{\mathrm{f},k}\right)\right)\\
&= \sum_{l=0}^{\infty}\sum_{j\in I_k}\left(q_j\phi_j \mathrm{e}^{-\gamma_j\left(t_{\mathrm{c},k}+lt_{\mathrm{f},k}-t_{\mathrm{p},j}\right)}\prod_{\substack{i\in I_k\\ i\neq j}}\frac{\phi_i \mathrm{e}^{-\gamma_i\left(t_{\mathrm{c},k}+lt_{\mathrm{f},k}-t_{\mathrm{p},i}\right)}}{\phi_i+\gamma_i t_{\mathrm{p},i}}\right)\\
&= \sum_{l=0}^{\infty}\frac{\mathrm{e}^{-\sum_{i\in I_k}\gamma_i\left(t_{\mathrm{c},k}+lt_{\mathrm{f},k}-t_{\mathrm{p},i}\right)}}{\prod_{i\in I_k}\left(1+\frac{\gamma_i t_{\mathrm{p},i}}{\phi_i}\right)}\sum_{j\in I_k} q_j\left(\phi_j+\gamma_j t_{\mathrm{p},j}\right) \qquad (3.50)\\
&= \frac{\mathrm{e}^{-\sum_{i\in I_k}\gamma_i\left(t_{\mathrm{c},k}-t_{\mathrm{p},i}\right)}}{\prod_{i\in I_k}\left(1+\frac{\gamma_i t_{\mathrm{p},i}}{\phi_i}\right)}\left(\sum_{l=0}^{\infty}\mathrm{e}^{-lt_{\mathrm{f},k}\sum_{i\in I_k}\gamma_i}\right)\sum_{j\in I_k} 3600\gamma_j\\
&= 3600\frac{\mathrm{e}^{-\sum_{i\in I_k}\gamma_i\left(t_{\mathrm{c},k}-t_{\mathrm{p},i}\right)}\sum_{i\in I_k}\gamma_i}{1-\mathrm{e}^{-t_{\mathrm{f},k}\sum_{i\in I_k}\gamma_i}}\prod_{i\in I_k}\frac{\phi_i}{\phi_i+\gamma_i t_{\mathrm{p},i}}, \qquad \forall i: t_{\mathrm{p},i} < t_{\mathrm{c},k},
\end{aligned}
$$

where flow rate is expressed as

$$q_j = \frac{3600}{\mathbb{E}[T_j]} = \frac{3600\,\gamma_j}{\phi_j+\gamma_j t_{\mathrm{p},j}}. \qquad (3.51)$$

Equation (3.50) can also be expressed as

$$
\begin{aligned}
C_{\mathrm{p},k} &= \frac{3600\gamma\prod_{i\in I_k} R_{\Upsilon,i}\left(t_{\mathrm{c},k}\right)}{1-\mathrm{e}^{-\gamma t_{\mathrm{f},k}}}\\
&= \frac{3600\gamma R_{\Upsilon,I_k}\left(t_{\mathrm{c},k}\right)}{1-\mathrm{e}^{-\gamma t_{\mathrm{f},k}}},
\end{aligned} \qquad (3.52)
$$

where $\gamma = \sum_{i\in I_k}\gamma_i$, and

$$R_{\Upsilon,I_k}(\upsilon) = \mathrm{e}^{-\sum_{i\in I_k}\gamma_i\left(\upsilon-t_{\mathrm{p},i}\right)}\prod_{i\in I_k}\frac{\phi_i}{\phi_i+\gamma_i t_{\mathrm{p},i}} = \prod_{i\in I_k} R_{\Upsilon,i}(\upsilon) \qquad (3.53)$$

is the lag distribution of the superimposed process.

The model of Tanner (1967) can be obtained from equation (3.50) by acknowledging that $t_{\mathrm{p},i} = t_{\mathrm{p}}$, $\phi_i = 1-\lambda_i t_{\mathrm{p}}$, and $\gamma_i = \lambda_i = q_i/3600$:

$$C_{\mathrm{p},k} = q_{\mathrm{M},k}\frac{\mathrm{e}^{-\lambda\left(t_{\mathrm{c},k}-t_{\mathrm{p}}\right)}}{1-\mathrm{e}^{-\lambda t_{\mathrm{f},k}}}\prod_{i\in I_k}\left(1-\lambda_i t_{\mathrm{p}}\right), \qquad (3.54)$$

where $q_{\mathrm{M},k} = 3600\lambda = \sum_{i\in I_k} q_i$. See also Gipps (1982). Fisk (1989) has extended Tanner's result to include the case where different lanes have different critical gaps. Hagring (1998*a*, 1998*b*) has extended Tanner's formula for superimposed M3 headway distributions having equal follower headways, but allowing lanes to differ in critical gaps and follow-up times. Fisk and Hagring observed that capacity is greatest when traffic is evenly distributed among lanes. Then bunching is least and bunch overlap is greatest for a given total major flow rate.

For a single priority stream the equation 3.50 reduces to equation 3.19. Equation 3.50 can be used to obtain the capacity across multiple independent streams having any combination of negative exponential, shifted exponential, and M3 headway distributions.

The potential capacity across two streams i and j having Cowan's M3 headway distribution with equal minimum headways (t_p) is

$$C_{p,k} = \frac{3600\phi_i\phi_j(\gamma_i + \gamma_j)e^{-(\gamma_i+\gamma_j)(t_{c,k}-t_p)}}{(\phi_i + \gamma_i t_p)(\phi_j + \gamma_j t_p)\left(1 - e^{-t_{f,k}(\gamma_i+\gamma_j)}\right)}, \qquad t_p < t_{c,k}. \tag{3.55}$$

This equation is identical with the equation 8 of Troutbeck (1986). Figure 3.11 displays a set of curves identical with Fig. 1 of Troutbeck (1986). It shows that major stream bunching increases minor stream capacity, even in the case of two independent priority streams.

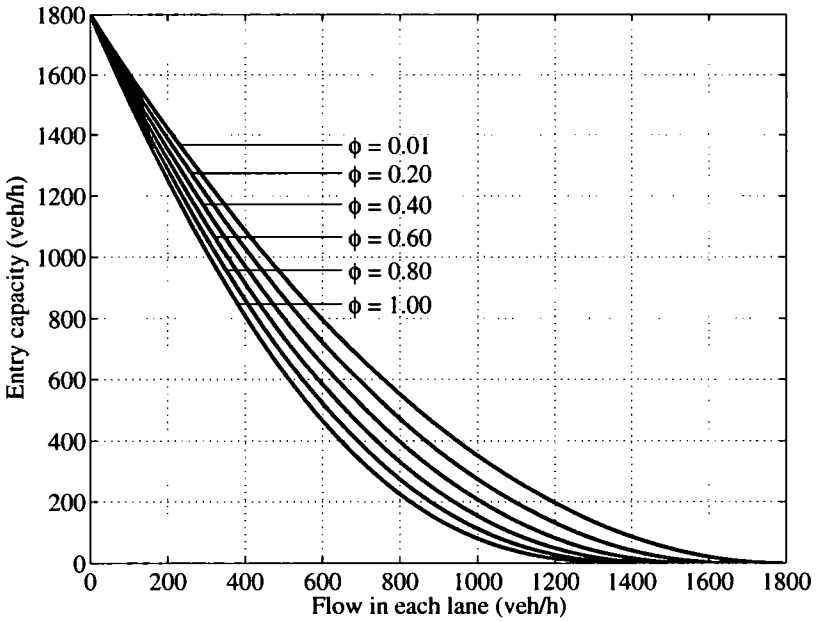

Figure 3.11: Entry capacity at an intersection having two identical priotity streams with minimum headway $t_p = 2\,s$ and different proportions (ϕ) of free vehicles, and minor stream critical gap $t_c = 4\,s$ and follow-up time $t_f = 2\,s$ (see Troutbeck 1986)

Troutbeck (1991) described a modification of a single-lane capacity model, which gives good estimates of the two-lane model. He presented an iterative procedure to estimate the parameters for the modified model. Although Troutbeck & Brilon (1997) suggested that there are no practical reasons to increase the complexity of calculations by using multi-lane models, it can be questioned whether the two-lane model (3.55) is more complicated to use than a one-lane model (3.19) with parameters estimated by an iterative procedure. Brilon (1988*a*) has favored simple capacity formulas (3.12, 3.27, and (3.30)) based on the summation of conflicting major streams, because it gives lower capacity estimates than multi-lane model, and thus does not overestimate actual capacity.

Hagring (1998*b*) has demonstrated the superiority of multi-lane models, especially when critical gaps are lane specific. In this case equation (3.40) should be modified for lane-specific critical gaps and follow-up times:

$$C_{p,k} = \sum_{l=0}^{\infty} \sum_{j \in I_k} \left[q_j R_j(t_{c,j} + l t_{f,j}) \prod_{\substack{i \in I_k \\ i \neq j}} R_{\Upsilon,i}(t_{c,i} + l t_{f,i}) \right]. \tag{3.56}$$

The capacity model for M3 distributed component-stream headways becomes

$$C_{p,k} = 3600 \frac{e^{-\sum_{i \in I_k} \gamma_i (t_{c,i} - t_{p,i})} \sum_{i \in I_k} \gamma_i}{1 - e^{-\sum_{i \in I_k} t_{f,i} \gamma_i}} \prod_{i \in I_k} \frac{\phi_i}{\phi_i + \gamma_i t_{p,i}}, \qquad \forall i : t_{p,i} < t_{c,i}. \quad (3.57)$$

When the intra-bunch headways $t_{p,i}$ are equal in all component streams, the capacity equation by Hagring (1998*b*) is obtained:

$$\begin{aligned} C_{p,k} &= 3600 \frac{e^{-\sum_{i \in I_k} \gamma_i (t_{c,i} - t_p)} \sum_{i \in I_k} \gamma_i}{1 - e^{-\sum_{i \in I_k} t_{f,i} \gamma_i}} \prod_{i \in I_k} \frac{\phi_i}{\phi_i + \gamma_i t_{p,i}} \\ &= \frac{3600 \Gamma e^{-\sum_{i \in I_k} \gamma_i (t_{c,i} - t_p)}}{1 - e^{-\sum_{i \in I_k} t_{f,i} \gamma_i}} \prod_{i \in I_k} \frac{\phi_i q_i}{3600 \gamma_i}, \end{aligned} \quad (3.58)$$

where $\Gamma = \sum_{i \in I_k} \gamma_i$. Different critical gaps for each lane may reflect the assumption that the values increase as the distance of the conflicting lane from the stop line increases, and that crossing and merging operations may have different critical gaps for the same minor movement (Fisk & Tan 1989). Li, Wang & Jiang (2003) have extended the multi-lane model to a case where the minor flow consists of two classes of vehicles.

3.4 Potential capacity of roundabout approaches

3.4.1 Background

The capacity of a stream or a lane at an unsignalized intersection is usually defined as the stop-line capacity. It is restricted by the arrivals and queues of higher priority vehicles and pedestrians and by minimum headways between departing vehicles. In addition, limited length of turning lanes may restrict capacity upstream of an intersection.

Hagring (1996*a*) has pointed out that roundabouts can have additional capacity restrictions at weaving sections, especially due to heavy vehicles, and at exits[6], where capacity may be limited by crossing pedestrians. That is, capacity restrictions apply to both inflows, outflows, and circulating flows of a roundabout.[7] However, most theoretical studies of roundabout capacity have focused on entry or stop-line capacity. Consequently, the discussion below describes the capacity of an approach at a roundabout. The effect of pedestrians on exit flows can be estimated using the procedure in section 3.8. If the capacity of weaving sections is critical, the use of simulation models is suggested.

All circulating vehicles in a roundabout have merged to the circulating stream. The gap-acceptance process at roundabout entries increase bunching in the circulating flow. On the other hand, exiting vehicles "combine headways". The processes of entering and exiting streams modify the shape of the headway distribution of circulating flow (see Hagring 2001). Although theoretical methods usually assume that the minor stream does not modify the circulating flow rate, iterative techniques can be used to address the interdependency of entering and circulating flows.

3.4.2 Historical overview

The first estimates of roundabout capacity were more or less rules of thumb. In 1930's Watson (1933) suggested that there should be a four-second headway between successive vehicles in each traffic stream. This would allow 900 pc/h to merge under favorable

[6]Preliminary results in Germany indicate that the maximum outflow from a one-lane roundabout with a rather narrow exit is about 1,200 veh/h (Brilon, Wu & Bondzio 1997).

[7]This is of course a simplistic description of roundabout capacity. The operation of traffic streams at a roundabout is a process of many complex merging and weaving interactions.

conditions. Watson suggested a 15 % margin for pedestrian traffic, obtaining a capacity estimate of 1,500 pc/h as the maximum sum of major and minor flows at a roundabout merge. Heavy vehicles required a six-second time interval.

Another early rule of thumb was given by Hammond & Sorenson (1941), who suggested a capacity limitation of about 3,000 vehicle per hour at any one point. The minimum radius for the central island was 150 feet (50 m) and the width of the circulatory roadway 25–35 feet (8–11 m). Shrope (1952) provided an extensive empirical analysis of one roundabout in Latham, New York.

One of the first capacity models was proposed by Clayton (1941, 1945) as:

$$C_p = s\left[n - \frac{\alpha}{90}\left(n - \frac{4}{3}\right)\right]. \tag{3.59}$$

The parameters of the model were saturation flow rate (s = 1200 veh/h), number of entry lanes (n), and "maximum weaving angle" (α, angle between the diagonals of a weaving area). This model was later recommended by the British Ministry of Transport (Clayton 1955).

The most significant of the early roundabout capacity models was developed by Wardrop (1957) at the British Road Research Laboratory. Based on measurements under test conditions the maximum flow through a weaving section was found to be

$$C_p = \frac{4.9(w_w + w_a)(4l_w - 3w_w)(3 - p_w)}{l(0.56 + p_{HV})} \quad \text{pc/h}, \tag{3.60}$$

where w_w and l_w are the width and the length of a weaving area (Fig. 3.12), w_a is average approach width (Fig. 3.13), p_w is the proportion of weaving traffic to total traffic in weaving section, and p_{HV} is the proportion of "medium or heavy" vehicles, including busses. The equation was further developed to the following form (Road Research Laboratory 1965):

$$C_p = \frac{108w_w\left(1 + \frac{w_a}{w_w}\right)\left(1 - \frac{p}{3}\right)}{1 + \frac{w_w}{l_w}} \quad \text{pc/h}. \tag{3.61}$$

This "practical capacity" was about 80 per cent of the capacity formula (3.60) above.

At old British roundabouts, described by these models, neither vehicles already at a roundabout nor those entering were given priority (Ashworth & Laurence 1978). The operations were best described as weaving rather than merging or gap acceptance maneuvers (McDonald & Armitage 1978). It was possible that vehicles "blocked back" from an adjoining weaving section and so impeded the exiting flow (Road Research Laboratory 1965). This "locking effect" limited the capacity of a roundabout, as illustrated in the delay/flow curve of Figure 3.14 (Webster 1960).

When circulating flow was given priority, the locking problem was avoided and capacity was increased approximately by 10 % (Blackmore 1963), being comparable to the best traffic signal systems (Blackmore 1970). Consequently, an offside priority rule was introduced in Britain in November 1966 (Duff 1968, Kimber 1980). It required entering drivers to give way to circulating vehicles. Long weaving sections to absorb queues were no longer necessary, enabling the design of smaller roundabouts (Kimber 1980). This offside-priority rule is nowadays the prevailing policy worldwide.

In the 70's the Wardrop's model was found to be no longer applicable in Britain (Ashworth & Field 1973, Philbrick 1977), and some gap-acceptance models based

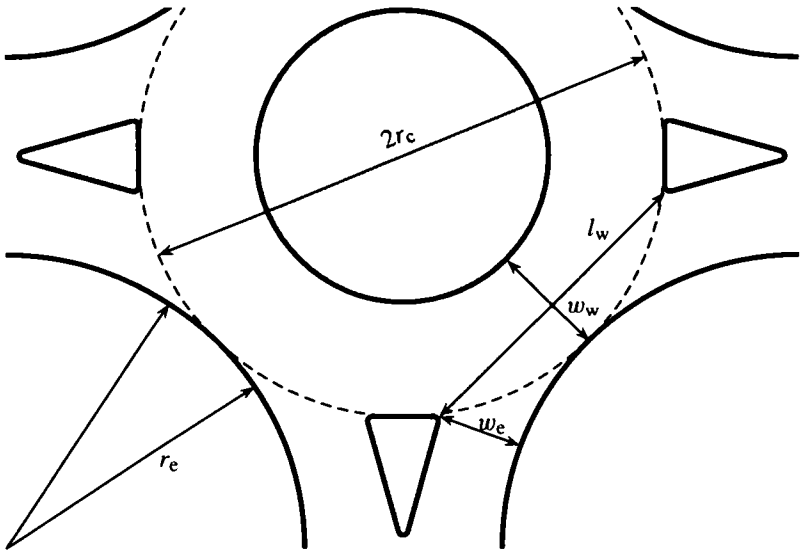

Figure 3.12: Roundabout geometry parameters

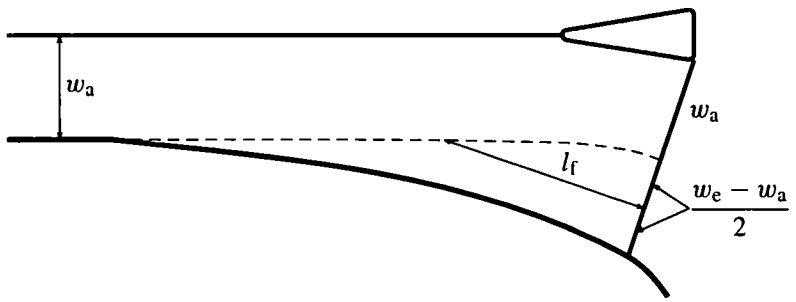

Figure 3.13: Flared entry parameters

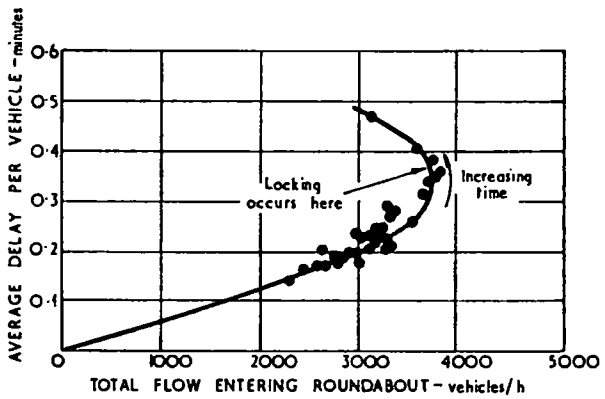

Figure 3.14: The effect of "locking" at a roundabout (Webster 1960, Road Research Laboratory 1965)

on Tanner's model (3.24) were developed (Armitage & McDonald 1974, McDonald & Armitage 1978, Ashworth & Laurence 1978) as well as linear regression models (Philbrick 1977). The current British methodology is based on linear regression models (O'Flaherty 1997).

3.4.3 Current methodologies

The British linear model for roundabout capacity is (Kimber 1980)

$$C_p = \begin{cases} a_1(a_2 - a_3 q_M), & \text{if } a_3 q_M \le a_2 \\ 0, & \text{if } a_3 q_M > a_2, \end{cases}$$

where

$$a_1 = 1 - 0.00347(\phi_e - 30) - 0.978\left(r_e^{-1} - 0.05\right)$$
$$a_2 = 303 a_4$$
$$a_3 = 0.210 a_5$$
$$a_4 = w_a + \frac{w_e - w_a}{1 + 2a_6}$$
$$a_5 = 1 + \frac{0.5}{1 + e^{(2r_c - 60)/10}}$$
$$a_6 = \frac{w_e - w_a}{l_f}.$$

Parameters are described in Figures 3.12 and 3.13. Parameter ϕ_e is the entry angle; i.e., conflict angle between entering and circulating streams. Parameters w_e, w_a, l_f, r_c, and r_e are in meters, ϕ_e is in degrees, and C_p and q_M are in pc/h. Kimber (1980) has presented more detailed descriptions of the parameters as well as their ranges in the data base.

In Norway the potential capacity of a roundabout is estimated as (Statens Vegvesen 1985, Aakre 1998)

$$C_p = 275 a_1 - 0.282 q_M (1 + 0.2 a_1) \quad \text{pc/h.} \tag{3.62}$$

The coefficient a_1 is defined as

$$a_1 = w_a + \frac{w_e - w_a}{1 + 2a_2}$$
$$a_2 = \frac{1.6(w_e - w_a)}{l_f},$$

where w_e is the entry width (Fig. 3.12) and l_f is the entry flare length (Fig. 3.13).

Other examples of linear capacity models have been presented by Louah (1988), Simon (1991), and Hakkert et al. (1991). Regression models based on exponential capacity equations (3.27) have been presented by Stuwe (1991), Brilon & Stuwe (1993), Guichet (1997), and Aagaard (1995), among others.

A gap-acceptance model for roundabouts requires an appropriate headway distribution for circulating streams and the estimation of critical gaps and follow-up times, adjusted for the roadway (geometric) conditions of the roundabout. If a roundabout is analyzed as a series of T-intersections, the equations for potential capacity in section 3.2 can be

applied. HCM2000 (Transportation Research Board 2000, Troutbeck 1997*b*) suggests the potential capacity model (3.12) based on exponential headways and a stepwise gap-acceptance function. The same equation is used in DanKap (Vejdirektoratet 1999*b*). German HBS 2001 applies the Siegloch model (3.27). All these manuals apply the same model for roundabouts as for other unsignalized intersections. The Swedish Capcal 2 has a special headway distribution for circulating flow (SNRA 1995*c*). The method is described in section 5.4.

The Australian method (Austroads 1993) applies the M3 model (3.19), which is also used in the SIDRA software package (Akçelik 1998). The parameters γ and ϕ are estimated using equations (3.20) and (3.21). The intra-bunch headway t_p is two seconds for one-lane roundabouts and one second for multi-lane roundabouts (Akçelik & Troutbeck 1991, Austroads 1993). Multi-lane traffic flows are reduced to one-lane flows modified to have a shorter intra-bunch gap and flow rate equal to the total flow rate on all circulatory lanes (Troutbeck 1991). In later SIDRA versions the intra-bunch headways have been defined as follows (Akçelik 1998):

$$\begin{aligned} t_p &= 2.0 \text{ s} && \text{for single-lane circulating flow} \\ &= 1.2 \text{ s} && \text{for two-lane circulating flow} \\ &= 1.0 \text{ s} && \text{for circulating flow with more than two lanes} \end{aligned}$$

If lane flows are not equal, the intra-bunch headway is calculated as a flow-weighted average of intra-bunch headways of the streams contributing to the circulating flow. The effect of vehicles exiting to the subject approach is ignored (Troutbeck 1991). The effect of limited priority has also been evaluated (see page 60).

Hagring (1998*b*) has developed a new Swedish method to estimate roundabout capacity. He uses the M3 model (3.19), which he has extended for multi-lane highways with lane-dependent critical gaps and follow-up times. The capacity equation (3.58) and its derivation has been presented above. The intra-bunch headway is 1.8 seconds, which has been used in the old Swedish capacity manual (Statens vägverk 1977, Anveden 1988) and verified by Hagring (1996*b*). The proportion of free headways is obtained by a relation $\phi_i = 0.910 - 1.545 q_i/3600$ (Hagring 1998*b*, Hagring 2000). The Tanner distribution (2.41) with $\phi_i = 1 - t_p q_i/3600$ was also found to give good results in capacity estimation. In a recent paper (Hagring et al. 2003) estimated the proportion of free headways as $\phi_i = 0.914 - 1.549 q_i/3600$. This model indicated that the allocation of traffic on lanes and thus the origin-destination flows in a roundabout have a considerable effect on capacity (Hagring 2000), as Akçelik (1997) had suggested earlier.

3.5 Movement capacity of Rank 3 streams

3.5.1 Description of the procedure

The estimation of Rank 3 stream k movement capacity proceeds in four stages:

1. The potential capacity ($C_{p,i}$) of a conflicting Rank 2 stream i is determined using the procedures described above.

2. An adjustment factor ($f_{a,i}$, fraction of time available for gap acceptance in stream i) is evaluated using $C_{p,i}^{-1}$ as the average service time of stream i server. This procedure is repeated for all conflicting Rank 2 streams.

3. The gap acceptance capacity $C_{a,k}$ of stream k is estimated assuming that no stream i vehicles are waiting for entry and all major streams are independent.

4. The movement capacity of stream k is the gap acceptance capacity multiplied by the adjustment factor

$$C_{m,k} = f_{a,i} C_{a,k}, \tag{3.63}$$

or

$$C_{m,k} = f_{l,i} C_{p,k}, \tag{3.64}$$

where $f_{l,i}$ is the impedance factor describing the fraction of potential capacity available as movement capacity. In case of several conflicting Rank 2 streams the adjustment or impedance factors are combined.

The estimation of factors $f_{a,i}$ and $f_{l,i}$, and gap-acceptance capacity $C_{a,k}$ is discussed below, but first it is necessary to take a closer look at queue discharge processes.

3.5.2 Queuing model for Rank 3 stream capacity

Figure 3.15 displays a simplified presentation of traffic streams at a T-intersection. The minor-road left-turn vehicles (stream 7, Rank 3) must give way to streams 2 and 4. Streams 2 and 4 are, however, not independent. The Rank 2 stream 4 must yield to Rank 1 stream 2. Thus stream 7 vehicles can enter the intersection only if there is a gap larger than the critical gap in the combined major stream (2 and 4) *and* no stream 4 vehicles are waiting for entry. Potential capacity, which assumes independent priority streams (Section 3.3), would overestimate the capacity. A modified approach is required.

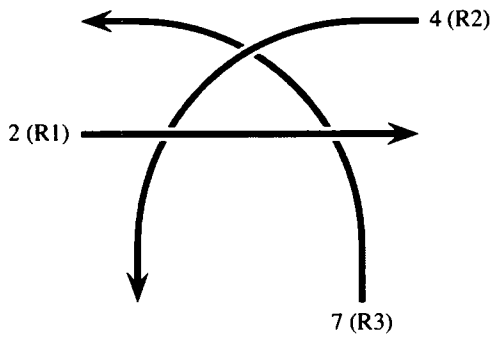

Figure 3.15: Three ranks of streams at a T-intersection

The time available for Rank 3 vehicles consists of two types of periods: *i*) Rank 2 stream queuing and queue discharge periods, and *ii*) gap acceptance periods. During gap acceptance periods all major-stream (Rank 1 and Rank 2) vehicles can proceed without delay, and priority streams can be considered independent. When the proportion of time, number of major-stream headways, and the headway distribution of the superimposed process available for Rank 3 gap acceptance are known, the capacity of a Rank 3 stream can be calculated. In order to do this, the queuing model has to be described in detail.

Figure 3.16 displays a queuing model description of Rank 2 stream i vehicles blocking the entry of Rank 3 stream k vehicles. As vehicle 1 enters the queue of stream i, Rank 1 vehicles block the entry of both Rank 2 and Rank 3 vehicles. When the antiblock starts, vehicle 1 enters service, and the busy period of the server begins. During the service time $t_{f,i}$ no other stream i vehicle can enter service. Vehicle 2 has to wait for the service of vehicle 1 to complete. As vehicle 1 departs, vehicle 2 enters service.

Busy period ends as vehicle 2 departs service. The length of the busy period is $2t_{f,i}$. An isolated vehicle 3 arrives to an empty system. As it enters the queue, the service starts immediately. It blocks stream k for the time of the critical gap $t_{c,k}$.

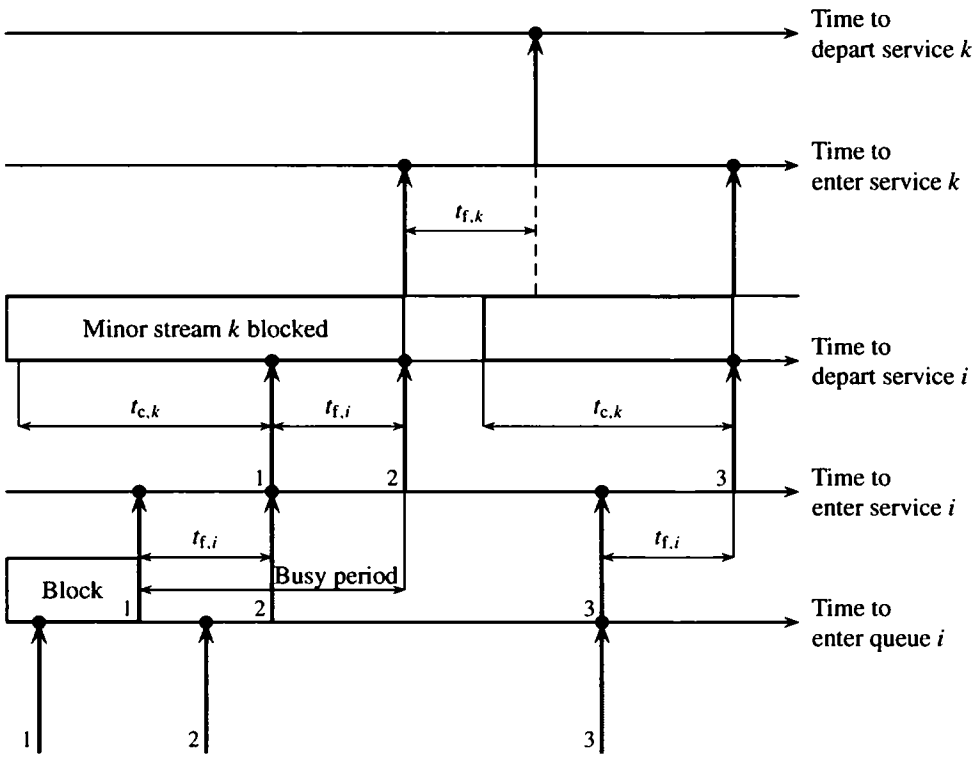

Figure 3.16: A queuing model having service times interrupted by blocks

The block of minor stream k terminates as the server of stream i becomes idle. After that the server of stream k starts service. The blocks and antiblocks in Figure 3.16 are described in terms of priority stream service departure times. Accordingly, the major stream arrival times in Figure 2.11 on page 43 should also be interpreted as service departure times. As Rank 1 flows decrease, the Rank 2 stream approaches an M/D/1 queuing system, and the departure flow approaches the model of Tanner (see page 41).

If $t_{f,i}$ is interpreted as the travel time from the stop line to the conflict point, the service starts when a vehicle crosses the stop line and ends when the vehicle has passed the conflict point. In this case the utilization factor of the server is the sum of utilization factors for all component streams (see section 3.10).

The queuing analogy should not be stretched too far. When an acceptable gap follows a stream i vehicle, a stream k vehicle does not—safety permitting—have to wait for $t_{f,i}$ before it can enter the intersection. The possibility of overlapping service times between conflicting streams cannot be excluded.

In the basic queuing model of Figure 3.16 each stream has a separate server with service time equal to the follow-up time. Service is interrupted by blocks created by higher priority vehicles. Haight (1963) described this model by stating that in an unsignalized intersection a vehicle arriving to an intersection with no queue does not necessarily receive immediate service.

If interruptions in the operation of stream i server are included in the service time, the average service time of queued vehicles is the inverse of capacity ($\bar{S}_{q,i} = C_i^{-1}$). As

Figure 3.17 displays, in this model vehicle 1 enters service immediately, and service time includes the time ($W_{e,i}^{(1)}$) spent waiting for the block termination. Service begins when a vehicle enters the stop line and terminates $t_{f,i}$ after the vehicle has crossed the stop line. Neither a Rank 2 *nor* a Rank 3 vehicle can cross the stop line before the follow-up time $t_{f,i}$ has elapsed.

Vehicle 1 departs service $t_{f,i}$ after the termination of the block, and the next vehicle enters service. Major stream arrivals frequently extend the service times of minor stream vehicles beyond the follow-up time. The dashed arrow displays the virtual departure time; i.e., the departure time assuming that vehicle 1 had arrived during an antiblock.

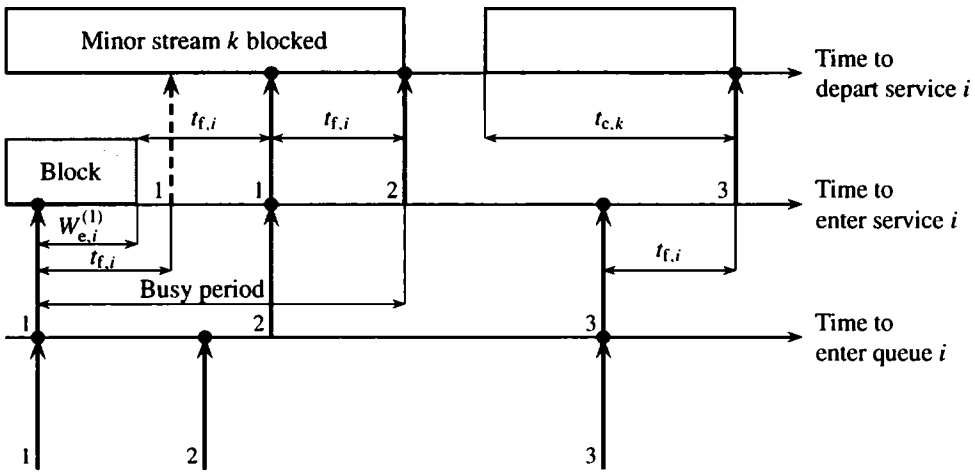

Figure 3.17: A queuing model having service times extended by blocks

In both models the service departure times of stream i vehicles are equal. In both models the busy period ends as server i becomes idle. During busy periods the entry of stream i vehicles may be blocked by Rank 1 vehicles. The starting time of a busy period is, however, different in the models. The model in Figure 3.17 includes in the busy period the time that the first vehicle is waiting for an antiblock, while this time is excluded from the busy period in model 3.16. Because a Rank 2 vehicle waiting for entry prevents the entry of a Rank 3 vehicle, this time period is not available for gap acceptance. Accordingly, the capacity of a Rank 3 stream should be estimated using the model in Figure 3.17. In this model service time is the sum of two components: *waiting time at yield/stop line* and *follow-up time* (Yeo & Weesakul 1964). See Section 4.2 for more details.

According to Kimber, Summersgill & Burrow (1986) a queuing vehicle enters service when the previous vehicle has crossed the yield/stop line. Follow-up time is at the beginning of a service time, before a queuing vehicle reaches the yield/stop line. For non-queuing vehicles service begins when they arrive to the yield/stop line, and service time does not include the follow-up time. In this model follow-up time is interpreted as the time required for a queuing vehicle to move to the yield/stop line. The length of the service time before a minor stream vehicle reaches the yield/stop line depends on the departure time of the vehicle ahead. See also Kremser (1964).

In this report it is assumed that service of all vehicles begins when they reach the yield/stop line. After crossing the yield/stop line a vehicle is being served until the end of the follow-up time, as displayed in Figure 3.17 (see Weiss & Maradudin 1962, Dunne

& Buckley 1972, Daganzo 1977, Pöschl 1983). Follow-up time is interpreted as a safety zone behind a vehicle crossing a yield/stop, which postpones the opportunity of the next vehicle to enter the yield/stop line, and also the departure of a lower priority vehicle. The definition of service time is the same for all vehicles, also for vehicles arriving during the follow-up time of the previous vehicle. The measurement of a follow-up time is initialized when a vehicle crosses the yield/stop line.

3.5.3 Rank 2 queue discharge

Let us assume that the arrival processes of all streams are Poisson (see Section 2.3.3). Minor stream i vehicles accept lags and headways that are not shorter than the critical gap ($t_{c,i}$). The minimum interdeparture time of minor-stream vehicles is equal to the follow-up time ($t_{f,i}$).

The utilization factor of a server in a Rank 2 stream i is

$$\rho_i = \frac{q_i \bar{S}_i}{3600} \approx \frac{q_i}{C_{p,i}} = \rho_i', \tag{3.65}$$

where ρ_i' is the D/C ratio, and the potential capacity $C_{p,i}$ is calculated using the equation (3.12) above. Utilization factor ρ_i is the fraction of time that server i is busy. The average service time $\bar{S}_i$ is approximately equal to the inverse capacity. (See section 4.2 for details.) For the sake of simplicity, the utilization factor (ρ) and the D/C ratio (ρ') are here assumed equal, unless otherwise stated.

The fraction of randomly arriving (Poisson) vehicles in stream i having to wait for service is equal to the fraction of vehicles arriving when the server is busy, which is equal to the utilization factor ρ_i (Khintchine 1960). These vehicles discharge from a queue and their headways cannot be used by minor stream drivers. Other $(1 - \rho_i)$ vehicles enter the intersection without queuing, although they may have had to wait for an antiblock at the stop line.

The number of queue discharge headways per hour is $\rho_i q_i$. Because the average queue discharge headway is $C_{p,i}^{-1}$, the fraction of time required for queue discharge is $\rho_i q_i C_{p,i}^{-1} = \rho_i^2$. During queue discharge the departure flow rate of stream i is $C_{p,i} = q_i \rho_i^{-1}$. The flow rate can be expressed as the sum of flows during the queue discharge and free departure periods:

$$q_i = \rho_i^2 \frac{q_i}{\rho_i} + (1 - \rho_i^2) q_i^*, \tag{3.66}$$

where q_i^* is the average flow rate during the free departure periods. The vehicles departing during the free departure periods do not have to wait for service, although the service times may be extended by higher priority vehicles. The average flow rate during the free departure periods can be solved from equation (3.66) as

$$q_i^* = \frac{q_i}{1 + \rho_i}. \tag{3.67}$$

The average free departure headway of stream i can now be expressed as

$$\bar{t}_i^* = \frac{3600}{q_i^*} = 3600 \left(\frac{1}{q_i} + \frac{1}{C_{p,i}} \right). \tag{3.68}$$

It is the sum of average arrival headway and average service time. If Rank 1 flows approach zero, $C_{p,i}^{-1}$ approaches $t_{f,i}$ and the average free departure headway in stream i approaches $\lambda_i^{-1} + t_{f,i}$.

Following Figure 3.18 an analysis period τ of stream i can be divided into two distinct time periods: queue discharge and free departures. During a queue-discharge period of length $\rho_i^2\tau$ the departure flow rate is $C_{\mathrm{p},i}$. The free departure period lasts for $(1-\rho_i^2)\tau$, and has flow rate $q_i(1+\rho_i)^{-1}$.

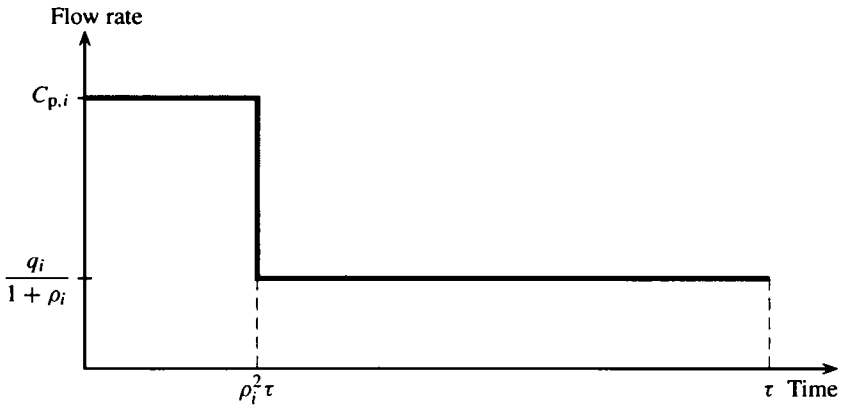

Figure 3.18: Flow rates during queue-discharge and free-flow periods

As presented in equation (3.7), capacity is the product of expected departures during a randomly selected headway multiplied by the expected number of headways per time unit. The number of queue discharge headways in stream i is $\rho_i q_i$. The number of headways available for gap acceptance is $(1-\rho_i)q_i$ (Gipps 1982). Because no headway can be shorter than the follow-up time, the headway distribution should be modified as $f_i\left(t \mid T \geq t_{\mathrm{f},i}\right)$ (Dunne & Buckley 1972, Siegloch 1973).

3.5.4 Rank 3 capacity with no Rank 1 conflict

Dunne & Buckley (1972) have studied the capacity of a Rank 3 stream with no Rank 1 conflict, but Rank 2 stream modified by filtering through a Rank 1 stream. A similar model is discussed here, but in this model a Rank 3 vehicle cannot proceed, if a Rank 2 vehicle is waiting for entry.

If Rank 3 vehicles can ignore other priority streams besides stream i (as in Fig. 3.19), the movement capacity of a Rank 3 stream k is:

$$\begin{aligned} C_{\mathrm{m},k} &= (1-\rho_i)q_i \int_0^\infty \alpha(t) f_i\left(t \mid T \geq t_{\mathrm{f},i}\right) \mathrm{d}t \\ &= \frac{(1-\rho_i)q_i}{R_i\left(t_{\mathrm{f},i}\right)} \int_0^\infty \alpha(t) f_i(t) \mathrm{d}t \\ &= \frac{(1-\rho_i)}{R_i\left(t_{\mathrm{f},i}\right)} C_{\mathrm{p},k}, \end{aligned} \tag{3.69}$$

where $C_{\mathrm{p},k}$ is the potential capacity obtained by the methods above. The capacity is adjusted for Rank 2 queues by $(1-\rho_i)$ and for the modified headway distribution by $\left[R_i\left(t_{\mathrm{f},i}\right)\right]^{-1}$. For a stepwise gap acceptance function (3.9) the capacity is obtained as

$$\begin{aligned} C_{\mathrm{m},k} &= (1-\rho_i)q_i \sum_{j=0}^{\infty} R_i\left(t_{\mathrm{c},k} + jt_{\mathrm{f},k} \mid T \geq t_{\mathrm{f},i}\right) \\ &= \frac{(1-\rho_i)q_i}{R_i\left(t_{\mathrm{f},i}\right)} \sum_{j=0}^{\infty} R_i\left(t_{\mathrm{c},k} + jt_{\mathrm{f},k}\right). \end{aligned} \tag{3.70}$$

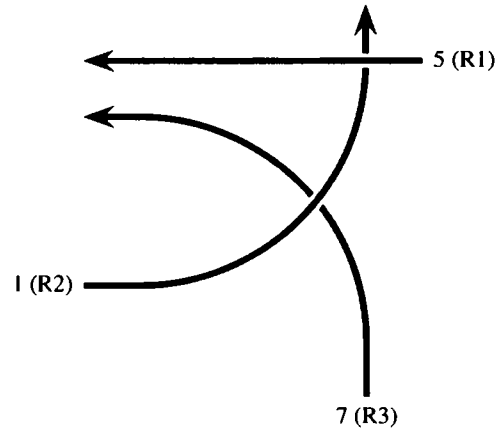

Figure 3.19: Three ranks of streams with no conflict between ranks 1 and 3

For random (exponential) headways in stream i and no Rank 1 flow the movement capacity of a Rank 3 stream k is

$$\begin{aligned} C_{\mathrm{m},k} &= \frac{(1-\rho_i)q_i}{\mathrm{e}^{-\lambda_i t_{\mathrm{f},i}}} \times \frac{\mathrm{e}^{-\lambda_i t_{\mathrm{c},k}}}{1-\mathrm{e}^{-\lambda_i t_{\mathrm{f},k}}} \\ &= \frac{(1-\rho_i)q_i \mathrm{e}^{-\lambda_i (t_{\mathrm{c},k}-t_{\mathrm{f},i})}}{1-\mathrm{e}^{-\lambda_i t_{\mathrm{f},k}}}. \end{aligned} \tag{3.71}$$

The equation has the same form as Tanner's capacity formula (3.24). This was to be expected, because in the absence of Rank 1 flows $\rho_i = \lambda_i t_{\mathrm{f},i}$, and the Rank 2 flow i is a departure process from an M/D/1 queuing system (see also Dunne & Buckley 1972). Constrained headways have a fixed length, and unconstrained headways follow the shifted exponential distribution.

3.5.5 Time available for gap acceptance

Harders (1968) proposed that, when no Rank 2 vehicles are queuing, the movement capacity of Rank 3 streams can be estimated assuming independent priority streams.[8] When there is a queue of Rank 2 stream i vehicles, no Rank 3 stream k vehicles can enter the intersection. Thus the movement capacity of stream k can be expressed as

$$C_{\mathrm{m},k} = p_{0,i} C_{\mathrm{p},k}, \tag{3.72}$$

where $p_{0,i}$ is the probability of empty queue in stream i, and $C_{\mathrm{p},k}$ is the potential capacity of stream k assuming independent priority streams.

Harders (1968) observed that the flow rate in a Rank 2 stream i can be expressed as the sum of delayed and undelayed vehicles. During a proportion of time $1 - p_{0,i}$ vehicles discharge from queue at flow rate $C_{\mathrm{p},i}$. When there is no queuing, a vehicle can enter the intersection without delay, if there is an antiblock in the Rank 1 stream j and the headway in the Rank 2 stream i is longer than the follow-up time $t_{\mathrm{f},i}$. Assuming Poisson arrivals Harders expressed flow rate q_i as

$$q_i = (1 - p_{0,i}) C_{\mathrm{p},i} + p_{0,i} \chi q_i, \tag{3.73}$$

where χ is the probability of an antiblock in the Rank 1 stream j and a headway larger than the follow-up time in Rank 2 stream i:

$$\begin{aligned} \chi &= \mathbb{P}\{\Upsilon_j \geq t_{\mathrm{c},i}\}\, \mathbb{P}\{T_i \geq t_{\mathrm{f},i}\} \\ &= \mathrm{e}^{-t_{\mathrm{c},i} q_j / 3600} \mathrm{e}^{-t_{\mathrm{f},i} q_i / 3600} \\ &= \mathrm{e}^{(t_{\mathrm{c},i} q_j + t_{\mathrm{f},i} q_i)/3600}. \end{aligned} \tag{3.74}$$

[8]This assumption is correct for Poisson arrivals only. As Rank 2 queue clears, the first vehicle in a Rank 3 stream queue faces not a gap but a lag.

The probability of empty queue in stream i was then obtained as

$$p_{0,i} = \frac{C_{p,i} - q_i}{C_{p,i} - \chi q_i}. \tag{3.75}$$

Harders called $p_{0,i}$ an *impedance factor*. Figure 10-5 in HCM 1985 (Transportation Research Board 1985) is based on this equation (see Brilon 1988*a*).

In HCM2000 (Transportation Research Board 2000) the impedance factor $p_{0,i}$ is the probability that at a random time instant the system in stream i is empty; i.e.,

$$p_{0,i} = 1 - \rho_i \approx 1 - \frac{q_i}{C_{p,i}} = 1 - \rho_i', \qquad \rho_i \leq 1, \tag{3.76}$$

where the utilization factor (ρ_i) of the queuing system in stream i is approximated as the D/C ratio (ρ_i'), q_i is the arrival flow rate, and $C_{p,i}$ is the potential capacity of stream i. Brilon (1988*a*) and Grossmann (1991) have demonstrated that equation (3.76) gives acceptable results. Equation (3.72) is used to calculate the movement capacity.

This method has three problems:

1. The impedance factor p_0 is interpreted as the fraction of time available for gap acceptance, whereas it should be interpreted as the fraction of headways available for gap acceptance, as shown in Section 3.1.

2. The utilization factor ρ overestimates the impedance effect of a Rank 2 stream.

3. The distribution of Rank 2 stream headways during the gap acceptance periods should be modified to exclude headways shorter than the follow-up time $t_{f,i}$ and to adjust the flow rate during free-departure conditions accordingly (Siegloch 1973).

These modifications are discussed below.

When a priority vehicle in queuing models of Figures 3.16 and 3.17 has departed service, the next vehicle in the same stream or in a minor stream can enter service. The critical gaps for Rank 3 vehicles are evaluated backward from these time instants.

The critical gap of a minor stream includes the follow-up times of priority stream vehicles. Thus, the blocking effect of vehicle 1 in Figure 3.17 does not start as a vehicle enters service, but from the "virtual departure time" (dashed arrow) that it would have departed service if the entry was not blocked by Rank 1 vehicles. It is also obvious, that the blocking effect of an isolated vehicle 3 is $t_{c,k}$, not $t_{c,k} + t_{f,i}$. The follow-up time of an isolated vehicle should be included as time available for Rank 3 gap acceptance. The time period blocked by a freely departing vehicle is equal to the critical gap, and it is considered in the gap acceptance process.[9] This is evident, if we consider a situation having no Rank 1 flow and no queuing in a Rank 2 stream. The impedance factor should be equal to unity. Consequently, the *time period blocked by queuing Rank 2 vehicles is the busy period minus the follow-up time.*

If a busy period in stream i ends at time τ, the following idle time is the lag $\Upsilon_i(\tau)$ remaining at time τ. For random (Poisson) arrivals the average idle period is equal to the average lag, which is equal to the average headway λ_i^{-1}. If the average length of a busy period is $\mathbb{E}[T_{bp,i}]$ and the average length of an idle period is $\mathbb{E}[T_{ip,i}] = \lambda_i^{-1}$, then

[9] Akçelik (1994*a*) includes the follow-up times of all major stream vehicles in antiblocks, but subtracts follow-up time from critical gap.

for a queuing process with Poisson arrivals holds (Gross & Harris 1974)

$$\frac{\rho_i}{1-\rho_i} = \frac{\mathbb{E}[T_{\mathrm{bp},i}]}{\mathbb{E}[T_{\mathrm{ip},i}]} = \lambda_i \, \mathbb{E}[T_{\mathrm{bp},i}]. \tag{3.77}$$

The expected length of a busy period is now obtained as

$$\mathbb{E}[T_{\mathrm{bp},i}] = \frac{\rho_i}{\lambda_i(1-\rho_i)}. \tag{3.78}$$

The average busy cycle is the expected sum of busy and idle periods:

$$\mathbb{E}[T_{\mathrm{bc},i}] = \mathbb{E}[T_{\mathrm{bp},i}] + \mathbb{E}[T_{\mathrm{ip},i}] = \frac{\rho_i}{\lambda_i(1-\rho_i)} + \frac{1}{\lambda_i} = \frac{1}{\lambda_i(1-\rho_i)}. \tag{3.79}$$

The proportion of randomly arriving (Poisson) vehicles having to wait for service is the proportion of vehicles arriving during a busy period (see Khintchine 1960):

$$p_{\mathrm{w},i} = \frac{\lambda_i \, \mathbb{E}[T_{\mathrm{bp},i}]}{\lambda_i \, \mathbb{E}[T_{\mathrm{bc},i}]} = \rho_i. \tag{3.80}$$

This proportion does not include the vehicles, whose service initiated the busy periods. The proportion of time available in a Rank 1 stream for gap acceptance is obtained as

$$\begin{aligned} f_{\mathrm{a},i} &= 1 - \frac{\mathbb{E}[T_{\mathrm{bp},i}] - t_{\mathrm{f},i}}{\mathbb{E}[T_{\mathrm{bc},i}]} \\ &= 1 - \rho_i + \frac{t_{\mathrm{f},i}}{\mathbb{E}[T_{\mathrm{bc},i}]} \\ &= (1 + \lambda_i t_{\mathrm{f},i})(1-\rho_i) \\ &= \left(1 + \frac{q_i t_{\mathrm{f},i}}{3600}\right)\left(1 - \frac{q_i}{C_i}\right). \end{aligned} \tag{3.81}$$

This is the proportion of time during which queuing stream i vehicles do not block the entry of Rank 3 vehicles; i.e., the proportion of time during which the Rank 2 departure headways (real and virtual) follow the shifted exponential distribution. As capacity approaches $t_{\mathrm{f},i}^{-1}$, the impedance factor approaches the probability $1-\rho_i^2$ of no queue (at most one customer in system) in an M/G/1 queuing system.[10] If stream i is congested ($\rho_i > 1$), the server does not have idle periods and the adjustment factor is zero. In order to avoid negative values of $f_{\mathrm{a},i}$, the equation should be slightly modified:

$$\boxed{f_{\mathrm{a},i} = \left(1 + \frac{q_i t_{\mathrm{f},i}}{3600}\right)\left(1 - \frac{q_i}{C_i}\right)_+}. \tag{3.82}$$

As Figure 3.20 displays, the factor $f_{\mathrm{a},i}$ assigns a larger proportion of time to gap acceptance than $p_{0,i} = 1 - \rho_i$. The difference between $p_{0,i}$ and $f_{0,i}$ increases as potential capacity $C_{\mathrm{p},i}$ increases, because then busy cycles become shorter.

[10] Kendall (1951) has shown that for Poisson arrivals the probability of a queue length left behind by a departing customer is geometric: $p_n = (1-\rho)\rho^n$. Thus the probability that a departing customer leaves behind at most one customer is $(1-\rho) + (1-\rho)\rho = 1-\rho^2$. For Poisson arrivals this is also the queue size distribution for a outside observer (see Cooper 1981); i.e., the probability that at a random time instant no vehicles are waiting for service. A process having Poisson arrivals also has the PASTA (Poisson arrivals see time averages) property (Wolff 1989).

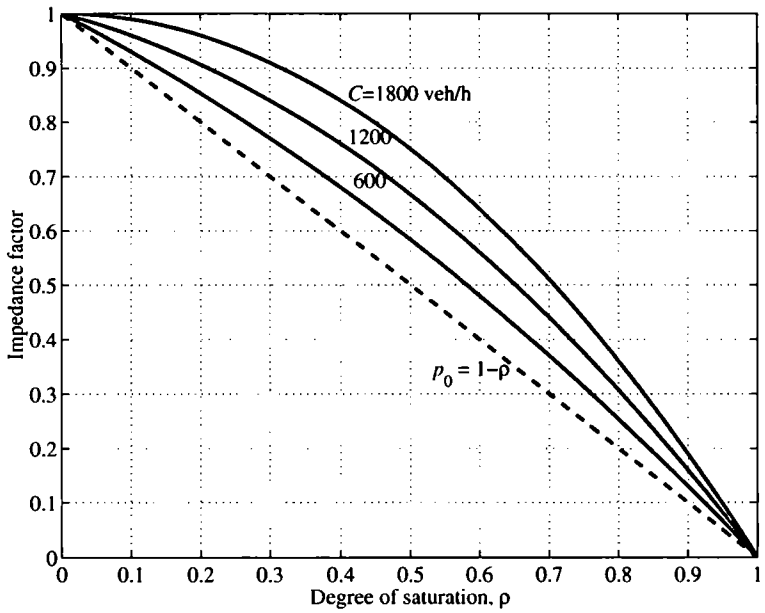

Figure 3.20: Two impedance factors: p_0 (dashed line) and f_a (solid curves)

In Figure 3.20 the follow-up time is $t_{f,i} = 2$ seconds. Capacity 1,800 veh/h is attained, when there is no conflicting higher priority traffic. Even then the impedance factor decreases to zero as the D/C ratio increases to unity. This indicates that the model accounts for a bottleneck effect. Because the discharge headway of vehicles entering the intersection cannot be shorter than $t_{f,i}$, a turning movement may have queue formation even though there is no conflicting higher priority traffic. Furthermore, at low degrees of saturation the drop in the time available for gap acceptance is not as steep as $p_{0,i}$ indicates.

Because $f_{a,i}$ is the time available for gap acceptance, the number of Rank 1 stream j headways available for gap acceptance[11] is $f_{a,i}q_j$. As noted above, the number of Rank 2 stream i headways available is $(1 - \rho_i)q_i$. The adjustments are different, because Rank 2 headways during a gap acceptance period are all larger than $t_{f,i}$, including the first one.

3.5.6 Gap availability for Rank 3 vehicles

The discussion above has demonstrated that the fraction of Rank 2 stream i headways available for Rank 3 gap acceptance is $1 - \rho_i$. These may be headways of either real or virtual stream i departures. The fraction of time $f_{a,i}$ available for gap acceptance is given by equation (3.82), which also gives the fraction of Rank 1 stream j headways available for gap acceptance. The total number of available headways per hour is

$$q_M^* = (1 - \rho_i)q_i + f_{a,i}q_j = (1 - \rho_i)\left[q_i + \left(1 + \frac{q_i t_{f,i}}{3600}\right)q_j\right]. \qquad (3.83)$$

[11] In capacity estimation the lags and headways available for gap acceptance can be assumed to form a continuous time period during which the nonqueuing major-stream vehicles arrive. See Figure 3.18. The resulting headways are available for gap acceptance.

In order to derive the equation for movement capacity, it is necessary to obtain the distribution of headways during the gap acceptance periods. As indicated earlier these are headways of either real of virtual priority stream departures.

Traffic flow is described as a point process, where the location of a point on a time axis describes the departure time of a vehicle from a service process. A Rank 3 vehicle observes two point processes: process 'I' for Rank 1 departures and process 'II' for Rank 2 departures. Let us assume that all arrivals can be described as a Poisson process. Process I is independent of other streams, so that its headways follow the negative exponential distribution with location parameter λ_I. The headways available for gap acceptance in process II follow shifted exponential distribution with scale parameter λ_{II}, which is equal to the scale parameter of the exponential arrival headway distribution. The location parameter (minimum headway) is equal to the follow-up headway $t_p = t_{f,II}$. Because departure times of delayed vehicles have been replaced by virtual departure times, the virtual flow rate of stream II during gap acceptance periods is

$$q_{a,II} = 3600\lambda_{a,II} = \frac{3600\lambda_{II}}{1 + \lambda_{II} t_{f,2}}. \tag{3.84}$$

which is the flow rate of the shifted exponential headway process.

Because all service times in the Rank 2 stream exceeding $t_{f,2}$ have been excluded, these two processes can be considered independent. The process observed by the Rank 3 vehicles is the superposition of processes 1 and 2. The survivor function of intervals (headways) in a superimposed process of two component processes is

$$R(t) = p_I R_I(t)\, R_{\Upsilon,II}(t) + p_{II} R_{II}(t)\, R_{\Upsilon,I}(t)\,, \tag{3.85}$$

The proportions of points from both component processes are

$$p_I = \frac{\lambda_I}{\lambda_I + \lambda_{a,II}} = \frac{\lambda_I(1 + \lambda_{II} t_p)}{\lambda_I(1 + \lambda_{II} t_p) + \lambda_{II}} \tag{3.86}$$

$$p_{II} = \frac{\lambda_{a,II}}{\lambda_I + \lambda_{a,II}} = \frac{\lambda_{II}}{\lambda_I(1 + \lambda_{II} t_p) + \lambda_{II}}. \tag{3.87}$$

where $\lambda_{a,II} = \lambda_{II}(1+\lambda_{II} t_p)^{-1}$. The same results are obtained, if p_I and p_{II} are calculated with $\lambda_{a,I} = f_{a,II}\lambda_I = (1+\lambda_{II} t_p)(1-\rho_{II})\lambda_I$ and $\lambda_{a,II} = (1-\rho_{II})\lambda_{II}$. The survivor function can now be expressed as

$$\begin{aligned} R(t) &= \left(\frac{p_I}{1 + \lambda_{II} t_p} + p_{II}\right) e^{-(\lambda_I+\lambda_{II})t + \lambda_{II} t_p} \\ &= \frac{\lambda_I + \lambda_{II}}{\lambda_I(1 + \lambda_{II} t_p) + \lambda_{II}} e^{-(\lambda_I+\lambda_{II})t + \lambda_{II} t_p}, \qquad t \geq t_p. \end{aligned} \tag{3.88}$$

If $t_p = 0$, we get the survivor function of negative exponential distribution with scale parameter $\lambda = \lambda_I + \lambda_{II}$, as expected.

3.5.7 Movement capacity under one Rank 2 stream

When minor stream gap acceptance follows the step function (3.9), the movement capacity of a Rank 3 stream k can be obtained as

$$\begin{aligned}
C_{m,k} &= q_M \sum_{i=0}^{\infty} R(t_{c,k} + i t_{f,k}) \\
&= \frac{3600(1-\rho_{II})(\lambda_I(1+\lambda_{II}t_p)+\lambda_{II})(\lambda_I+\lambda_{II})}{\lambda_I(1+\lambda_{II}t_p)+\lambda_{II}} \sum_{i=0}^{\infty} e^{-(\lambda_I+\lambda_{II})(t_{c,k}+it_{f,k})+\lambda_{II}t_p} \\
&= 3600(1-\rho_{II})(\lambda_I+\lambda_{II}) e^{-(\lambda_I+\lambda_{II})t_{c,k}+\lambda_{II}t_p} \sum_{i=0}^{\infty} e^{-(\lambda_I+\lambda_{II})it_{f,k}} \\
&= 3600(1-\rho_{II})(\lambda_I+\lambda_{II}) \frac{e^{-(\lambda_I+\lambda_I)t_{c,k}+\lambda_{II}t_p}}{1-e^{-(\lambda_I+\lambda_{II})t_{f,k}}} \\
&= \boxed{(1-\rho_{II})(q_I+q_{II}) \frac{e^{|-(q_I+q_{II})t_{c,k}+q_{II}t_p|/3600}}{1-e^{-(q_I+q_{II})t_{f,k}/3600}},} \qquad t_p < t_{c,k} \\
&= f_{II} C_{p,k},
\end{aligned} \tag{3.89}$$

where

$$\boxed{f_{II} = \frac{(1-\rho_{II})}{e^{-q_{II}t_p/3600}}} \tag{3.90}$$

is the impedance factor due to Rank 2 stream II queuing, $t_p = t_{f,II}$ is the follow-up time of the Rank 2 stream, and $C_{p,k}$ is the potential capacity (3.12) assuming a Poisson priority stream with flow rate $q_I + q_{II}$, critical gap $t_{c,k}$, and follow-up time $t_{f,k}$. The Rank 1 priority streams used in the analysis of ρ_{II} may be different than the Rank 1 priority streams of stream k. The denominator in the impedance factor is the probability of a headway or lag larger than t_p in the Poisson process of the Rank 2 stream. It adjusts the capacity for the filtered headway distribution (and lower flow rate) of the Rank 2 stream during the periods available for Rank 3 gap acceptance. The result is similar to equation (3.70). The relation between f_{II} and the HCM2000 impedance factor $p_{0,II}$ is

$$f_{II} = \frac{p_{0,II}}{e^{-q_{II}t_{f,II}/3600}}. \tag{3.91}$$

If $q_{II} = 0$, equation (3.89) is equal to the capacity equation (3.12) for Poisson priority flow. If $q_I = 0$, equation (3.89) is equal to Tanner's formula (3.24), as indicated in example 3.1 on page 83.

Capacity equation (3.89) can be obtained directly from equation (3.46) by setting number of headways $q_I^* = (1+\lambda_{II}t_p)(1-\rho_{II})q_I$, $q_{II}^* = (1-\rho_{II})q_{II}$, scale parameters $\theta_I = \lambda_I$, $\theta_{II} = \lambda_{II}$, and minimum headways $t_{f,I} = 0$ and $t_{f,II} = t_p$:

$$\begin{aligned}
C_{m,k} &= \frac{e^{-(\lambda_I+\lambda_{II})t_{c,k}+\lambda_{II}t_p}(q_I+q_{II})(1+\lambda_{II}t_p)(1-\rho_{II})}{\left(1-e^{-(\lambda_I+\lambda_{II})t_{f,k}}\right)(1+\lambda_{II}t_p)} \\
&= (1-\rho_{II})(q_I+q_{II}) \frac{e^{|-(q_I+q_{II})t_{c,k}+q_{II}t_p|/3600}}{1-e^{-(q_I+q_{II})t_{f,k}/3600}}, \qquad t_p < t_{c,k}
\end{aligned} \tag{3.92}$$

Figure 3.21 displays the capacity of a Rank 3 stream with different Rank 2 and total (Rank 1 + Rank 2) major-stream flow rates. The critical gap of both Rank 2 and Rank

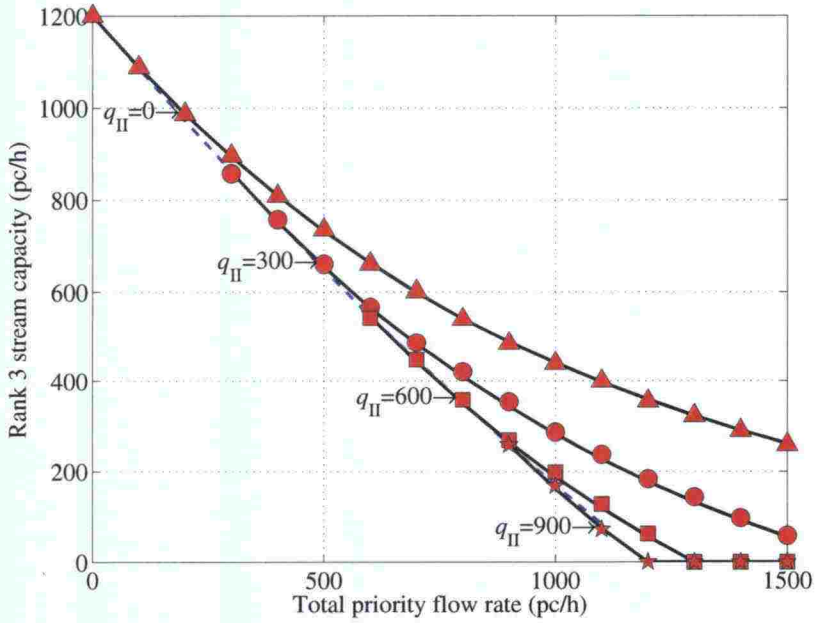

Figure 3.21: Movement capacity of a Rank 3 stream with different Rank 2 (q_{II}) and total priority flow rates. Critical gaps and follow-up times of both Rank 2 and Rank 3 streams are 5 s and 3 s, respectively. Capacities were calculated with equation (3.89) and Monte Carlo simulation (markers). Dashed curve shows Tanner's capacity (3.24) with no Rank 1 flow and Rank 2 stream minimum headway equal to the follow-up time.

3 vehicles is five seconds and follow-up time three seconds. The capacities of equation (3.89) are compared with results of Monte Carlo simulations.

If there are no priority flows, the capacity is $3600/t_{f,k} = 1200$ veh/h. For zero Rank 2 flows Rank 3 capacity is obtained with the equation (3.12) for Poisson priority flow, displayed as the upper curve in Figure 3.21. For zero Rank 1 flows the capacity is obtained with Tanner's capacity formula (3.24), displayed as a dashed curve in Figure 3.21. When $q_I = 0$ veh/h and $q_{II} = 1200$ veh/h, no headways are available for Rank 3 gap acceptance, and Rank 3 capacity is zero. The Rank 3 capacities for other proportions of Rank 1 and Rank 2 flows are found approximately between the capacity formulas (3.12) and (3.24).

Figure 3.22 displays a comparison of equation (3.89) with HCM2000 capacities. (The HCM adjustment factor 2 for left-turn flows has not been applied.) Dashed curves display the respective capacities with no Rank 1 flows. This is the major difference between equation (3.89) and HCM2000. The latter excludes the follow-up times of all Rank 2 vehicles from the time available for Rank 3 gap acceptance and assumes exponential priority stream headways. Equation (3.89) includes the follow-up times of non-queuing Rank 2 vehicles in the time available for Rank 3 gap acceptance and assumes shifted exponential priority stream headways. It gives a lower Rank 2 flow rate during the gap acceptance periods than the average arrival rate of the (exponential) Rank 2 stream. Consequently, HCM2000 gives much lower capacities at low Rank 1 flows.

Stream 7 at a T-intersection (Fig. 2.3) must give way to Rank 1 streams 2 and 5, and

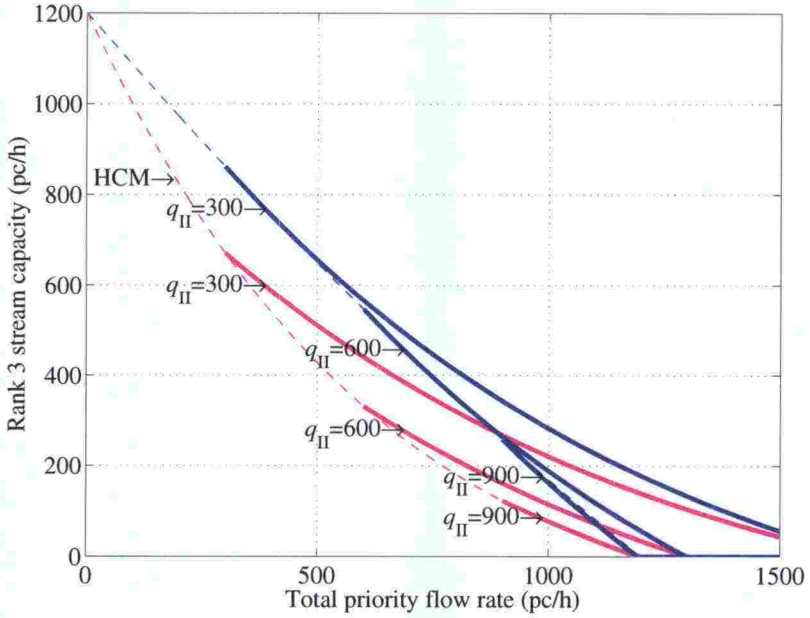

Figure 3.22: Movement capacity of a Rank 3 stream: Equation 3.89 (blue curves) compared with HCM2000 capacities (magenta). Dashed curves display capacities with no Rank 1 flows.

Rank 2 stream 4. Movement capacity is calculated as

$$\boxed{C_{\mathrm{m},7} = f_4 C_{\mathrm{p},7},} \tag{3.93}$$

where

$$\boxed{f_4 = \frac{1 - \frac{q_4}{C_{\mathrm{p},4}}}{\mathrm{e}^{-q_4 t_{\mathrm{f},4}/3600}}.} \tag{3.94}$$

The priority streams of stream 4 used in the calculation of $C_{\mathrm{p},4}$ are $I_4 = \{2, 3\}$. Potential capacity $C_{\mathrm{p},7}$ is calculated assuming priority streams $I_7 = \{2, 4, 5\}$. Rank 1 priority flow is $q_2 + q_5$ plus the possible effect of the major road right-turn stream 3. Rank 2 stream is q_4.

3.5.8 Movement capacity under two Rank 2 streams

In a four-leg intersection (Fig. 2.2, page 26) minor road through streams 8 and 11 have Rank 3. They must give way to Rank 2 streams 1 and 4 (major road left turns). Stream 1 must give way to Rank 1 streams 5 and 6, and stream 4 must give way to streams 5 and 6. The priority streams of minor streams 8 and 11 are $I_8 = \{1, 2, 4, 5, 6\}$ and $I_{11} = \{1, 2, 3, 4, 5\}$.

The impedance factor f_4 of major-road left-turn stream 4 is given above. The impedance factor of stream 1 is likewise

$$\boxed{f_1 = \frac{1 - \rho_1}{\mathrm{e}^{-q_1 t_{\mathrm{f},1}/3600}} = \frac{1 - \frac{q_1}{C_{\mathrm{p},1}}}{\mathrm{e}^{-q_1 t_{\mathrm{f},1}/3600}}.} \tag{3.95}$$

It is the proportion of capacity available due to major stream queuing. Because the queuing processes of streams 1 and 4 are independent, it can be assumed that the

combined impedance factor is the product

$$\boxed{f_{1\wedge 4} = f_1 f_4.} \tag{3.96}$$

This is indeed the case, as will be shown next.

If the other Rank 2 stream is ignored, the proportion of time available for gap acceptance in streams 1 and 4 is

$$\begin{aligned} f_{a,1} &= \left(1 + \frac{q_1 t_{f,1}}{3600}\right)\left(1 - \frac{q_1}{C_1}\right), \qquad q_1 < C_1 \\ f_{a,4} &= \left(1 + \frac{q_4 t_{f,4}}{3600}\right)\left(1 - \frac{q_4}{C_4}\right), \qquad q_4 < C_4. \end{aligned} \tag{3.97}$$

These factors are probabilities that at a random time instant gap acceptance is not restricted by queuing vehicles in the respective stream. Because the queuing processes are independent, the probability that at a random time instant gap acceptance is not restricted by queuing vehicles in either stream is the product

$$f_{a,1\wedge 4} = f_{a,1} f_{a,4}. \tag{3.98}$$

Because this is also the proportion of vehicles in Rank 1 streams arriving during gap acceptance periods, the number of vehicles observed in these streams during the gap acceptance periods is

$$\begin{aligned} q_{a,2} &= f_{a,1\wedge 4} q_2 \\ q_{a,3} &= f_{a,1\wedge 4} q_3 \\ q_{a,5} &= f_{a,1\wedge 4} q_5 \\ q_{a,6} &= f_{a,1\wedge 4} q_6. \end{aligned} \tag{3.99}$$

Of the "free headways" in stream 1 (4) only headways of vehicles arriving during the non-queuing periods of stream 4 (1) can be considered for gap acceptance. Thus,

$$\begin{aligned} q_{a,1} &= f_{a,4}(1 - \rho_1) q_1 \\ q_{a,4} &= f_{a,1}(1 - \rho_4) q_4. \end{aligned} \tag{3.100}$$

Streams 2, 3, 5, and 6 are assumed to be Poisson processes with parameters $\lambda_2 = q_2/3600$, $\lambda_3 = q_3/3600$, $\lambda_5 = q_5/3600$, and $\lambda_6 = q_6/3600$. During the gap acceptance periods streams 1 and 4 are assumed to have shifted exponential headway distributions with scale parameters $\lambda_1 = q_1/3600$ and $\lambda_4 = q_4/3600$ and location parameters equal to the follow-up times $t_{f,1}$ and $t_{f,4}$.

During the time periods available for gap acceptance Rank 2 streams are not blocked by Rank 1 vehicles, so that all streams 1, 2, 4, and 5 can be considered independent. The capacity of streams 8 and 11 can be obtained using equation (3.46) as

$$\begin{aligned} C_{m,8} &= (1 - \rho_1)(1 - \rho_4) \frac{q_M e^{(-q_M t_{c,8} + q_1 t_{f,1} + q_4 t_{f,4})/3600}}{1 - e^{q_M t_{f,8}/3600}} \\ &= \frac{(1 - \rho_1)(1 - \rho_4)}{e^{-q_1 t_{f,1} - q_4 t_{f,4}}} \times \frac{q_M e^{-q_M t_{c,8}/3600}}{1 - e^{q_M t_{f,8}/3600}} \\ &= \boxed{f_{1\wedge 4} \frac{q_M e^{-q_M t_{c,8}/3600}}{1 - e^{q_M t_{f,8}/3600}},} \end{aligned} \tag{3.101}$$

where $q_M = q_1 + q_2 + q_4 + q_5 + q_6$. Likewise, the movement capacity of minor stream 11 is

$$C_{m,11} = f_{1\wedge4}\frac{q_M e^{-q_M t_{c,11}/3600}}{1 - e^{q_M t_{f,11}/3600}}, \tag{3.102}$$

where $q_M = q_1 + q_2 + q_3 + q_4 + q_5$. If $\rho_1 \geq 1$ or $\rho_4 \geq 1$, Rank 3 capacities are zero.

In the calculation of q_M the major-road through flows are adjusted for the possible effects of nonconflicting right-turn streams (stream 3 on stream 8 and stream 6 on stream 11). However, in the estimation of Rank 2 capacities this adjustment is not made, but the effect of major road right-turn streams is considered directly.

3.6 Movement capacity of Rank 4 streams

Rank 4 streams 7 and 10 (left turns from minor road) in four-legged intersections must give way to streams of three higher ranks. A Rank 4 vehicle can enter the intersection when there is an acceptable gap in the priority streams and no conflicting Rank 2 or Rank 3 queues. These queues are, however, not independent. The queues of a Rank 3 stream can discharge when there is a gap larger than the critical gap in Rank 1 and Rank 2 priority streams, and conflicting Rank 2 queues are empty. No analytical equations for Rank 4 stream capacity estimates have been presented (Troutbeck & Brilon 1997).

For Rank 4 stream 7 (10) the conflicting Rank 3 stream is the opposing through stream 11 (8). Conflicting Rank 2 streams are the major-road left-turn streams 1, 4 and the opposing minor road right turning stream 12 (9). The latter stream has no effect on the Rank 3 queues in stream 11 (8). If the major road has separate lanes for entering streams 7 (10) and 12 (9), the streams do not have a conflict.

Because of the mutual dependency of queues, conflicting Rank 2 and Rank 3 queues occur more simultaneously than would be the case, if the queuing processes were independent. Ignorance of this dependency would give too low capacity estimates. Brilon & Großmann (1991) have developed by simulation a corrected probability:

$$p_{z,i} = 0.65 p_{0,1\wedge4\wedge i} - \frac{p_{0,1\wedge4\wedge i}}{p_{0,1\wedge4\wedge i} + 3} + 0.6\sqrt{p_{0,1\wedge4\wedge i}}, \tag{3.103}$$

where $p_{z,i}$ is the probability of empty queues in major road left-turn streams 1, 4, and minor road through stream i, and $p_{0,1\wedge4\wedge i} = p_{0,1} p_{0,4} p_{0,i}$ (see Grossmann 1991, Kyte et al. 1996). This equation is also used in HCM2000 (Transportation Research Board 2000). As Figure 3.23 displays, the corrected probability (thick curve) is larger than the simple product $p_{0,1\wedge4\wedge i}$ (diagonal line). The movement capacity of streams 7 and 10 is calculated as

$$\begin{aligned} C_{m,7} &= p_{z,11} p_{0,12} C_{p,7} \\ C_{m,10} &= p_{z,8} p_{0,9} C_{p,10}. \end{aligned} \tag{3.104}$$

The German HBS2001 (FGSV 2001) uses a different approach:

$$p_{z,i} = \frac{1}{1 + \dfrac{1 - p_{0,1} p_{0,4}}{p_{0,1} p_{0,4}} + \dfrac{1 - p_{0,i}}{p_{0,i}}}. \tag{3.105}$$

The queues of all conflicting priority streams are considered as a single queue. M/M/1 queueing systems are assumed (Brilon, Wu & Bondzio 1997).

Equation (3.105) can also be expressed as

$$p_{z,i} = \frac{p_{0,1\wedge4\wedge i}}{p_{0,1\wedge4} + p_{0,i} - p_{0,1\wedge4\wedge i}}, \tag{3.106}$$

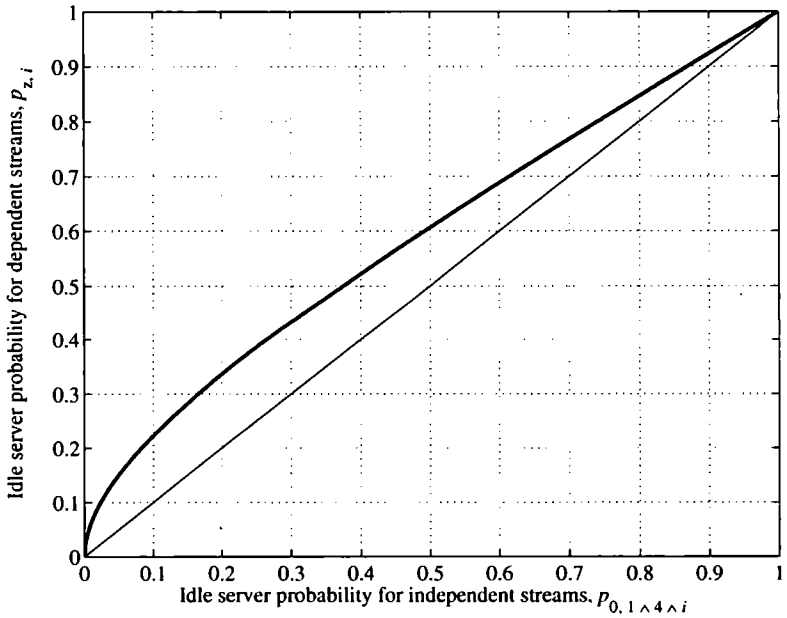

Figure 3.23: Corrected probability of empty queues in streams 1, 4, and i (8 or 11) (Brilon & Großmann 1991)

which can be interpreted as the probability of an idle server in all streams 1, 4, and i under the condition that a server is known to be idle either in both left-turn streams 1 and 4 or in stream i. All service processes are assumed to be independent. The HCM2000 equations (3.104) are used to obtain the movement capacities of streams 7 and 10.

Figure 3.24 displays the German impedance factor against different values of $p_{0,1\wedge4}$ and $p_{0,i}$. When there is no traffic in major-road left-turn streams ($p_{0,1\wedge4} = 1$), the probability of a queue-free state in all priority streams is $p_{0,i}$, as expected. As Figure 3.25 displays, the HCM2000 impedance factor is not consistent under these conditions. The same observation can be made, when there is no traffic in stream i; i.e., $p_{0,i} = 1$. Consequently, equation (3.103) does not fulfill the necessary marginal conditions (Brilon, Wu & Bondzio 1997).

Brilon & Wu (2002) described these approaches as pragmatic simplifications, which are only of an approximative nature. They chose to propose an even simpler approximation (see section 3.10), which is easier to use in practical applications. However, below is described a theoretically more solid approach.

The potential capacity $C_{p,k}$ of a Rank 4 stream k is given by equation (3.12), where the major flow rate q_M is the sum of conflicting higher priority streams. Following equation (3.89) this capacity should be adjusted for the utilization ratio of the server and the modified headway distributions of higher priority streams.

First it is necessary to define a utilization factor of a service system with two streams (i and j) of units (vehicles). The average arrival rates are λ_i and λ_j, and average service times $\bar{S}_i$ and $\bar{S}_j$. The utilization factor is the product of average arrival rate and the average service time. The average arrival rate of units is $\lambda_i + \lambda_j$ and the average service

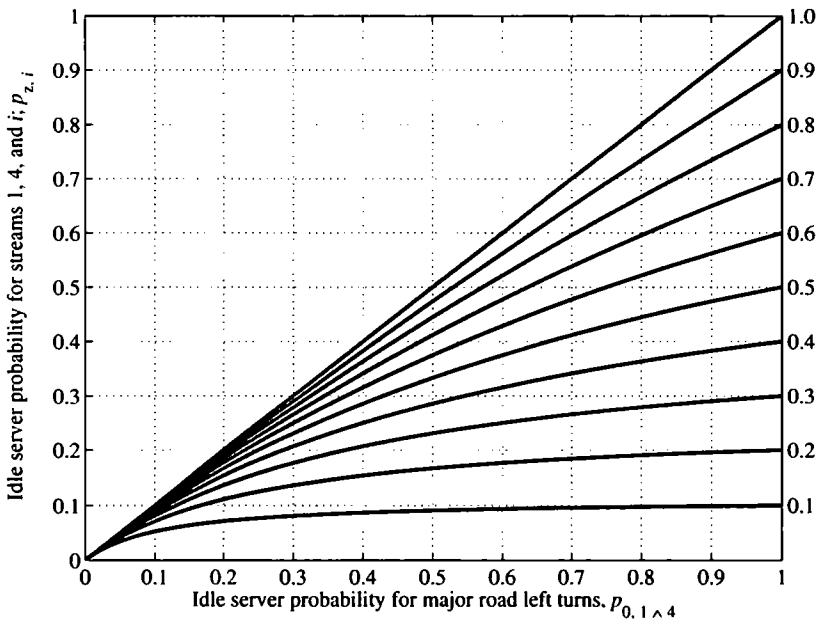

Figure 3.24: German impedance factor $p_{z,i}$ with different values of $p_{0,1\wedge4}$ and $p_{0,i}$ (right) (FGSV 2001)

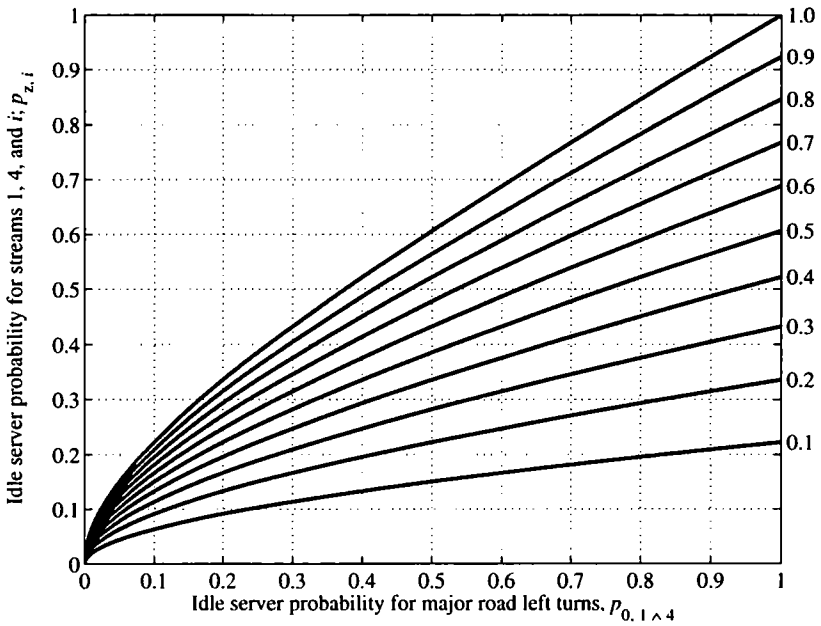

Figure 3.25: HCM2000 impedance factor $p_{z,i}$ with different values of $p_{0,1\wedge4}$ and $p_{0,i}$ (right)

time is the weighted average

$$S = \frac{\lambda_i \bar{S}_i + \lambda_j \bar{S}_j}{\lambda_i + \lambda_j}. \tag{3.107}$$

The utilization factor of the service system is

$$\rho_{i,j} = (\lambda_i + \lambda_j)\bar{S} = \lambda_i \bar{S}_i + \lambda_j \bar{S}_j = \rho_i + \rho_j, \tag{3.108}$$

which is the sum of the utilization factors of the component streams.

The impedance factor $p_{z,i}$ is now derived following the queuing model in Figure 3.16, in which Rank 3 service is interrupted while a Rank 2 vehicle is being served. Because only one server can be busy at one time, the utility factors are additive.

Let us now assume that stream i has Rank 2 and stream j has Rank 3. The arrival rates are $q_i = 3600\lambda_i$ and $q_j = 3600\lambda_j$. Rank 2 stream i has follow-up time $t_{f,i}$ and average service time $\bar{S}_i = 3600/C_{m,i}$. The utilization factor is $\rho_i = \lambda_i \bar{S}_i$. Rank 3 stream j has follow-up time $t_{f,j}$ and movement capacity $C_{m,j}$. The utilization factor ρ_j is different from the demand-to-capacity (D/C) ratio $\rho'_j = q_j/C_{m,j}$. Because stream j vehicles are served only during the fraction $1 - \rho_i$ of time, the average service time is $\bar{S}_j = 3600(1 - \rho_i)/C_{m,j}$ and the utilization factor $\rho_j = \lambda_j \bar{S}_j = (1 - \rho_i)\rho'_j$. This gives an interesting interpretation for the D/C ratio of a Rank 3 stream:

$$\rho'_j = \frac{\rho_j}{1 - \rho_i}. \tag{3.109}$$

The D/C ratio of a Rank 3 stream j gives the probability that at a random time instant a stream j vehicle is being served (waiting for a gap or a follow-up time) under the condition that there are no Rank 2 vehicles in the service system.

The utilization factor of the total service system is

$$\rho_{i,j} = \rho_i + \rho_j = \rho_i + (1 - \rho_i)\rho'_j = \rho_i + \rho'_j - \rho_i \rho'_j, \tag{3.110}$$

which is the probability that there is a vehicle in the service system. The probability of an empty system is now obtained directly as

$$1 - \rho_{i,j} = 1 - \left[\rho_i + (1 - \rho_i)\rho'_j\right] = (1 - \rho_i)(1 - \rho'_j). \tag{3.111}$$

The queuing processes are not independent, but the effect of stream i on the queuing process of stream j is carried in the D/C ratio ρ'_j, as demonstrated above (3.109). For a four-leg intersection this indicates that

$$p_{z,i} = p_{0,1\wedge 4} p_{0,i} = p_{0,1} p_{0,4} p_{0,i}. \tag{3.112}$$

This is displayed in figure 3.26 and as the diagonal line in figure 3.23. It should, however, be observed that the model discussed here includes also a capacity adjustment for the headway distribution of Rank 2 and Rank 3 streams, which adjustment is not included in HCM2000. In addition, equation (3.69) gives higher capacities and lower utilization factors than HCM2000 for Rank 3 streams, which increases the Rank 4 capacity.

The discussion above gives an important result: Capacities of Rank 2, 3, and 4 streams are calculated in a hierarchical order. The capacities of higher priority streams are used as input in the capacity estimation of lower priority flows. These capacity estimates contain all the information necessary about the hierarchy of streams. *When the capacities of major streams are known, their relative priorities can be ignored in the capacity estimation of a minor flow.* If q_i is the flow rate of a stream, which is in a set I_k of

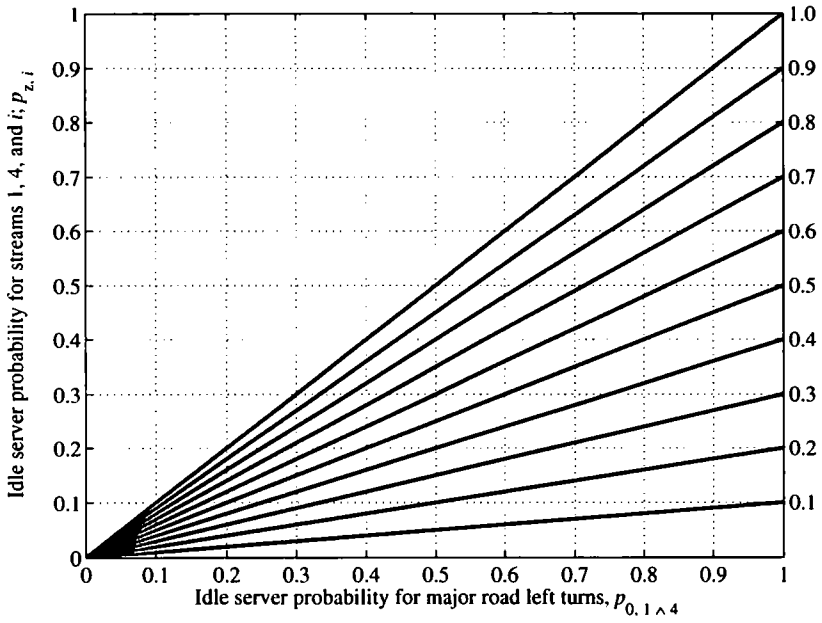

Figure 3.26: Linear impedance factor $p_{z,i}$ with different values of $p_{0,1\wedge4}$ and $p_{0,i}$ (right)

priority streams (Ranks 2 and 3) of minor stream k, the movement capacity of stream k can be expressed as

$$C_{m,k} = \frac{\prod_{i\in I_k} p_{0,i}}{e^{-\sum_{i\in I_k} q_i t_{f,i}/3600}} C_{p,k}, \tag{3.113}$$

where $C_{p,k}$ is the potential capacity of stream k assuming that all major streams are independent, $p_{0,i} = 1 - \rho_i'$, and ρ_i' is the D/C ratio of stream i. This equation can be used to estimate the movement capacity of both Rank 3 and Rank 4 streams.

The set I_k includes only priority streams of Rank 2 and Rank 3. If a Rank 1 stream j with minimum headway $t_{p,j}$ is included in I_k, the headways in stream j are assumed to follow Tanner's distribution. This is equivalent to assuming a conflicting "Rank 0" stream with no traffic. Accordingly, $\rho_j = q_j t_{p,j}/3600$.

Figures 3.27 and 3.28 display the movement capacities of equation (3.113) compared with Monte Carlo simulations. Figures 3.29 and 3.30 show that equation (3.113) gives higher capacities than HCM2000. No adjustments for conflicting flows, as in HCM2000 Exhibit 17-4, have been made.

The movement capacities of streams 7 and 10 are

$$C_{m,7} = \frac{p_{0,1}p_{0,4}p_{0,11}p_{0,12}C_{p,7}}{e^{-(q_1 t_{f,1}+q_4 t_{f,4}+q_{11} t_{f,11}+q_{12} t_{f,12})/3600}} \tag{3.114}$$

$$C_{m,10} = \frac{p_{0,1}p_{0,4}p_{0,8}p_{0,9}C_{p,10}}{e^{-(q_1 t_{f,1}+q_4 t_{f,4}+q_8 t_{f,8}+q_9 t_{f,9})/3600}}, \tag{3.115}$$

where $C_{p,k}$ is the potential capacity of stream k (7 or 10) assuming that all major streams are independent and have negative exponential headway distributions with scale parameter $\lambda_i = q_i/3600$. The possible effect of nonconflicting major-road right-turn streams (3 and 6) should be included in the major-road through-stream (2 and 5) flow rates.

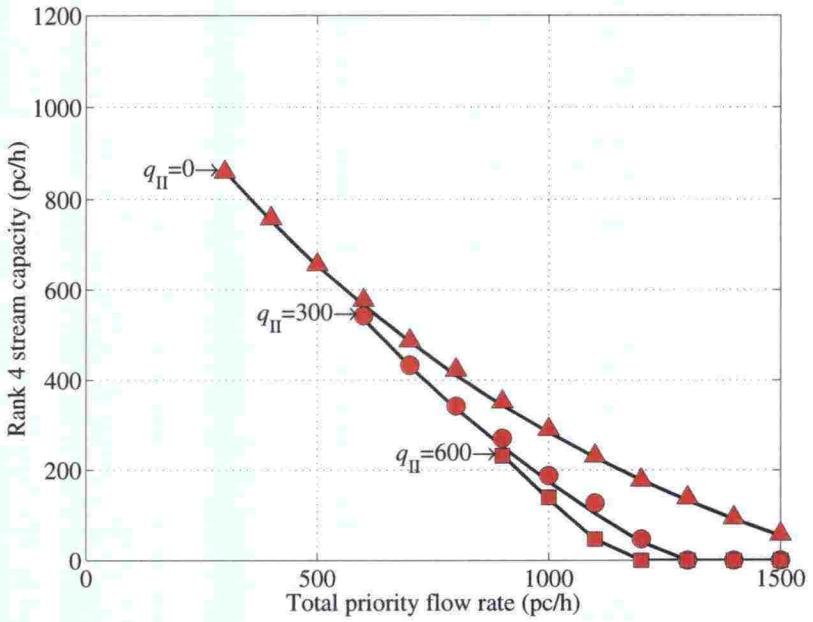

Figure 3.27: Movement capacity (3.113) of a Rank 4 stream when Rank 3 flow rate is $q_{III} = 300$ *veh/h compared with Monte Carlo simulations (markers)*

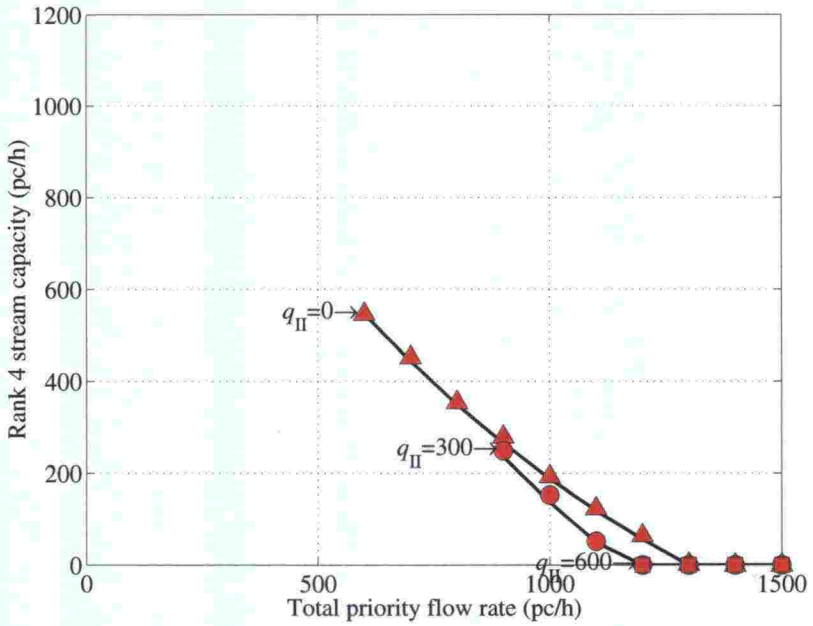

Figure 3.28: Movement capacity (3.113) of a Rank 4 stream when Rank 3 flow rate is $q_{III} = 600$ *veh/h compared with Monte Carlo simulations (markers)*

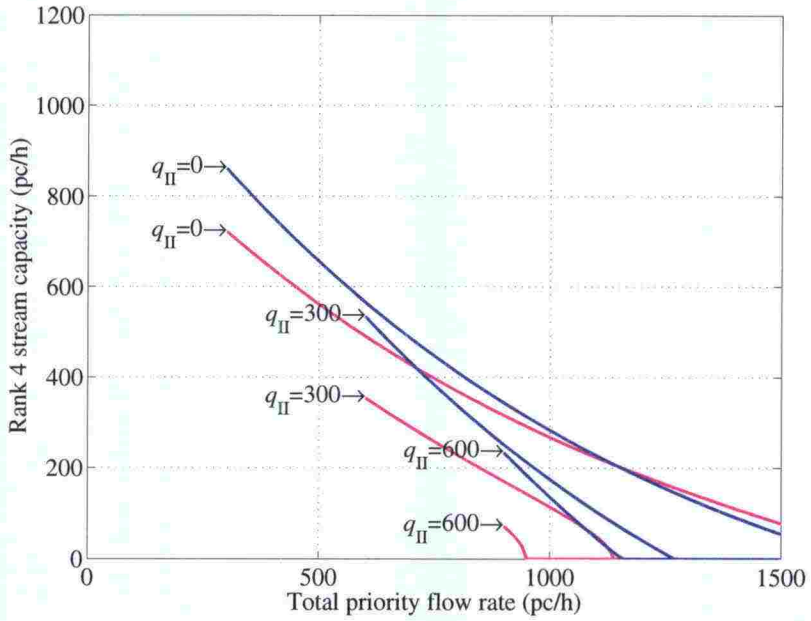

Figure 3.29: Movement capacity (3.113) of a Rank 4 stream when Rank 3 flow rate is $q_{III} = 300$ *veh/h (blue curves) compared with HCM2000 (magenta curves)*

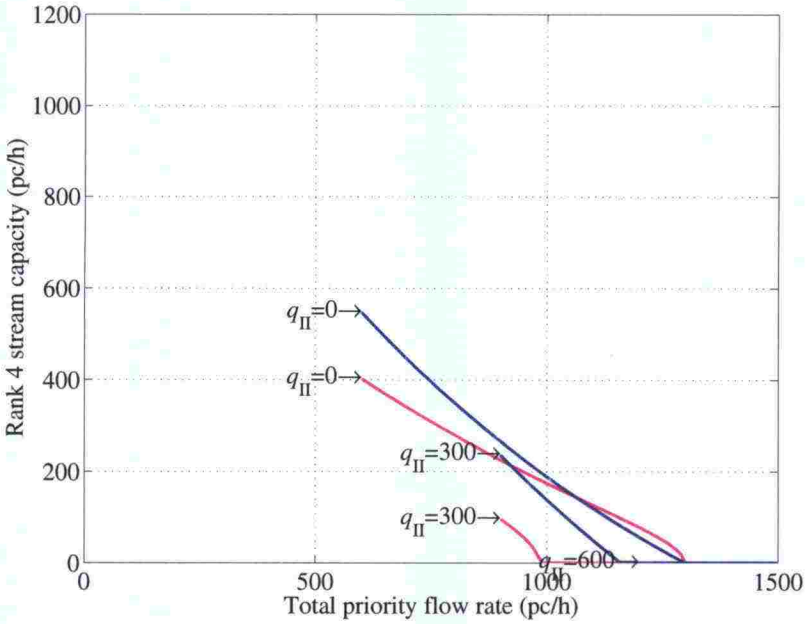

Figure 3.30: Movement capacity (3.113) of a Rank 4 stream when Rank 3 flow rate is $q_{III} = 600$ *veh/h (blue curves) compared with HCM2000 (magenta curves)*

3.7 Shared lanes

On shared lanes multiple streams are combined. If an approach in a four-leg intersection has only one lane, all three streams (left, through, and right) share the same lane.

Hawkes (1966) described a minor-road lane shared by left-turn and right-turn vehicles as an embedded Markov chain (see page 118 below). Fisk & Tan (1989) have modeled a lane shared by two movements as an M/M/1 queuing system with two customer types. The third approach, which is followed here, was presented by Harders (1968). Its is simple and widely applied.

If the movement capacity of stream i is $C_{m,i}$, the average departure headway (service time) from a continuous queue is

$$\bar{S}_{q,i} = \frac{1}{C_{m,i}}. \tag{3.116}$$

The average service time on a lane sharing n streams is

$$\bar{S}_q = \sum_{i=1}^{n} p_i \bar{S}_{q,i} = \sum_{i=1}^{n} \frac{p_i}{C_{m,i}}, \tag{3.117}$$

where p_i is the proportion of stream i on the lane

$$p_i = \frac{q_i}{\sum_{i=1}^{n} q_i} = \frac{q_i}{q}, \tag{3.118}$$

and q is the total flow rate on the shared lane. The shared lane capacity is (Harders 1968, Catchpole & Plank 1986)

$$\boxed{C = \frac{1}{\bar{S}_q} = \frac{1}{\sum_{i=1}^{n} \frac{p_i}{C_{m,i}}} = \frac{q}{\sum_{i=1}^{n} \rho_i},} \tag{3.119}$$

where $\rho_i = q_i / C_{m,i}$. If a shared lane includes Rank 1 streams (major road through and/or right movements) the movement capacity $C_{m,i}$ of a Rank 1 stream i is equal to the saturation flow rate s_i.

The discussion above considers the capacity of a lane shared by several movements. Mathematically these movements are vehicles with different gap acceptance properties. Accordingly, it is possible to extend equation (3.119) to estimate the capacity of lanes shared by any types of heterogeneous vehicles (passenger cars, trucks, RV's) and drivers (men, women, older drivers) (Troutbeck & Brilon 1997). The capacity of a stream having a heterogeneous mixture of vehicle types is the harmonic mean of capacities for each vehicle type, weighted by the frequency of the vehicle type in the subject stream (Catchpole & Plank 1986). That is, the capacity is the inverse of average service times. In fact, this approach is valid for all traffic systems where traffic flows of different capacities are using the same service facility (Kyte et al. 1996).

If Rank 1 (major road through and right turn) vehicles share a lane with a left turn movement, the Rank 1 vehicles may be delayed because of left turning vehicles waiting for an acceptable gap. These delayed Rank 1 vehicles increase the time required for queue discharge on the shared lane. The impedance effect of a shared lane can be estimated following a method proposed by Harders (1968).

Let us assume that a lane is shared by left-turn and through movements. The D/C ratio of the left-turn movement (ρ_L) is obtained following equation (3.65). It is the

fraction of time required for the queue discharge of left-turn vehicles. On a shared lane this fraction of time is increased by the through vehicles joining the queue. Let (ρ_a) designate the fraction of time required for the discharge of through vehicles. Undelayed through vehicles do not form a queue.

The fraction of time required by queue discharge on a shared lane is

$$\rho_S = \rho_L + \rho_a. \tag{3.120}$$

Because through vehicles are assumed to arrive following a Poisson process, the fraction of delayed through vehicles is ρ_S. The fraction of time required by the discharge of delayed through vehicles is

$$\rho_a = \rho_S \frac{q_T}{s_T} = \rho_S \rho_T, \tag{3.121}$$

where q_T, s_T, and ρ_T are the arrival rate, saturation flow rate and D/C ratio of the through stream, respectively. The factor ρ_S is now obtained as (Harders 1968)

$$\rho_S = \rho_L + \rho_S \rho_T = \frac{\rho_L}{1 - \rho_T}. \tag{3.122}$$

If a lane is shared also by a right turning stream having D/C ratio ρ_R, the total utilization factor of Rank 1 streams is the sum $\rho_T + \rho_R$, which gives

$$\boxed{\rho_S = \frac{\rho_L}{1 - (\rho_T + \rho_R)}}. \tag{3.123}$$

Since the 1994 edition (Transportation Research Board 1994) HCM has suggested the use of ρ_S in stead of ρ_L ($L = 1, 4$) to take into account the impedance effect of queue formation on a shared lane.

It should be noted that the fraction of time ρ_S includes all headways less than the follow-up time in the left-turn stream, but not in the through or right-turn streams. Consequently, the headway distribution of the left-turn stream during the time intervals available for Rank 3 and Rank 4 gap acceptance is shifted exponential. The headway distributions of the Rank 1 streams are, however, unmodified (i.e., negative exponential).

3.8 Pedestrian effects

Pedestrians can cross a road in groups. A follow-up time needs to be considered only at very high pedestrian volumes, when pedestrian enter the crosswalk in several rows. The follow-up time is then applied to rows of pedestrians.

The problems regarding pedestrians in the hierarchy of traffic streams have been discussed above (page 28). No rank was assigned to pedestrian flows, because they break the hierarchical structure of vehicular-stream priorities. Because pedestrians do not have an absolute priority, but drivers and pedestrians "negotiate" the priority, the gap acceptance theory is of a limited use.

Below a simple method is presented to estimate the impedance effects of pedestrian (and cyclist) flows. The method is similar to the methods in the HCM2000 (Transportation Research Board 2000) and in the Additive Conflict Flows methodology described in section 3.10.

When a pedestrian or a group of pedestrians crosses a lane of width w_l meters at speed v_p m/s, the lane is blocked for time interval

$$t_{pb} = \frac{w_l}{v_p}. \tag{3.124}$$

Lane width can be adjusted for the length of pedestrian groups.

If pedestrians cross a road in groups of average size n_g, the average number of pedestrian groups per hour is

$$q_g = \frac{q_p}{n_g}, \tag{3.125}$$

where q_p is the hourly flow rate of pedestrians. Furthermore, if vehicles in minor stream k give priority to a fraction $p_{k,j}$ of pedestrian groups in pedestrian stream j, the fraction of time a lane is blocked by pedestrians can be obtained as

$$\rho_j = p_{k,j}\frac{q_g t_{pb}}{3600}. \tag{3.126}$$

It is assumed that pedestrians and vehicles "negotiate" the priority. If a group of pedestrians is given priority, their crossing time is unavailable for gap acceptance. If a group of pedestrians is not given priority, it is assumed that they walk across the road together with the next group of pedestrians that has obtained priority.

At high pedestrian flow rates the pedestrian impedance factor $p_{0,j} = 1 - \rho_j$ should be adjusted for follow-up times between rows of pedestrians crossing a road. Otherwise the pedestrian impedance factor is applied in the same way as the impedance factors of vehicular streams.

3.9 Passenger-car equivalencies

Equation (3.119) can be used to estimate the capacity of a stream consisting of different classes of vehicles with different gap-acceptance properties. Each vehicle class is considered as a separate stream. Brilon (1988*b*) used this approach to confirm the German passenger-car equivalencies presented by Jessen (1968).

The effect of passenger-car equivalencies are not evaluated in this research. It is suggested that the same adjustment factors are used as for the signalized intersections (Luttinen & Nevala 2002).

3.10 Excursion: Additive Conflict Flows methodology

Brilon & Wu (2001, 2002) have suggested the Additive Conflict Flows (ACF) procedure as a third capacity analysis method, besides the empirical regression technique and the gap acceptance procedure. They proposed that the theoretical background of ACF is easier to understand than the theory of gap acceptance. ACF can also better analyze pedestrian and cyclist flows as well as the limited priority effects. The draft chapter for unsignalized intersection capacity analysis is based on the ACF (Brilon & Miltner 2002).

The estimation of ACF parameters has been considered easier than the estimation of gap acceptance parameters. The major advantage is that the capacity of a stream can be calculated as a function of traffic volumes of other streams in a single step. In gap acceptance theory the capacities of higher priority flows are required as parameters for Rank 3 and 4 stream capacity calculations.

The capacity of stream k is the maximum discharge flow rate ($q_{max,k}$) multiplied by the proportion (p_0) of time available for queue discharge:

$$C_k = q_{max,k}p_0 = \frac{3600}{t_{q,k}}p_0, \tag{3.127}$$

where $t_{q,k}$ is the length of time that the conflict area is occupied by a discharging stream k vehicle. It is similar to the follow-up time $t_{f,k}$ in the gap acceptance models. The

probability p_0 that the conflict area is not occupied by another stream is the product

$$p_0 = p_{0,q} p_{0,a}, \tag{3.128}$$

where $p_{0,q}$ is the probability of no queuing or discharging major stream vehicles and $p_{0,a}$ is the probability of no approaching major stream vehicles.

The probability that a conflict area is not blocked by queuing or discharging stream i vehicles is $p_{0,q,i} = 1 - \rho_i = 1 - \lambda_i t_{q,i}$. As in signalized intersections, the D/C ratio (ρ_A) of major streams in a conflict area (A) is calculated as the sum of the degrees of saturation of conflicting major streams, so that

$$p_{0,q,A} = 1 - \rho_A = 1 - \sum_{i \in A} \rho_i = 1 - \sum_{i \in A} \lambda_i t_{q,i} = 1 - \sum_{i \in A} \frac{q_i t_{q,i}}{3600}. \tag{3.129}$$

If a minor stream crosses several conflict areas, the probability that no area is blocked by queuing or discharging vehicles is the product

$$p^*_{0,q} = \prod_j p_{0,q,j}, \tag{3.130}$$

where the multiplication is over all conflict areas. Conflict areas are assumed to operate independently, acknowledging that the assumption is not always realistic.

The probability $p_{0,a,i}$ that a conflict area is not blocked by an approaching stream i vehicle is expressed as the probability that a gap is larger than a time period $t_{a,i}$; i.e.,

$$p_{0,a,i} = \mathbb{P}\{T_i > t_{a,i}\} = R_i(t_{a,i}), \tag{3.131}$$

where the time period $t_{a,i}$ is the time period that the conflict area is blocked by an approaching vehicle in major movement i. It is comparable to the shortest acceptable headway $t_{o,i} = t_{c,i} - t_{f,i}/2$, but contrary to the gap acceptance models, the time period $t_{a,i}$ is related to major stream, not minor stream. For exponential headways the probability is

$$p_{0,a,i} = e^{-t_{a,i} q_i / 3600}, \tag{3.132}$$

The probability that conflict area A is not blocked by approaching vehicles is

$$p_{0,a,A} = \prod_{i \in A} p_{0,a,i} = e^{-\sum_{i \in A} t_{a,i} q_i / 3600}. \tag{3.133}$$

Because all conflict periods have been excluded, the headways in all priority streams can be assumed independent. If a minor stream crosses several conflict areas, the probability that no area is blocked by approaching vehicles is the product

$$p^*_{0,a} = \prod_j p_{0,a,j} = e^{-\sum_i t_{a,i} q_i / 3600}, \tag{3.134}$$

where j runs over all conflict groups and i runs over all major streams. None of the major streams should be counted twice.

The capacity of a minor stream k involved in more than one conflict group is

$$\begin{aligned} C_k &= \frac{3600}{t_{q,k}} p^*_{0,q} p^*_{0,a} \\ &= \frac{3600}{t_{q,k}} \prod_j \left(1 - \sum_{i \in j} \frac{q_i t_{q,i}}{3600}\right) e^{-\sum_{i \in l_k} q_i t_{a,i} / 3600}, \end{aligned} \tag{3.135}$$

where j runs over all conflict areas, and I_k is the set of all conflicting priority streams of stream k.

Probabilities of priorities for pedestrians are used to adjust the capacity for pedestrian movements. Probability of pedestrian priority gives the fraction of pedestrians considered occupying the conflict area in the capacity analysis. The same approach can be used to adjust the capacity for limited priority.

In conclusion: The capacity of a minor stream k is the product of maximum flow rate $q_{\max,k}$ and the time available for queue discharge. This time is obtained in two steps. First, busy periods are excluded. Secondly, during the remaining time the priority stream is considered as a superposition (sum) of all conflict flows (hence the name "ACF"), and the time periods having lags less than $t_{a,i}$ are excluded. The parameters $t_{a,i}$ are related to major streams, not minor streams. If a minor stream crosses several conflict areas, these are assumed independent, but each major stream is used only once in the calculations.

The proportion of occupancy (ρ_A) of queueing/discharging movements across a conflict area (A) is based on discharge headways ($t_{q,i}$, $i \in A$), not on movement capacities as in the gap acceptance theory. Consequently, the capacity of a minor flow can be calculated in a single step. Rank 1 vehicles are also included in the queuing process of a service area. This assumption reduces the capacity estimate. In fact, if all major streams are assumed to have Rank 2 and the minor stream is assumed to have Rank 3, ACF and HCM2000 give very similar results, as a comparison of Figures 3.31 and 3.22 indicates. (Parameters used in Figure 3.31 are described below.)

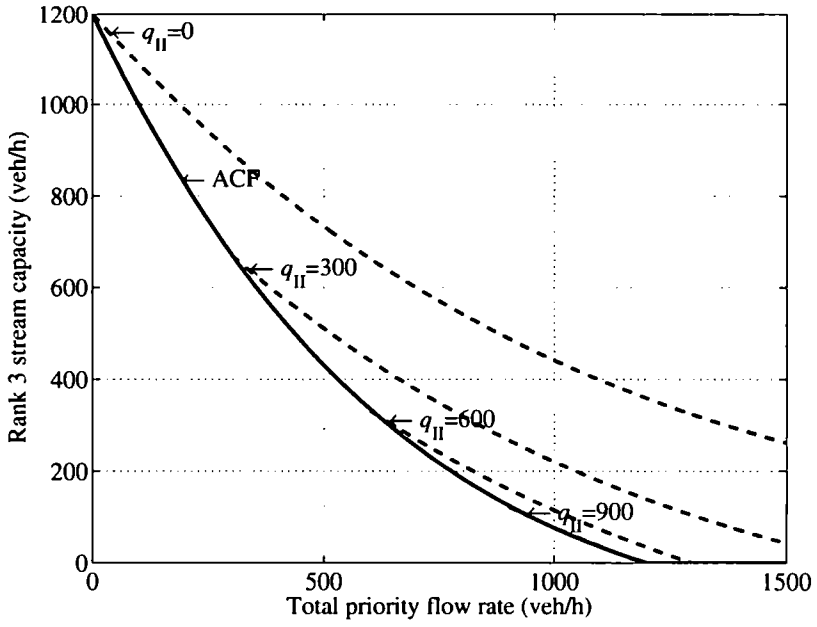

Figure 3.31: Capacity of a Rank 3 stream, when Rank 2 flow rate is q_{II} veh/h, according to HCM2000 (dashed curves) and ACF (solid curve)

Figure 3.32 displays a queuing model for the ACF procedure. The model is microscopic for major streams and macroscopic for minor streams. The discussion above (Sections 3.5.3 and 3.5.5) about the time available for gap acceptance and the major stream headway distributions during these time periods is relevant here also.

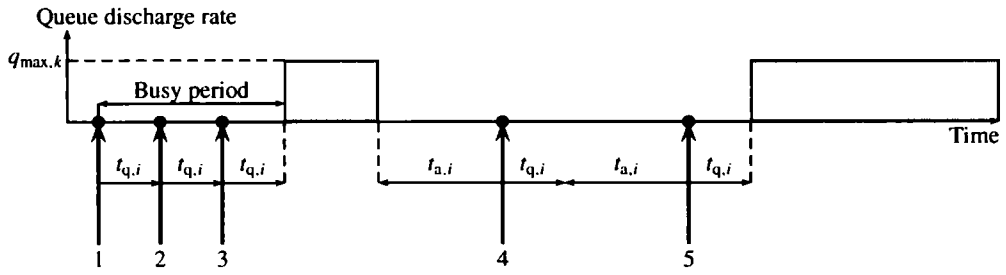

Figure 3.32: ACF queuing model for major stream i and minor stream k

Parameters $t_{a,i}$ and $t_{q,i}$ are estimated using statistical procedures based on goodness of fit between observed and estimated capacities. Because the hierarchy of major streams is ignored, the estimates of $t_{q,i}$ may be sensitive to the distribution of the total priority flow between different priority streams. The estimation procedure can adjust the estimates of $t_{a,i}$ for the fact that an isolated major stream vehicle blocks a minor stream for time period $t_{a,i} + t_{q,i}$, not for $t_{a,i}$.

Figures 3.31 and 3.33 display comparisons of HCM2000 and ACF capacities for Rank 3 and Rank 4 movements. The critical gap was $t_c = 5$ s and follow-up time $t_f = 3$ s in the HCM method for all movements. In the ACF method all movements had $t_q = t_f = 3$ s and $t_a = t_c - t_f/2 = 3.5$ s. Because the interactions between major streams are reduced to a simple queuing process, the distribution of total priority flow among different priority streams does not affect the ACF capacity estimate, when t_q and t_a are the same for all movements. Consequently, the Rank 3 capacity according to ACF is approximately equal to the HCM2000 capacity when all major flows are assigned to a Rank 2 movement.

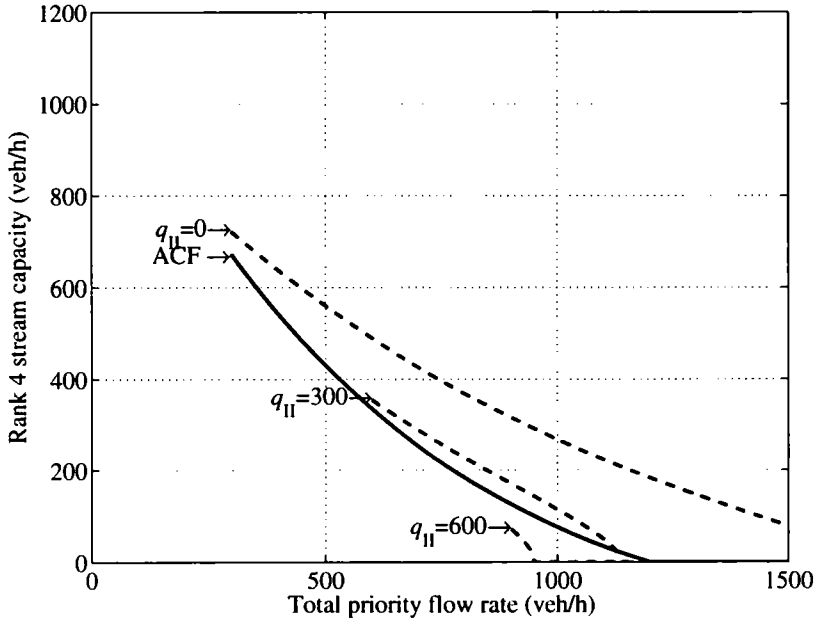

Figure 3.33: Capacity of a Rank 4 stream, when Rank 3 flow rate is $q_{III} = 300$ veh/h, according to HCM2000 (dashed curves) and ACF (solid curve)

4 DELAYS AT UNSIGNALIZED INTERSECTIONS

4.1 Definitions of delay

Delay indicates an excess time consumed in a transportation facility in comparison to a reference value, which Kimber et al. (1986) have called a *comparator*. It is a performance measure experienced by road users. Although it has been shown that the users' perception of quality of service may be difficult to measure (Pécheux, Pietrucha & Jovanis 2000), delay is a widely used service measure for intersections (see Transportation Research Board 2000, FGSV 2001). Delay is also a fundamental parameter in the economic analysis of highway investments.

In capacity analysis a continuous queue at a subject lane was assumed. The details of the queuing process were insignificant. Because delay is the time difference between a realized and an ideal operation time, an analysis of the queuing process is necessary in delay models.

Queuing processes at unsignalized intersections have been described above in sections 2.4 and 3.5.2. Definitions of delays experienced in these processes are described below. For a more detailed analysis the reader is referred to Leutzbach & Köhler (1974), McDonald, Hounsell & Kimber (1984), Kimber et al. (1986), Lapierre & Steierwald (1987), and Akçelik (1998).

In delay models driver behavior and gap-acceptance theory must be described in terms of queuing theory. A vehicle at a stop or yield line is in *service*, vehicles waiting for service behind the first vehicle are in *queue*, and vehicles approaching the intersection upstream of the queue are *arriving* vehicles (Fig. 4.1). Queuing vehicles and the vehicle in service are in the *system*. In queuing theory a distinction is made between the mean *waiting time in queue* and the mean *waiting time in the system* (Gross & Harris 1998). Acceleration, deceleration, and the physical dimensions of vehicles are ignored. In traffic flow theory the physical dimensions and other properties of vehicles and transportation facilities must be considered. Consequently, delay is more appropriate as a performance measure than waiting time.

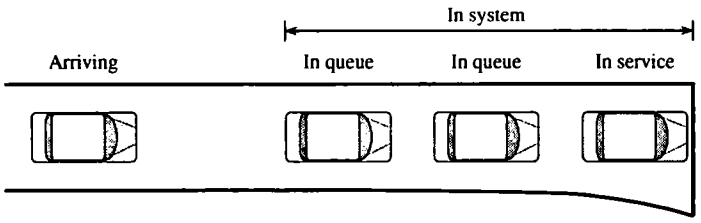

Figure 4.1: Vehicles at an intersection approach

According to HCM2000 (Transportation Research Board 2000) *total delay* is the sum of all components of delay:

- *Control delay* is measured by comparison with the uncontrolled condition
- *Traffic delay* results from vehicular interaction causing drivers to reduce their speed below the free-flow speed
- *Geometric delay* is caused by geometric features requiring vehicles to reduce their speed in negotiating a facility
- *Incident delay* is the time loss due to an incident, compared with the no-incident condition.

Total delay is the difference between the travel time actually experienced and the reference travel time (comparator) that would result during base conditions, in the absence of control, traffic, geometric, or incident delay. In the analysis of unsignalized intersections delays caused by vehicular interaction (traffic delays) are included in control delays. The effects of incidents, such as road maintenance, should be analyzed separately. Consequently, the most important delay components at unsignalized intersections are control and geometric delays.

Figure 4.2 displays two space-time trajectories of an isolated vehicle at a yield-controlled intersection. The first trajectory describes a vehicle entering the intersection without any vehicular interaction. The vehicle approaches the intersection at approach cruise speed (v_a), decelerates (A–C) until it reaches the negotiation speed (v_n), proceeds with that speed some distance (C–F_1), and accelerates (F_1–G_1) to exit cruise speed (v_e). The details of the trajectory within the intersection are ignored (see McDonald et al. 1984, Kimber et al. 1986, Akçelik 1998).

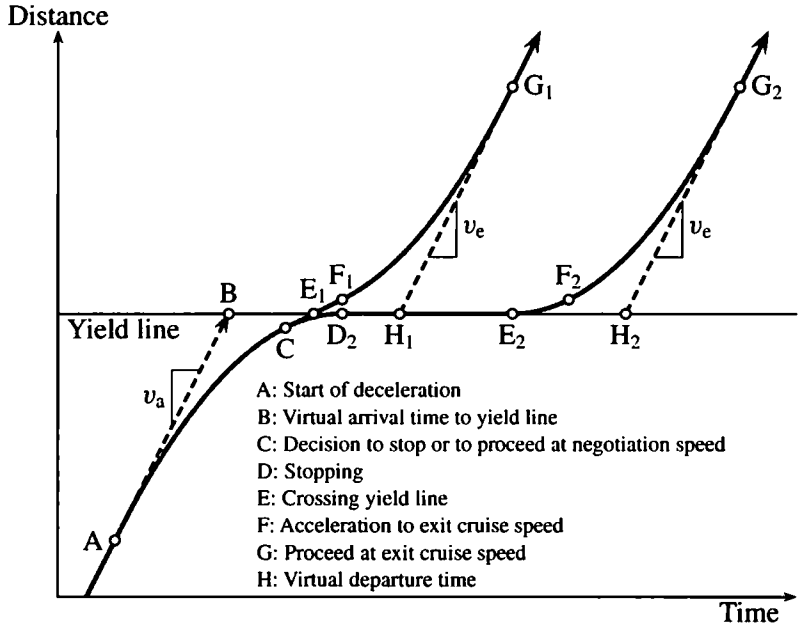

Figure 4.2: Trajectories of an isolated vehicle at a yield-controlled intersection

In the comparator trajectory, vehicles enter the intersection at approach cruise speed (v_a) and depart at exit cruise speed (v_e), with an instantaneous change of speed at yield line. The time lost due to deceleration, negotiation speed, and acceleration is the time interval between virtual arrival and departure times $T(B, H_1)$. Because this excess time is based on the geometry of the intersection, not on any traffic interactions or traffic control, the lost time is called *geometric delay*

$$W_g^{(1)} = T(B, H_1). \tag{4.1}$$

It is the sum of deceleration delay $W_d^{(1)} = T(B, C)$, negotiation delay $W_n^{(1)} = T(C, F_1)$, and acceleration delay $W_a^{(1)} = T(F_1, H_1)$. Accordingly, the geometric delay of vehicle i is

$$W_g^{(i)} = W_d^{(i)} + W_n^{(i)} + W_a^{(i)} \tag{4.2}$$

(Kyte et al. 1996). It includes the delay caused by speed reduction in order to check for possible conflicts, even if there are none. In this discussion the time lost due to

checking is included in the negotiation delay.

Kimber et al. (1986) call W_g the measurable geometric delay. Pure geometric delay is the delay of an isolated vehicle knowing that it is safe to drive through an intersection immediately on arrival. It is a theoretical, under normal operating conditions non-measurable delay.

If a vehicle has to stop, it decelerates and stops ($A–D_2$), waits for the next antiblock ($D_2–E_2$), accelerates to negotiation speed ($E_2–F_2$), proceeds, and accelerates to the exit cruise speed ($F_2–G_2$). At stop-controlled intersections minor road vehicles have to stop, even if the major stream lag is safe for entry.

Total delay is the difference between virtual arrival and departure times

$$W_t^{(2)} = T(B, H_2). \tag{4.3}$$

For a vehicle that waits at the yield line, but does not queue, the total delay is the sum of deceleration delay, stop delay, negotiation delay, and acceleration delay:

$$W_t^{(i)} = W_d^{(i)} + W_s^{(i)} + W_n^{(i)} + W_a^{(i)}. \tag{4.4}$$

Total delay can also be defined as the travel time between two points upstream and downstream of the intersection, unaffected by it, subtracted by the travel time of the comparator:

$$W_t^{(2)} = T(A, G_2) - [T(A, B) + T(H_2, G_2)]. \tag{4.5}$$

For a vehicle coming to a complete stop deceleration and acceleration delays are larger than these components in the geometric delay. If no negotiation delay is assumed for a stopping vehicle ($W_n^{(i)} = 0$), all delays are caused by vehicular interactions, and geometry does not cause any additional delay.

In Figure 4.2 it is assumed that geometry does not cause any extra delay to a stopping vehicle. However, compared to a vehicle able to cross the intersection without any vehicular interaction, the extra delay, "net control delay", is $T(H_1, H_2)$. If a turning vehicle first accelerates to an exit negotiation speed and it can accelerate to exit cruise speed only after exiting the intersection, geometric delay cannot be ignored, but delay due to geometry is much less than the geometric delay W_g (without control delay). This indicates a dependency between control delay and geometric delay, and suggests two alternative definitions:

1. A *control-oriented* definition of control delay measures all delays $T(B, H_2)$ due to traffic signs and vehicular interactions. As total delays increase, the impact of geometric conditions decreases. Geometric delay is the extra delay due to geometry. It is the difference between total delay and control delay:

   $$W_g' = W_t - W, \tag{4.6}$$

   According to this definition, geometric delay is a function of control delay. In Figure 4.2 a stopped vehicle (2) can accelerate from stop to exit cruise speed without any additional delay due to geometry (negotiation speed). The control-oriented model assigns no geometric delay to this vehicle.

2. A *comparator-oriented* definition uses geometric delay as a comparator, so that control delay is the difference between total delay and geometric delay

   $$W = W_t - W_g. \tag{4.7}$$

   This is the actual excess delay $T(H_1, H_2)$ caused by traffic signs and vehicular interactions.

The definition of control delay in HCM2000, as presented above, suggests a comparator-oriented definition. It is also compatible with the general definition of delay given in the beginning of this section. According to Troutbeck (2000) the control delay comprises the time spent queuing, the service time, and deceleration and acceleration delays *at speeds below negotiation speed.* In the discussion below the comparator-oriented definition of control delay is assumed.

In queuing models vehicles are assumed to arrive with instantaneous deceleration, and all stopping vehicles are assumed to stop at the stop/yield line and stack vertically. The arrival time to the system is the earliest time instant (E_1 in Figure 4.2) that the vehicle would be able to cross the stop/yield line in case of no vehicular interaction. The queue discipline is first-in-first-out (FIFO); i.e., vehicles depart in the same order as they have arrived.

Figure 4.3 displays vehicle trajectories assuming no geometric delay, so that control delay is equivalent to total delay. Deceleration and acceleration rates are finite and queues have a physical length.

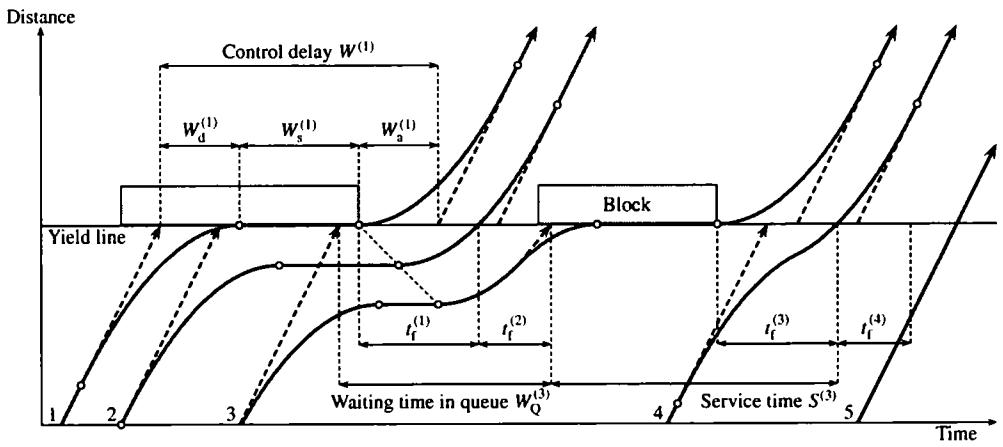

Figure 4.3: Vehicle trajectories for a through movement at a yield-controlled intersection with no geometric delay

Vehicular delays at an unsignalized intersection can be described in terms of waiting times in queuing systems as follows: A vehicle enters the system (queue or service) at its virtual arrival time. This is the virtual arrival time under prevailing geometric conditions (E_1 in Figure 4.2). It is the first time instant that the vehicle can cross the yield line in case of an antiblock. *Waiting time in queue* (W_Q) begins when a vehicle enters a queue and ends when the vehicle enters the yield line. The virtual arrival time from the queue to yield line is assumed, because it is the time instant that a vehicle would cross the yield line in case of an antiblock. When a vehicle enters the yield line, its *service time* (S) begins (see section 3.5.2). The *waiting time in system* is the sum of waiting time in queue and service time: $W_S = W_Q + S$. Average control delay can now be expressed as

$$\begin{aligned} \bar{W} &= \bar{W}_Q + \bar{S} - t_f + \bar{W}'_a \\ &= \boxed{\bar{W}_S - t_f + \bar{W}'_a.} \end{aligned} \tag{4.8}$$

If a vehicle can cross the yield line without stopping (vehicles 2 and 4), its acceleration delay is smaller than the acceleration delay of a stopped vehicle.[1] When $\bar{W}'_a$

[1]Greenshields, Shapiro & Ericksen (1947) made a distinction between functional and chronotropic

is defined as the average acceleration delay in excess of negotiation and acceleration delays, $T(E_1, H_1)$, due to geometric conditions, equation (4.8) is compatible with the comparator-oriented definition of control delay.

The follow-up times in Figure 4.3 have different lengths. This is caused by the early acceleration of vehicles accepting a lag. At signalized intersections the longer discharge headways for the first few discharging vehicles are a well know phenomenon (see King & Wilkinson 1976, Briggs 1977, Teply & Jones 1991, Niittymäki & Pursula 1997). If a stream has to observe a stop sign, the vehicles cannot benefit from early acceleration. In mathematical models all follow-up times of a stream under given traffic conditions are usually assumed to be constant. This approach has some empirical support from the measurements by Koivisto (1999).

The discussion here applies to delays of minor stream vehicles. Concerning disturbances in a Rank 1 stream the reader is referred to section 3.7 (see also Bonneson & Fitts 1999).

Figure 4.4 displays an input-output diagram of a minor stream (see also Daganzo 1997). The vertical distance between the curves indicates the number of vehicles in the system at a given time, assuming that vehicles form a vertical stack at the stop line (see Fig. 2.13). The horizontal distance between the curves gives the waiting time in system of a given vehicle. The area between the curves is equal to the cumulative delay during the observation period.

4.2 Service times

4.2.1 Definition of service time

In queuing systems service time is the time that a customer spends at a counter. At unsignalized intersections the service time of a vehicle begins when it reaches the yield/stop line. The entry time is the virtual entry time; i.e., the first time instant that the vehicle could cross the stop line in case on an antiblock (see Figure 4.3). Service time ends when the follow-up time has passed since the vehicle has crossed the stop line. Accordingly, service time is the sum of a waiting time at the yield/stop line during a block and the follow-up time, as described in Section 3.5.2.

Vehicles can enter service either from a queue or without queuing. Queuing vehicles enter service immediately when the service of the vehicle ahead has been completed. It is evident that the remaining lag is not shorter than $t_c - t_f$. Isolated (non-queuing) vehicles arrive to an empty system at a random time instant, but after the follow-up time has passed since the previous vehicle had crossed the stop line. The arrival process of vehicles that find an empty system is not independent of the arrival process of vehicles in the major stream (Daganzo 1977). Because the expected state of the major stream at the beginning of the service time is different for queuing and isolated vehicles, they have different service time distributions. The service time distribution of all minor stream vehicles is a mixture of service time distributions for queuing and isolated vehicles.

The basic properties of service times for both arrival types is discussed next. In order to describe the dynamics behind the service processes, the equations for average service

decelerations. *Functional* deceleration is necessary to adjust speed for intersection geometry or to obey a stop sign. A vehicle may accelerate as soon as the specific deceleration or stopping function has been fulfilled. *Chronotropic* deceleration ("chronoceleration") occurs when motion beyond a specific point cannot be continued until after a specific time instant, such as the beginning of an antiblock or end of the follow-up time. A driver may save time by an early deceleration so that the vehicle can enter an intersection at the beginning of an antiblock or at the end of a follow-up time at a higher speed than possible with a later deceleration. See the trajectory of vehicle 4 in Figure 4.3.

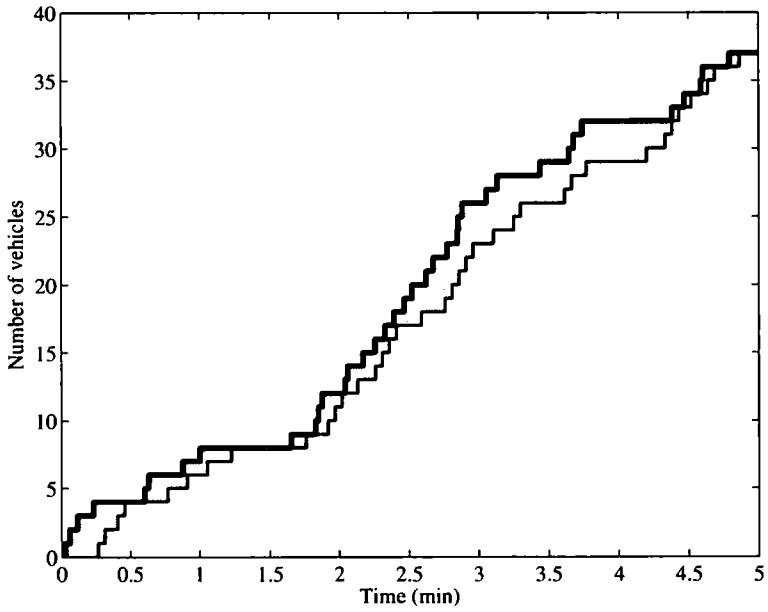

Figure 4.4: Cumulative arrivals (thick curve) and departures (thin curve) of a minor stream (major flow 800 veh/h, minor flow 400 veh/h, $t_c = 5\,s$, $t_f = 3\,s$, exponential headway distributions)

times are derived. In order to keep the mathematics simple, the second moments of the service time distributions are presented with bibliographic references only.

4.2.2 Average service time of queuing vehicles

Under saturated conditions a minor stream vehicle enters service immediately after the service of the previous vehicle has ended. This is demonstrated by vehicle 2 in Figure 3.17. The vehicle enters a yield/stop line (service) exactly t_f after the previous vehicle has crossed the stop line. The remaining lag is not shorter than $t_c - t_f$. If the lag is greater than or equal to t_c, the vehicle can cross the yield/stop line immediately. The probability of no waiting at a yield/stop line is

$$p_{q,0} = \mathbb{P}\{\, \Upsilon \geq t_c \mid \Upsilon \geq t_c - t_f \,\} = \frac{R_\Upsilon(t_c)}{R_\Upsilon(t_c - t_f)}. \tag{4.9}$$

When the major stream headways are exponentially distributed the probability is

$$p_{q,0} = \frac{R_\Upsilon(t_c)}{R_\Upsilon(t_c - t_f)} = e^{-\lambda t_f}. \tag{4.10}$$

For vehicles discharging from the yield/stop line immediately upon entry the service time is equal to the follow-up time t_f.

The time interval from the beginning of an antiblock to the beginning of the next antiblock can be called a *cycle* (c). The average service time of vehicles discharging from a queue is the average cycle length divided by the average number of discharging vehicles (D_c) in a cycle:

$$\bar{s}_q = \frac{\mathbb{E}[c]}{\mathbb{E}[D_c]}. \tag{4.11}$$

The average cycle length is the sum of a headway $T \geq t_c$ and the sum of consecutive headways shorter than the critical gap. If major stream headways are exponentially distributed, a headway $T \geq t_c$ follows shifted exponential distribution with mean

$$\mathbb{E}[\, T \mid T \geq t_c \,] = \frac{1}{\lambda} + t_c. \tag{4.12}$$

In order to estimate the expected sum of gaps in a block, we need to derive the expectation of a sum of a random number of i.i.d. random variables. Let $X \stackrel{\mathrm{d}}{=} \{\, T \mid T < T_c \,\}$ be a headway shorter than the critical gap. The sum $Y_N = X_1 + \cdots + X_N$ of N consecutive headways shorter than the critical gap has expectation

$$\mathbb{E}[Y_N] = \mathbb{E}\left[\sum_{i=1}^{N} X_i\right] = \mathbb{E}\left[\mathbb{E}\left[\sum_{i=1}^{n} X_i \mid N = n\right]\right], \tag{4.13}$$

where $X_1, \ldots, X_n$ is a random sample of variate X, and the inner expectation has been conditioned[2] on the event $N = n$. Because X_i and N are independent, the conditional expectation is

$$\mathbb{E}\left[\sum_{i=1}^{n} X_i \mid N = n\right] = \mathbb{E}\left[\sum_{i=1}^{n} X_i\right] = n\,\mathbb{E}[X_i] = n\,\mathbb{E}[X]. \tag{4.14}$$

This is the expected value of the sum assuming that the number (n) of consecutive headways shorter than the critical gap is known. However, as the number (N) of headways is a random variable, the expectation of Y_N is (Goodman 1988)

$$\mathbb{E}[Y_N] = \mathbb{E}[N\,\mathbb{E}[X]] = \mathbb{E}[N]\,\mathbb{E}[X]. \tag{4.15}$$

Thus, the expected value of the sum is the expected number of headways shorter than the critical gap multiplied by their expected length. Ross (1996) has given the result (4.15) using moment generating functions.

A headway is shorter than the critical gap with probability

$$p_g = \mathbb{P}\{T < t_c\} = F(t_c), \tag{4.16}$$

and the probability of n consecutive headways shorter than the critical gaps follows the geometric distribution

$$p_n = p_g^n(1 - p_g). \tag{4.17}$$

The expected number of consecutive headways $T_i < t_c$ is obtained from equation (2.11) as

$$\mathbb{E}[N] = \frac{p_g}{1 - p_g} = \frac{F(t_c)}{R(t_c)} = \mathrm{e}^{\lambda t_c} - 1. \tag{4.18}$$

The expected length of a headway shorter than the critical gap is

$$\begin{aligned}
\mathbb{E}[X] &= \mathbb{E}[\, T \mid T < t_c \,] \\
&= \int_0^{t_c} t\, f(t \mid t < t_c)\, \mathrm{d}t \\
&= \frac{1}{F(t_c)} \int_0^{t_c} t\, f(t)\, \mathrm{d}t \\
&= \frac{1}{1 - \mathrm{e}^{-\lambda t_c}} \left[\mathrm{e}^{-\lambda t} \left(-t - \frac{1}{\lambda}\right)\right]_0^{t_c} \\
&= \frac{1}{\lambda} - \frac{t_c}{\mathrm{e}^{\lambda t_c} - 1}.
\end{aligned} \tag{4.19}$$

[2]For conditional expectations see e.g. Grimmett & Welsh (1986).

The expected cycle length can now be expressed as

$$\begin{aligned}\mathbb{E}[c] &= \mathbb{E}[\,T \mid T \geq t_c\,] + \mathbb{E}[N]\,\mathbb{E}[\,T \mid T < t_c\,] \\ &= \frac{1}{\lambda e^{-\lambda t_c}}.\end{aligned} \tag{4.20}$$

The number of departures during a headway $T \geq t_c$ follows the geometric distribution

$$\mathbb{P}\{\,D_c = d \mid T \geq t_c\,\} = p_{q.0}^{d}\left(1 - p_{q.0}\right). \tag{4.21}$$

The expectation is obtained following equation (2.9) as

$$\mathbb{E}[D_c] = \frac{1}{1 - p_{q.0}}. \tag{4.22}$$

For exponential headways $p_{q.0} = e^{-\lambda t_f}$ and $\mathbb{E}[D_c] = (1 - e^{-\lambda t_f})^{-1}$.

The average service time of vehicles discharging from a queue (arriving while server was busy) is now obtained as

$$\bar{S}_q = \frac{\mathbb{E}[c]}{\mathbb{E}[D_c]} = \frac{1 - e^{-\lambda t_f}}{\lambda e^{-\lambda t_c}}. \tag{4.23}$$

This is the inverse of capacity equation (3.12), as expected. Consequently, this approach can be used as an alternative derivation of the capacity equation. For a more rigorous derivation of $\bar{S}_q$ see Kremser (1962), who also derived the second moment of the service time as

$$\mathbb{E}\left[S_q^2\right] = \frac{2e^{\lambda t_c}}{\lambda^2}\left[\left(e^{\lambda t_c} - \lambda t_c\right)\left(1 - e^{-\lambda t_f}\right) - \lambda t_f e^{-\lambda t_f}\right]. \tag{4.24}$$

The average waiting time at yield/stop line for vehicles discharging from a queue is

$$\bar{W}_q = \bar{S}_q - t_f = \frac{1 - e^{-\lambda t_f}}{\lambda e^{-\lambda t_c}} - t_f. \tag{4.25}$$

After each vehicle there is a time period t_f during which the next vehicle is moving to the yield/stop line and no vehicles are waiting at the stop line. This time interval is part of the service time of the first vehicle and the queuing time of the second vehicle.

4.2.3 Average service time of isolated vehicles

An isolated (non-queuing) minor stream vehicle (vehicles 1 and 3 in Figure 3.17) arrives, when the server is idle, and enters service (yield/stop line) immediately. The vehicle can arrive after t_f has passed since the last vehicle in the preceding queue has crossed the yield/stop line. No major stream vehicle can arrive until $t_c - t_f$ has passed since the server became idle. However, it is possible that a major stream vehicle arrives before the isolated minor stream vehicle reaches the stop line.

If a subject vehicle is blocked by higher priority vehicles, as vehicle 1 in Figure 3.17, it must wait for the next antiblock. Once the antiblock starts, the vehicle crosses the yield/stop line immediately. However, the server is busy until the follow-up time has passed. Thus, the service time, $\bar{S}_e$, of a vehicle arriving to an empty system is the sum of average waiting time at stop line W_e and the follow-up time t_f (Yeo & Weesakul 1964).

An isolated vehicle enters an intersection at a random time and can enter the yield/stop line without queuing. If the vehicle enters during an antiblock, it can depart immediately. Let us assume that, when a non-queuing minor stream vehicle arrives, the major

stream is in steady state (see, however, Daganzo 1977). The probability of no wait is equal to the probability of a lag greater than or equal to the critical gap:

$$p_{e,0} = \mathbb{P}\{\Upsilon \geq t_c\} = R_\Upsilon(t_c)\,. \tag{4.26}$$

This is equal to the "transparency"; i.e., the percentage of time a driver would consider it safe to merge or cross the major stream (Herman & Weiss 1961, Weiss 1963, Allan 1968).

The vehicle has to stop and wait if the lag available is shorter that the critical gap. The probability of wait is

$$p_{e,1} = \mathbb{P}\{\Upsilon < t_c\} = F_\Upsilon(t_c)\,. \tag{4.27}$$

If headways are independent and identically distributed, the probability that the next headway (gap) cannot be accepted is

$$p_g = \mathbb{P}\{T < t_c\} = F(t_c)\,, \tag{4.28}$$

and the probability that a driver has to wait for one lag and $n-1$ gaps (n vehicles) is

$$p_n = p_{e,1} p_g^{n-1}(1 - p_g). \tag{4.29}$$

If major stream headways follow the negative exponential distribution, lag and gap distributions are equal:

$$F_\Upsilon(t_c) = F(t_c) = 1 - e^{-\lambda t_c}, \tag{4.30}$$

and $p = p_{e,1} = p_g$, so that $p_n = p^n(1-p)$. This is a geometric distribution with expectation obtained from equation (2.11) as follows:

$$\mathbb{E}[N] = \frac{p}{1-p} = e^{\lambda t_c} - 1. \tag{4.31}$$

The expected length of a headway shorter than the critical gap is given in equation (4.19) as

$$\mathbb{E}[\,T \mid T < t_c\,] = \frac{1}{\lambda} - \frac{t_c}{e^{\lambda t_c} - 1}. \tag{4.32}$$

Following equation 4.15 the average waiting time during a block for a vehicle arriving to an empty system can be expressed as the product of the expectations (Greenshields & Weida 1952):

$$\bar{W}_e = \mathbb{E}[N]\;\mathbb{E}[\,T \mid T < t_c\,] = \boxed{\frac{e^{\lambda t_c} - 1}{\lambda} - t_c.} \tag{4.33}$$

The first term in the equation is the average service time of vehicles departing from a queue with follow-up time equal to critical gap.[3] $\bar{W}_e$ is the lower limit for minor stream average delay (Transportation Research Board 1997). As the major flow (λ) approaches zero, the first part in the equation approaches t_c, and $\bar{W}_e$ approaches zero.

Because Adams (1936) was the first to present the result, it is also called the *Adams' delay*. He solved the problem in terms of the average waiting time of pedestrians

[3]When follow-up time (t_f) is equal to critical gap (t_c) the potential capacity under exponential major stream arrivals is obtained from equation (3.12) as follows:

$$C_p = \frac{\lambda e^{-\lambda t_c}}{1 - e^{-\lambda t_c}} = \frac{\lambda}{e^{\lambda t_c} - 1}.$$

See Grabe (1954).

attempting to cross a traffic stream. Because follow-up times are ignored, average service time approaches zero and capacity tends to infinity at very low major flow rates. The distribution of this waiting time has been studied by Garwood (1940), Tanner (1951), and Mayne (1954). Tanner (1951) and McNeil & Weiss (1974) have derived the variance of this waiting time

$$\sigma_e^2 = \frac{e^{2\lambda t_c} - 2\lambda t_c e^{\lambda t_c} - 1}{\lambda^2} \tag{4.34}$$

as well as the mean and variance of the waiting time for isolated minor stream vehicles at a yield controlled intersection, when the critical lag is shorter than the critical gap. Figure 4.5 demonstrates that standard deviation σ_e is slightly higher than the Adams' delay, which indicates a larger variation than exponentially distributed waiting times would have. Cowan (1984) has generalized the Adams' formula for M3 distributed major stream headways.

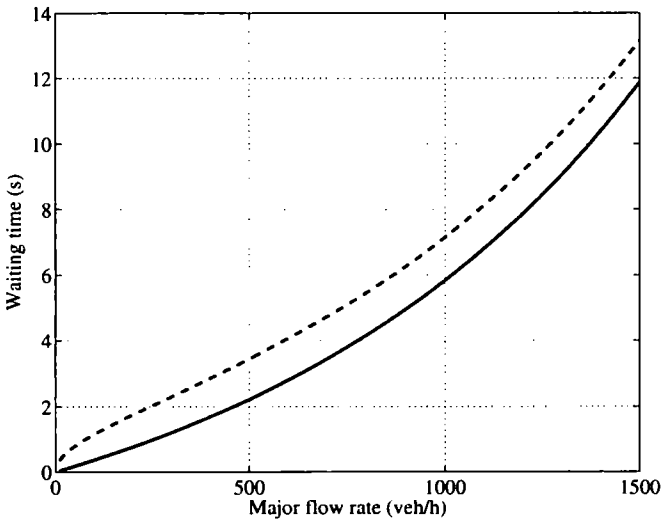

Figure 4.5: Mean ($\bar{W}_e$, solid line) and standard deviation (σ_e, dashed line) of waiting time for isolated vehicles, when major stream headway distribution is exponential, $t_c = 5\,s$, and $t_f = 3\,s$

When a vehicle has found an acceptable lag or gap, it enters the intersection. If there is another vehicle behind the subject vehicle, it can enter the intersection after the follow-up time has passed. Until that time, the server is busy (Fig. 3.17). Accordingly, the average service time of isolated vehicles is (Kremser 1962)

$$\boxed{\bar{S}_e = \bar{W}_e + t_f = \frac{e^{\lambda t_c} - 1}{\lambda} - (t_c - t_f).} \tag{4.35}$$

At very low major flow rates the average service time of an isolated vehicle ($\bar{S}_e$) approaches the follow-up time (t_f), as Figure 4.6 demonstrates. As major flow rate increases, the average service time for isolated vehicles increases slightly more steeply than the average service time of queuing vehicles. (In some papers $\bar{W}_e$ has been used in stead of $\bar{S}_e$, which explains differences in the results.)

The second moment of the service time has been derived by Kremser (1962) as

$$\boxed{\mathbb{E}[S_e^2] = 2\left(\frac{e^{\lambda t_c} - 1}{\lambda} - t_c\right)\left(\frac{e^{\lambda t_c}}{\lambda} + t_f - t_c\right) + t_f^2 - t_c.} \tag{4.36}$$

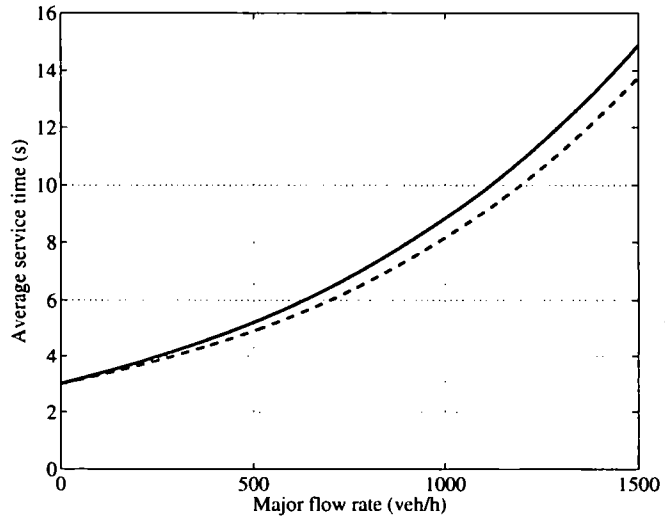

Figure 4.6: Average service time of isolated vehicles ($\bar{S}_e$, solid line) compared with the average service time of queuing vehicles ($\bar{S}_q$, dashed line) when major stream headway distribution is exponential, $t_c = 5\,s$, and $t_f = 3\,s$

As stated above, this discussion was based on the assumption that, when an isolated (non-queuing) minor stream vehicle arrives, the major stream is in steady state. Kremser (1964) and Daganzo (1977) have demonstrated that this assumption is not correct. An isolated minor stream vehicle can arrive only when the server is idle. When the server becomes idle, there must be a lag $\Upsilon \geq t_c - t_f$. Consequently, the arrival process of isolated minor stream vehicles and the arrival process in the major stream are not independent.

Let us assume that the last vehicle in a minor-stream (i) queue departed at time 0 so that the busy period ended at time t_f. Thus, the arrival time (τ) of an isolated minor stream vehicle can not be earlier than t_f, and the arrival time (τ_k) of the next major stream (k) vehicle can not be earlier than t_c. The lag found by the isolated minor stream vehicle is (Daganzo 1977)

$$\Upsilon(\tau) = \begin{cases} t_c - \tau + X, & \text{if } t_f \leq \tau < t_c \\ X, & \text{if } t_c \leq \tau, \end{cases} \tag{4.37}$$

where X follows the negative exponential distribution with scale parameter λ_k (see Figure 4.7). If $t_f = t_c$, a non-queuing vehicle cannot enter before the critical gap has passed since the previous departure, and the lag is exponentially distributed.

If the arrival time of the minor stream vehicle is $\tau \geq t_c$, the lag is exponentially distributed:

$$f_1(\upsilon) = \lambda_k e^{-\lambda_k \upsilon}. \tag{4.38}$$

If the minor stream vehicle arrives before the critical gap of the previous vehicle has passed, the lag follows the shifted exponential distribution with location parameter $t_c - \tau$; i.e.,

$$f_2(\upsilon, \tau) = \lambda_k e^{-\lambda_k(\upsilon + \tau - t_c)}. \tag{4.39}$$

A given lag υ can realize with different arrival times. If the lag is $\upsilon \geq t_c - t_f$, the minor stream vehicle can have arrived at any time in the interval $t_f \leq \tau < t_c$. However, a lag

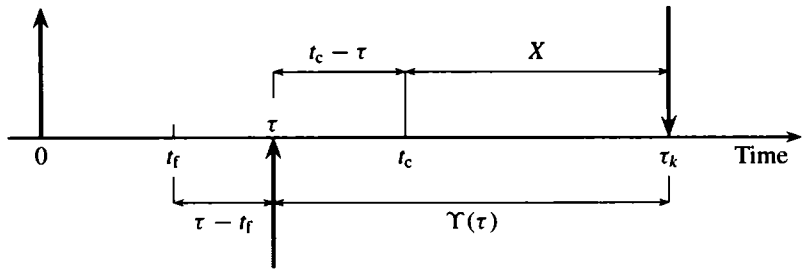

Figure 4.7: Lag for an isolated minor stream vehicle arriving before the critical gap has passed since the departure of the preceding vehicle

$\upsilon < t_c - t_f$ is only possible, if $\tau > t_c - \upsilon$. The density function of the lag distribution is obtained as

$$f_\Upsilon(\upsilon) = \begin{cases} \mathbb{P}\{\tau > t_c\}\, f_1(\upsilon) + \int_{t_c-\upsilon}^{t_c} f(\tau)\, f_2(\upsilon, \tau)\, d\tau, & \text{if } \upsilon < t_c - t_f \\ \mathbb{P}\{\tau > t_c\}\, f_1(\upsilon) + \int_{t_f}^{t_c} f(\tau)\, f_2(\upsilon, \tau)\, d\tau, & \text{if } \upsilon \geq t_c - t_f, \end{cases} \tag{4.40}$$

where $f(\tau)$ is the density function of the minor stream arrival times.

When the minor stream arrival process is Poisson with flow rate λ_i, the probability density function of minor stream arrival time (given that it is larger than the follow-up time) is

$$f(\tau) = \lambda_i e^{-\lambda_i(\tau - t_f)}. \tag{4.41}$$

The probability that a non-queuing vehicle arrives after the critical gap has passed since the last departure is

$$\mathbb{P}\{\tau > t_c\} = \int_{t_c}^{\infty} f(\tau)\, d\tau = e^{-\lambda_i(t_c - t_f)}. \tag{4.42}$$

The density function of the lag distribution can now be expressed as (Daganzo 1977)

$$f_\Upsilon(\upsilon) = \begin{cases} e^{-\lambda_i(t_c-t_f)}\lambda_k e^{-\lambda_k \upsilon} + \int_{t_c-\upsilon}^{t_c} \lambda_i e^{-\lambda_i(\tau - t_f)} \lambda_k e^{-\lambda_k(\upsilon+\tau-t_c)}\, d\tau, & \text{if } \upsilon < t_c - t_f \\ e^{-\lambda_i(t_c-t_f)}\lambda_k e^{-\lambda_k \upsilon} + \int_{t_f}^{t_c} \lambda_i e^{-\lambda_i(\tau - t_f)} \lambda_k e^{-\lambda_k(\upsilon+\tau-t_c)}\, d\tau, & \text{if } \upsilon \geq t_c - t_f, \end{cases} \tag{4.43}$$

which gives (Daganzo 1977)

$$f_\Upsilon(\upsilon) = \begin{cases} \dfrac{\lambda_k e^{-\lambda_i(t_c-t_f)}}{\lambda_i + \lambda_k} \left(\lambda_k e^{-\lambda_k \upsilon} + \lambda_i e^{\lambda_i \upsilon}\right), & \text{if } \upsilon < t_c - t_f \\ \dfrac{\lambda_k e^{-\lambda_k \upsilon}}{\lambda_i + \lambda_k} \left(\lambda_k e^{-\lambda_i(t_c-t_f)} + \lambda_i e^{\lambda_k(t_c-t_f)}\right), & \text{if } \upsilon \geq t_c - t_f. \end{cases} \tag{4.44}$$

When $t_c = t_f$, equation (4.44) reduces to the negative exponential lag density (2.15). This indicates that the assumption of steady state at time τ is correct only when the critical gap is equal to the follow-up time (Daganzo 1977, Kremser 1964).

The probability of no wait is

$$\begin{aligned} p_{e,0} &= \mathbb{P}\{\Upsilon > t_c\} \\ &= \int_{t_c}^{\infty} f_\Upsilon(\upsilon)\, d\upsilon \\ &= \frac{e^{-\lambda_k t_c}}{\lambda_i + \lambda_k} \left(\lambda_k e^{-\lambda_i(t_c-t_f)} + \lambda_i e^{\lambda_k(t_c-t_f)}\right). \end{aligned} \tag{4.45}$$

Daganzo (1977) has pointed out that this probability is always larger than the probability (4.26) based on exponential lags. Models based on equation 4.26 tend to predict longer delays.

The probability of not accepting a lag is

$$\begin{aligned} p_{e.l} &= 1 - p_{e.0} \\ &= 1 - \frac{e^{-\lambda_k t_c}}{\lambda_i + \lambda_k}\left(\lambda_k e^{-\lambda_i (t_c - t_f)} + \lambda_i e^{\lambda_k (t_c - t_f)}\right). \end{aligned} \tag{4.46}$$

The average service time for an isolated vehicle was derived by Daganzo (1977) as

$$\bar{S}_e = p_{e.l}\left[-\mathcal{L}'_\Upsilon(0) - (e^{\lambda_k t_c} + 1)\mathcal{L}'_T(0)\right] + t_f, \tag{4.47}$$

where $\mathcal{L}_\Upsilon$ and $\mathcal{L}_T$ are the Laplace transforms of rejected lags and gaps, respectively. The first derivatives of these transforms at parameter value zero are (Daganzo 1977)

$$\begin{aligned} \mathcal{L}'_\Upsilon(0) = \frac{\lambda_k e^{-\lambda_i (t_c - t_f)}}{p_{e.l}(\lambda_i + \lambda_k)} \Bigg[&\left(t_f - t_c + \frac{1}{\lambda_i}\right) e^{\lambda_i (t_c - t_f)} - \frac{1}{\lambda_i} + e^{-\lambda_k t_c}\left(t_c - \frac{1}{\lambda_k}\right) - \frac{1}{\lambda_k} \\ &+ \frac{\lambda_i e^{(\lambda_i + \lambda_k)(t_c - t_f)}}{\lambda_k^2}\left(e^{-\lambda_k t_c}(\lambda_k t_c + 1) - e^{-\lambda_k (t_c - t_f)}\left[\lambda_k (t_c - t_f) + 1\right]\right) \Bigg] \end{aligned} \tag{4.48a}$$

$$\mathcal{L}'_T(0) = \frac{t_c e^{-\lambda_k t_c}}{1 - e^{-\lambda_k t_c}} - \frac{1}{\lambda_k}. \tag{4.48b}$$

Pöschl (1983) has presented the second moment $\mathbb{E}[S_e^2]$ of the service time. The equation is, however, not reproduced here, because it is even more complicated than the equation for average service time. According to Daganzo (1977) the magnitude of error when assuming an exponentially distributed lag density (2.15) instead of the correct density function (4.44) is not likely to be large for most reasonable values of parameters.

4.3 Delays under steady-state conditions

4.3.1 Queuing as a stochastic process

Let us assume that the average arrival rate of a minor stream is λ. Vehicles cross the stop line following the gap acceptance procedure. Vehicles waiting for entry form a vertical stack at the stop line and are served following the first-come-first-served principle. Under steady state conditions the arrival process and the service process stay unchanged, the average arrival rate does not exceed capacity, and queues have reached an equilibrium state.

The state of the process at time τ is described by the number $N(\tau)$ of vehicles in the system. When a minor stream vehicle arrives, the state of the process increases by one unit. When a minor stream vehicle departs the intersection (t_f after crossing the stop line), the state of the process decreases by one unit. It is assumed that only one vehicle can arrive or depart simultaneously.

Cooper (1981) has presented an important theorem, which can be applied in the queuing process under discussion:

> In any queuing system for which the realizations of the state process are step functions with only unit jumps (positive or negative), the equilibrium state distribution just prior to arrival epochs is the same as that just following departure epochs. In addition, when the input is Poisson this distribution is the same as the outside observers distribution.

Consequently, if minor stream arrivals are assumed to be Poisson, it is only necessary to describe the queuing process at times of departure from service (see also Tanner 1962). This approach will be followed here.

Let δ_n be the service departure time of vehicle n. The time interval between two consecutive service departure times is $T_n = \delta_n - \delta_{n-1}$. If the number of vehicles in the system after departure n is N_n, the number of vehicles in the system immediately after the next departure is (Neuts 1989)

$$N_{n+1} = (N_n - 1)_+ + A(\delta_n, \delta_{n+1}) = (N_n - 1)_+ + A_{n+1}, \qquad \text{for } n \geq 1, \tag{4.49}$$

where A_{n+1} is the number of arrivals between departures n and $n+1$. The number of vehicles in the system after the next departure depends only on the number of vehicles in the system after current departure and the number of arrivals between the current and the next departures. This type of process is called an *embedded Markov chain* (see Kendall 1951, Kendall 1953, Ross 1996). At transition points (times of departure from service) the process behaves like a discrete-time Markov chain having a one-step transition probability matrix

$$\mathbf{P} = \begin{bmatrix} p_{00} & p_{01} & p_{02} & \cdots \\ p_{10} & p_{11} & p_{12} & \cdots \\ 0 & p_{21} & p_{22} & \cdots \\ 0 & 0 & p_{32} & \cdots \\ \vdots & \vdots & \vdots & \ddots \end{bmatrix}, \tag{4.50}$$

where p_{ij} is the probability that between two consecutive departures the number of vehicles in the system changes from i to j. Because $\mathbf{P}$ is a stochastic matrix, its rows sum to one:

$$\sum_{j=0}^{\infty} p_{ij} = 1. \tag{4.51}$$

The transition probabilities can be derived from equation (4.49). If $i \in \{1, 2, 3, \dots\}$ a vehicle (n) arrives to stop line (service) immediately when the previous vehicle $(n-1)$ has departed service. The transition interval between departures $n-1$ and n is the service time of vehicle n. The probability p_{ij} of transition from state i to $j \in \{i-1, i, i+1, \dots\}$ is the probability α_{j-i+1} of $j-i+1$ arrivals during the service time. Because the arrival process is Poisson, it is not necessary to know the backward waiting time (see Figure 2.6 on page 32) at the time of service completion.

If $i = 0$ a vehicle (n) arrives to stop line (service) some time after the previous vehicle $(n-1)$ has departed service. The transition interval between departures $n-1$ and n is the idle time of the server plus the service time of vehicle n. However, vehicle $n+1$ cannot arrive before vehicle n. The probability p_{0j} of transition from state 0 to $j \in \{0, 1, 2, \dots\}$ is the probability β_j of j arrivals during the service time of vehicle n that has arrived during an idle period. The transition probability matrix can be expressed as

$$\mathbf{P} = \begin{bmatrix} \beta_0 & \beta_1 & \beta_2 & \cdots \\ \alpha_0 & \alpha_1 & \alpha_2 & \cdots \\ 0 & \alpha_0 & \alpha_1 & \cdots \\ 0 & 0 & \alpha_0 & \cdots \\ \vdots & \vdots & \vdots & \ddots \end{bmatrix}. \tag{4.52}$$

The transition probabilities are independent on n and depend on i and j only through their difference. The rows sum to one:

$$\begin{aligned} \sum_{k=0}^{\infty} \alpha_k &= 1 \\ \sum_{k=0}^{\infty} \beta_k &= 1. \end{aligned} \tag{4.53}$$

Let $f_q(u)$ and $f_e(u)$ be the probability density functions of service time distributions for vehicles arriving to a queue and to an empty system, respectively. Because minor stream arrivals are Poisson, the transition probabilities are

$$\begin{aligned} \alpha_k &= \int_0^{\infty} \frac{(\lambda u)^k}{k!} e^{-\lambda u} f_q(u)\, du \\ \beta_k &= \int_0^{\infty} \frac{(\lambda u)^k}{k!} e^{-\lambda u} f_e(u)\, du. \end{aligned} \tag{4.54}$$

These are probabilities of k arrivals during a service period. The process is equivalent to an M/G2/1 queuing system. If $f_q(u) = f_e(u)$, the transition probability matrix describes an M/G/1 queuing system (see Neuts 1989).

4.3.2 M/G/1 model

If the arrival pattern of vehicles approaching an intersection in one lane is assumed to follow the Poisson process, and vehicles are served by a single server having some general i.i.d. service pattern, the system can be described as an M/G/1 queuing process.[4] Because all service times are assumed to be independent and identically distributed, $\alpha_i = \beta_i$. The transition probabilities are

$$\alpha_k = \int_0^{\infty} \frac{(\lambda u)^k}{k!} e^{-\lambda u} f_S(u)\, du \tag{4.55}$$

where $f_S(u)$ is the probability density function of service times. The one-step transition probability matrix is

$$\mathbf{P} = \begin{bmatrix} \alpha_0 & \alpha_1 & \alpha_2 & \cdots \\ \alpha_0 & \alpha_1 & \alpha_2 & \cdots \\ 0 & \alpha_0 & \alpha_1 & \cdots \\ 0 & 0 & \alpha_0 & \cdots \\ \vdots & \vdots & \vdots & \ddots \end{bmatrix}. \tag{4.56}$$

Let us define

$$\pi_j = \lim_{k \to \infty} \mathbb{P}\{N_k = j\}, \qquad j \in \{0, 1, 2, \dots\} \tag{4.57}$$

as the stationary (equilibrium) probability that in the long run the system is found in state j. These probabilities can be expressed as

$$\begin{aligned} \pi_j &= \pi_0 p_{0j} + \sum_{i=1}^{j+1} \pi_i p_{ij} \\ &= \pi_0 \alpha_j + \sum_{i=1}^{j+1} \pi_i \alpha_{j-i+1}, \qquad j \in \{0, 1, 2, \dots\}. \end{aligned} \tag{4.58}$$

[4] In Kendall's (1953) notation M/G/1 stands for Markovian (Poisson) arrival process / General service time distribution / 1 server.

The process can reach state j, if it first reaches some other state i from which it moves to state j. The probabilities sum to unity

$$\sum_{j=0}^{\infty} \pi_j = 1. \tag{4.59}$$

This can be used as a normalization equation in further analysis.

The average waiting times can be derived either from the stationary probabilities (4.58) which have probability-generating function

$$G_\pi(z) = \sum_{j=0}^{\infty} \pi_j z^j = \frac{(z-1)\mathcal{L}_S(\lambda - \lambda z)}{z - \mathcal{L}_S(\lambda - \lambda z)}(1-\rho), \tag{4.60}$$

where $\mathcal{L}_S(\cdot)$ is the Laplace transform of the service-time distribution function, or directly from equation (4.49) using mean values (Cooper 1981). The average waiting time in queue is given by the *Pollaczek-Khintchine formula* (Pollaczek 1930, Khintchine 1960, Kendall 1951)[5]:

$$\bar{W}_{\mathrm{G.Q}} = \frac{\rho \bar{S}}{2(1-\rho)}\left(1 + \frac{\sigma_S^2}{\bar{S}^2}\right) = \frac{\rho \bar{S}\left(1 + C_S^2\right)}{2(1-\rho)}, \tag{4.61}$$

where $\bar{S}$ is the mean and σ_S^2 is the variance of service times, $\rho = \lambda \bar{S}$ is the server utilization factor, λ is the arrival rate, and $C_S = \sigma_S / \bar{S}$ is the coefficient of variation of service times. If $\bar{S}$ is assumed to be equal to inverse capacity, the utilization factor is equal to the D/C ratio. Because under low D/C conditions this assumption underestimates ρ, it underestimates delay also. The average waiting time in the system, including the service time, is (Gross & Harris 1998)

$$\begin{aligned} \bar{W}_{\mathrm{G.S}} &= \bar{W}_{\mathrm{G.Q}} + \bar{S} \\ &= \bar{S}\left(1 + \frac{\rho\left(1 + C_S^2\right)}{2(1-\rho)}\right) \\ &= \boxed{\bar{S}\left(1 + \frac{\rho\kappa}{1-\rho}\right)}, \end{aligned} \tag{4.62}$$

where $\kappa = (1 + C_S^2)/2$ is the *randomness constant* (Transportation Research Board 1997). It indicates how rapidly the average delay increases with the D/C ratio (Troutbeck 1986). Because $\sigma_S^2 = \mathbb{E}[S^2] - \bar{S}^2$, the randomness constant is

$$\kappa = \frac{\mathbb{E}[S^2]}{2\bar{S}^2}. \tag{4.63}$$

Observing that $\rho/\bar{S} = \lambda$, the waiting times can be expressed as

$$\bar{W}_{\mathrm{G.Q}} = \frac{\lambda\, \mathbb{E}[S^2]}{2(1-\rho)} \tag{4.64a}$$

$$\bar{W}_{\mathrm{G.S}} = \bar{S} + \frac{\lambda\, \mathbb{E}[S^2]}{2(1-\rho)}. \tag{4.64b}$$

[5]Khintchine presented the result in 1932 in a paper in Russian, independently of Pollaczek (Cooper 1981).

Little's (1961) formula

$$\bar{L} = \lambda \bar{W} \tag{4.65}$$

gives the average number of vehicles in system or in queue, depending on the type of average waiting time ($\bar{W}$) used in the equation. Queue length distributions have been studied by Heidemann (1991) and Wu (1994). Little's formula (4.65) can also be used to estimate average delay, when the average queue length is known. Daganzo (1977), however, warns about some pitfalls in this technique, especially in connection with the embedding technique.

In order to apply equation 4.62, the mean ($\bar{S}$) and variance (σ_S^2) of service times must be estimated. It is usually suggested that the average service time of queuing vehicles ($\bar{S}_q = C^{-1}$) is used (Transportation Research Board 1997), although it may slightly underestimate service times and delays (see Fig. 4.6).

The variance σ_S^2 depends on the service time distribution. If all service times are assumed constant, $\sigma_S^2 = 0$, $\kappa = 0.5$, and the average waiting time in queue is

$$\bar{W}_{D.Q} = \frac{\rho \bar{S}}{2(1-\rho)} = \frac{\rho^2}{2\lambda(1-\rho)}. \tag{4.66}$$

This queuing process is called M/D/1, where D stands for deterministic service times. The assumption that all vehicles wait an equal time at yield/stop line is, of course, unrealistic. The M/D/1 model has found better applications in the delay estimation of signalized intersections (Webster 1958).

If both interarrival time (headway) and service time distributions are assumed to be negative exponential, the queuing process is called M/M/1. In the negative exponential distribution the standard deviation is equal to the mean ($\sigma_S = \bar{S}$), so that $C_S = 1$ and $\kappa = 1$. The waiting times are obtained from the Pollaczek-Khintchine formula (4.61) as

$$\bar{W}_{M.Q} = \frac{\rho \bar{S}}{1-\rho} \tag{4.67a}$$

$$\bar{W}_{M.S} = \frac{\bar{S}}{1-\rho}. \tag{4.67b}$$

According to Kimber & Hollis (1979) and Fisk & Tan (1989) the M/M/1 model will produce a good approximation to a M/G/1 model having similar average service times.

The variation in service times doubles the waiting time in a queue over that in an M/D/1 system ($\bar{W}_{M.Q} = 2\bar{W}_{D.Q}$). If $\bar{S}$ is the inverse of capacity (C), the waiting time in system can be expressed as the inverse of reserve capacity

$$\bar{W}_{M.S} = \frac{3600}{C-q}. \tag{4.68}$$

The relationship between delay and reserve capacity has been discussed e.g. by Brilon (1988*b*) and Tracz, Chodur & Gondek (1990). This relationship demonstrates the central role of a good capacity estimate in delay estimation. At high degrees of saturation small errors in capacity estimates will result in significant errors in delay estimates (Kyte, Dixon & Basavaraju 2003).

Because service times cannot be shorter than the follow-up time, a possible model for service time distribution is the shifted exponential distribution, which has mean $\bar{S} = t_f + \theta^{-1}$ and standard deviation $\sigma_S = \theta^{-1} = \bar{S} - t_f$ (Luttinen 1996). The coefficient

of variation is $C_S = 1 - t_f/\bar{S}$. This indicates that the shifted exponential service time model gives smaller delays than the M/M/1 model. Shifted exponential service time distribution with location parameter equal to the follow-up time is equivalent to the assumption of negative exponential waiting time distribution at yield/stop line.

The randomness constant is obtained as

$$\kappa = 1 + \frac{t_f}{\bar{S}}\left(\frac{t_f}{2\bar{S}} - 1\right). \tag{4.69}$$

The average waiting time in the system can now be calculated as

$$\begin{aligned} \bar{W}_{M',S} &= \frac{\bar{S} + \rho t_f\left(\frac{t_f}{2\bar{S}} - 1\right)}{1-\rho} \\ &= \bar{W}_{M,S} + \frac{\rho t_f}{1-\rho}\left(\frac{t_f}{2\bar{S}} - 1\right). \end{aligned} \tag{4.70}$$

Because $t_f/(2\bar{S}) < 1$, the waiting time $\bar{W}_{M',S}$ is less than $\bar{W}_{M,S}$.

The M/G/1 models discussed so far have ignored that vehicles arriving to an empty system have different average service times ($\bar{S}_e$) than queuing vehicles ($\bar{S}_q$). In addition, the variance of service times is based on arbitrary assumptions, not on solid theory.

In an M/G/1 queuing process the proportion of time the server is busy is equal to the utilization factor $\rho = \lambda\bar{S}$. The distribution of service times is a *mixture* of two distributions. The proportion ρ of service times are from the distribution f_q for queuing vehicles (see Section 3.5.3), and the proportion $1 - \rho$ are from the distribution f_e for isolated vehicles:

$$f_S(s) = \rho f_q(s) + (1-\rho) f_e(s). \tag{4.71}$$

The average service time can be estimated as (SNRA 1995*b*, Pöschl 1983)

$$\bar{S} = \rho\bar{S}_q + (1-\rho)\bar{S}_e \tag{4.72}$$

The service quotients for queuing (ρ_q) and non-queuing vehicles (ρ_e) are

$$\rho_q = \lambda\bar{S}_q \tag{4.73a}$$

$$\rho_e = \lambda\bar{S}_e. \tag{4.73b}$$

The D/C ratio and the average service time are now obtained in terms of component flows as (Pöschl 1983)

$$\rho = \lambda\bar{S} = \frac{\rho_e}{1 + \rho_e - \rho_q} \tag{4.74}$$

$$\bar{S} = \frac{\bar{S}_e}{1 + \rho_e - \rho_q} \tag{4.75}$$

The probability that a randomly arriving vehicle finds the system empty is (Yeo 1962)

$$p_0 = 1 - \rho = \frac{1 - \rho_q}{1 + \rho_e - \rho_q}. \tag{4.76}$$

The second moment of the mixed service time distribution is

$$\begin{aligned} \mathbb{E}[S^2] &= \rho\,\mathbb{E}\left[S_q^2\right] + (1-\rho)\,\mathbb{E}\left[S_e^2\right] \\ &= \frac{\rho_e\,\mathbb{E}\left[S_q^2\right] + (1-\rho_q)\,\mathbb{E}\left[S_e^2\right]}{1 + \rho_e - \rho_q}. \end{aligned} \tag{4.77}$$

The average waiting time in queue is obtained from equation (4.64a) as

$$\begin{aligned}\bar{W}_{G.Q} &= \frac{\lambda\,\mathbb{E}[S^2]}{2(1-\rho)} \\ &= \frac{\lambda}{2(1-\rho_q)}\left(\rho_e\,\mathbb{E}\left[S_q^2\right] + (1-\rho_q)\,\mathbb{E}\left[S_e^2\right]\right).\end{aligned} \tag{4.78}$$

The average waiting time in system is obtained by adding the average service time to $\bar{W}_{G.q}$:

$$\begin{aligned}\bar{W}_{G.S} &= \bar{S} + \bar{W}_{G.q} \\ &= \boxed{\frac{\bar{S}_e}{1+\rho_e-\rho_q} + \frac{\lambda}{2(1-\rho_q)}\left(\rho_e\,\mathbb{E}\left[S_q^2\right] + (1-\rho_q)\,\mathbb{E}\left[S_e^2\right]\right).}\end{aligned} \tag{4.79}$$

4.3.3 M/G2/1 model

It is possible to apply the M/G/1 model with a service time distribution that takes into account the dependency between the major stream arrivals and the arrivals of non-queuing minor stream arrivals. However, the M/G/1 model assumes that consecutive service times are independent (Gross & Harris 1998); i.e., a sequence of service times for queuing and non-queuing vehicles follows geometric distribution (cf. Cooper 1981). The service times distributions behind transition probabilities α_i and β_i (4.55) are equal. In assigning service times to customers the M/G/1 model does not make any distinction between vehicles actually queuing or not queuing.

Yeo (1962) has presented a modified model, M/G2/1, which assigns service time S_q to queuing customers and service time S_e to customers arriving to an empty system. The one-step transition probability matrix is given as in equation 4.52, and transition probabilities follow equation 4.54 (see Neuts 1989). The average waiting time in queue is (Yeo 1962)

$$\bar{W}_{G2.Q} = \frac{\lambda\left(\rho_e\,\mathbb{E}\left[S_q^2\right] + (1-\rho_q)\,\mathbb{E}\left[S_e^2\right]\right)}{2(1-\rho_q)(1+\rho_e-\rho_q)}. \tag{4.80}$$

This differs from equation (4.78) by factor $(1+\rho_e-\rho_q)^{-1}$. When average service times for queuing and non-queuing customers are equal, the service quotients are also equal ($\rho_e = \rho_q$), and M/G2/1 model reduces to an M/G/1 model.

The average waiting time in system can be expressed as (Pöschl 1983)

$$\begin{aligned}\bar{W}_{G2.S} &= \bar{S} + \bar{W}_{G2.Q} \\ &= \boxed{\frac{\bar{S}_e + \frac{\lambda}{2(1-\rho_q)}\left(\rho_e\,\mathbb{E}\left[S_q^2\right] + (1-\rho_q)\,\mathbb{E}\left[S_e^2\right]\right)}{1+\rho_e-\rho_q}.}\end{aligned} \tag{4.81}$$

Yeo & Weesakul (1964) have used the M/G2/1 model for the analysis of delays at unsignalized intersections.

In an M/G/1 queuing system the distribution of queue lengths at service completion times is equivalent to the queue size distribution at random times (see footnote 10 on page 85.) Heidemann (1991) has shown that the M/G2/1 system also has this property.[6] He also demonstrated that Little's formula (4.65) can be applied in M/G2/1 systems.

[6] Daganzo (1977) warns against assuming the equivalency between queue length distributions at a random time and at the arrival time of a major stream vehicle (see Evans, Herman & Weiss 1964).

Lertworawanich & Elefteriadou (2003) have estimated storage (queue) lengths of left-turn lanes. They found that, compared to the M/G2/1 model, the M/M/1 model provided good estimates, except at near-capacity conditions.

4.3.4 Tanner's delay model

Tanner (1962) described major stream as departures from an M/D/1 queuing system with minimum headway t_p (see page 41) and average arrival rate λ_1, and assumed a Poisson process with average arrival rate λ_2 for minor stream arrivals. Minor stream vehicles cannot enter the intersection at shorter intervals than the follow-up time (t_f) and not within the critical gap (t_c) *after the previous major-stream vehicle.*

A block starts with a major-stream vehicle more than t_c behind the previous major-stream vehicle, and ends a time t_c after a vehicle being separated from the next major-stream vehicle by more than t_c. The model is similar to the extension principle in traffic signals (Fig. 2.12). Because $t_c > t_p$, the lag following a block is exponentially distributed. The lag distribution is the same for both queuing and isolated vehicles.

Tanner modeled the queuing process at an unsignalized intersection as an embedded Markov chain (see page 118) with two types of regeneration points:

1. The instants at which minor-stream vehicles cross the stop line
2. The ends of blocks in the major stream, if not included in the first type

These definitions are based on the description of gap acceptance, which is slightly different from the description used in this report. See footnote 6 on page 44.

The state of the system at a regeneration point of type 1 is the number of minor stream vehicles waiting after one has crossed the stop line. The state of the system at regeneration point of type 2 is x. The transition probability from state i to j ($i = x, 0, 1, 2, \ldots$; $j = x, 0, 1, 2, \ldots$) is p_{ij}. The system can now be described by a transition matrix

$$\mathbf{P} = \begin{bmatrix} p_{xx} & p_{x0} & p_{x1} & p_{x2} & \cdots \\ p_{0x} & p_{00} & p_{01} & p_{02} & \cdots \\ 0 & p_{10} & p_{11} & p_{12} & \cdots \\ 0 & 0 & p_{21} & p_{22} & \cdots \\ 0 & 0 & 0 & p_{32} & \cdots \\ \vdots & \vdots & \vdots & \vdots & \ddots \end{bmatrix}. \tag{4.82}$$

The results of the study, however, indicated that the average queue length just after service was the same as at random instant. Consequently, type 2 regeneration points can be considered redundant, and matrix 4.82 can be reduced to matrix 4.50 with appropriate adjustments to the transition probabilities. The passing of a major stream vehicle has no effect on minor stream queues, when no minor stream vehicles are waiting at stop line or arrive during the block.

The probability p_{ij} of transition from $i \in \{1, 2, 3, \ldots\}$ to $j \in \{i-1, i, i+1, \ldots\}$ is the probability of $j - i + 1$ arrivals during a service time, which is either the follow-up time t_f or a lag Υ_1 shorter than t_f plus a block (T_b):

$$p_{ij} = \mathbb{P}\{t_f \leq \Upsilon_1, A(t_f) = j - i + 1\} + \mathbb{P}\{\Upsilon_1 < t_f, A(\Upsilon_1 + T_b) = j - i + 1\}. \tag{4.83}$$

The probability of k arrivals during a transition interval is

$$\begin{aligned}\alpha_k &= \mathbb{P}\{t_f \le \Upsilon_1, A(t_f) = k\} + \mathbb{P}\{\Upsilon_1 < t_f, A(\Upsilon_1 + T_b) = k\} \\ &= e^{-\lambda_1 t_f}\frac{(\lambda_2 t_f)^k}{k!}e^{-\lambda_2 t_f} + \int_0^{t_f}\lambda_1 e^{-\lambda_1 v}\int_0^{\infty}\frac{[\lambda_2(v+y)]^k}{k!}e^{-\lambda_2(v+y)}f_b(y)\,dy\,dv \\ &\qquad k \in \{0, 1, 2, \dots\}, \quad (4.84)\end{aligned}$$

where $f_b(y)$ is the probability density function of block lengths (T_b). Tanner (1953) has given its moment generating function, from which the expected block length can be obtained as

$$\mathbb{E}[T_b] = \frac{e^{\lambda_1(t_c - t_p)}}{\lambda_1(1 - \lambda_1 t_p)} - \frac{1}{\lambda_1}. \quad (4.85)$$

If a departing vehicle leaves the system empty ($i = 0$), Tanner's (1962) model (4.82) considers the possibility of transition to state x as:

$$\begin{aligned}p_{0x} &= \mathbb{P}\{\Upsilon_1 < \Upsilon_2, A(T_b) = 0\} \\ &= \frac{\lambda_1}{\lambda_1 + \lambda_2}\int_0^{\infty} e^{-\lambda_2 y} f_b(y)\,dy. \quad (4.86)\end{aligned}$$

The transition takes place, if a major-stream vehicle arrives before a minor-stream vehicle and no minor-stream vehicles arrive during the ensuing block y (Fig. 4.8).

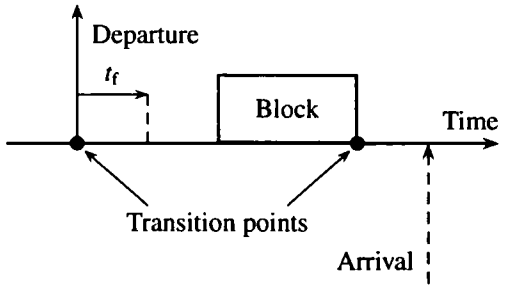

Figure 4.8: Transition $0 \to x$ in Tanner's (1962) model

The state 0 stays unchanged (Fig. 4.9), if one minor-stream vehicle arrives *a*) during the follow-up time in antiblock, *b*) after follow-up time but before the next major-stream vehicle, *c*) during a lag $\Upsilon_1 < t_f$ or adjacent block, or *d*) during a block that has started after the follow-up time:

$$\begin{aligned}p_{00} &= \mathbb{P}\{t_f \le \Upsilon_1, A(t_f) = 1\} + \mathbb{P}\{t_f \le \Upsilon_2 < \Upsilon_1\} \\ &\quad + \mathbb{P}\{\Upsilon_1 < t_f, A(\Upsilon_1 + T_b) = 1\} + \mathbb{P}\{t_f \le \Upsilon_1 < \Upsilon_2, A(T_b) = 1\}. \quad (4.87)\end{aligned}$$

This becomes (Tanner 1962)

$$\begin{aligned}p_{00} &= e^{-\lambda_1 t_f}\lambda_2 t_f e^{-\lambda_2 t_f} + \frac{\lambda_2}{\lambda_1 + \lambda_2}e^{-(\lambda_1+\lambda_2)t_f} \\ &\quad + \int_0^{t_f}\lambda_1 e^{-\lambda_1 v}\int_0^{\infty}\lambda_2(v+y)e^{-\lambda_2(v+y)}f_b(y)\,dy\,dv \\ &\quad + \frac{\lambda_1}{\lambda_1 + \lambda_2}e^{-(\lambda_1+\lambda_2)t_f}\int_0^{\infty}\lambda_2 y\, e^{-\lambda_2 y} f_b(y)\,dy. \quad (4.88)\end{aligned}$$

By collecting terms we obtain

$$p_{00} = \frac{e^{-(\lambda_1+\lambda_2)t_f}}{\lambda_1+\lambda_2}\left(\lambda_2(1+\lambda_1 t_f+\lambda_2 t_f)+\lambda_1\int_0^\infty \lambda_2 y\, e^{-\lambda_2 y} f_b(y)\, dy\right) + \int_0^{t_f}\lambda_1 e^{-\lambda_1 v}\int_0^\infty \lambda_2(v+y)e^{-\lambda_2(v+y)} f_b(y)\, dy\, dv. \quad (4.89)$$

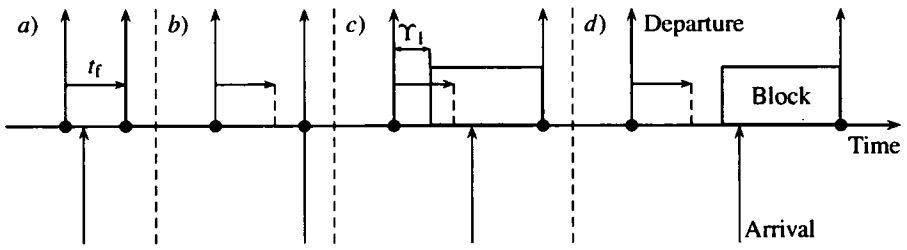

Figure 4.9: Possible ways for transition 0 → 0 in Tanner's (1962) model

The state of the system shifts from state 0 to state $j \in \{1, 2, 3, \dots\}$, if $j+1$ vehicles arrive *a*) during a follow-up time in antiblock, or *b*) during a lag $\Upsilon_1 < t_f$ or adjacent block, or *c*) during a block initiated by a major-stream vehicle arriving later than t_f after the previous transition point but before the next minor-stream vehicle:

$$p_{0j} = \mathbb{P}\{t_f \le \Upsilon_1, A(t_f) = j+1\} + \mathbb{P}\{\Upsilon_1 < t_f, A(\Upsilon_1 + T_b) = j+1\} + \mathbb{P}\{t_f \le \Upsilon_1 < \Upsilon_2, A(T_b) = j+1\}, \qquad j \in \{1, 2, 3, \dots\}. \quad (4.90)$$

This can be expressed as (Tanner 1962)

$$p_{0j} = \frac{(\lambda_2 t_f)^{j+1}}{(j+1)!}e^{-(\lambda_1+\lambda_2)t_f} + \int_0^{t_f}\lambda_1 e^{-\lambda_1 v}\int_0^\infty \frac{[\lambda_2(v+y)]^{j+1}}{(j+1)!}e^{-\lambda_2(v+y)} f_b(y)\, dy\, dv + \frac{\lambda_1}{\lambda_1+\lambda_2}e^{-(\lambda_1+\lambda_2)t_f}\int_0^\infty \frac{(\lambda_2 y)^{j+1}}{(j+1)!}e^{-\lambda_2 y} f_b(y)\, dy, \qquad j \in \{1, 2, 3, \dots\}. \quad (4.91)$$

Transition probabilities p_{0j} are analogous with the probability p_{00} in cases *a*, *c*, and *d*. Case *b* does, however, not have an analogy, because service time is zero and it does not allow any queue accumulation.

If the system is empty when a block ends, the system remains in state x, if a major-stream vehicle arrives before a minor-stream vehicle and no minor-stream vehicles arrive during the ensuing block; i.e., $p_{xx} = p_{0x}$. A state x is followed by state 0 if the next vehicle is from the minor stream or if the next vehicle is from the major stream and exactly one minor-stream vehicle arrives during the block (Tanner 1962):

$$\begin{aligned} p_{x0} &= \mathbb{P}\{\Upsilon_2 < \Upsilon_1\} + \mathbb{P}\{\Upsilon 1 < \Upsilon_2, A(T_b) = 1\} \\ &= \frac{\lambda_2}{\lambda_1+\lambda_2} + \frac{\lambda_1}{\lambda_1+\lambda_2}\int_0^\infty \lambda_2 y\, e^{-\lambda_2 y} f_b(y)\, dy. \end{aligned} \quad (4.92)$$

Similarly (Tanner 1962)

$$\begin{aligned} p_{xj} &= \mathbb{P}\{\Upsilon 1 < \Upsilon_2, A(T_b) = j+1\} \\ &= \frac{\lambda_1}{\lambda_1+\lambda_2}\int_0^\infty \frac{(\lambda_2 y)^{j+1}}{(j+1)!}e^{-\lambda_2 y} f_b(y)\, dy, \qquad j \in \{1, 2, \dots\}. \end{aligned} \quad (4.93)$$

Now all elements in the transition probability matrix **P** (4.82) have been defined.

The regeneration point of type 1 in this model is the time instant that a minor stream vehicle crosses the stop line. The follow-up time is not included in waiting time. The average waiting time in system is obtained by adding t_f to the Tanner's delay ($\bar{W}_2$), as suggested by Heidemann (1991). The equation is

$$\boxed{\bar{W}_S = \bar{W}_2 + t_f = \frac{\mathbb{E}[T_b^2]}{2a_1} + \frac{\lambda_2}{\lambda_1} a_1 e^{-\lambda_1 t_f}(e^{\lambda_1 t_f} - \lambda_1 t_f - 1)}{1 - \lambda_2 a_1 (1 - e^{-\lambda_1 t_f})} + t_f, \tag{4.94}$$

where

$$a_1 = \mathbb{E}[T_b] + \lambda_1^{-1} = \frac{e^{\lambda_1 (t_c - t_p)}}{\lambda_1 (1 - \lambda_1 t_p)}. \tag{4.95}$$

If the major flow is Poisson ($t_p = 0$), the waiting time becomes

$$\bar{W}_S = \bar{W}_2 + t_f = \frac{\lambda_1 e^{\lambda_1 t_f}(e^{\lambda_1 t_c} - \lambda_1 t_c - 1) + \lambda_2 e^{\lambda_1 t_c}(e^{\lambda_1 t_f} - \lambda_1 t_f - 1)}{\lambda_1 [\lambda_1 e^{\lambda_1 t_f} - \lambda_2 e^{\lambda_1 t_c}(e^{\lambda_1 t_f} - 1)]} + t_f. \tag{4.96}$$

Dunne & Buckley (1972) observed that for an isolated vehicle the average waiting time during a block (Adams' delay) according to equation 4.94 is

$$\bar{W}_e = \lim_{\lambda_2 \to 0} \bar{W}_2 = \frac{\mathbb{E}[T_b^2]}{2a_1}. \tag{4.97}$$

Capacity (3.24) can be expressed as

$$\begin{aligned} C_p &= \frac{\lambda_1 (1 - \lambda_1 t_p) e^{-\lambda_1 (t_c - t_p)}}{1 - e^{-\lambda_1 t_f}} \\ &= [a_1 (1 - e^{-\lambda_1 t_f})]^{-1}, \end{aligned} \tag{4.98}$$

so that the demand-to-capacity ratio of the minor stream is

$$\rho = \frac{\lambda_2}{C_p} = \lambda_2 a_1 (1 - e^{-\lambda_1 t_f}). \tag{4.99}$$

Delay equation (4.94) can now be rewritten as (Dunne & Buckley 1972)

$$\bar{W}_2 = \frac{\bar{W}_e + a_2 \rho}{1 - \rho}, \tag{4.100}$$

where

$$\begin{aligned} a_2 &= \frac{e^{\lambda_1 t_f} - \lambda_1 t_f - 1}{\lambda_1 (e^{\lambda_1 t_f} - 1)} \\ &= \frac{1}{\lambda_1} - \frac{t_f}{e^{\lambda_1 t_f} - 1} \end{aligned}$$

The waiting time in system can be expressed as

$$\begin{aligned} \bar{W}_S &= \bar{W}_2 + t_f \\ &= \bar{S}_e \left[1 + \left(1 + \frac{a_2 - t_f}{\bar{S}_e} \right) \frac{\rho}{1 - \rho} \right]. \end{aligned} \tag{4.101}$$

This has the structure of the Pollaczek-Khintchine formula (4.61), assuming that the randomness constant is given as

$$\begin{aligned}\kappa &= 1 + \frac{a_2 - t_f}{\bar{S}_e} \\ &= 1 + \frac{1}{\bar{S}_e}\left(\frac{1}{\lambda_1} - \frac{t_f}{1 - e^{-\lambda_1 t_f}}\right)\end{aligned} \tag{4.102}$$

and $\bar{S}_e = \bar{W}_e + t_f$ is the average service time of isolated vehicles (see Section 4.2.3).

Thus, the average delay equation (4.94) of Tanner (1962) can be expressed in terms of an M/G/1 queuing system. Pöschl (1983) has demonstrated numerically that Tanner's model is compatible with the M/G/1 model. See also Heidemann (1991). Also when major-stream headways follow Cowan's (1975, 1984, 1987) M3 model (see Section 2.3.6), the delay equation can be expressed in the form of the Pollaczek-Khintchine formula (Troutbeck 1990, Troutbeck & Walsh 1994).

The discussion above has demonstrated that the theoretical queuing models have a close connection with gap acceptance theory. Troutbeck & Walsh (1994) have remarked that with proper service-time distributions queuing theory gives exactly the same estimates as gap acceptance theory. They preferred gap acceptance theory, because it is based on documented driver behavior. However, in this report queuing theory is preferred mainly for three reasons: *i*) Queuing theory allows the application of sophisticated capacity models without leading to very complex delay models. *ii*) Queuing models use capacity as a parameter, so that delay estimates are compatible with capacity estimates. *iii*) Queuing models are easier to analyze under transient (time-dependent) conditions than gap acceptance models. This is the theme of the next section.

4.4 Delays under transient conditions

4.4.1 Definition of a transient state

The models discussed above assume steady-state conditions (see section 3.1). It is assumed that all conditions remain similar, with only random variation, during the analysis period, and that earlier conditions (such as a peak period) do not have any significant effect on the analysis period. However, the conditions during an analysis period are often transient, because

- flow rates, or other conditions, are changing,
- the system cannot reach equilibrium because flow rates exceed capacity, and/or
- preceding conditions still have an effect on the performance of the system.

During a transient period the performance measures of the system are time dependent.

The parameters, such as flow rates, of the models are usually given as averages over the analysis period. Because delay is not a linear function of flow rates, but increases more steeply at high flow rates, the use of average parameter values under transient conditions make the results biased. The analysis should be performed for several shorter analysis periods, describing flow rates as a step function, and with a proper consideration of initial queues (Kimber & Hollis 1978, Fisk & Tan 1989).

When conditions are stable, but have changed recently, it takes some time before the effect of earlier conditions becomes negligible. Steady state conditions are obtained only after a transient phase. For example, after a peak period, when flow rates have

decreased, it takes some time before the queues have reached equilibrium. Also during a peak period it takes some time before the queues reach an equilibrium state. The problem of an initial transient period is well known in simulation theory (e.g., Bratley, Fox & Schrage 1987, Kleijnen 1987).

Morse (1958) has estimated that the "relaxation time" of a queuing system with one exponential channel and finite storage capacity is approximately $(\sqrt{C} - \sqrt{q})^{-2}$ (see also Kleinrock 1976). As flow rates approach capacity, relaxation time increases to infinity. If flow rates exceed capacity, queues increase constantly, and no equilibrium is reached.

It is apparent that oversaturated systems are in a transient state. For degrees of saturation below but near unity the relaxation times are likely to span over observation periods. Consequently, transient analysis is called for, if conditions change during the analysis period and/or if the D/C ratio is near or above unity.

4.4.2 Oversaturated conditions

Overflow delay

If the average arrival rate exceeds capacity, the intersection is oversaturated. The expected number of arrivals during a time period τ is $A(\tau) = q\tau$. The average departure rate is equal to the capacity C, so that $D(\tau) = C(\tau) = C\tau$, assuming a constant capacity during the observation period.

If the queue length in the beginning of the observation period is $L(0)$, the queue at the end of the observation period is $L(\tau) = L(0) + A(\tau) - D(\tau)$.[7] Because under oversaturated conditions $A(\tau) > D(\tau)$, the system is in a *nonequilibrium* state, and the queue length increases constantly.

A fluid analogy model for unsignalized intersections was described in section 2.5. Figure 4.10 displays a fluid-analogy model for a case where demand flow rate instantaneously increases above the capacity at the beginning of the observation period. The area between $A(\tau)$ and $C(\tau)$ curves is the overflow delay (Gazis & Potts 1965); i.e., the excess waiting time due to oversaturation. The fluid analogy model ignores the service times and the stochastic component of delay (Fig. 4.11). When queues are long, the magnitude of of discontinuities is small relative to the average values (Kleinrock 1976).

To estimate the overflow delay it is only necessary to know the initial queue $L(0)$, arrival flow rate $q(t)$, capacity C, and the length of the observation period τ. A special strength of the fluid analogy overflow model is that a similar approach can be applied to estimate overflow delay for different kinds of facilities, such as freeways (May & Keller 1967) and signalized intersections (Gazis & Potts 1965, Luttinen & Nevala 2002).

The overflow queue is

$$L_o(\tau) = L(0) + A(\tau) - C(\tau), \tag{4.103}$$

assuming that the overflow condition continues over the whole time interval (cf. Catling 1977):

$$\forall u \in (0, \tau]: L(0) + A(u) - C(u) > 0. \tag{4.104}$$

If the overflow period starts in the beginning of the analysis period and there is no initial queue, then $L_o(\tau) = A(\tau) - C(\tau)$. For a constant arrival rate and capacity the overflow

[7] Because at oversaturated conditions server is always busy, the departure rate from the system is equal to the rate of customers moving from the queue to the service. The number of customers in the system is $N(\tau) = L(\tau) + 1$.

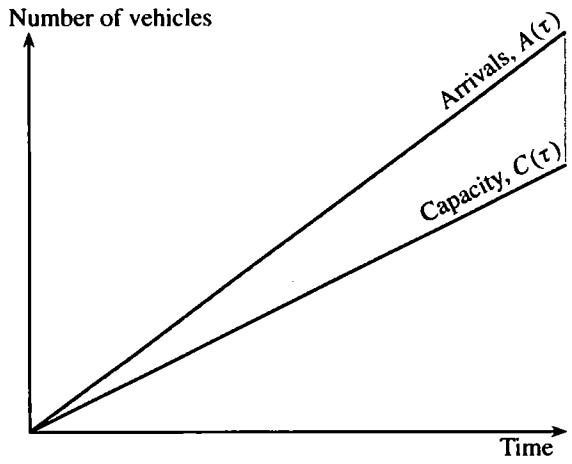

Figure 4.10: Fluid analogy model for overflow delay

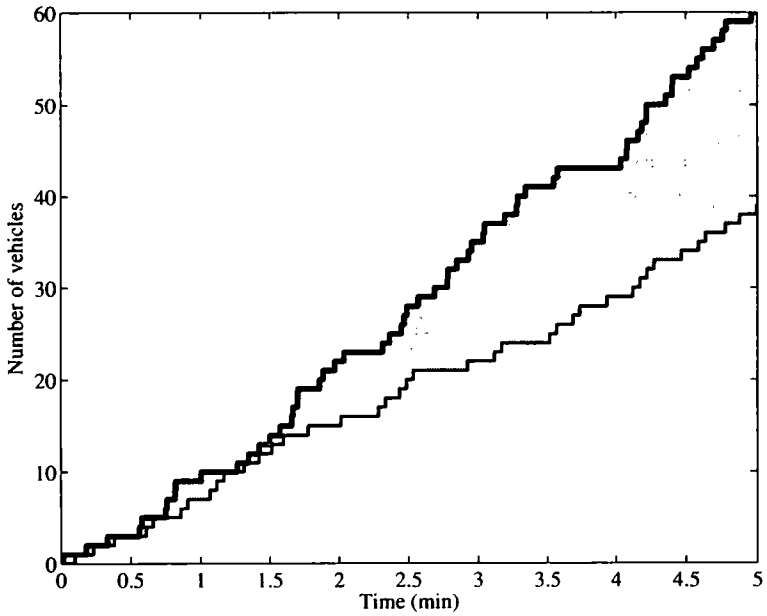

Figure 4.11: Cumulative arrivals (thick curve) and departures (thin curve) at an oversaturated minor approach (major flow 800 veh/h, minor flow 700 veh/h, $t_c = 5\,s$, $t_f = 3\,s$, exponential headway distributions)

queue is $L_o(\tau) = \tau(q - C) = C\tau(\rho - 1)$. If the overflow queue at time instant τ_1 is $L_o(\tau_1)$, the overflow queue at $\tau_2 > \tau_1$ is

$$L_o(\tau_2) = L_o(\tau_1) + A(\tau_2) - A(\tau_1) - C(\tau_2) + C(\tau_1) = L_o(\tau_1) + C(\rho - 1)(\tau_2 - \tau_1). \tag{4.105}$$

Under condition (4.104) the equation holds also for $\rho < 1$.

The cumulative overflow delay (Figure 4.12) during interval $(0, \tau]$ is the area between the cumulative arrival curve and the capacity curve (Gazis & Potts 1965, May & Keller 1967):

$$W_o(\tau) = \int_0^\tau L_o(u)\,du = \frac{\tau^2}{2}(q - C) = \frac{C\tau^2}{2}(\rho - 1). \tag{4.106}$$

This delay includes the overflow delay accumulated until τ, that is the overflow delay 0PQ of vehicles $C(\tau)$ and the overflow delay PQR of vehicles $A(\tau) - C(\tau)$ accumulated up to time τ. If there is an initial overflow queue $L(0) > 0$, the cumulative delay is

$$W_o(\tau) = \int_0^\tau L_o(u)\,du = L(0)\tau + \frac{C\tau^2}{2}(\rho - 1). \tag{4.107}$$

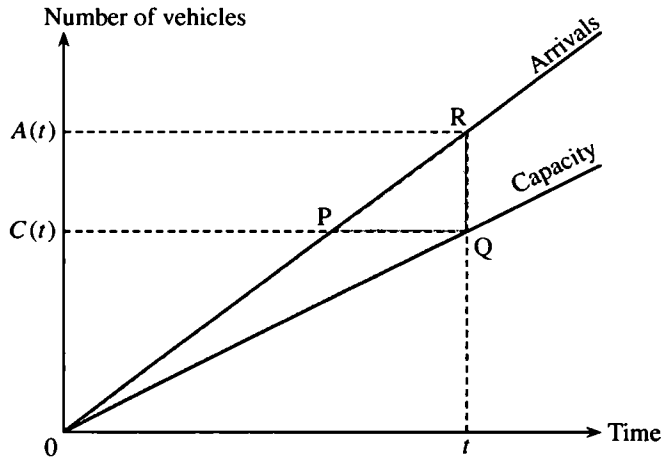

Figure 4.12: Overflow delay based on queue sampling

The delay includes delays suffered by vehicles in the initial overflow queue, and excludes all delays suffered after time τ (Kimber & Hollis 1979). The initial queue captures all relevant information about the history of the system (Heidemann 2002). Consequently, the cumulative delays based on queue sampling are additive: $\tau_1 < \tau_2 < \tau_3$: $W_o(\tau_1, \tau_3) = W_o(\tau_1, \tau_2) + W_o(\tau_2, \tau_3)$. Because the delay is based on the measurement of queue lengths, this approach is called the *queue-sampling method*. Delay estimation based on the measurement of individual vehicle delays is called the *path-trace method* (Rouphail & Akçelik 1992).

The average queue-sampling overflow delay per vehicle (Fig. 4.13) is obtained by dividing the cumulative overflow delay by the number of departures $C\tau$ (Neuburger 1971, Hurdle 1984):

$$\bar{W}_o(\tau) = \frac{W_o(\tau)}{C\tau} = \frac{L(0)}{C} + \frac{\tau}{2}(\rho - 1). \tag{4.108}$$

The method overestimates the average overflow delay, because it includes also the delay PQR. The average deterministic waiting time in system under oversaturated conditions

is obtained as the sum of average service time and the average overflow delay (Troutbeck 2000)

$$\bar{W}_{D,S}(\tau) = \frac{1}{C} + \bar{W}_o(\tau) = \frac{1}{C} + \frac{L(0)}{C} + \frac{\tau}{2}(\rho - 1)\,. \qquad (4.109)$$

As the length of the oversaturation period increases, the curve becomes steeper, and in the limit becomes vertical, as analysis period approaches infinity.

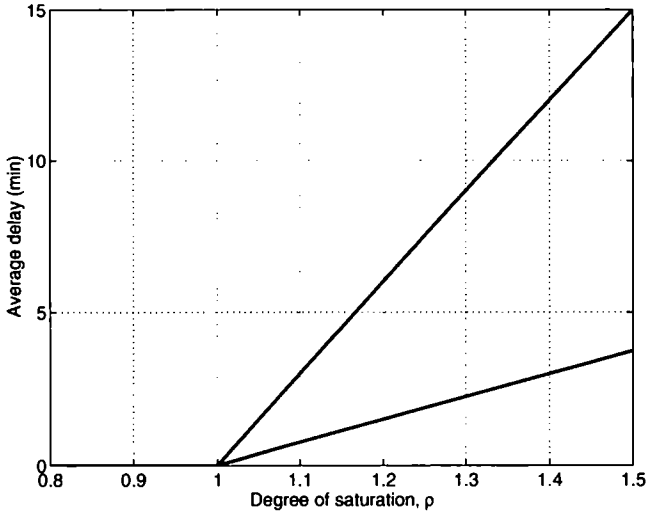

Figure 4.13: Average overflow delay for oversaturation periods of length 15 and 60 minutes

Peak period delay

At oversaturated conditions the queues increase constantly, and the system does not reach equilibrium. In the extreme, after infinite time, there will be an infinite queue. The analysis of equilibrium conditions is apparently implausible, when the system is oversaturated. There will be available neither infinite time for queue accumulation nor infinite space for the queues. Severe oversaturation has also an impact on traffic demand, as some traffic redistributes into the surrounding network an avoids the oversaturated intersection (Kimber, Marlow & Hollis 1977). Consequently, oversaturation is always a peaked phenomenon lasting only for a limited length of time (Neuburger 1971, Yagar 1977).

The discussion above provides some tools for the analysis of oversaturation during a peak period. In order to estimate the delay during a peak period we need to know the maximum flow rate and the shape of the demand pattern. May & Keller (1967) suggested triangular or trapezoid shaped demand patterns (Fig. 4.14). Kimber & Hollis (1978) defined a low-definition (rectangular) and a high-definition (piecewise constant) pattern.

Let us assume a rectangular demand pattern with peak flow $q_P > C$ lasting for time τ_P, after which the flow rate decreases to $q < C$. The time $(0, \tau_P]$ is the *peak period*. There is no initial queue, $L(0) = 0$, in the system. During the time interval $(0, \tau_P)$ the overflow queue increases at rate $C(\rho_P - 1)$ and reaches its maximum $L_o(\tau_P) = C\tau_P(\rho_P - 1)$, where $\rho_P = q_P/C > 1$ is the D/C ratio during the peak period (Fig. 4.15). After τ_P the queue length decays at rate $C(\rho - 1)$, where $\rho < 1$ is the D/C ratio after the peak

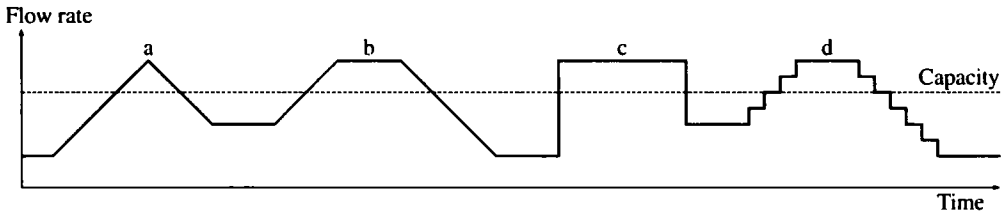

Figure 4.14: Triangular (a), trapezoidal (b), rectangular (c), and piecewise constant (d) demand patterns

period (Kimber & Hollis 1978). The overflow queue is

$$L_o(\tau) = \begin{cases} C\tau(\rho_P - 1), & \text{if } 0 < \tau \leq \tau_P \\ L_o(\tau_P) - C(\tau - \tau_P)(1 - \rho), & \text{if } \tau_P < \tau \leq \tau_o \end{cases} \tag{4.110}$$

The *overflow period* ends at τ_o, when the overflow queue vanishes:

$$L(\tau_o) = L_o(\tau_P) - C(\tau_o - \tau_P)(1 - \rho) = 0. \tag{4.111}$$

The length of the overflow period is determined by the length of the peak period and the D/C ratio during and after the peak period (see Kimber & Hollis 1978):

$$\tau_o = \tau_P + \frac{L_o(\tau_P)}{C(1 - \rho)} = \frac{(\rho_P - \rho)\tau_P}{1 - \rho}. \tag{4.112}$$

This result can also be obtained more directly by equating the number of overflow vehicles to the capacity during time interval $(0, \tau_o]$ (Rouphail & Akçelik 1992):

$$q_P\tau_P + q(\tau_o - \tau_P) = C\tau_o. \tag{4.113}$$

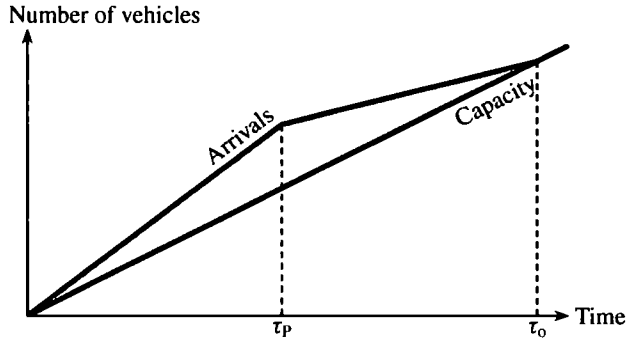

Figure 4.15: Overflow delay due to a rectangular peak flow pattern

The cumulative overflow delay is the area of the triangle in Figure 4.15 (cf. Kimber & Hollis 1978):

$$W_o(\tau_o) = \int_0^{\tau_o} L_o(u)\,du = \frac{C\tau_P^2(\rho_P - 1)(\rho_P - \rho)}{2(1 - \rho)}. \tag{4.114}$$

Since the queue increases and decreases in a linear fashion the average queue length during time interval $(0, \tau_o]$ is half the maximum queue length of $L_o(\tau_P)$ (Neuburger 1971), and the delay is

$$W_o(\tau_o) = \frac{\tau_o}{2} L_o(\tau_P). \tag{4.115}$$

Because the delay includes the area of the total triangle, the results for both queue-sampling and path-trace methods agree, and the bias in the average overflow delay disappears.

The average overflow delay per vehicle is obtained by dividing the cumulative overflow delay with the number $C\tau_o$ of vehicles experiencing overflow delay:

$$\bar{W}_o = \frac{W_o(\tau_o)}{C\tau_o} = \frac{L_o(\tau_P)}{2C} = \frac{\tau_P}{2}(\rho_P - 1). \tag{4.116}$$

The same result can also be derived using the Little's formula (4.65), which states that the average queue length is equal to the product of average waiting time and the arrival rate (Little 1961). Because during the interval $(0, \tau_o]$ the average queue length is $\bar{L}_o(\tau_p)/2$, and the average arrival rate to the overflow queue is equal to the departure rate (capacity), we obtain

$$W_o = \frac{L_o(\tau_P)}{2C} = \frac{\tau_P}{2}(\rho_P - 1). \tag{4.117}$$

As equation (4.108) shows, this delay is equal to the average queue-sampling delay during time interval $(0, \tau_P]$.

The average overflow delay does not depend on the D/C ratio after the peak. Because the average overflow queue length $L_o(\tau_P)/2$ does not change with ρ, the delay per vehicle does not increase, although ρ increases. The time period of high average delays, however, becomes longer.

Equation (4.116) gives the average overflow delay per vehicle *during the overflow period* $(0, \tau_o]$. Kimber & Hollis (1978) have attributed the excess delay to the vehicles $A(\tau_P) = C\rho_P\tau_P$ of the peak itself:

$$\bar{W}_o = \frac{W_o(\tau_o)}{C\rho_P\tau_P} = \frac{\tau_P(\rho_P - 1)(\rho_P - \rho)}{2\rho_P(1 - \rho)}. \tag{4.118}$$

One should be careful, if this average delay is used to estimate the cumulative overflow delay.

Using the queue-sampling method the cumulative delays over consecutive time periods can be summed. The calculations should consider the initial queue at the start of the analysis period. Rouphail & Akçelik (1992) have discussed the delay estimates based on the path-trace method.

4.4.3 Coordinate-transformation method

Oversaturation is usually a peaked phenomenon lasting only for a limited length of time. For a peak period of limited length the average delay can not increase to infinity. Consequently, the steady-state approach breaks down at high degrees of saturation (Rouphail, Tarko & Li 1997).

At D/C ratios considerably above unity the queues are very large and the effects of random variation can be ignored (Yagar 1977). The average overflow delay approaches the deterministic overflow delay W_o presented above. On the other hand, for D/C ratios considerably below unity the probability of overflow due to random fluctuations is very low, and the steady-state results appear to be plausible. When the D/C ratio is near unity the average delay is above the fluid analogy model but below the steady-state model (see Hurdle 1984).

The stochastic nature of a peak period has been studied analytically by de Smit (1971), Newell (1971) and others. The fluid approximation suggests some analogy with flooding theory (see Prabhu 1965, Gani 1969). Haight (1963) used a transition matrix (Markov chain) for queue length probabilities. The most commonly used approach is, however, based on a combination of a steady-state model and a deterministic oversaturation model.

The average delay curve of the steady-state model approaches asymptotically the vertical line $\rho = 1$. If it is assumed that the average time-dependent delay curve should approach the deterministic overflow curve, the new delay curve can be obtained by a coordinate transformation suggested by Kimber et al. (1977) and Catling (1977). Originally the method was applied in the Transyt program (Robertson 1969) by P. D. Whiting.

The horizontal difference between the time-dependent waiting-time curve and the deterministic waiting-time curve is $\rho_D - \rho$ (Fig. 4.16). If the time-dependent curve approaches asymptotically the deterministic curve in the same way as the steady-state curve approaches asymptotically the vertical line $\rho = 1$, then the following relation holds (Kimber & Hollis 1979):

$$1 - \rho_n = \rho_D - \rho, \tag{4.119}$$

where ρ_n and ρ_D are the degrees of saturation giving the same steady-state and deterministic average waiting times, respectively, as the transformed average waiting time $\bar{W}_T$ for D/C ratio ρ.

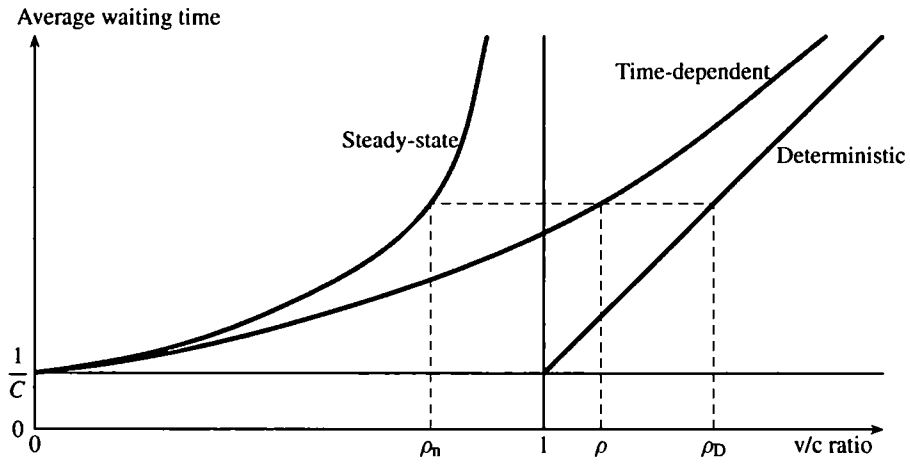

Figure 4.16: Coordinate transformation for waiting times in the system

The average deterministic waiting time in system is (Kimber & Hollis 1979)

$$\bar{W}_{D,S} = \frac{1}{C} + \frac{L(0)}{C} + \frac{\tau}{2}(\rho_D - 1). \tag{4.120}$$

Because this is equal to the transformed waiting time $\bar{W}_{T,S}$ for D/C ratio ρ, we obtain

$$\rho_D = \frac{2}{\tau}\left(\bar{W}_{T,S} - \frac{1 + L(0)}{C}\right) + 1. \tag{4.121}$$

Equation (4.119) can now be expressed as

$$\frac{2}{\tau}\left(\bar{W}_{T,S} - \frac{1 + L(0)}{C}\right) + \rho_n - \rho = 0 \tag{4.122}$$

The equivalent D/C ratio (ρ_n) for the steady-state model can be obtained from a steady-state waiting-time equation. This equation should describe the waiting time in system, including the service time.

If the steady-state waiting time is estimated using the M/G/1 model (4.62), ρ_n can be expressed as

$$\rho_n = \frac{C\bar{W}_{T,S} - 1}{C\bar{W}_{T,S} - 1 + \kappa}. \tag{4.123}$$

The time dependent average waiting time in the system can be solved from the quadratic equation

$$\frac{2C}{\tau}\bar{W}_{T,S}^2 - \left(\rho - 1 + \frac{2[L(0) + 2 - \kappa]}{C\tau}\right) C\bar{W}_{T,S} + (1-\kappa)\left(\rho + \frac{2[L(0)+1]}{C\tau}\right) - 1 = 0 \tag{4.124}$$

as (Catling 1977, Kimber & Hollis 1979)

$$\bar{W}_{T,S} = a_1 + \sqrt{a_1^2 + a_2}, \tag{4.125}$$

where

$$a_1 = \frac{\tau}{4}(\rho - 1) + \frac{L(0) + 2 - \kappa}{2C}$$
$$a_2 = \frac{\tau}{2C}\left[1 - (1-\kappa)\left(\rho + \frac{2[L(0)+1]}{C\tau}\right)\right].$$

The negative branch of the solution has no physical significance (Kimber & Hollis 1979).

In an M/M/1 system with no initial queue $\kappa = 1$, $L(0) = 0$, and

$$\rho_n = 1 - \frac{1}{C\bar{W}_{T,S}}. \tag{4.126}$$

The time-dependent average waiting time in the system is (see also Kimber et al. 1977, Troutbeck 2000)

$$\boxed{\bar{W}_{T,S} = \frac{\tau}{4}(\rho - 1) + \frac{1}{2C} + \sqrt{\left(\frac{\tau}{4}(\rho - 1) + \frac{1}{2C}\right)^2 + \frac{\tau}{2C}}.} \tag{4.127}$$

It can also be obtained directly from equation (4.125) as

$$\bar{W}_{T,S} = a_1 + \sqrt{a_1^2 - a_2}, \tag{4.128}$$

where

$$a_1 = \frac{\tau}{4}(\rho - 1) + \frac{1}{2C}$$
$$a_2 = \frac{\tau}{2C}.$$

Because $\rho - 1 = C^{-1}(q - C)$, the average waiting time can be expressed also in terms of capacity and reserve capacity (see Brilon 1991, FGSV 2001).

If the assumption (4.119) of equivalent differences between D/C ratios is replaced by an assumption of equivalent proportions (Heidemann 2002)

$$\frac{\rho}{\rho_D} = \rho_n, \tag{4.129}$$

the equation for an M/M/1 system with no initial queue is

$$\left[\frac{2}{\tau}\left(\bar{W}_{T,S} - \frac{1}{C}\right) + 1\right]\left[1 - \frac{1}{C\bar{W}_{T,S}}\right] - \rho = 0. \tag{4.130}$$

The time-dependent average waiting time in the system is obtained as the larger root of the equation above, which gives

$$\boxed{\bar{W}_{T,S} = \frac{1}{C} + \frac{\tau}{4}\left(\rho - 1 + \sqrt{(\rho-1)^2 + \frac{8\rho}{C\tau}}\right).} \tag{4.131}$$

This formula was suggested by Akçelik & Troutbeck (1991), and it has been adopted in the HCM2000 (Transportation Research Board 2000) with a slight modification.

The German method (FGSV 2001) uses a coordinate-transformation approach with parameters based on simulation and field measurements (Brilon et al. 1994). Instead of D/C ratio the reserve capacity is used as a parameter in the model.

As Hurdle (1984) remarks, the coordinate-transformation method is not a result of any detailed analysis of queue behavior. The only justifications for the method is that it provides a smooth transition from steady-state analysis to time-dependent analysis in a way that satisfies the intuitive ideas of what ought to happen. Also, the method does not consider the length of the overflow-queue discharge process following the peak period.

Heidemann (2002) has derived exact formulas for means and variances of queue lengths and waiting times in M/G/1 systems under transient conditions. The means and variances were obtained by numerical methods. They were shown to depend on the shape of the service time distribution, not only on its first and second moments. However, the coordinate-transformation approximations presented by Kimber & Hollis (1979) and Akçelik & Troutbeck (1991) were found to agree fairly well with the exact results. The method of Kimber & Hollis (1979) performed slightly better than the method of Akçelik & Troutbeck (1991).

Equation (4.131) gives the time-dependent average waiting time in the system. Following equation 4.8 the average time-dependent control delay can be expressed as

$$\bar{W}_T = \bar{W}_{T,S} - t_f + \bar{W}'_a, \tag{4.132}$$

where $\bar{W}'_a$ is the average acceleration delay.

5 PERFORMANCE ANALYSIS METHODOLOGIES

5.1 Performance measures

Capacity describes the maximum performance of a traffic facility. Capacity is, however, not a sufficient measure for the analysis of an intersection, because operating conditions may be unreasonably low for traffic demand below, but near capacity. The first edition of Highway Capacity Manual (Bureau of Public Roads 1950) addressed this issue by defining a *practical capacity.*[1] It is "the maximum number of vehicles that can pass a given point on a roadway or in a designated lane during one hour without the traffic density being so great as to cause unreasonable delay, hazard, or restriction to the drivers' freedom to maneuver under the prevailing roadway and traffic conditions."

The second edition (Highway Research Board 1965) developed this idea further by introducing *levels of service.* Practical capacity was replaced by *service volumes* representing specific volumes related to operating conditions collectively termed 'level of service' (LOS). A service volume was "the maximum number of vehicles that can pass over a given section of a lane or roadway in one direction on multilane highways (or in both directions on a two- or three-lane highway) during a specified time period while operating conditions are maintained corresponding to the selected or specified level of service." No specific analysis procedure was presented for unsignalized intersections. The manual suggested that capacities and service volumes were estimated by the signalized intersection criteria; i.e., load factor. Signal split was to be calculated on the basis of the relative volumes on intersecting roads and inversely on the basis of their relative widths.

The third edition of HCM (Transportation Research Board 1985) presented an analysis procedure based on the German methodology. Reserve capacity was used as a level-of-service criterion. This approach is still used in Finland. In later updates of HCM the "average total delay" was adopted as a service measure (Transportation Research Board 1994). Total delay was defined as "the total elapsed time from when a vehicle stops at the end of the queue until the vehicle departs from the stop line."

The fourth edition of HCM (Transportation Research Board 2000) uses *control delay* as a service measure for both signalized and unsignalized intersections (Table 5.1). While reserve capacity is a practical engineering measure, delay is a measure experienced directly by road users. Control delay includes initial deceleration delay, queue move-up time, stopped delay, and final acceleration delay. The same service measure is also used in the German manual HBS 20001 (FGSV 2001), as displayed in Table 5.1.

Table 5.1: Average control delay as a LOS criterion in HCM2000 (Transportation Research Board 2000) and HBS 2001 (FGSV 2001)

LOS	HCM 2000	HBS 2001
A	≤ 10	≤ 10
B	≤ 15	≤ 20
C	≤ 25	≤ 30
D	≤ 35	≤ 45
E	≤ 50	> 45
F	> 50	v/c > 1

[1]This concept is still in use. In the Australian guidelines (Austroads 1988) "practical absorption capacity" is defined as 80 % of the theoretical "absorption capacity". The Australian Sidra model (Akçelik 1998), however, applies the HCM level-of-service criteria.

Kyte et al. (1996) suggested both delay and queue length as LOS criteria. However, according to the German manual (FGSV 2001) queue length cannot be considered as a level-of-service criterion but a factor in intersection design.

The discussion below describes the analysis methodologies used in the United States (HCM), Denmark (DanKap), Sweden (Capcal 2), and Finland (Capcal) to estimate the capacity and average delay at unsignalized intersections and roundabouts. The German Additive Conflict Flows methodology has been described in Section 3.10. For further information about current German capacity analysis procedures the reader is referred to HBS 2001 (FGSV 2001). It is assumed that the reader is familiar with the theory presented above.

5.2 U.S. methodology

HCM2000 (Transportation Research Board 2000) Chapter 17 describes analysis methods for two-way stop-controlled (TWSC) intersections, all-way stop-controlled (AWSC) intersections and roundabouts. The manual suggests that with appropriate changes in key parameters an analyst can apply the TWSC method to yield-controlled intersections.

The analysis procedures are extensively described in the manual. Background information is presented in Contractor's Final Report (Kyte et al. 1996). The roundabout methodology follows the suggestions of Troutbeck (1997*b*). The outline of the HCM2000 method is displayed in Figure 5.1.

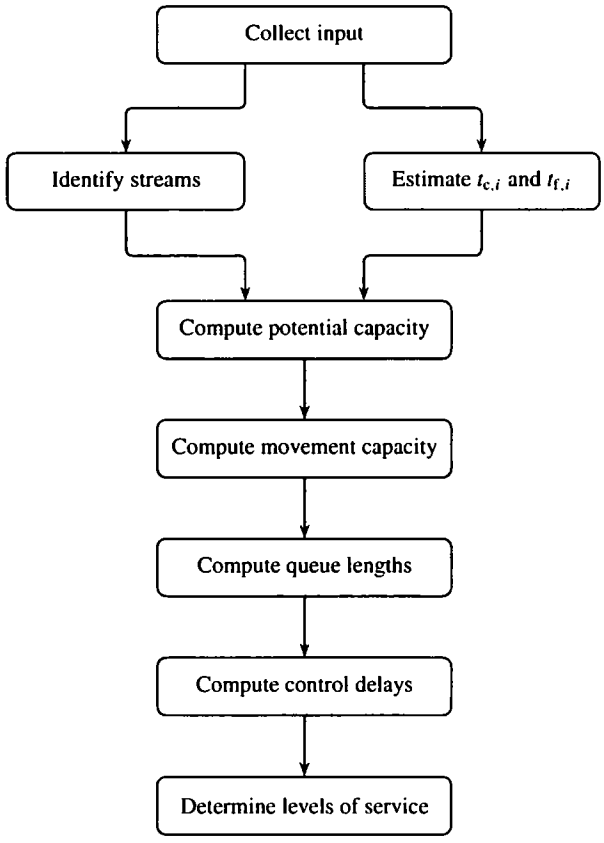

Figure 5.1: HCM2000 analysis methodology for unsignalized intersections (Transportation Research Board 2000)

HCM2000 assumes Poisson arrivals and constant critical gaps and follow-up times. It

allows an analysis of short peak periods. Because the theoretical basis of HCM2000 has been extensively discussed above, only a short overview will be given here.

Traffic streams at an unsignalized intersection are classified following Figures 2.2 and 2.3. Pedestrian flows along the major road have Rank 1 and those across the major road have Rank 2. Conflicting flow rates are the flow rates of conflicting streams, with a some exceptions:

- If a minor stream merging to an N-lane road and is in conflict with a major stream i in one lane only, the conflicting flow rate is q_i/N.
- One half of the right-turn movement exiting before conflict area is included in major stream
- The effect of left-turn major-stream flows is twice their number
- For a minor-road left-turn movement only half of the opposing through and right-turn flow rates are included as conflicting flow rate.

At roundabouts the vehicles passing in front of the entering vehicle are counted as the major flow. At most well-designed roundabouts the exiting traffic can be ignored.

Base values for *critical gaps* and *follow-up times* are displayed in Table 5.2. Adjustments for critical gap are made to account for the presence of heavy vehicles, approach grade, T-intersections, and two-stage gap acceptance. The follow-up time is adjusted for the presence of heavy vehicles.

Table 5.2: Base values for critical gaps and follow-up times for an unsignalized intersection with a two or four-lane major road in HCM2000 (Transportation Research Board 2000)

	Critical gap (s)		Follow-up
Movement	2-lane	4-lane	time (s)
Major left	4.1	4.1	2.2
Minor right	6.2	6.9	3.3
Minor through	6.5	6.5	4.0
Minor left	7.1	7.5	3.5

For one-lane roundabouts HCM2000 uses the critical gaps and follow-up times suggested by Troutbeck (1997*b*), as displayed in Table 5.3. An upper bound and a lower bound for the capacity is estimated. The analysis procedure can be applied if the circulating flow does not exceed 1,200 veh/h. No analysis procedure is presented for multi-lane roundabouts.

Table 5.3: Critical gaps and follow-up times for roundabouts in HCM2000 (Transportation Research Board 2000)

	Critical gap (s)	Follow-up time (s)
Upper bound	4.1	2.6
Lower bound	4.6	3.1

The *potential capacity* (3.12) is calculated assuming a Poisson arrival process on major streams. The *impedance* factor of a Rank 2 stream i is the probability $p_{0,i} = 1 - \rho_i$ that the system is empty. See discussion in Section 3.5.5. The impedance factor for multiple conflicting Rank 2 streams is obtained by multiplication. For Rank 4 streams

the impedance factor to account for conflicting Rank 2 and Rank 3 queues is obtained using the adjustment (3.103) of Brilon & Großmann (1991).

The effect of a *pedestrian* stream j is estimated by a pedestrian blockage factor

$$\rho_j = \frac{q_g t_{pb}}{3600}, \tag{5.1}$$

where q_g is the number of pedestrian groups per hour, and t_{pb} is the average duration of time the lane is blocked by a pedestrian group (see Section 3.8). The pedestrian impedance factor is obtained as $p_{0,j} = 1 - \rho_j$. This factor is combined with other impedance factors ($p_{0,i}$) by multiplication.

The estimation of shared lane capacity in HCM2000 is described in Section 3.7. The capacity estimation of a flared approach is described at the end of this section.

Although HCM2000 suggests the use of simulation models and field data to assess the effects of *upstream signals*, the manual presents a rather detailed procedure for the task. As platoons from a signalized intersections arrive at an unsignalized intersection, four flow regimes result:

1. No platoons
2. Platoon from the left only
3. Platoon from the right only
4. Platoons from both directions.

A minor stream is considered to be blocked if a platoon is traveling in a conflicting stream. During the unblocked period the major stream is assumed to be random with flow rate

$$q_{M,u} = \begin{cases} \dfrac{q_M - s_M(1 - p_{M,u})}{p_{M,u}}, & \text{if } q_M > s_M(1 - p_{M,u}) \\ 0, & \text{otherwise,} \end{cases} \tag{5.2}$$

where q_M is the total flow rate of the major stream, s_M is the saturation flow rate of the major stream, and $p_{u,j}$ is the proportion of time that the minor stream is unblocked by major stream platoons. The capacity of the minor stream j is

$$C_j = p_{u,j} C_{u,j}, \tag{5.3}$$

where $C_{u,j}$ is the capacity assuming a continuous random flow rate $q_{M,u}$ in the major stream.

If a wide median allows minor stream vehicles to cross the major road in two phases, the capacity is analyzed in two stages. The *two-stage gap acceptance* analysis procedure in HCM2000 follows the method developed by Brilon et al. (1996) and Brilon & Wu (1999). See also Luttinen (1998).

The *95th-percentile queue length* of a minor stream j is estimated as

$$\begin{aligned} L_{95,j} &= 900\tau \left(\frac{q_j}{C_j} - 1 + \sqrt{\left(\frac{q_j}{C_j} - 1\right)^2 + \frac{\dfrac{3600}{C_j} \times \dfrac{q_j}{C_j}}{150\tau}} \right) \frac{C_j}{3600} \\ &= \frac{\tau C_j}{4} \left(\rho_j - 1 + \sqrt{(\rho_j - 1)^2 + \frac{24\rho_j}{\tau C_j}} \right), \end{aligned} \tag{5.4}$$

where τ is the length of the analysis period. The queue length can also be expressed in terms of reserve capacity ($\kappa_j = C_j - q_j$) as

$$L_{95,j} = \frac{\tau}{4}\left(-\kappa_j + \sqrt{\kappa_j^2 + \frac{24q_j}{\tau}}\right). \tag{5.5}$$

The service measure of unsignalized intersections in HCM2000 is the *average control delay*. The definition of control delay in HCM2000 has been discussed in section 4.1. The formula (4.131) suggested by Akçelik & Troutbeck (1991) is used, but with an additional value of five seconds to "account for the deceleration of vehicles from free-flow speed to the speed of vehicles in queue and the acceleration of vehicles from the stop line to free-flow speed."[2] The delay equation is

$$\boxed{\bar{W}_j = \frac{3600}{C_j} + 900\tau\left(\rho_j - 1 + \sqrt{(\rho_j - 1)^2 + \frac{8\rho_j}{\tau C_j}}\right) + 5.} \tag{5.6}$$

The level-of-service criteria are presented in Table 5.1.

HCM2000 considers a *flared minor-road approach* as an approach with an additional short lane. The traffic in the flared lane consists of a right turn movement having flow rate q_R and a left+through movement having flow rate q_{LT}. The capacity of a flared lane is estimated by interpolation between the capacity of two separate lanes and the capacity C_{SH} of a shared lane.

The capacity of a shared lane is calculated as described above. The capacity of a separate-lane condition is calculated using equation[3]

$$C_S = \min\left\lfloor C_R\left(1 + \frac{q_{LT}}{q_R}\right), C_{LT}\left(1 + \frac{q_R}{q_{LT}}\right)\right\rfloor, \tag{5.7}$$

where $\lfloor\cdot\rfloor$ is the floor function (Spanier & Oldham 1987). For a movement $k \in \{R, LT\}$ considered to operate in a separate lane the average queue length is estimated using the Little's formula (4.65) as

$$\bar{L}_k = \frac{\bar{W}_k q_k}{3600}, \tag{5.8}$$

where $\bar{W}_k$ is the average control delay of movement k assuming a separate lane. The required storage space (vehicles) for the approach to operate effectively as separate lanes is estimated as

$$L_r = \max_{k\in\{R,LT\}} \langle \bar{L}_k + 1 \rangle, \tag{5.9}$$

where $\langle\cdot\rangle$ is the nearest integer (rounding) function (Spanier & Oldham 1987). The capacity of a flared lane is obtained by interpolation between the shared lane capacity (C_{SH}) and the capacity (C_S) assuming two separate lanes:

$$C = \begin{cases} (C_S - C_{SH})\dfrac{L_s}{L_r} + C_{SH}, & \text{if } L_s < L_r \\ C_S, & \text{if } L_s \geq L_r, \end{cases} \tag{5.10}$$

[2]This description indicates a possible overlap in control delay and geometric delay. See discussion in Section 4.1. HCM2000 does not subtract the follow-up time (see equation (4.132).

[3]This equation and some other details of the method are described in a correction sheet (TRB Committee A3A10, Highway Capacity and Quality of Service 2003). It contains also some corrections for the upstream-signal effects procedure.

where L_s is the actual storage capacity of the flare.

If the required storage does not exceed the actual storage, capacity (5.10) and delay are calculated assuming separate lanes. The average control delay is calculated as

$$\bar{W} = \frac{q_{LT}\bar{W}_{LT} + q_R\bar{W}_R}{q_{LT} + q_R}, \qquad (L_s \geq L_r) \tag{5.11}$$

where $\bar{W}_{LT}$ and $\bar{W}_R$ are the average control delays of left+through and right-turn movements, respectively, assuming separate lanes. The probability or frequency of storage overflow are not considered. If the storage is less than required, the average control delay is calculated using the capacity estimate in Equation 5.10 for $L_s < L_r$.

5.3 Danish methodology

DanKap (Vejdirektoratet 1999*b*, Vejdirektoratet 1999*a*) estimates potential capacity using the gap acceptance model (3.12) which assumes Poisson arrivals, as does HCM2000 (Transportation Research Board 2000). The impedance factors and the effect of shared lanes are calculated using the same methods as in HCM2000. Traffic volume and capacity are given in terms of passenger cars per analysis period, not as pc/h.

Separate critical gaps (see Tables 5.4 and 5.5) are defined for bicycles and other unregistered vehicles. The critical gap used in the calculations is the weighted average of critical gaps for bicycles and motorized vehicles. The follow-up time is 3.0 s for all movements. No distinction is made even between yield and stop controlled approaches.

*Table 5.4: Base values for critical gaps and follow-up times for an unsignalized intersection with a two or four-lane major road in DanKap (Vejdirektoratet 1999*b*)*

	Critical gap (s)					Follow-up
	Passenger cars				Bicycles	time
	Yield control		Stop control		and other	
Movement	2-lane	4-lane	2-lane	4-lane	unregistered	(s)
Major right	—	—	—	—	2.5	3.0
Major left	5.5	6.0	—	—	2.5	3.0
Minor right	5.5	5.5	6.5	6.5	2.5	3.0
Minor through	6.0	7.0	7.0	8.0	2.5	3.0
Minor left	7.0	8.0	8.0	9.0	2.5	3.0

*Table 5.5: Base values for critical gaps and follow-up times for a roundabout in DanKap (Vejdirektoratet 1999*a*)*

	Critical gap (s)		Follow-up
Entry lanes	PCs	Bicycles	time (s)
1	4.5	2.5	2.8
2	4.0	—	2.6

Traffic streams are classified following Figures 2.2 and 2.3. Conflicting flow rates are the flow rates of conflicting streams. Major stream right-turn movements exiting before the conflict area can be multiplied with a factor between zero and one. It is recommended that these right-turn movements are ignored (Aagaard 1998). Conflicting bicycle flows along the major road (movements 2 and 5) are included in the analysis. Pedestrian flows are ignored. The passenger-car equivalents used to express vehicle counts as equivalent number of passenger cars are displayed in Table 5.6.

Table 5.6: Passenger-car equivalents in DanKap (Vejdirektoratet 1999a)

Gradient	Vehicle category			
(%)	Motorcycles etc.	PCs and vans	Trucks and buses	Semi-trailers etc.
+4	0.7	1.4	3.0	6.0
+2	0.6	1.2	2.0	3.0
0	0.5	1.0	1.5	2.0
-2	0.4	0.9	1.2	1.5
-4	0.3	0.8	1.0	1.2

The capacity of a roundabout entry is adjusted for pedestrians (f_p) and exiting traffic (f_e) effects as

$$C = f_p f_e C_p. \tag{5.12}$$

If the traffic flow exiting before the conflict area is less than 400 pc/τ the adjustment factor is $f_e = 1$. Otherwise it is $f_e = 0.9$. These values are based on measurements at only one roundabout, and therefore are very uncertain (Aagaard 1998).

In a one-lane entry of a roundabout the adjustment f_p for pedestrians depends both on the crossing pedestrian volume (ped/τ) and the circulating volume (pcu/τ) of both motorized vehicles and bicycles (Table 5.7). If no pedestrians cross the entry, $f_p = 1$. These adjustments follow the results of German empirical research (Brilon, Wu & Bondzio 1997). For a two-lane entry the adjustment is $f_p = 1.0$.

Table 5.7: Adjustment factor f_p for crossing pedestrian flows at a one-lane entry to a roundabout according to DanKap (Vejdirektoratet 1999b)

Motorized veh +	Pedestrians (ped/τ)			
bicycle flow (pcu/τ)	100	200	300	400
0	0.99	0.93	0.87	0.81
100	0.99	0.93	0.87	0.82
200	0.99	0.94	0.88	0.83
300	0.99	0.94	0.89	0.84
400	0.99	0.95	0.90	0.86
500	0.99	0.95	0.91	0.88
600	0.99	0.96	0.93	0.90
700	0.99	0.97	0.95	0.93
800	0.99	0.98	0.97	0.96
900	0.99	1.00	1.00	1.00
1000	1.00	1.00	1.00	1.00

The time-dependent delay formula (4.131) suggested by Akçelik & Troutbeck (1991) is used in DanKap. But unlike in HCM2000, no additional component for deceleration and acceleration delay is used. DanKap does not present any level-of-service criteria.

The 95 and 99-percentile queue lengths for lane j are evaluated recursively from equation (Aagaard 1998)

$$\bar{\rho}_j = \frac{2L_a}{\tau C_j} + \left(\frac{100 - a}{100}\right)^{1/(L_a+1)}, \tag{5.13}$$

where L_a is the queue length exceeded a percent of time in the analysis period (τ), $\bar{\rho}_j$ is the average D/C ratio during the analysis period, and C_j is the capacity. This equation stems from the research of Wu (1994).

5.4 Swedish methodology

5.4.1 Analysis procedure

The Swedish capacity analysis software Capcal implements the procedures of the capacity manual (Statens vägverk 1977). Capcal 2 procedures for unsignalized intersections (SNRA 1995*b*) and roundabouts (SNRA 1995*c*) have been slightly modified from the previous version. Capcal 3 is a MS-Windows version of the software with some enhancements. The software version referred to in this report is Capcal 2.10.

Figure 5.2 displays the main steps in Capcal 2 methodology. Mean service times are used to estimate degrees of saturation, which are the major parameters in the estimation of MOEs, such as capacity, delay and queue lengths. Roundabouts are treated as a series of T-intersections. In TV131 roundabouts were analyzed as short merge areas.

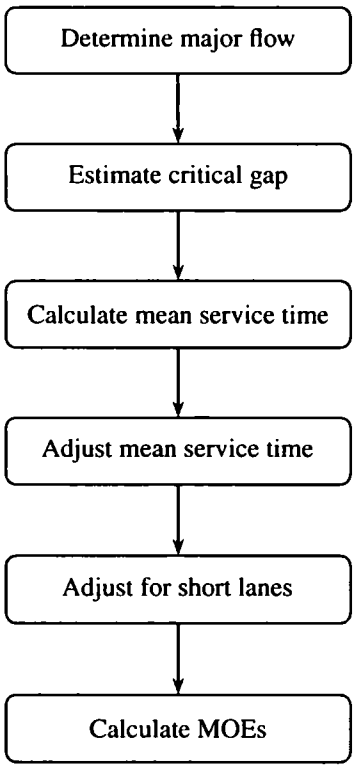

Figure 5.2: Capcal 2 analysis methodology for unsignalized intersections (SNRA 1995b)

The performance measures provided by the method are: capacity, delay, queue length, and the proportion of stopping vehicles. The Swedish method does not present any level-of-service criteria.

Although Capcal 2 is used in Finland, the Finnish guidelines (Tiensuunnittelutoimisto 1978) and software (Tiensuunnittelutoimisto 1987, Kehittämiskeskus 1991) still follow the Swedish capacity manual TV131 (Statens vägverk 1977). Consequently, the differences between Capcal 2 and the old method will be described. The new roundabout capacity analysis methodology developed by Hagring (1998*b*) has been described in section 3.4.

5.4.2 Major flows

For each minor stream the conflicting higher priority flows a determined. Major flow is the sum of these higher priority flows. In crossing conflicts the whole crossing flow is added to the major flow. In a merging conflict the flow rate of the merging major flow rate is divided by the number of lanes in the exit, where the merging occurs. Major-road right-turn vehicles are ignored if they do not have conflict with the minor stream. Bicycles and pedestrians having a crossing conflict with the subject movement have an equivalency value of 0.5. Bicycles having a merging conflict are ignored.

The major flow is adjusted for the possible effect of a wide median by an additive adjustment

$$f_M = -0.4 \min \{q_R, cq_L\}, \tag{5.14}$$

where q_R is the major-road through flow rate from the right and q_L is the major-road through flow rate from the left. For a left-turn minor movement onto a two-lane exit $c = 0.5$, otherwise $c = 1$. The effect of major-road left-turn movements is ignored. This is a simplification of the method proposed by Tanner (1951).

Capcal 2 has a unique way of defining major flows at a roundabout. The vehicular interactions can be described as three different cases (Hagring 1996*b*, Hagring 1998*b*):

1. Weaving occurs when the circulating flow leaves the roundabout at an exit upstream to the exit of the minor flow. The entire circulating flow is included in the major flow.

2. Merging occurs when the circulating flow and the minor flow leave the roundabout at the same exit. Only part of the circulating flow is included in the major flow, based on the roundabout geometry.

3. No interaction occurs when the circulating flow leaves the roundabout downstream to the exit of the minor flow. The circulating flow is not included in the major flow. It is possible that a minor flow has no major flow at all, despite there being circulating vehicles.

These interactions are summarized in table 5.8. These principles have been derived from literature and traffic engineering judgement (Bergh 1991).

Table 5.8: Interactions between major and minor stream at a roundabout according to Capcal 2 (Hagring 1996b)

Minor stream	Major stream		
	Left side approach		Opposite approach
	Through	Left turn	Left turn
Right turn	Merging	No interaction	Merging
Through	Weaving	Merging	Weaving
Left turn	Weaving	Weaving	Weaving

The new Swedish roundabout capacity analysis procedure developed by Hagring (1998*b*) uses the conventional way of defining major flow: it includes the circulating vehicles up to the entry point considered. At a two-lane roundabout also the vehicles circulating in the inner lane are included in the major flow of the minor stream vehicles in the curb lane. Different kinds of interactions are, however, described by different (lane-specific) critical gaps.

5.4.3 Critical gaps

The base values for critical gaps (t_c) in Capcal 2 are displayed Table 5.9. Table 5.10 is from the old manual. Critical gaps increase with the level of maneuvering difficulty and higher major road speed limits. Stop controlled approaches have larger critical gaps than yield controlled. Follow-up times t_f are $0.6t_c$ (Nordqvist et al. 1973).

Table 5.9: Base values for critical gaps in Capcal 2 (SNRA 1995b)

	Major road speed limit					
	50 km/h		70 km/h		90 km/h	
Movement	Yield	Stop	Yield	Stop	Yield	Stop
Major left	4.8	4.8	5.7	5.7	6.7	6.7
Minor right	5.0	5.7	5.9	6.6	6.9	7.5
Minor through	5.1	5.8	6.0	6.7	7.0	7.6
Minor left	5.3	6.0	6.2	6.9	7.2	7.8

Table 5.10: Base values for critical gaps in TV131 (Statens vägverk 1977)

	Major road speed limit				
	50 km/h		70 km/h		90 km/h
Movement	Yield	Stop	Yield	Stop	Stop
Major left	5.0	—	5.8	—	6.5
Minor right	4.8	5.5	6.0	6.5	7.2
Minor through	5.2	5.8	6.0	6.5	7.0
Minor left	5.3	6.0	6.2	6.8	7.5

The critical gaps in Table 5.9 assume 10 % of heavy vehicles in the subject movement. For other percentages the additive adjustment is $f_{HV} = p_{HV} - 0.1$, where p_{HV} is the proportion of heavy vehicles. That is, heavy vehicles are assigned one second longer critical gaps than passenger cars (Hagring 1997). In the old manual the adjustment was $f_{HV} = 2(p_{HV} - 0.1)$; i.e., heavy vehicles were assigned two seconds larger critical gaps.

If the major road has more than two lanes, critical gaps are increased, but if the intersection allows two-stage gap acceptance, critical gaps are reduced (Table 5.11). For right-turn movements critical gaps are adjusted for curb radius r (meters) and angle α (degrees):

$$f_r = 1 - \left(1 + \frac{r - 12}{18}\right)\left(1 - \frac{\alpha - 90}{120}\right). \tag{5.15}$$

If the major road is one way, the critical gaps of minor road through and left-turn movements are reduced by 0.5 s.

Table 5.11: Critical gap adjustment for wide median and number of major-road lanes (SNRA 1995b)

Two-stage	Lanes		
gap acceptance	2	3–4	> 4
No	0	0.3	0.6
Yes	-0.5	0	0.3

TV131 had also an adjustment for the size of urban area or rural conditions (lower critical gap in densely populated areas), but this correction has been omitted in Capcal 2.

The critical gaps for 90 km/h roads was altered as a correction for rural conditions (SNRA 1995*b*). The old version of Capcal adjusted the critical gap for gradients, but in Capcal 2 the adjustment is made to lane capacity.

For roundabouts specific critical gaps are defined for right-turn movements $t_{c,r}$ and for crossing movements $t_{c,c}$ based on the width/length ratio of the weaving section:

$$t_{c,r} = 3.06 + 1.1\frac{w_w}{l_w} + 2.375\frac{w_w^2}{l_w^2} \tag{5.16}$$

$$t_{c,c} = 3.06 + 2.6\frac{w_w}{l_w} + 2.75\frac{w_w^2}{l_w^2}, \tag{5.17}$$

where w_w is the width and l_w is the length of the weaving section (SNRA 1995*c*). Additive adjustments are applied to the base values.

Hagring (1996*b*) has found this method to give too short critical gaps. His equation for critical gaps at a roundabout is

$$t_c = 3.91 - 0.0278l_w + 0.121w_w + 0.592(i - 1), \tag{5.18}$$

where i is the entry lane (1 for right lane, 2 for left lane). The values are about 0.5 seconds greater than the critical gaps estimated by Capcal. Later Hagring (1998*b*) estimated critical gaps for two-lane roundabouts by making distinction between both entry lanes and circulating lanes (Table 5.12). The follow-up time is $t_f = 2.4$ s on both entry lanes. See also Hagring (2000).

Table 5.12: Average critical gaps in two-lane roundabouts according to Hagring (1998b)

Entry lane	Circulating lane	
	Outer	Inner
Right	4.273	3.998
Left	4.615	4.403

5.4.4 Average service times

The most important measure in the Swedish methodology is the average service time (x). Under queuing conditions the average service time is the reciprocal of capacity; i.e., $\bar{S}_q = C^{-1}$. Service times $\bar{S}_q$ can be measured under moderate queuing conditions, while the measurement of capacity requires long periods of continuous queues (Nordqvist et al. 1973). This point has been later emphasized by Akçelik (1998).

The Swedish capacity manual (Statens vägverk 1977) recognizes three major stream headway distributions (Bergh 1991):

1. Tanner's M/D/1 headway model (2.44) is used when the major flow occupies one lane only. This model is used as a major-stream headway model for major road left-turn and minor road right-turn movements. The minimum headway is $t_p = 1.8$ s.

2. Exponential major-stream headway model is used for minor streams having conflicts with major streams on two lanes; i.e., minor-road through and left-turn movements on a two-lane major road, and major-road left-turn movements on a multi-lane road. In addition, the exponential headway model is used for minor road right-turn movements to a multi-lane road.

3. Pearson type III (gamma) distribution (see Luttinen 1991, Luttinen 1996) is used when traffic signals are within 300 m on the major road. It is also used for minor-road through and left-turn movements, when the major road has four or more lanes. The application of this model was influenced by a paper by Voigt (1973).

Since, eventually, no empirical data was found to support the Pearson III distribution, Capcal 2 has replaced it with the exponential distribution (Anveden 1988, Bergh 1991). Accordingly, Tanner's distribution is used for major-road left turns and minor road right turns on two-lane major roads. In all other cases the exponential headway distribution is assumed. At roundabouts the headway distribution is a mixture of random (exponential) headways and a platoon model leading to the following expression of average service time for queuing vehicles (SNRA 1995*c*):

$$\bar{S}_q = (1 - p_q)\bar{S}_1 + p_q\bar{S}_2 \tag{5.19}$$

where

$$\bar{S}_1 = \frac{1 - e^{-\lambda t_f}}{\lambda e^{-\lambda t_c}} \tag{5.20}$$

$$\bar{S}_2 = \frac{\left(e^{\lambda(t_c - t_f)} - e^{0.6\lambda(t_c - t_f)}\right)\left(1 - e^{-0.542\lambda t_c}\right)}{0.146\lambda} \tag{5.21}$$

$$p_q = 0.29\lambda e^{0.25 t_c}. \tag{5.22}$$

For vehicles departing from a queue the average service time is the reciprocal of the capacity. When major-stream headways follow the Tanner's M/D/1 model, the average service time under queuing conditions is (SNRA 1995*b*)

$$\bar{S}_q = \frac{1 - e^{-\lambda t_f}}{\lambda\left(1 - \lambda t_p\right) e^{-\lambda(t_c - t_p)}}, \tag{5.23}$$

which is the inverse of the corresponding capacity equation (3.24). For exponential major-stream headways the average service time under queuing conditions is (SNRA 1995*b*)

$$\bar{S}_q = \frac{1 - e^{-\lambda t_f}}{\lambda e^{-\lambda t_c}}, \tag{5.24}$$

which is the inverse of capacity equation (3.12).

For an isolated vehicle, arriving to stop line after the follow-up time has passed since the last departure, the average service time $\bar{S}_e$ is assumed to be either the follow-up time (t_f) or the average waiting time ($\bar{W}_e$) of an isolated vehicle (4.33), whichever is larger (SNRA 1995*b*):

$$\bar{S}_e = \max\{t_f, W_e\}. \tag{5.25}$$

Because waiting time (4.33) is used in stead of service time (4.35), it is necessary to set follow-up time as a lower limit for service time in order to avoid capacity estimates larger than t_f^{-1}.

The average service time is defined as

$$\bar{S} = \rho\bar{S}_q + (1 - \rho)\bar{S}_e. \tag{5.26}$$

Because the D/C ratio (ρ) is a function of the average service time, an iterative procedure is required. The following estimate is used as an initial value

$$\tilde{\rho} = \lambda\bar{S}_e = \frac{q\bar{S}_e}{3600}. \tag{5.27}$$

The variance ratio of service times is estimated as

$$C_S^2 = \frac{\bar{S}_q + \bar{S}_e}{2\bar{S}_q}. \tag{5.28}$$

If the major road has wide shoulders, the interaction with minor-road right-turn vehicles can be viewed as a merging procedure. The maximum merging rate of minor stream vehicles is $(1500 - q_M)_+$, where q_M is the conflicting major flow rate. If $\bar{S}_q$ or $\bar{S}_e$ are larger than the average service time of the merge, they are replaced with the latter.

The impedance effect of higher priority queues is estimated by multiplying the service time with an adjustment factor (Hagring 1997)

$$f_q = \frac{1}{\prod_{j=1}^{m}(1 - \rho_j)}, \tag{5.29}$$

where ρ_j is the D/C ratio for secondary major stream j, and m is the number of secondary higher priority movements, which have to yield to streams of higher rank.

5.4.5 Capacity

Capacity is defined as the stationary outflow from a lane having a continuous queue, assuming that the flow rates of all other traffic streams are given (Nordqvist et al. 1973, Anveden 1988). The capacity of a lane k sharing movements $i \in I$ is calculated as

$$C_k = \frac{f_C}{\sum_{i \in I} \bar{S}_{q,i} \frac{q_i}{q_k}}, \tag{5.30}$$

where f_C is the correction factor for lane capacity, $\bar{S}_{q,i}$ is the service time under queuing conditions of movement i, q_i is the flow rate per movement i in lane k, and $q_k = \sum_{i \in I} q_i$ is the total flow rate in lane k. The correction factor f_C includes corrections for bicycles, lane widths, and gradients.

5.4.6 Delay

The components of delay in the Swedish methods are defined as (Nordqvist et al. 1973, Anveden 1988)

- *Total delay* (W_t) is the additional time consumption per vehicle above the time consumption of traffic entering the intersection at the same speed as upstream of the intersection and exiting at the same speed as traffic flows downstream of the intersection.
- *Geometric delay* (W_g) is the hypothetical total delay if there were no interactions between different vehicle movements and no control devices (stop signs) causing delay.
- *Interaction delay* (W) is the delay caused by control devices and interactions between different vehicle movements; i.e., $W = W_t - W_g$.

Total delay has a physical interpretation. Geometric and interaction delays do, however, not correspond to any two different parts in a time-space trajectory of a vehicle (Anveden 1988).

Geometric delay has a deceleration and an acceleration component

$$\bar{W}_g = \bar{W}_{gd} + \bar{W}_{ga} = \frac{(v_a - v_n)^2}{2a_d v_a} + \frac{(v_e - v_n)^2}{2a_a v_e}, \tag{5.31}$$

where v_a is approach speed, v_e is exit speed, v_n is the negotiation speed, and a_d and a_a are deceleration and acceleration constants, respectively. Total delay is the sum of interaction delay and geometric delay. However, it is assumed that at least some part of the deceleration component in the geometric delay should be ignored, because deceleration to some extent takes place when a vehicle catches up a queue. For simplicity, total delay is calculated as (SNRA 1995*b*)

$$\bar{W}_t = \max\left\{\bar{W}, \bar{W}_{gd}\right\} + \bar{W}_{ga}. \tag{5.32}$$

This indicates a control-oriented definition of the interaction delay. In the old manual all acceleration delays were included in the geometric delay (Anveden 1988).

Total interaction delay is calculated as the sum of the average waiting time in queue and the average service time

$$\bar{W} = \bar{W}_q + \bar{S}. \tag{5.33}$$

The follow-up time is not subtracted, because it may not be included in the service time $\bar{S}_e$ (5.25) of isolated vehicles. Acceleration delay due to control is not included.

Under degrees of saturation less than 0.8 the waiting time in queue is calculated using the Pollaczek-Khintchine formula (4.61) with variance ratio given by equation 5.28. For a major-stream through+left lane ρ in the numerator is replaced by the D/C ratio of the left-turn movement only, while no change is done in the denominator. When $\rho > 1.4$, the fluid-analogy model (4.116) is applied. For $0.8 \leq \rho \leq 1.4$ the average waiting time in queue is interpolated between the two cases.

In TV131 the P-K formula (4.61) was used for $\rho \leq 0.9$. The method could not be applied when the D/C ratio was $\rho > 0.9$. The variance ratio was estimated as a function of ρ and calibrated by simulation and field measurements. As a result, the estimate for the average waiting time was a function of ρ only (Hanson 1978).

5.4.7 Short lanes

A short lane can be blocked by a queue on the adjacent lane (a) extending beyond the short lane. A long lane can be blocked by a queue extending beyond the storage space L_s of an adjacent short lane. If a lane is blocked a new lane allocation is done by an iterative procedure.

In an analysis procedure for short lanes Capcal 2 calculates the queue length for the lane (m) having the higher D/C ratio ($\rho_m = \max\{\rho_a, \rho_s\}$) of the two lanes. The Pollaczek-Khintchine formula for average queue length in an M/G/1 system

$$\bar{L}_m = \frac{\left(1 + C_S^2\right)\rho_m}{2(1 - \rho_m)} \tag{5.34}$$

is used for degrees of saturation $\rho \leq 0.8$. At higher degrees of saturation the queue length is estimated by an application of the Little's formula (4.65)

$$\bar{L}_m = \lambda_m \bar{W}_m. \tag{5.35}$$

In the old Swedish manual (Statens vägverk 1977) the probability of storage overflow was calculated as

$$\mathbb{P}\left\{L_s < \bar{L}_m\right\} = \left(\frac{\bar{L}_m}{\bar{L}_m + 1}\right)^{L_s}. \tag{5.36}$$

In Capcal 2 the short lane is treated as an ordinary lane, if $\bar{L}_m \leq L_s$. The probability or frequency of blocking are not considered. If a lane is blocked, the average waiting time in queue is taken to be the same as for the adjacent lane, which is considered to be a slight overestimation. The utilization factor of the short lane is calculated as

$$\rho_s = 1 - \left(\frac{\lambda_s}{\lambda_a + \lambda_s}\right)^{L_s} - \left(\frac{\lambda_a}{\lambda_a + \lambda_s}\right)^{L_s}. \quad (5.37)$$

5.5 Finnish methodology

The Finnish guidelines (Tiensuunnittelutoimisto 1978) and the Finnish Capcal software (Tiensuunnittelutoimisto 1987, Kehittämiskeskus 1991) follow the Swedish capacity manual TV131 (Statens vägverk 1977), which was described above. The differences between the Finnish method and the TV131 method are described below.

The Swedish policy favors speed limits 50, 70, 90, and 110 km/h, while in Finland 50, 60, 80, 100, and 120 km/h are most commonly used. The highest speed limit (120 km/h) is posted on freeways only. To reflect this difference in speed limits the critical gap table (5.13) has been adjusted for Finnish conditions. The adjustment factors for critical gap and the follow-up time $t_f = 0.6t_c$ follow the Swedish method.

Table 5.13: Base values for critical gaps in the Finnish guidelines (Tiensuunnittelutoimisto 1978)

	Major road speed limit (km/h)							
	50 km/h		60 km/h		80 km/h		100 km/h	
Movement	Yield	Stop	Yield	Stop	Yield	Stop	Yield	Stop
Major left	5.0	—	5.8	—	6.2	—	6.8	—
Minor right	4.8	5.5	5.4	6.0	6.4	6.9	7.0	7.5
Minor through	5.6	6.4	6.0	6.8	6.7	7.4	7.2	7.8
Minor left	5.9	6.7	6.4	7.2	7.3	8.1	8.0	8.8

The estimation of capacity, delay and other performance measures follows the Swedish TV131 (Statens vägverk 1977) methodology. The level-of-service criteria (Table 5.14) follow the criteria in HCM 1985 (Transportation Research Board 1985). The service measure is "reserve capacity", which is the inverse of average waiting time in system in a M/M/1 queuing model. See section 4.3.2 for details.

Level of service can also be determined from Figure 5.3, which is based on Table 5.14 slightly modified. The D/C ratio (Table 5.15) is used as an alternative service measure.

Table 5.14: Level-of-service criteria in Finland (Pursula & Ristikartano 1988, Tie- ja liikennetekniikka 2001)

Level of service	Reserve capacity (veh/h)
A	400–
B	300–399
C	200–299
D	100–199
E	0– 99
F	$q > C$

Based on field measurements Uusiheimala (1995) suggested new ranges for critical gaps (Table 5.16). See also Niittymäki & Uusiheimala (1996). In particular, the critical gaps for major road left turns and minor road right turns appeared to need some

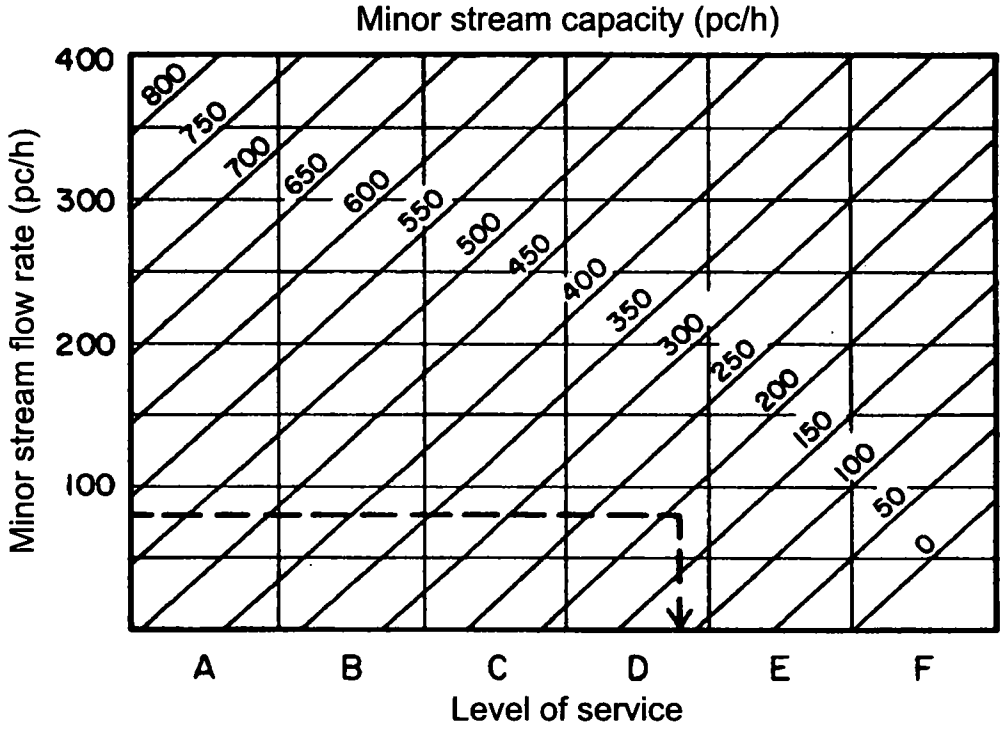

Figure 5.3: Level of service according to the Finnish guidelines (Tie- ja liikennetekniikka 2001)

Table 5.15: Alternative quality-of-service criteria in Finland (Tie- ja liikennetekniikka 2001)

Quality of service	D/C ratio
Good	0.00–0.50
Fair	0.50–0.70
Tolerable	0.70–0.85
Bad	0.85–1.00
Very bad	1.00–

adjustment (Pursula & Peltola 1998). The results were used to recommend new critical gaps to be implemented in the HUTSIM simulation software (Table 5.17). Some of these adjustments were very significant, as a comparison of Tables 5.13 and 5.17 reveals.

Table 5.16: New ranges for critical gaps suggested by Uusiheimala (1995)

	Major road speed limit (km/h)			
	50	60	80	100
Critical gap (s)	3–5.5	4–6	6–8	7–8

Figure 5.4 displays a chart for a rough assessment of a roundabout according to the old Finnish guidelines (Tiehallitus 1992). The upper edge of the gray area can be interpreted as the practical capacity of a one-lane roundabout. Pedestrian and bicycle flows crossing an entry are added to the circulating flow. If the distance between an exit and an entry is less than 15 meters, 30 % of exiting flow is added to the circulating flow. The pce factor for trucks and vans is 1.5 and for semi-trailers 2.0.

These capacity estimates were found to be too small at low circulating flow rates

Table 5.17: Recommended critical gaps for simulation of unsignalized intersections (Pursula et al. 1997)

	Major road speed limit (km/h)							
	50 km/h		60 km/h		80 km/h		100 km/h	
Movement	Yield	Stop	Yield	Stop	Yield	Stop	Yield	Stop
Major left	4.0	—	4.5	—	5.5	—	6.0	—
Minor right	4.0	5.0	4.5	5.5	6.5	7.0	7.0	7.5
Minor through	5.0	6.0	5.5	6.5	7.0	7.0	7.0	7.5
Minor left	5.5	6.3	6.0	6.8	7.0	8.0	8.0	8.8

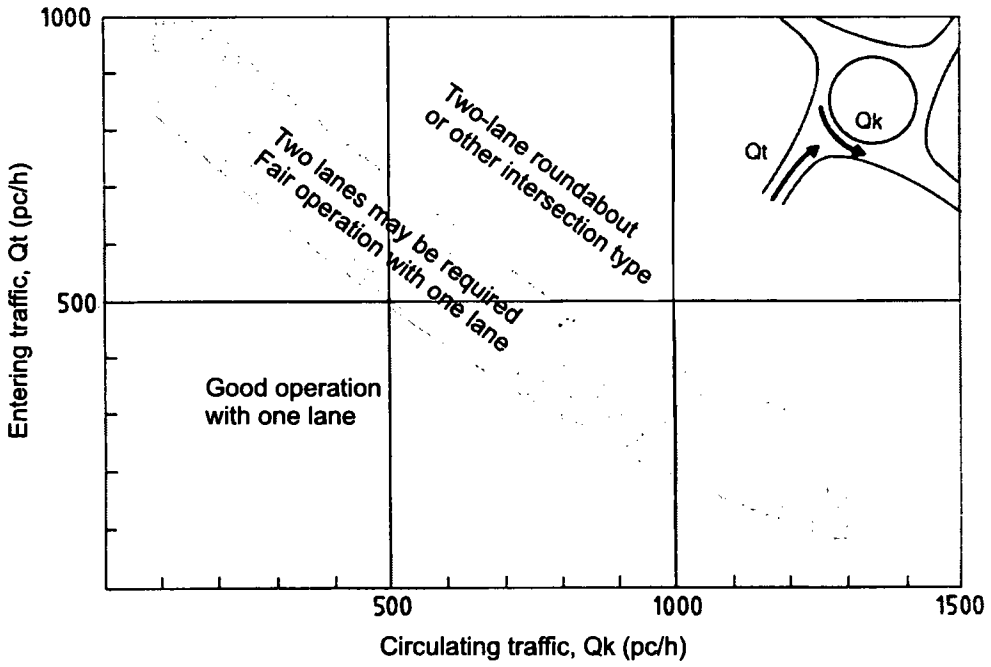

Figure 5.4: Operation of a roundabout according to the old Finnish guidelines (Tiehallitus 1992)

(Liimatainen 1997). The new guidelines (Tie- ja liikennetekniikka 2001) have a slightly corrected chart (Figure 5.5). For a more detailed capacity estimation it is suggested that a roundabout is analyzed as a series of T-intersections with critical gap $t_c = 4.8$ s (Liimatainen 1997). The value is slightly higher that the lower bound in HCM2000 (Table 5.3). Hagring & Niittymäki (1997) have demonstrated that in Denmark, Finland, and Sweden there is a general trend of diminishing critical gaps with increasing roundabout size.

The guidelines do not give specific capacity estimates. The empirical studies (Jormalainen 1991, Kehittämiskeskus 1996) were not able to find congested conditions at roundabouts under study. The results, however, suggested that the Finnish version of Capcal (TV131 method) overestimated the capacity of roundabouts. The reason for this was probably in the estimation of critical gaps (Kehittämiskeskus 1996). This was also suggested by the Swedish studies of Hagring (1996*b*), as discussed in section 5.4.3. The new Swedish capacity model developed by Hagring has given capacity estimates very close to Finnish simulation results (Hagring & Niittymäki 1997, Pursula et al. 1997).

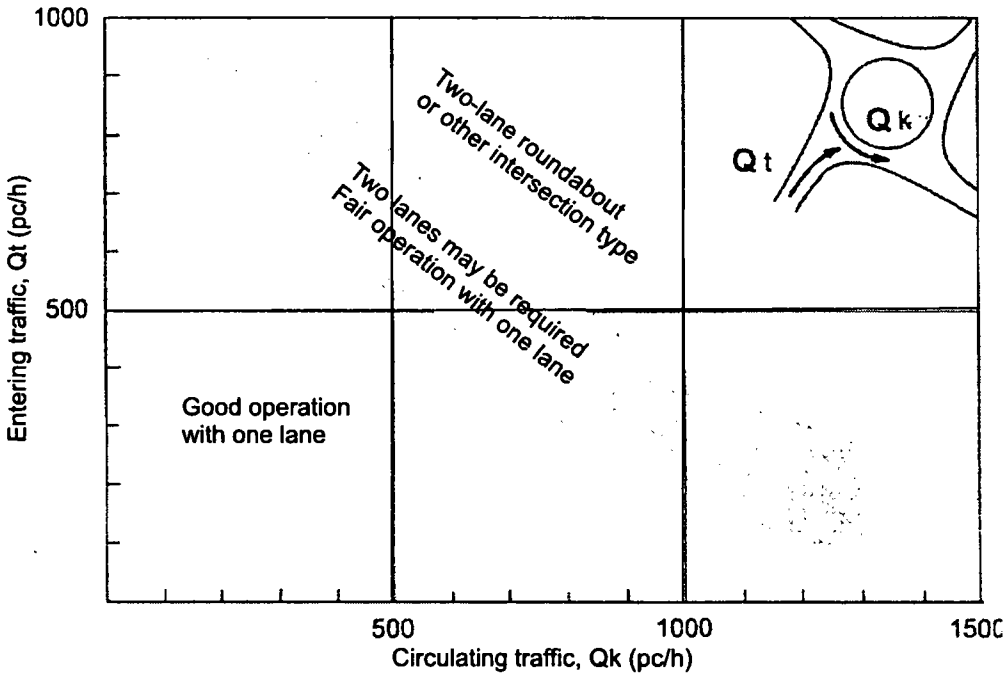

Figure 5.5: Operation of a roundabout according to the current Finnish guidelines (Tie- ja liikennetekniikka 2001)

6 SIMULATION STUDIES

6.1 Hutsim as a simulation tool

A Finnish object-oriented simulation software, HUTSIM, was used in simulation experiments. It has three components: HUTEDI, HUTSIM, and HUTSIM-analyzer. HUTEDI is a simulation model editor. HUTSIM is a microscopic traffic simulator. HUTSIM-Analyzer is a postprocessor.

HUTSIM has been under development at the Helsinki University of Technology (HUT) since 1989. The stochastic properties of traffic flow and the conflicts with other traffic flows can be described and analyzed with sufficient accuracy. HUTSIM was originally developed for the analysis of signalized intersections, but it has been extended for the analysis of unsignalized intersections, roundabouts (Fig. 6.1), small networks, and highway sections as well. The version of HUTSIM used in this research was 4.21.

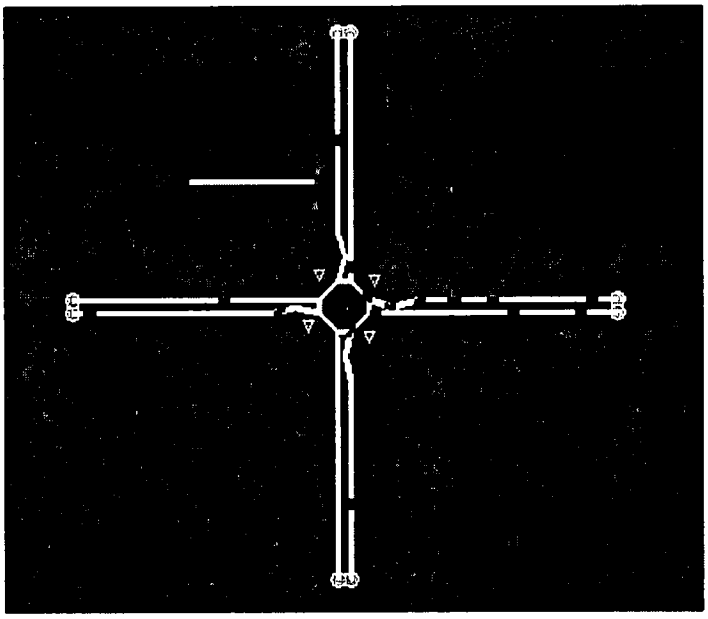

Figure 6.1: HUTSIM *roundabout model*

The building blocks of HUTSIM are object-oriented programming and rule-based interaction dynamics. The most important models to control the movement of vehicles are:

1. Vehicle acceleration and deceleration models
2. Car-following model
3. Lane-changing model.

Kosonen (1999) has described each model in detail.

Lane segments are modeled as links or "pipes", in which vehicles move. The main properties of "vehicle objects", initialized at generation are identification number, vehicle type, length, desired speed and destination. Traffic signals as well as stop and yield signs are "obstacle signals" connected to pipes (Kosonen 1996).

For unsignalized intersections HUTSIM applies a traffic-signal analogy approach: "red signal" (stop) during blocks and "green signal" (go) during antiblocks. Stop sign gives

a red (stop) signal until a minor stream vehicle approaching the stop line has come to a stop. "Stop" signal activates the deceleration model. "Go" signal has no effect on vehicle movements. Yield and stop signs are both obstacles in vehicles' path and "sight objects". They open the drivers' sight to vehicles outside of their own driving path.

In HUTSIM the vehicular interactions at an unsignalized intersection are slightly different from the gap acceptance models. Safety lag v_s in HUTSIM is the minimum acceptable lag (from the rear of a minor-stream vehicle to the front of a major-stream vehicle) at conflict point, whereas critical gap is the minimum acceptable headway or lag that a driver at a stop/yield line observes. A safety lag is used in HUTSIM, because it is possible to use the same parameter value for all vehicle types (Koivisto 1999). Safety lags may follow a statistical distribution (Kosonen 1996). However, in this study, they were constant.

The lanes and driving paths at an intersection are modeled as pipes. Stop/yield line is typically at the end of a yielding pipe. Conflict point is usually at the end of a major stream pipe, which may be connected to the same pipe as the yielding pipe. Figure 6.2) presents a simple illustration of a yield-sign object, which controls two conflict points. A more realistic simulation arrangement requires separate sign objects for all conflict points.

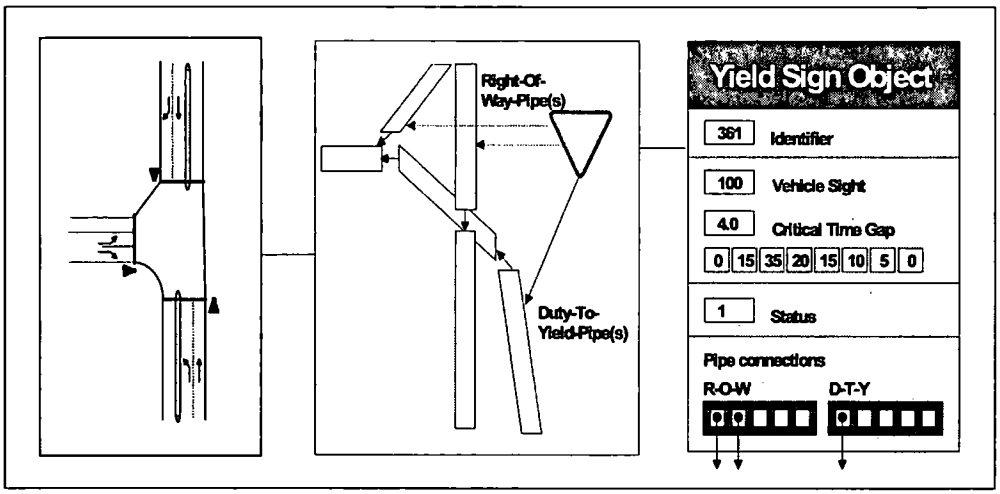

Figure 6.2: The yield-sign object in HUTSIM *(Kosonen 1996). The "Critical Time Gap" in the figure refers to "safety lag".*

When the distance (d_y) of a yielding vehicle to a conflict point is shorter than the maximum sight distance d_s, the yield sign indicates whether it is safe to proceed ("go") or not ("stop"). When a minor-stream vehicle approaches the intersection at speed v_y and the next major-stream vehicle is approaching with speed v_M at distance d_M from the conflict point, the yield sign gives a stop signal if

$$\left(\frac{d_M}{v_M} < \frac{d_y + l_y}{v_y} + v_s \text{ AND } \frac{v_y^2}{2d_y} < \alpha_{max}\right) \text{ OR } d_y > d_s, \tag{6.1}$$

where l_y is the length of the yielding vehicle.[1] The conflict point is the collision point of the rear bumper of a yielding vehicle and the front bumper of the major stream vehicle. The yield sign will give a stop signal, if the time distance at conflict point, when a minor

[1] Equation 6.1 is a slightly modified version of the equation of Kosonen (1996).

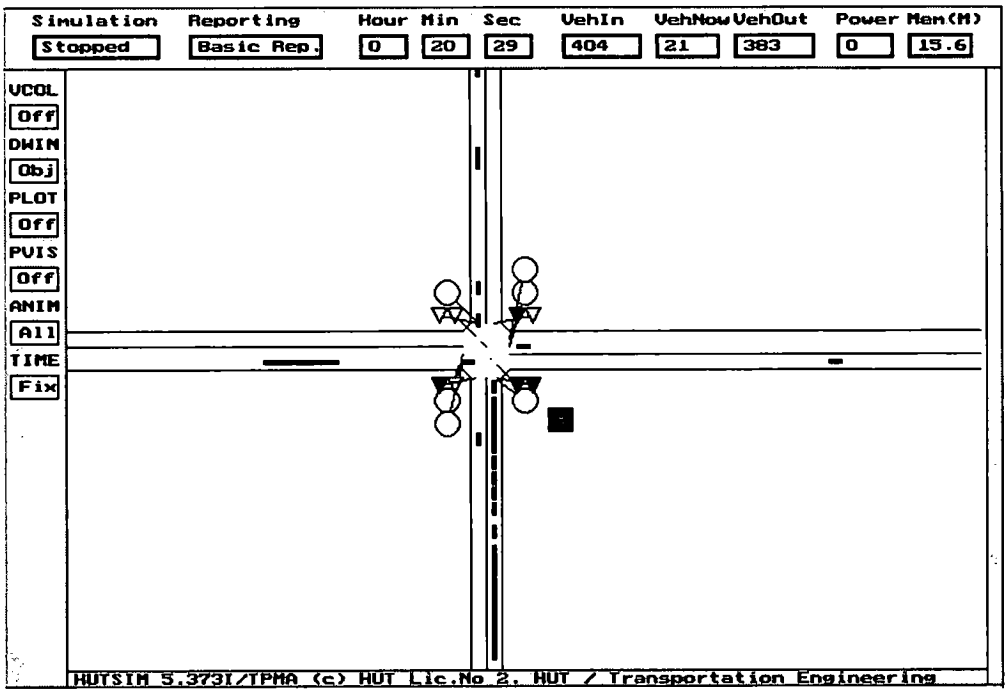

Figure 6.3: Simulation screen in HUTSIM

stream vehicle has passed it, to the next approaching major stream vehicle is shorter than the safety lag υ_s and the minor stream vehicle is able to stop without exceeding the maximum deceleration rate. If multiple major-stream lanes (pipes) are connected to one yield or stop sign, the status of the sign is determined by the first vehicle in all pipes to enter the conflict point. As long as the distance d_y to the yield sign is longer than the maximum sight distance d_s, the driver observes it as a stop signal. A short sight distance forces the vehicle to slow down and prepare to stop. (Kosonen 1996)

Major-stream vehicles are assumed to drive at their current speed, possible future accelerations or decelerations are not predicted. Acceleration is accounted for a stopped or nearly stopped minor-stream vehicle, but its driving time to conflict point may be overestimated for some slowly moving vehicles. Accordingly, the safety-lag estimate used in the decision making may be inaccurate. In order to minimize the number of inconsistent operations the conflict points were set to the stop lines.

Rule 6.1 considers driving times to a conflict point. In general, the operations of simulated vehicles are based on the properties of the vehicle, environment, control, and other vehicles stored in a data base, not on driver's observations. Thus, HUTSIM cannot be used to analyze the gap acceptance process, when observation of major road vehicles exiting before the conflict point is unclear. However, HUTSIM can model the modification of the headway distribution of through vehicles due to the deceleration of right turning vehicles in a shared lane.

Critical gap in HUTSIM is the sum three components:

1. Occupancy time (t_M) of a major stream vehicle at a conflict point
2. Occupancy (t_m) of a minor stream vehicle at the conflict point
3. Safety lag (υ_s) to the arrival of the next priority vehicle to the conflict point

The minor stream vehicle can enter the conflict point immediately after the major stream vehicle has passed it, no safety interval is defined, neither has the conflict point any physical dimensions. A critical lag is the sum of components 2 and 3 above. For a given safety lag the critical gap is larger than the critical lag. Although all vehicles obey the same safety lag, the minimum acceptable gaps and lags may be different for different vehicles, depending on vehicle dynamics and the initial speed of a minor-stream vehicle.

For a major-stream vehicle having length l_v and driving at speed v, the occupancy time at a conflict point is $t_M = l_v/v$. The stop or yield line is assumed to locate at the conflict point. For a stopped minor-stream vehicle having the same length l_v and acceleration rate a, the occupancy time at a conflict point is $t_m = \sqrt{2l_v/a}$. The critical gap is obtained as

$$\begin{aligned} t_c &= t_M + t_m + v_s \\ &= \frac{l_v}{v} + \sqrt{\frac{2l_v}{a}} + v_s. \end{aligned} \tag{6.2}$$

In HUTSIM passenger cars have length $l_v = 4$ m and acceleration rate $a = 1.6$ The difference between a critical gap and a safety lag is about 2.5 s, when $v = 50$ km/h and about 2.4 when $v = 100$ km/h. If a minor-stream vehicle passes a conflict point at a negotiation speed of 30 km/h, the difference $t_c - v_s$ is approximately 0.8–0.6 seconds.

The vehicle-dynamics parameters are independent of traffic conditions. Accordingly, follow-up times in HUTSIM are not related to major stream flow rates or waiting times.

HUTSIM has a more realistic model for vehicle dynamics than gap acceptance and queuing models. Compared to signalized intersections, where the status of signals follows explicitly defined rules, the modeling of unsignalized intersections is much more complicated. In HUTSIM the decision making processes of drivers at unsignalized intersections are not more sophisticated than the mathematical gap acceptance models. HUTSIM has not been calibrated to model the variation in the behavior of a driver or between drivers. Although safety lags between drivers may follow a statistical distribution, HUTSIM assumes consistent drivers. The criticism directed at gap acceptance models is in many respects also valid for HUTSIM, as well as for many other simulation models (see Hagring 1996*a*).

6.2 Calibration of Hutsim for unsignalized intersections

6.2.1 Vehicle-dynamics parameters

HUTSIM has been extensively calibrated and validated for Finnish signalized intersections (Niittymäki 1993, Niittymäki & Pursula 1994, Niittymäki 1998). The microscopic and macroscopic properties of the system were measured, the HUTSIM parameters were calibrated, and the macro-level results were compared with field measurements. The results of HUTSIM were considered very reliable. It can be assumed that the vehicle-dynamics parameters are similar in both signalized and unsignalized intersections. The calibration and application of HUTSIM for roundabouts has been reported by (Hagring 1997, Pursula et al. 1997).

During this study field data were collected to further calibrate HUTSIM for the analysis of unsignalized intersections, including roundabouts. The results of these measurements have been reported by Koivisto (1999). Only a short overview will be given here.

In HUTSIM the departure processes at unsignalized intersections are simulated using the rules and parameters of vehicle dynamics (Table 6.1). Critical gaps and follow-up times are not used as parameters. Because changing the safety lag has no effect

on vehicle dynamics parameters, HUTSIM cannot be used to study, for example, the possible correlation between critical gaps and follow-up times.

Table 6.1: Vehicle dynamics parameters for unsignalized intersections in HUTSIM *(Pursula et al. 1997, Koivisto 1999)*

		Vehicle class				
		Passenger car		City bus	Tram	Truck
Parameter	Unit	Normal	Maximum			
Acceleration	m/s^2	1.6		1.2	1.3	1.0–1.2
Deceleration	$-m/s^2$	1.9	3.2	1.3	1.3	1.2
		All vehicle classes				
Follower gap	s	1.2				
Starting response time	s	0.9				

The arrivals were generated following a shifted exponential headway distribution with a minimum arrival-time headway $t_p = 0.5$ seconds. The cumulative distribution function of the headway distribution was

$$F(t) = \begin{cases} 0, & \text{if } t < 0.5\,s \\ 1 - e^{-\theta(t-0.5)}, & \text{if } t \geq 0.5\,s. \end{cases} \tag{6.3}$$

The random number seed in a HUTSIM run was the same in all simulation runs. Thus, it was possible to replicate the same traffic input with different control parameters. However, it was not possible to analyze the variance of results with given control parameters.

6.2.2 Follower gaps

Follower gap is the desired time interval (from back bumper to front bumper) between two consecutive vehicles. When major-stream flow rate is low, follow-up time is the the most important parameter to describe minor-stream capacity, and follower gap is the most important parameter to describe the follow-up time. The follower gap in HUTSIM was calibrated both by direct follower-gap measurements and by verifying that the resulting follow-up times are realistic.

Follow-up times were measured at eight roundabouts. The diameter (d) of the central island ranged from 8 to 55 meters. The measured follow-up times decreased slightly with increasing diameter (Koivisto 1999):

$$t_f = 2.2506 - 0.0043d, \qquad R^2 = 0.31. \tag{6.4}$$

When the follower gap in HUTSIM was set to 1.2 s, the resulting follow-up times were slightly higher than obtained in the field measurements. With follower gap 1.1 s HUTSIM slightly underestimated the follow-up times.—Compared to international guidelines the measured follow-up times were very short.

Follow-up times were also measured at three T-intersections. The results were evaluated by movement and by queue position. For major-road left turns and minor-road right turns the follow-up times were about 2.0–2.1 seconds. For minor-road left-turn movements the follow-up time was about 2.25 seconds. These data were, however, from one intersection only.

With follower gap set to 1.2 seconds HUTSIM overestimated the follow-up times, except for minor-road left turns, for which HUTSIM produced good estimates. When the follower gap was set to 1.1 seconds, the follow-up times produced by HUTSIM were close

to field measurements. The follow-up times at a minor-road left-turn were, however, underestimated.

The follower gaps were also measured directly. The follower gap of 1.2 seconds was found to better describe the field measurements, and it was used in the simulation runs. It may underestimate capacities in some cases, but it is not likely to produce unrealistically high capacities. Follower gap 1.2 seconds is the default value in HUTSIM.

6.2.3 Driving speeds

Acceleration ceases when a vehicle has attained its target speed or the maximum speed at current location, such as a roundabout. Target speeds have a discrete distribution. Koivisto (1999) used the speed distributions in Table 6.2. In this study the average target speed was 80 km/h with 20 % of drivers having target speed 70 km/h and another 20 % having target speed 90 km/h. At the intersection the speed limit was, however, 60 km/h. This arrangement allowed the possibility of an arrival rate higher than the queue-discharge rate. For the major-road through stream this arrangement was not necessary. The average target speed was 60 km/h with 20 % of drivers having target speed 50 km/h and another 20 % having target speed 70 km/h. Figure 6.4 displays speed as a function of distance when a stopped vehicle accelerates at rate 1.6 m/s^2.

Table 6.2: Speed distributions used by (Koivisto 1999)

Target	Speed limit		
speed (km/h)	50 km/h	80 km/h	100 km/h
50	60 %		
60	40 %		
70		10 %	
80		40 %	
90		50 %	60 %
100			30 %
110			10 %

Maximum speeds of turning and circulating vehicles were calibrated with field measurements (Koivisto 1999). At roundabouts the driving speed v of passenger cars increases with the diameter r of the central island:

$$v = 26.676 + 0.0862r. \tag{6.5}$$

The speeds of vehicles turning right or left at a conventional unsignalized intersection are similar to the speeds at small roundabouts. The negotiation speed of left turning vehicles was set to 30 km/h and of minor-road through vehicles to 40 km/h.

6.2.4 Limited priority merge

Although not a calibration issue, a short discussion is presented here about the conditions under which HUTSIM simulation describes a limited priority merge (see page 60). Priority becomes limited if a merging vehicle cannot reach its target speed before a major stream vehicle driving with its target speed has reached the follower gap $t_{\min}$ behind the merged vehicle. When a merging vehicle passes the conflict point with speed v_0 and accelerates at constant acceleration rate a, the vehicle reaches its target

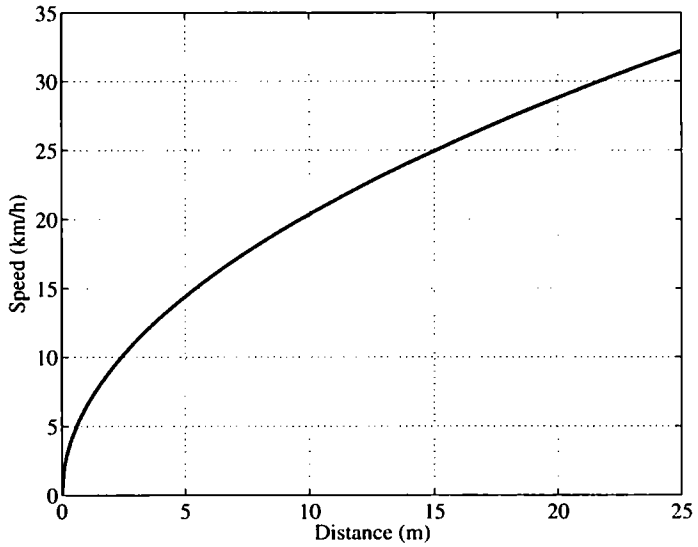

Figure 6.4: Speed as a function of distance with the default acceleration rate 1.6 m/s^2 of passenger cars in HUTSIM

speed v after time t_a and distance d_a:

$$t_a = \frac{v - v_0}{a} \tag{6.6}$$

$$d_a = \frac{v^2 - v_0^2}{2a}. \tag{6.7}$$

Limited priority merge takes place when the major stream vehicle drives the distance d_a in a time shorter than $t_a - v_s + t_{min}$, where v_s is the safety lag, and the speed of the major-stream vehicle is equal to the target speed (v) of the merging vehicle. In order to avoid limited priority, the safety lag should be

$$v_s \geq t_a - \frac{d_a}{v} + t_{min} = \frac{v - v_0}{a} - \frac{v^2 - v_0^2}{2av} + t_{min}. \tag{6.8}$$

Limited priority modifies the major stream headway distribution, which decreases capacity below the value expected under an unmodified headway distribution. This effect is largest under reasonably high major-stream flow rates, when gap forcing may produce shock waves in the major stream. Figure 6.5 displays an estimate of minimum safety lags required for absolute priority merge.

6.2.5 The effect of right-turn vehicles

If a turning vehicle decelerates from v_1 to v_2 at rate a, the deceleration takes time

$$t_d = \frac{v_1 - v_2}{a} \tag{6.9}$$

and distance

$$d_d = \frac{v_1^2 - v_2^2}{2a}. \tag{6.10}$$

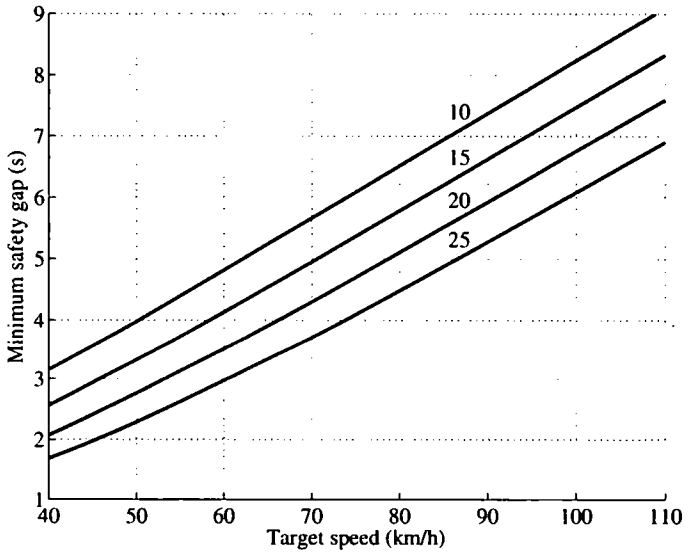

Figure 6.5: Minimum safety lag values in HUTSIM *to avoid gap forcing, when major and minor stream vehicles are all passenger cars with equal target speeds, and speeds of merging vehicles at conflict point range from 10 to 25 km/h*

The delay due to deceleration for a right turning vehicle is

$$W_d = t_d - \frac{d_d}{v_1}. \tag{6.11}$$

If a turning vehicle decelerates from 100 km/h to 30 km/h with rate 1.9 m/s^2, the delay of a right turning vehicle is 6.7 seconds. Because gap and lag estimation in HUTSIM is based on the assumption of constant speed, the delay in arrival time due to deceleration is not correctly estimated and the lag extension cannot be utilized by minor-stream vehicles. This decreases the simulated capacity. This is most likely the explanation for the low simulated capacities obtained by Koivisto (1999).

Imperfect estimation of priority-vehicle deceleration may happen in the real world also, but the effect is included in the critical gaps, if measured on field. If necessary, a specific adjustment should be defined. However, the performance of basic models should be evaluated without this effect.

It was considered necessary to perform the simulation studies with a limited number of movements. Because of the problems described above more reliable results could be obtained without any right-turn movements.

6.3 Simulated capacity of unsignalized intersections

6.3.1 Rank 2 capacity

For Rank 2 capacity analysis the stream arrangements displayed in Figure 6.6 were analyzed. The minor-stream left-turn movement (7) was the most important movement in the analysis. Because it has Rank 4, it can be analyzed with one, two, or three higher rank conflicting movements. The arrangements included all two-stream combinations used in the capacity analysis of Rank 3 and Rank 4 streams. The first three arrangements were used in Rank 3 and Rank 4 analysis. The last three arrangements were used in Rank 4 analysis only.

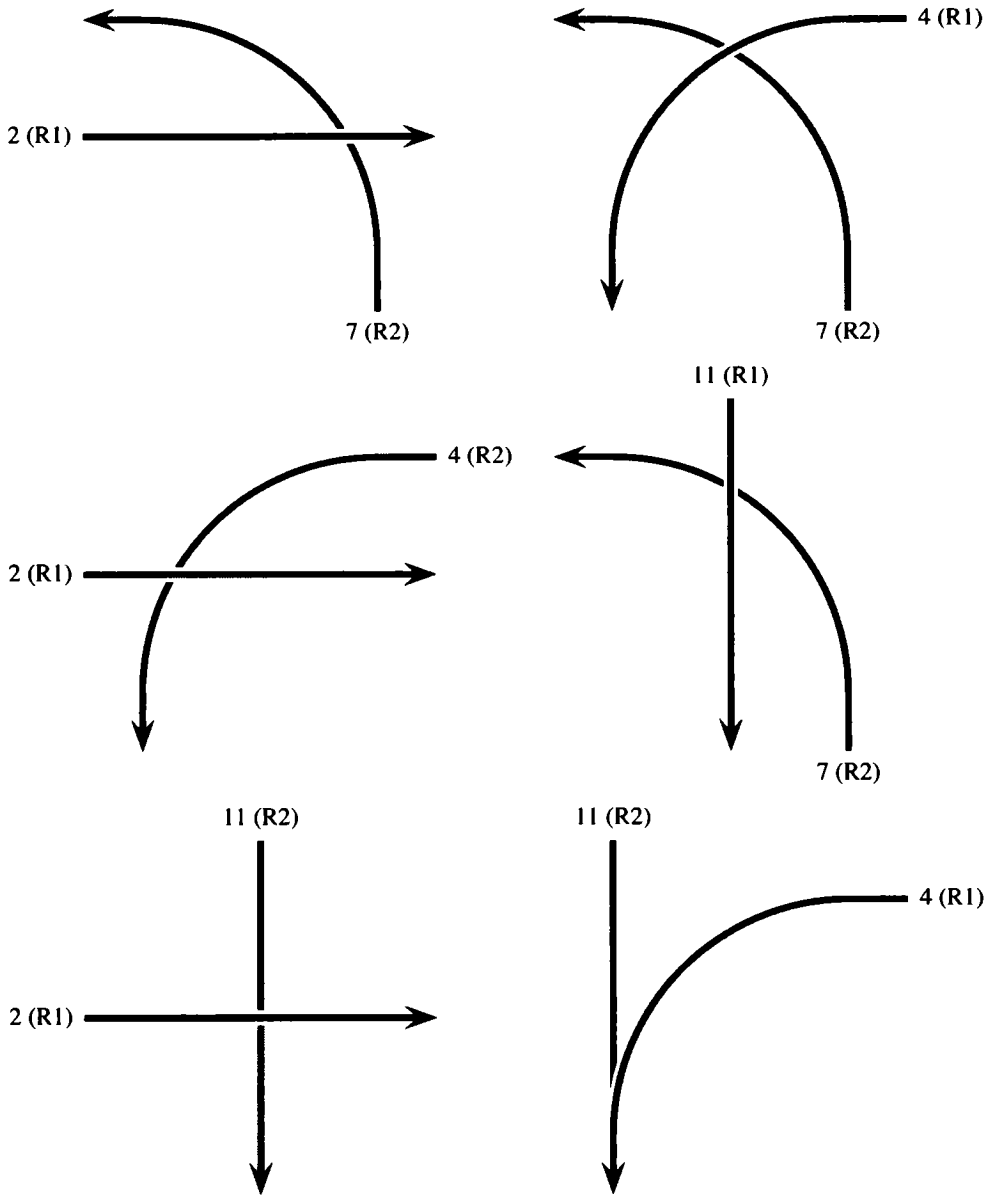

Figure 6.6: Simulated streams for Rank 2 capacity analysis

The safety lags in the HUTSIM runs were 2, 3, and 4 seconds. The minor roads and major-road left-turn streams had a yield-sign object with sight distance 200 meters. A stop sign was simulated by setting a yield-sign with a sight distance of 1.5 meters. In HUTSIM a yield-sign object gives a stop signal to an approaching vehicle until it is closer than the sight distance.

Capacity models were estimated using the least squares procedure. For the exponential capacity model (3.12) the estimated parameters were the critical gap (t_c) and the follow-up time (t_f). For the shifted exponential model (3.17) the minimum time headway (t_p) was also estimated. Critical gaps were estimated as initial critical gap (for a two-second safety lag) and an increment corresponding to one-second increment in a safety lag.

Figure 6.7 displays capacity estimates for a stop-controlled minor-road left-turn stream (7) crossing a major-road through stream (2). The capacity curves are approximately

linear, which suggests a shifted exponential capacity model. Shifted exponential distribution was the headway distribution used in the vehicle generation. Apparently, vehicular interactions before the intersection did not change the headway distribution significantly enough to be observed in the capacity models.

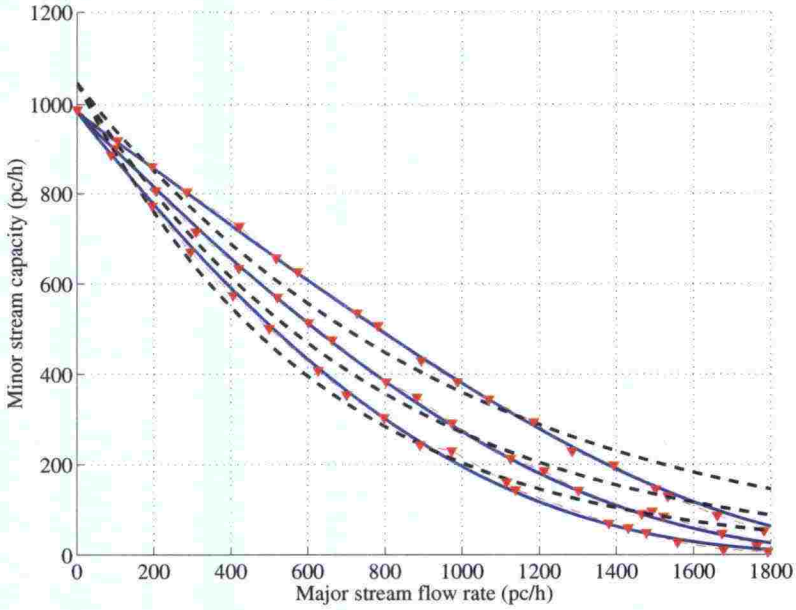

Figure 6.7: Capacity of a stop-controlled minor-road left-turn stream crossing a major-road through stream. Simulated (red triangles), exponential (solid blue) and shifted exponential (dashed black) capacity curves with safety lags 2 (upper), 3 (middle), and 4 (lower) seconds.

The shifted exponential model fits well the simulated capacities. The follow-up time 3.7 s (Table 6.3) indicates a capacity of 980 pc/h, when the major stream is negligible. Because the vehicle-dynamics parameters do not change with the safety lag, neither changes the follow-up time. The critical gap is approximately two seconds larger than the safety lag. The minimum major-stream headway (1.1 s) is approximately the same as the minimum headway parameter (1.2 s) in the simulation model.

Table 6.3: Gap-acceptance parameters for a minor-road left-turn stream crossing a major-road through stream

Parameter	Stop sign		Yield sign		Safety lag (s)
	Shifted exponential	Negative exponential	Shifted exponential	Negative exponential	
Critical gap (t_c)	4.2	5.4	4.7	5.8	2
	5.0	6.5	5.6	6.9	3
	5.9	7.5	6.5	7.9	4
Follow-up time (t_f)	3.7	3.4	2.1	2.1	
Min. headway (t_p)	1.1	0.0	0.9	0.0	

The critical gaps and follow-up times obtained by fitting the shifted exponential model describe driver behavior in the simulations better than the parameters for the negative exponential model. However, the application of the parameters of the shifted exponential capacity model in a negative exponential capacity model (Figure 6.8) overestimates

the simulated capacity.

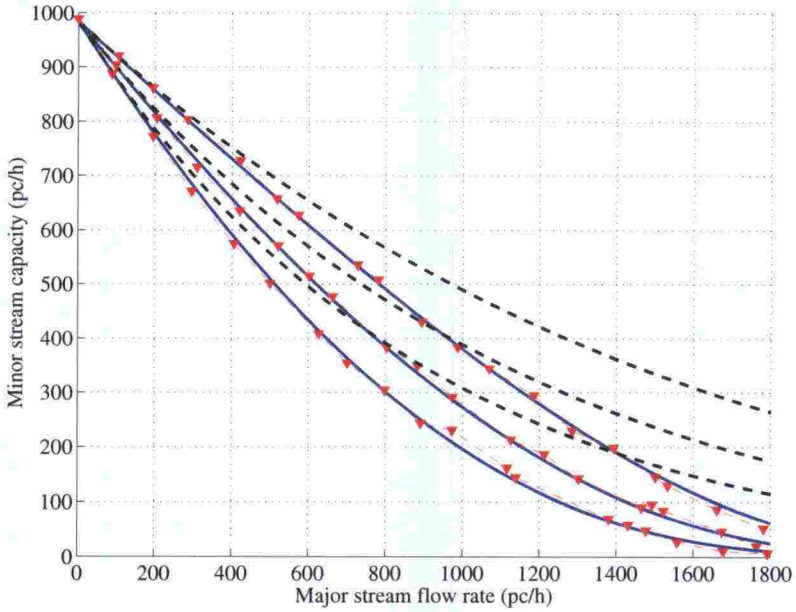

Figure 6.8: Capacity of a stop-controlled minor-road left-turn stream crossing a major-road through stream. Simulated (red triangles), exponential (solid blue) and shifted exponential (dashed black) capacity curves with safety lags 2 (upper), 3 (middle), and 4 (lower) seconds. Parameters obtained by fitting the shifted exponential model to the simulation results.

At a yield-controlled intersection the follow-up time is lower and critical gaps are higher. At low major-stream flow rates the capacity is higher, but approaches the capacity of a stop-controlled stream at high major-stream flow rates (Figure 6.9). One explanation for larger critical gaps at yield-controlled approaches may be that in HUTSIM a slow moving vehicle cannot always anticipate its acceleration while it estimates its arrival time to the conflict point. Accordingly, Table 6.3 describes the *relationships between safety lags and critical gaps at stop and yield controlled approaches in* HUTSIM. It should not be used to compare the effects of stop and yield signs at any intersection.

The critical-gap estimates for the exponential model are more than a second larger than the critical gaps for the shifted exponential model. The follow-up time is slightly lower (3.4 s). Because the exponential model has a stronger curvature than the simulated curves, the model overestimates the simulated capacity at low and high major-stream flow rates. At moderate conditions the model underestimates the simulated capacity.

Major-road left-turn vehicles (4) have to decelerate to the negotiation speed (30 km/h) before entering the intersection. Because in HUTSIM a minor-road left-turn vehicle (7) cannot anticipate this deceleration, minor-stream vehicles cannot use all acceptable lags. Accordingly, the critical gaps in the theoretical models must be increased (Table 6.4).

The shifted exponential capacity model gives again a better fit than the negative exponential model (Fig. 6.10). The capacity under negligible major-flow is, of course, the same as in the major-road through case (Fig. 6.7). The follow-up time estimates in both models are similar as in the major-road through case (Table 6.3). The critical gaps are, however, larger, especially for large safety-lag values.

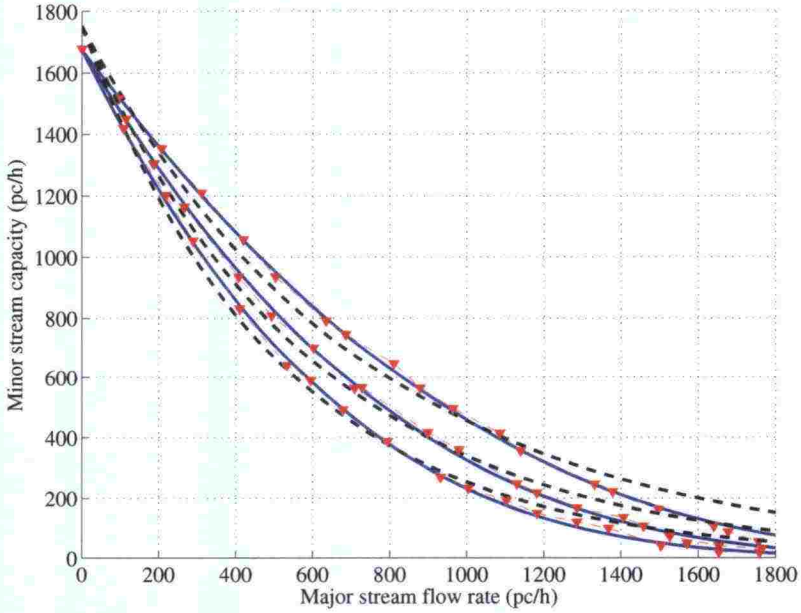

Figure 6.9: Capacity of a yield-controlled minor-road left-turn stream crossing a major-road through stream. Simulated (red triangles), exponential (solid blue) and shifted exponential (dashed black) capacity curves with safety lags 2 (upper), 3 (middle), and 4 (lower) seconds.

Table 6.4: Gap-acceptance parameters for a minor-road left-turn stream crossing a major-road left-turn stream

Parameter	Stop sign		Yield sign		Safety lag (s)
	Shifted exponential	Negative exponential	Shifted exponential	Negative exponential	
Critical gap (t_c)	5.6	7.4	6.6	8.1	2
	6.9	8.9	8.0	9.6	3
	8.3	10.4	9.3	11.0	4
Follow-up time (t_f)	3.7	3.5	2.2	2.1	
Min. headway (t_p)	1.3	0.0	1.0	0.0	

At a yield-controlled intersection follow-up times are smaller and stream capacity is higher, but it approaches the capacity of a stop-controlled stream at high major-stream flow rates (Fig. 6.11).

A major-road left-turn vehicle (4) does not have to stop, if it finds an acceptable lag in the major-road through stream (2). Consequently, the follow-up time and critical gaps are short (Table 6.5), and the capacity under low major-stream flow rates is high (Fig. 6.12). The critical gaps in the shifted exponential capacity model are approximately 1.6 seconds larger than the safety lag. In the negative exponential model the critical gaps are more than a second larger. The shifted exponential model has again a better fit, but the negative exponential model fits the simulated capacities better than in the case of a stop-controlled minor stream. The parameters are practically the same as for a yield-controlled minor-road left-turn stream (Table 6.3). In essence, the simulation models are the same.

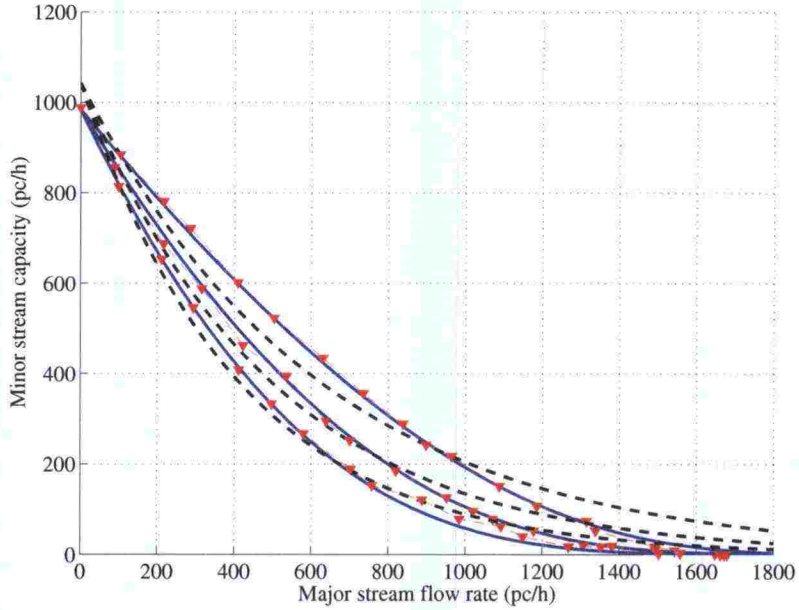

Figure 6.10: Capacity of a stop-controlled minor-road left-turn stream crossing a major-road left-turn stream. Simulated (triangles), exponential (solid blue) and shifted exponential (dashed black) capacity curves with safety lags 2 (upper), 3, and 4 (lower) seconds.

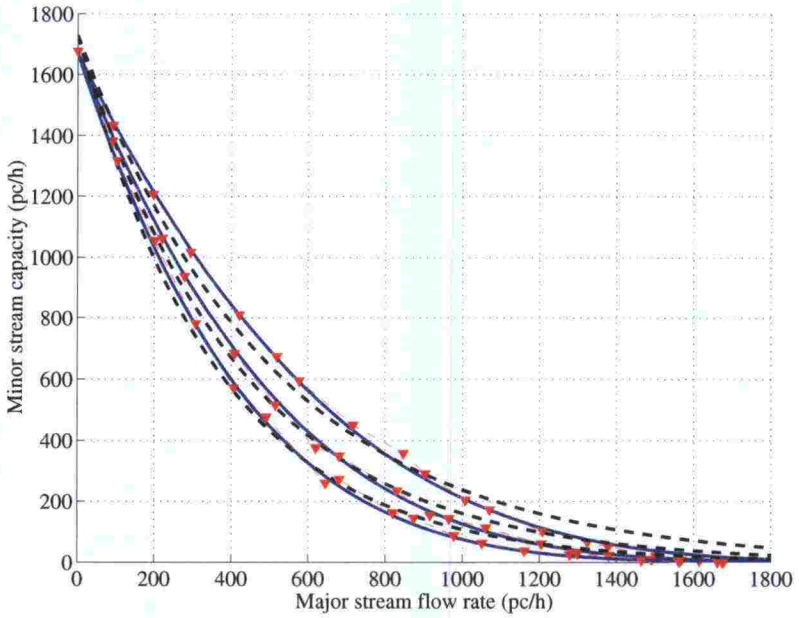

Figure 6.11: Capacity of a yield-controlled minor-road left-turn stream crossing a major-road left-turn stream. Simulated (triangles), exponential (solid blue) and shifted exponential (dashed black) capacity curves with safety lags 2 (upper), 3, and 4 (lower) seconds.

Table 6.5: Gap-acceptance parameters for a major-road left-turn stream crossing a major-road through stream

Parameter	Shifted exponential	Negative exponential	Safety lag (s)
Critical gap (t_c)	4.7	5.8	2
	5.6	6.9	3
	6.6	7.9	4
Follow-up time (t_f)	2.2	2.1	
Min. headway (t_p)	0.8	0.0	

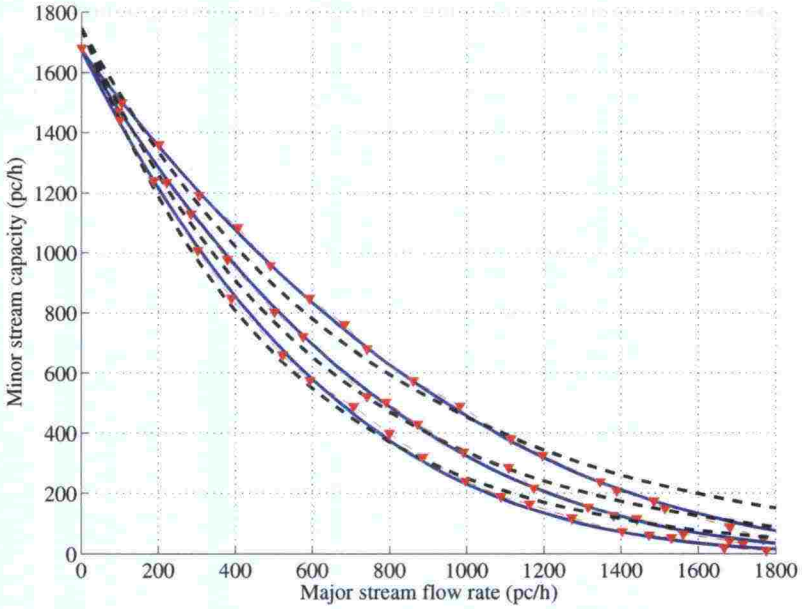

Figure 6.12: Capacity of a major-road left-turn stream crossing a major-road through stream. Simulated (triangles), exponential (solid blue) and shifted exponential (dashed black) capacity curves with safety lags 2 (upper), 3, and 4 (lower) seconds.

6.3.2 Rank 3 capacity

The capacity of a Rank 3 stream 7 was analyzed with the stream arrangement of Figure 6.13. The safety lag of stream 4 was two seconds. Stream 7 had a (simulated) stop sign and a three-second safety lag. A stop sign was simulated by setting a yield-sign with a sight distance of 1.5 meters.

The simulated capacity of a minor-road left-turn stream (7) is displayed in Figure 6.14. Simulated major-stream flow rates did not reach 1,800 pc/h, because at high Rank 1 flow rates the number of Rank 2 vehicles passing the intersection was restricted by Rank 2 capacity.

The critical gaps and follow-up times used in the estimation of the theoretical (3.89) and conventional (3.72) capacity models were obtained from the Rank 2 capacity analyses based on the shifted exponential model presented above (Tables 6.3, 6.4, and 6.5). Because the critical gaps of stream 7 were different for major streams 2 and 4, the critical gap used in the analysis was the weighted average of these two critical gaps.

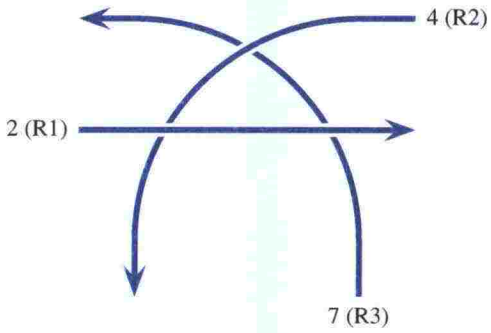

Figure 6.13: Simulated streams for Rank 3 capacity analysis

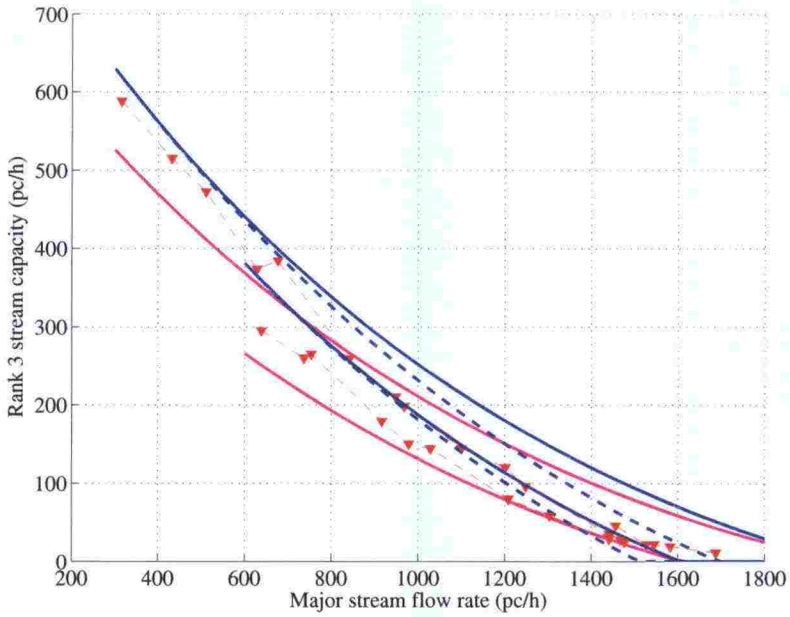

Figure 6.14: Rank 3 capacity of a stop-controlled minor-road left-turn stream (7) crossing major-road through (2) and left-turn (4) streams with left-turn flow rates 300 (upper curves) and 600 pc/h (lower curves). Simulated capacity (triangles), conventional capacity estimate (solid magenta) and theoretical capacity estimates(solid blue). Dashed blue curve displays the theoretical capacity estimate assuming a 1.8 second discharge headway for the Rank 1 stream.

The flow rates of the major movements were used as weighting factors.

The conventional capacity estimator is based on random arrivals and impedance factor $p_0 = 1 - \rho$, as used in both HCM2000 (Transportation Research Board 2000) and Capcal 2 (SNRA 1995*b*). As figure 6.8 demonstrates, the negative exponential capacity model (3.12) overestimates potential capacity at high major-stream flow rates. However, the impedance factor (3.76) in the conventional model gives too low capacity estimates. As a result, the conventional model gives too low capacity estimates at low major-stream flow rates, but at high flow rates the errors begin to cancel each other, and the capacity estimates are acceptable.

The theoretical model gives higher capacity estimates than the simulation model. Better estimates are obtained assuming a 1.8 s discharge headway for the Rank 1 stream.

Consequently, Rank 1 headways follow the Tanner model.

When a Rank 2 queue discharges, stopped vehicles accelerate to the negotiation speed. Because yielding vehicles in HUTSIM cannot anticipate the acceleration of higher-priority vehicles, a Rank 3 vehicle may enter the intersection when the Rank 2 queue starts to discharge. This causes a small positive bias in simulated capacities. This bias is largest (about 20 pc/h) at saturated conditions.

6.3.3 Rank 4 capacity

The capacity analysis of a Rank 4 stream (7) was based on the stream arrangement in Figure 6.15. Because a Rank 4 vehicle in HUTSIM could not anticipate the deceleration of a stopping Rank 3 vehicle, the resulting critical gaps were very high and capacities were very low. Better results were obtained in the analysis of a yield-controlled intersection.

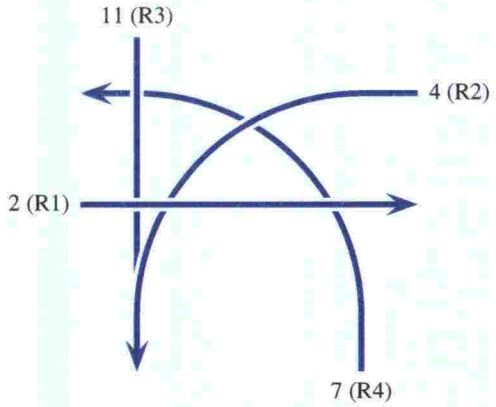

Figure 6.15: Simulated streams for Rank 4 capacity analysis

The capacity of a minor-road left-turn stream (7) crossing a minor-road through stream (11) is similar to the capacity of crossing the major-road left-turn stream (4). The only difference in the simulation model is a higher negotiation speed (40 km/h) for stream 11 than for stream 4 (30 km/h). Consequently, HUTSIM gives lower critical gaps (Table 6.6) and higher capacities for crossing the through stream (11). Again, this is not necessarily a reflection of reality, but a property of the simulation model. When negotiation speed is higher, the deceleration time is shorter, and the error in the estimated arrival time to the conflict point is smaller.

Table 6.6: Gap-acceptance parameters for a yield-controlled minor-road left-turn stream crossing a minor-road through stream

Parameter	Shifted exponential	Negative exponential	Safety lag (s)
Critical gap (t_c)	5.7	7.0	2
	7.1	8.5	3
	8.4	9.9	4
Follow-up time (t_f)	2.2	2.1	
Min. headway (t_p)	0.9	0.0	

The minor-road through stream (11) must yield to streams 2 and 4. Because the negotiation speed of stream 11 in the HUTSIM model is higher (40 km/h) than of stream 7 (30 km/h), the follow-up time is shorter (see Table 6.7). This gives a higher capacity at low major-stream flow rates (Figure 6.16). The critical gaps are larger when

merging with the major-road left-turn stream, because the left-turn stream has a lower negotiation speed (30 km/h) than the major-road through stream (60 km/h), and in HUTSIM the minor-road vehicles cannot anticipate the extension of a gap or a lag due to a deceleration.

Table 6.7: Gap-acceptance parameters for a yield-controlled minor-road through stream crossing a major-road through and left-turn streams

Parameter	Major through		Major left		Safety lag (s)
	Shifted exponential	Negative exponential	Shifted exponential	Negative exponential	
Critical gap (t_c)	4.9	6.0	6.9	8.3	2
	5.8	7.0	8.1	9.6	3
	6.8	8.1	9.3	10.9	4
Follow-up time (t_f)	2.0	1.9	2.0	1.9	
Min. headway (t_p)	0.8	0.0	0.9	0.0	

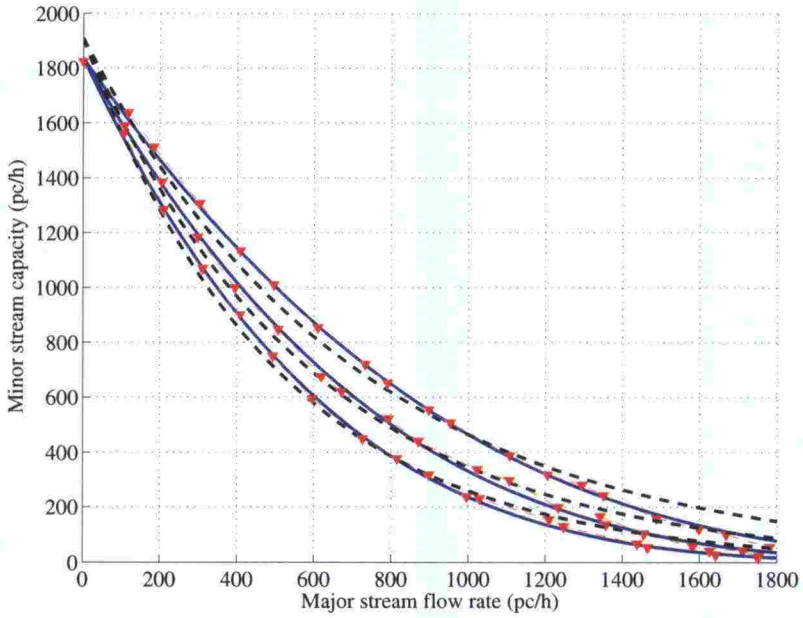

Figure 6.16: Capacity of a yield-controlled minor-road through stream crossing a major-road through stream. Simulated (triangles), exponential (solid blue) and shifted exponential (dashed black) capacity curves with safety lags 2 (upper), 3, and 4 (lower) seconds.

Simulated Rank 4 capacities and capacity estimates based on the conventional (3.104) and theoretical (3.114) models are displayed in Figure 6.17. The safety lag for the major-road left-turn stream (4) was 2.0 seconds, for the minor-road through stream (11) it was 2.5 seconds, and for the minor-road left-turn stream (7) the safety lag was 3.0 seconds. Longer safety lags at lower priority streams were used in order to minimize the number of "sneakers". The critical gaps and follow-up times were obtained from the shifted exponential capacity models in the Rank 2 analysis. For minor streams crossing several priority streams the critical gaps were estimated as averages weighted by the conflicting flow rates. For stream 11 the values were interpolated.

The simulated priority-stream flow rates were measured at exit points. At high flow rates

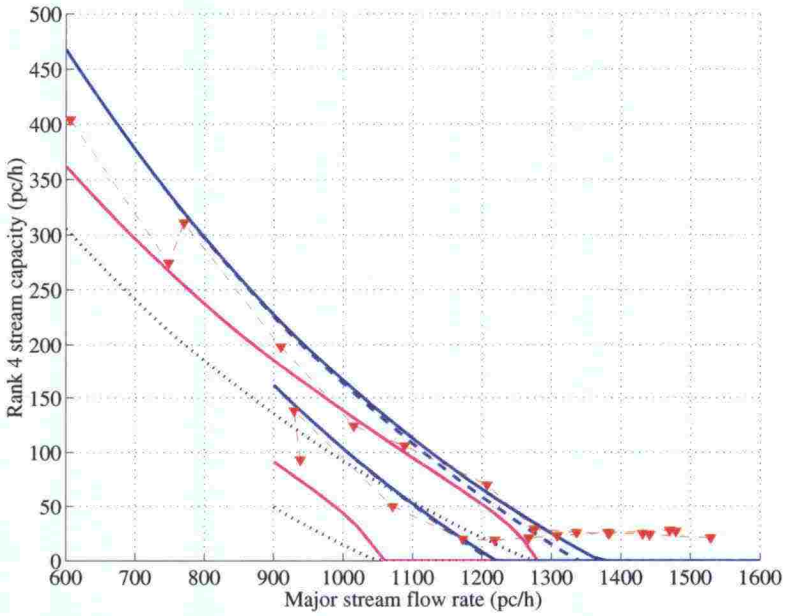

Figure 6.17: Rank 4 stream capacity at a yield-controlled intersection with Rank 3 flow rate 300 pc/h and Rank 2 flow rates 300 (upper curves) and 600 pc/h (lower curves). Simulated capacity (triangles), conventional capacity estimate (3.104, magenta) and theoretical capacity estimate (3.114, blue). Dashed blue curves display the theoretical capacity estimates assuming a 1.8 second discharge headway for the Rank 1 stream. Dotted black curves display the conventional capacity estimates without the additional adjustment (3.103).

capacity may have restricted the number of departures of Rank 2 or Rank 3 streams. Consequently, the total major-stream flow rate did not reach 1,800 pc/h, which was the maximum expected traffic generation rate; i.e. the demand.

The capacity did not decrease to zero at high major-stream flow rates, because in HUTSIM some Rank 4 vehicles departed while a Rank 2 or Rank 3 queue started to discharge, as discussed above. This factor increased the capacity at high major-stream flow rates by approximately 25 pc/h.

The conventional model slightly underestimates the simulated capacity. As observed in the Rank 3 analysis, the impedance factor (3.103) gives too low values, while the exponential model (3.12) with realistic parameter values tends to overestimate the simulated capacity (Fig. 6.8). The dotted curves display the conventional capacity estimates without the additional adjustment (3.103), as in Capcal 2. The estimates are too low. The adjustment (3.103) in HCM2000 improves the estimates considerably.

The theoretical model gives slightly too high capacity estimates, especially if the simulation results are adjusted for the effect of "sneakers". The assumption of a 1.8 second discharge headway in the Rank 1 stream has a minor decreasing effect on the results.

6.4 Simulated capacity of roundabouts

Figure 6.18 displays potential capacity estimates for two roundabouts based on HUTSIM simulations. Two central island diameters (8 m and 38 m) were used. Safety lag was two seconds. Capacity decreases almost linearly with increasing circulating flow. Larger diameter (d) increases capacity by approximately 50 pc/h. At low circulating flow rates

the increase in capacity is higher. Linear regression equations are

$$\hat{C}_p = 1436 - q_c \quad \text{pc/h}, \qquad d = 8\,\text{m} \tag{6.12a}$$

$$\hat{C}_p = 1484 - q_c \quad \text{pc/h}, \qquad d = 38\,\text{m} \tag{6.12b}$$

From the family of M3 capacity models (3.19) the shifted exponential ($\phi = 1$) model (3.17) gives the best fit, when minor stream capacity decreases linearly with increasing major stream flow rate. Figure 6.18 displays these models fitted for the simulation results. The critical gap was four seconds. The follow-up time was 2.5 s for the smaller roundabouts and 2.3 s for the larger roundabout. The saturation flow rate for $t_f = 2.5$ is 1,440 pc/h, which is close to the capacity of the smaller roundabout under very low circulating flow rates. For the larger roundabout the follow-up time $t_f = 2.3$ gives a higher saturation flow rate (1,565 pc/h) than predicted by the regression line (1,484 pc/h), but the simulation results indicate that the decrease in entry capacity is steeper at low circulating flow rates. For the larger roundabout the minimum headway in the circulating flow is $t_p = 1.8$ s, as in the Swedish models. For the smaller roundabout the results suggest a slightly larger ($t_p = 2.0$ s) minimum headway.

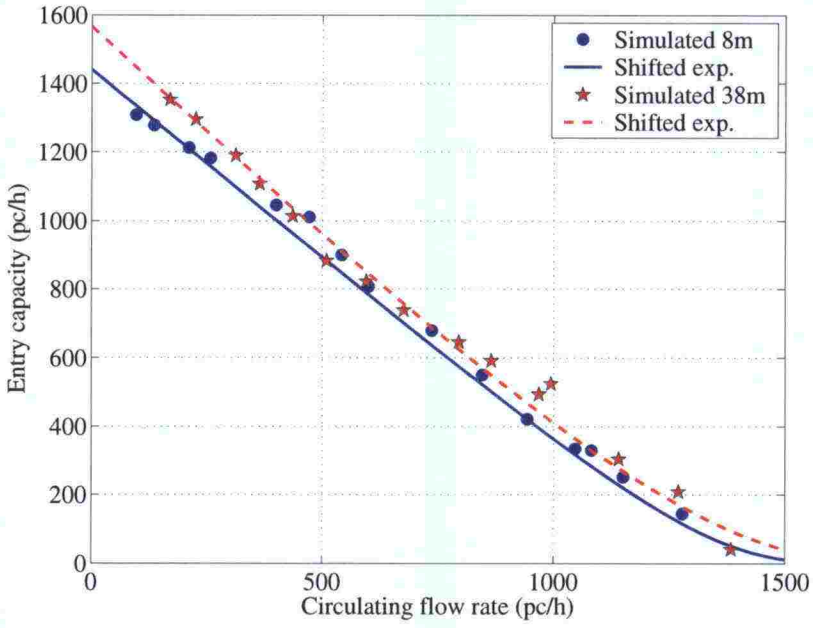

Figure 6.18: Capacity of a one-lane roundabout (simulation results and shifted exponential models) with critical gap $t_c = 4$ s and central island diameters 8 m and 38 m

The simulation results indicate a nearly linear relationship between entry capacity and circulating flow. Similar results have been obtained for two-lane roundabouts (Hagring 1997, Pursula et al. 1997). Linear capacity models have been supported by both empirical (Kimber & Coombe 1980) and theoretical (Troutbeck 2002) studies. The linearity is supposed to result from decreasing critical gaps and limited priority under high circulating flow rates. These phenomena are, however, not included in the simulation model.

The shifted exponential model suggested by the linear relationship is the headway model used in HUTSIM. When the follower gap in HUTSIM is 1.2 s, and circulating speeds are

about 30 km/h, the follower headway is approximately 1.8 s. Further research is needed to evaluate the effect of headway distributions on roundabout capacity.

6.5 Simulated delays

For delay analysis the operation of an intersection was simulated for 80 minutes. The first 10 minutes was an intialization interval, after which data was collected for 60 minutes (report interval). The final 10-minute interval was required by HUTSIM basic reporting system for vehicles that were generated during the "report interval" but departed the system after it.

Data was collected from detector output stored in a "delay file". The detector was located at the intersection exit point. Vehicles passing the detector during the report interval were included in the analysis. Accordingly, the delay analysis followed the path-trace method.

The analytical delay formulas are based on the queue-sampling method. At undersaturated conditions the results of path-trace and queue-sampling methods are similar. At oversaturated conditions the methods give different delay estimates, as demonstrated in Figure 4.12 on page 131. The queue-sampling overflow delay during a time period $(0, t]$ is the area 0QR, while the path-trace method gives overflow delay 0QP. In both methods the average delay is obtained by dividing the total delay by the number of departures, $C(t)$. The queue-sampling method overestimates the average delay, because it includes a delay component PQR of additional vehicles, which is not included in the path-trace method. On the other hand, the path-trace method does not include the delays accumulated to the vehicles in the queue. These vehicles have started to experience delays larger than the average delays of departed vehicles.

The delay of each vehicle was calculated from the HUTSIM delay file. The difference between the travel times from traffic generator to the intersection exit point under given conditions and under free conditions without a stop sign was used as an estimate of control delay. Because simulated minor-stream flow-rates were measured at exit point, they could not exceed capacity even though vehicle generation rate (demand) may have been higher.

The average control delay of a stop-controlled minor-road left-turn stream crossing a major-road through stream is displayed in Figure 6.19. The delay estimates were calculated according to the coordinate-transformation method using equations 4.131 and 4.132. The average acceleration delay was estimated as five seconds, following the HCM2000. A lower value would have fit better the simulation results, but the acceleration delays due to a "simulated stop sign" in HUTSIM may have been too low. A more detailed analysis of the acceleration delay would have required field data, which was not available for this research.

The capacity estimates were based on the shifted exponential capacity model (3.17) with parameters as in Table 6.3. The figure demonstrates that the coordinate transformation method gives reliable delay estimates, when capacity estimates are accurate.

HCM2000 calculates capacity (3.12) assuming negative exponential headways. To account for the effect of a stop sign, five seconds are added to the delay estimate of the coordinate-transformation method (4.131). The follow-up time is not subtracted from the waiting time in the system. The delay estimates are good, although they do not follow the simulation results as closely as the blue curves, which had capacity estimates based on the properties of the simulation model.

Figure 6.20 displays similar analysis for a yield-controlled approach. Because vehicles

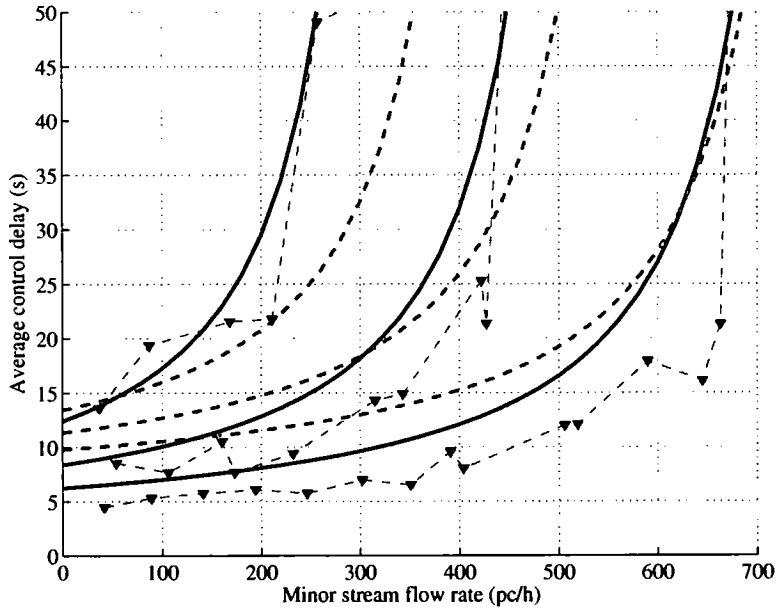

Figure 6.19: Average control delay of a stop-controlled minor-road left-turn stream crossing a major-road through stream having flow rates 300 (lower curve), 600 (middle), and 900 pc/h (upper). Simulated delays (red triangles) and delay estimates based on the coordinate-transformation method (shifted exponential capacity model, blue curves) and the HCM2000 method (dashed magenta curves).

accepting a lag do not stop, the average acceleration delay was calculated as

$$\bar{W}_a' = 5\left(1 - \frac{t_f C}{3600}\right) = 5 - \frac{t_f C}{720}. \tag{6.13}$$

It was assumed that the acceleration delay of a delayed vehicle is five seconds, and the proportion of undelayed vehicles is the proportion of actual capacity (C) to maximum capacity (t_f^{-1}).

The coordinate-transformation method again produces good delay estimates, when capacity estimates are based on the shifted exponential headway distribution. The delays are slightly overestimated, but the shape on the delay curves are very realistic.

Especially at low major-stream flow rates many delayed minor-stream vehicles can cross the yield line without stopping. A better acceleration delay estimate would have improved the delay estimates. It was, however, considered appropriate to keep the estimation of average acceleration delay very simple. The difference between the estimates would most likely have been in the range of 1–2 seconds, and the validation would have been possible only against simulation results.

HCM2000 delays were too high at low minor-stream flow rates. If five seconds (the adjustment for a stop sign) was subtracted, the delay estimates would have improved. Because HCM2000 capacity estimates were too high, delay estimates were too low at high flow rates.

It is evident that with good capacity estimates the coordinate-transformation method gives reliable delay estimates. It was also demonstrated that the HCM2000 delay estimation method (coordinate-transformation method) can be improved by subtracting

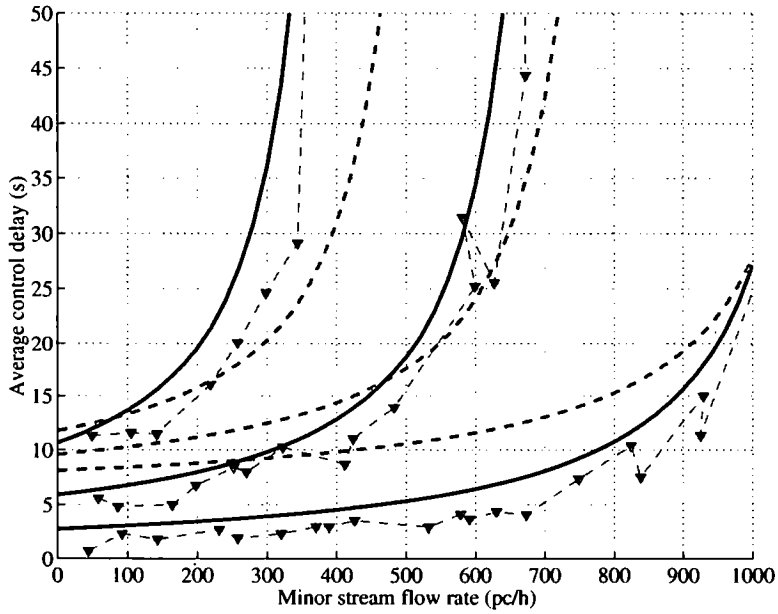

Figure 6.20: Average control delay of a yield-controlled minor-road left-turn stream crossing a major-road through stream having flow rates 300 (lower curve), 600 (middle), and 900 pc/h (upper). Simulated delays (red triangles) and delay estimates based on the coordinate-transformation method (shifted exponential capacity model, blue curves) and the HCM2000 method (dashed magenta curves).

the follow-up time from the waiting time in the system. A simple adjustment (6.13) for the acceleration delay at yield-controlled intersections was shown to give reasonable results.

7 CRITICAL GAPS AND FOLLOW-UP TIMES

7.1 Estimation methods

Critical gaps and follow-up times are measures of driver behavior at unsignalized intersections. Gap acceptance theory usually assumes that drivers are consistent and homogeneous. Gap acceptance is modeled by a step function (see Section 3.2.2), which indicates a constant critical gap and follow-up time for each movement. This assumption was used in the simulation studies also. In order to use the capacity and delay models, critical gaps and follow-up times have to be estimated.[1]

It is not possible to measure critical gaps directly. It is only possible to observe a driver either accepting or rejecting a gap. Under consistent behavior an accepted gap is an upper bound for the critical gap of the driver. Likewise, the largest rejected gap is a lower bound for the personal critical gap. If drivers are inconsistent, the estimation becomes even more complicated. It is not possible to observe a minimum acceptable gap/lag that may be different for different gaps/lags. Darzentas (1981) concludes that the distribution of accepted gaps/lags cannot be estimated from field data. However, probability distributions of gap acceptance created under the assumptions of consistent and inconsistent behavior are identical.

The capacity analysis methods described above assume consistent and homogeneous drivers. Gap acceptance can, accordingly, be described by a point estimate, a critical gap. The critical gap studies in Finland have been based on the Raff's method. Because recent international studies have indicated that the maximum likelihood method gives more accurate estimates, both of these methods have been applied in this research.

According to the *Raff's method* (Raff 1950) the critical gap (t_c) is the time-gap that has the property that the number of accepted gaps shorter than t_c is the same as the number of rejected gaps longer than t_c. A driver can accept only one gap, but reject any number of gaps. Raff observed that if all gaps were included in the analysis, rejected gaps had a too strong weight in the analysis.[2] Consequently, Raff considered only lags so that no more than one observation was collected for each driver. The number of observations was, however, greatly reduced. Consequentlt, Hewitt (1985) considered methods using only lags inferior to methods using both lags and gaps. In this study all gaps were included in the analysis so that the results were compatible with earlier Finnish critical gap studies.

Maximum likelihood method (ML) has been extensively used in statistical parameter estimation (Edwards 1974, Edwards 1992). A ML estimate has the highest likelihood of being the parameter of a hypothetical distribution which has generated the observations. Miller & Pretty (1968) suggested the ML method to estimate critical gaps. The method has been further developed and demonstrated to be one of the best critical-gap estimation methods (Hewitt 1985, Troutbeck 1992, Brilon, Koenig & Troutbeck 1997, Tian, Troutbeck, Kyte, Brilon, Vandehey, Kittelson & Robinson 2000).

7.2 Stop vs. yield control

Following the terminology of Greenshields et al. (1947) a stop sign indicates a *functional* deceleration and stop (see footnote on page 108). All vehicles must stop at stop line.

[1] If a linear gap acceptance function (see Section 3.2.3) is used, the number of discharging vehicles as a linear function of headway length has to be estimated. The shortest acceptable headway is $t_0 = \inf\{t: \alpha(t) > 0\}$.

[2] Raff also observed that a headway included the time interval that a major-stream vehicle occupied the conflict point, while it was unoccupied during the entire lag.

A yield sign, on the other hand, indicates a *chronotropic* deceleration. Minor stream vehicles must decelerate and maybe stop, if a block prevents their entry.[3]

A vehicle facing a yield sign does not have to stop, if it arrives during an antiblock. A vehicle arriving at the end of a block may decelerate early so that at the beginning of the block it may cross the stop line at a higher speed than possible otherwise. The vehicle may accept a shorter gap or lag than a stopping vehicle. Also the acceleration delay will be shorter. In addition, vehicles crossing a yield line during an antiblock may discharge with shorter follow-up times than vehicles having to stop at a stop line. The difference between these two control methods is largest at low degrees of saturation and low major stream flow rates, when the proportion of minor stream vehicles accepting lags is largest. As the major stream flow rate and the D/C ratio increase, more minor-stream vehicles have to stop at yield line and the difference between stop control and yield control decreases.

Some early German studies indicated that the priority rule has no influence on critical gaps and follow-up times (Brilon 1988*a*). In the current German guidelines (FGSV 2001) the follow-up times are different for yield and stop controlled intersections, but critical gaps are the same. The HCM 2000 (Transportation Research Board 2000) method is for stop-controlled intersections only. Capcal 2 (SNRA 1995*b*) gives different critical gaps for yield and stop controlled intersections. Follow-up times are also different ($t_f = 0.6t_c$). DanKap (Vejdirektoratet 1999*b*) has control-specific critical gaps, but the same follow-up times. Consequently, the guidelines that address both yield and stop control have either critical gaps, follow-up times, or both control specific.

The models used in this report assume that critical gaps and follow-up times are independent of major and minor stream flow rates. Yield controlled approaches are likely to have shorter critical gaps and follow-up times than stop controlled approaches, assuming that other conditions are similar.

The simulation results indicated clearly that follow-up times are different at yield and stop controlled intersections. Because the safety lag in HUTSIM was given as a parameter, the simulation results could not be used to estimate critical gaps.

7.3 Field studies

7.3.1 Data collection

The critical gap data available at the Helsinki University of Technology Laboratory of Transportation Engineering were supplemented by field measurements at eight intersections and nine roundabouts. Traffic operations were video recorded during peak hours. The data were collected and analyzed by the staff of the Laboratory. All locations were in the Southern Finland.

Intersections were chosen so that three different major-road speed limits were included: 50 km/h, 60 km/h, and 80 km/h. Three movements were studied:

1. Left turn from major road
2. Right turn from minor road
3. Left turn from minor road

Times, when a vehicle arrived to the stop-line and when a gap was accepted or rejected,

[3]This makes also the estimation of acceleration delay difficult at yield-controlled intersections.

were written down. This material was adequate to get the accepted and largest rejected gaps for the estimation of critical gap. The data contained mostly passenger cars.

Some of the not rejected headways were too long to give a realistic description of driver behavior. Consequently, very large rejected headways were excluded from the analysis, as described below.

7.3.2 Results

Although efforts were made to find intersections and time periods of high flow rates, the major streams were dominated by long headways. Because accepted headways were long, the information obtained about the upper bound of the critical gap was very limited. It is also possible that drivers were willing to reject gaps that they would have accepted under congested conditions, which may have resulted in too high lower bounds for the critical gap. Accordingly, both lower and upper bounds may have been overestimated.

The good supply of long headways appeared to distort especially the maximum likelihood estimates. For comparison, maximum likelihood estimates were calculated also for right-censored data. The maximum value for accepted gaps was set to 11 seconds for roundabouts and for intersections with major-road speed limit 50 or 60 km/h, and to 17 seconds when the speed limit was 80 km/h. The results are displayed in Appendix A. Raff's (1950) method was not very sensitive to censoring.

For each movement both average and weighted average were calculated (see Appendix A). The square root of sample size was used as the weighting factor. It became, however, apparent that more data was needed, especially under high D/C ratios, in order to obtain reliable critical-gap estimates. Until then the critical gaps presented by Pursula et al. (1997) and displayed in Table 5.17 are suggested as base values. The follow-up time estimate suggested by Jessen (1968)[4] $t_f = 0.6t_c$ can still be used as a base value. However, the capacity estimates are more reliable, if field-measured critical gaps and follow-up times are used.

For *roundabouts* the estimates in Table A.9 are in the range 4.0–4.7 s. No significant correlation was found between the roundabout size and the critical gaps. However, definite conclusions about the effect of roundabout geometry to critical gaps would require more field data.

For typical Finnish roundabouts the critical gaps as suggested by Hagring (1996*b*) and Capcal 2 (SNRA 1995*c*) are presented in Table 7.1 (see equations 5.18 and 5.16). The small (10 m) roundabout does not have approach islands, which makes the weaving section longer and the estimated critical gap shorter.

Table 7.1: Critical gaps for typical Finnish one-lane roundabouts according to equation (5.16) of Capcal 2 (SNRA 1995c) and equation 5.18 of Hagring (1996b)

Central island diameter d/m	Weaving section length l_w/m	Weaving section width w_w/m	Critical gap, t_c/s		
				Capcal 2	
			Hagring	Right turn	Crossing
10	21	10.0	4.5	4.1	4.9
20	23	8.5	4.3	3.8	4.4
40	30	7.0	3.9	3.4	3.8

[4]Later German studies, among others, have indicated that the direct correlation suggested by Jessen (1968) may not exist (Brilon 1988*a*).

Because the Finnish observations presented in Table A.9 do not indicate a correlation between critical gap and roundabout size, a single critical-gap value has been considered appropriate. The suggested *base value for a critical gap in Finnish one-lane roundabouts is 4.3 seconds*, which is close to the estimates in Table A.9. It is also the critical-gap estimate for a typical Finnish roundabout with central island radius of 20 m (Table 7.1), as well as the critical gap at a two-lane roundabout between traffic flows in outer circulating and entry lanes (Table 5.12), as estimated by Hagring (1998*b*). The suggested value is also in the range of the upper (4.1 s) and lower (4.6 s) bounds (Table 5.3) in HCM2000 (Transportation Research Board 2000), but slightly higher than the value 4.1 s suggested by the German HBS 2001 (FGSV 2001). For two-lane roundabouts the critical gaps suggested in Table 7.2 follow the results of Hagring (1998*b*).

Table 7.2: Suggested critical gaps and follow-up times for Finnish roundabouts

	One-lane roundabout		Two lane roundabout		
Entry	Critical	Follow-up	Critical gap		Follow-up
lane	gap	time	Outside lane	Inner lane	time
Right	4.3	2.3–2.5	4.3	4.0	2.4
Left			4.6	4.4	2.4

For two-lane roundabouts the follow-up time 2.4 s was suggested by Hagring (1998*b*). For one-lane roundabouts the follow-up time is calculated as

$$t_f = 2.5 - 0.0067(d - 8), \qquad 8 \le d \le 40, \tag{7.1}$$

where $d = 2(r_c - w_w)$ is the central island diameter. The resulting follow-up times are similar to the result (2.4 s) of Hagring (1996*b*) but shorter than suggested by HCM2000 (2.6–3.1 s), DanKap (2.6–2.8 s), and HBS 2001 (2.9 s)[5], which indicates that Finnish and Swedish roundabouts have higher capacity than the roundabouts in the U.S., Denmark, and Germany, when traffic flows are strongly dominated by one entry.

In the Australian guidelines (Austroads 1993) and in Sidra (Akçelik 1998) follow-up times at one-lane roundabouts are related to both roundabout size (inscribed circle diameter) and circulating flow rate. Follow-up times decrease with increasing diameter and increasing circulating flow rate. At low circulating flow rates the follow-up time ranges from 2.27 to 2.99 seconds, when the inscribed circle ranges from 80 to 20 meters (Austroads 1993). When the circulating flow approaches 1,500 veh/h the follow-up time can be as low as 1.7 seconds. In two-lane roundabouts with circulating flow rate 2,500 veh/h the follow-up time can be as low as 1.3 seconds. Sub-dominant streams have larger follow-up times than dominant streams.

The follow-up times suggested in Table 7.2 are still larger than the follow-up times obtained in field measurements (see equation 6.4). As the calibration studies indicated, with follower gap 1.2 s HUTSIM slightly overestimated follow-up times. The number of field measurements was, however, limited. In the light of international results, more field data are needed before lower follow-up times can be suggested.

The simulation results suggest that the minimum headway in circulating traffic is a function of central-island diameter (d):

$$t_p = 2.0 - 0.0067(d - 8), \qquad 8 \le d \le 40. \tag{7.2}$$

[5]New German research suggests 2.5 s as the follow-up time for a one-lane entry. (Thorsten Miltner at the German–Dutch–Finnish Seminar on Traffic Engineering at 8–9 June 2004 in Delft.)

In large roundabouts t_p is close to the value 1.8 s suggested by Hagring (1998*b*). In small roundabouts t_p is close to 2.0 s used in the Australian guidelines (Austroads 1993) and in Sidra (Akçelik 1998). The value 2.1 s used in the German guidelines (FGSV 2001) is slightly higher.

8 CONCLUSIONS AND RECOMMENDATIONS

8.1 Limitations of simulation experiments

Simulation tests reported above have been used to test analytical models against models with more advanced driver dynamics. The simulation software, HUTSIM, has been calibrated for Finnish unsignalized intersections, as described in Section 6.2. However, before making suggestions about capacity analysis methodologies it is necessary to briefly discuss the limitations of the simulation models.

The headway distribution used in the simulation models was shifted exponential. The distribution at specific locations is modified by target speed distributions, vehicular interactions, and roadway conditions. In the simulation models the distances from traffic generators to the intersection was short (less than one kilometer), which limited the effects of vehicular interactions.

In HUTSIM safety lag is the key parameter in gap acceptance. Drivers were assumed to be consistent and homogeneous. For a given safety lag at a yield-controlled intersection the critical gap was larger at high major-stream flow rates, when most vehicles had to stop at the yield line. However, studies on driver behavior have indicated that at high major-stream flow rates the critical gap may be shorter, not longer, than at low major-stream flow rates (see Section 2.4).

Minor-stream vehicles in HUTSIM cannot anticipate the acceleration or deceleration of major-stream vehicles. To some extent this may be realistic, but it is not validated. With a given safely lag critical gaps increase when major-stream vehicles decelerate. To minimize this effect all right-turn movements were eliminated from the simulation models.

On the other hand, Rank 3 (or 4) vehicles may enter the intersection while a Rank 2 (or 3) queue starts to discharge, because the vehicles cannot anticipate the acceleration of major-stream vehicles. This property of HUTSIM was demonstrated and its effect was discussed above. In the Rank 3 and Rank 4 cases analyzed the number of "sneakers" was not higher than 20–25 pc/h.

The shifted exponential capacity model (3.17) provided an excellent fit for the simulated Rank 2 capacities. These are, however, "tailor-made" capacity estimates for the simulation model. The main objective of the simulation experiments was the analysis of Rank3 and Rank 4 capacities. These results were consistent with the theory presented in this report.

8.2 Unsignalized intersections

Gap acceptance is still the dominating theory in the capacity analysis of unsignalized intersections. It is also the methodology suggested for the analysis of Finnish unsignalized intersections. This section describes the methodology for three and four-leg intersections. The capacity analysis of roundabouts is discussed in the next section.

The theory of capacity and delays at unsignalized intersections have been described in Chapters 3 and 4. These chapters present the theoretical background required to manually perform operational analysis of unsignalized intersections and to understand and evaluate published methodologies and capacity analysis software. For Rank 3 and Rank 4 capacity analysis a new theoretical approach has been developed.

In Chapter 5 three analysis methods were described: HCM2000, Capcal 2 and DanKap. All of them have been implemented as computer software. Of these three HCM2000 is the most advanced. It has procedures for shared lanes, flared lanes, heavy vehicles,

pedestrians, two-stage gap acceptance, and upstream signals.

The simulation studies in Section 6.3 indicated that capacity estimates based on the shifted exponential headway distribution give good approximations of potential capacity. Figure 8.1 displays a comparison of capacity models based on shifted exponential and Tanner's headway models. The minimum headway estimate for the shifted exponential models was about one second, which has been used in the figure. It is compared with Tanner's capacity (3.24) model with 1.8 second follower headways, as in the current Swedish and Finnish models. It is evident that Tanner's model is an appropriate model. With realistic parameters (estimated from the shifted exponential model based on simulation results) Tanner's model does not overestimate the simulated capacity as much as the negative exponential model (see Fig. 6.8).

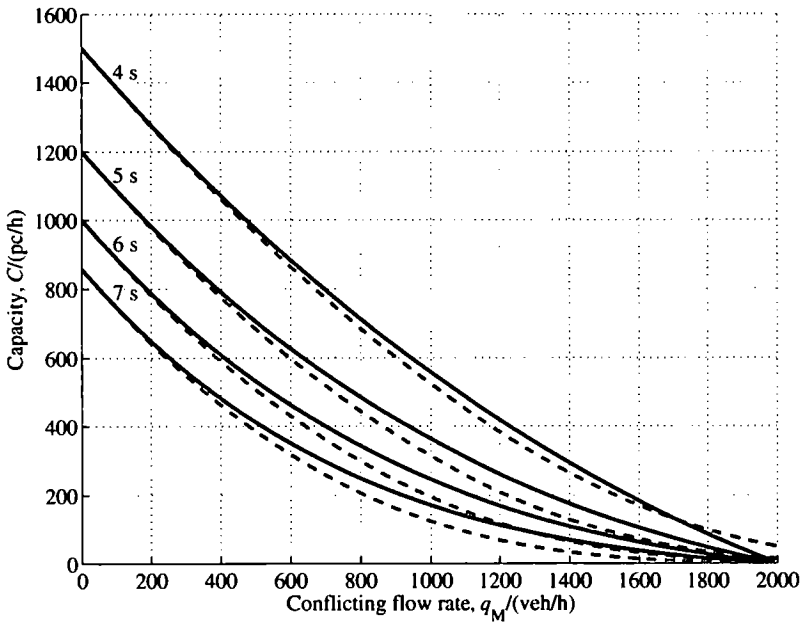

Figure 8.1: Potential capacity for priority-stream headways following Tanner's distribution (solid blue) and the shifted exponential distribution (dashed red). Minimum headways are 1.8 s for the Tanner model and 1 s for the shifted exponential model.

The simulation studies indicated that the new theoretical model for Rank 3 and Rank 4 headways gives good approximations of simulated capacities. The assumption of a 1.8 s minimum discharge headway (Tanner's model) in Rank 1 streams gives slightly better capacity estimates than the negative exponential model. For Rank 4 capacity the conventional (HCM2000) estimates may be slightly better than the theoretical model.

The new theoretical model with a 1.8 second discharge headway for Rank 1 streams is suggested for the analysis of Finnish unsignalized. Compared with the methods in HCM2000 and Capcal 2 the new method has several advantages:

1. Potential capacity estimates are in better agreement with simulation results than the estimates of HCM2000. For Rank 2 capacity analysis the method is the same as in Capcal 2.

2. Rank 3 capacity estimates are in better agreement with the simulation results than the estimates of HCM2000 and Capcal 2.

3. The Rank 4 capacity estimates of Capcal 2 are too low. The new estimates are similar to the HCM2000 estimates. Compared wit simulated capacities HCM2000 estimates are slightly too low, while the new estimates are slightly too high.

4. The new method has a more solid theoretical foundation, and it is not—at least not to the same extent as the HCM2000 method—based on cancellation of errors.

Consequently, it is suggested that the capacity of Finnish unsignalized intersections is estimated following equation (3.113), where the follower headway of Rank 1 streams is 1.8 seconds. The method is described in more detail in Chapter 3. Priority streams are those streams or substreams having an actual conflict with the minor stream, as discussed in Section 2.2. The critical gaps in Table 5.17 are used as base values. However, better results can always be obtained with field-measured values.

The effects of heavy vehicles were not analyzed in this research. For signalized intersections the adjustment factors of Capcal 2 (SNRA 1995*a*) were suggested (Luttinen & Nevala 2002). The same adjustment factors are suggested for unsignalized intersections.

Control delays can be estimated using the coordinate-transformation method with equations 4.131 and 4.132, as described in Chapter 4. Acceleration delay is five seconds for stop-controlled streams. For yield-controlled streams the simple estimate in equation 6.13 can be applied.

8.3 Roundabouts

The capacity of a roundabout entry can be estimated using the method (3.58) of Hagring (1998*b*), but assuming a shifted exponential headway distribution ($\phi = 1$) in the major flow. The capacity equation for entry lane k is

$$C_k = \frac{3600\Gamma e^{-\sum_{i=1}^{n}\gamma_i(t_{c,i}-t_p)}}{1-e^{-\sum_{i=1}^{n}t_f\gamma_i}}\prod_{i=1}^{n}\frac{q_i}{3600\gamma_i}, \tag{8.1}$$

where n is the number of circulating lanes (1 or 2), t_f is the follow-up time in entry lane k, $t_{c,i}$ is the critical gap in circulating lane i for the vehicle in entry lane k, t_p is the minimum (platoon) headway in a circulating lane, and $\Gamma = \sum_{i=1}^{n}\gamma_i$. The scale parameters are estimated as

$$\gamma_i = \frac{q_i}{3600 - q_i t_p}. \tag{8.2}$$

For a one-lane roundabout the equation simplifies to

$$C_k = \frac{qe^{-\gamma(t_c-t_p)}}{1-e^{-\gamma t_f}}, \tag{8.3}$$

the potential capacity (3.17) with major-stream headways following the shifted exponential distribution.

The exiting flows are assumed to have no effect of capacity. However, if local conditions indicate such an effect, the major flow in the outer circulating lane can be expressed as

$$q_1 = p_e q_e + q_{c,1}, \tag{8.4}$$

where $q_{c,1}$ is the actual circulating flow, q_e is the exiting flow rate, and p_e is the proportion of exiting flow included in the major flow. As a default $p_e = 0$.

Base values for critical gaps and follow-up times can be obtained from Table 7.2 on page 181. For one-lane roundabouts the follow-up time t_f and the minimum headway t_p can be estimated as functions of the central island diameter (d):

$$t_f = 2.5 - 0.0067(d - 8), \quad 8 \leq d \leq 40 \tag{8.5}$$

$$t_p = 2.0 - 0.0067(d - 8), \quad 8 \leq d \leq 40. \tag{8.6}$$

Figure 8.2 displays capacity estimates for one-lane roundabouts. At low circulating flow rates the capacity estimates are slightly higher than in the current guidelines (Fig. 5.5). When circulating flows are high, the new capacity estimates are lower than the current estimates. Better accuracy can be obtained, if the parameters are estimated using field data.

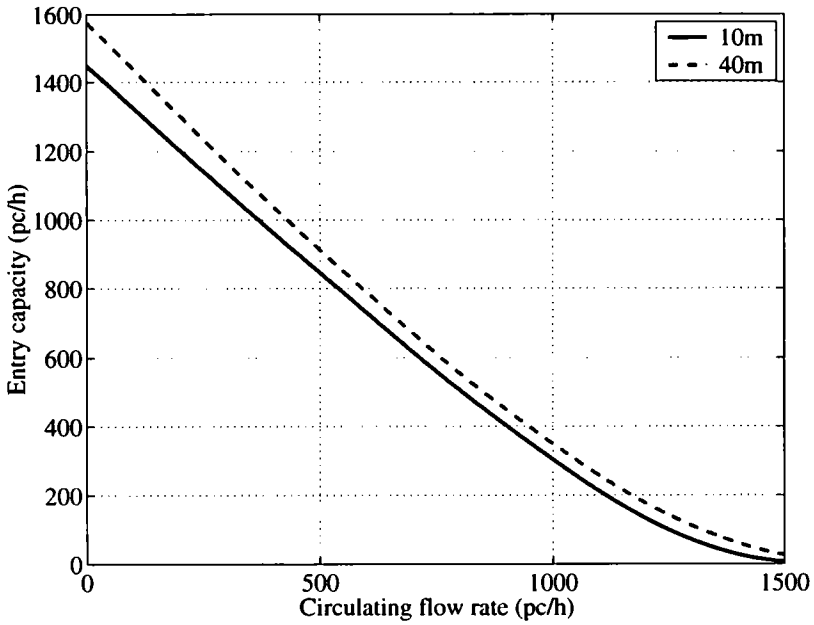

Figure 8.2: Capacity of Finnish one-lane roundabouts with central island diameters 10 m and 40 m

There was not enough field data to calibrate the HUTSIM simulation model for two-lane roundabouts. The methodology suggested is based on earlier simulation studies (Hagring 1997, Pursula et al. 1997), Swedish research (Hagring 1998*b*, Hagring et al. 2003) as well as on generalizations of the results for one-lane roundabouts.

At two-lane roundabouts the vehicles circulating in the inner lane are included in the major flow of the right entry lane. If the distribution of traffic between outer and inner lanes is not known, it can be approximated following the results of Hagring et al. (2003). As a default it is assumed that the outer lane is used by 55 % of left-turn vehicles, 95 % of through vehicles, and 100 % of right-turn vehicles. Lane changes from the inner lane to the outer lane are assumed to take place in the weaving area preceding the exit, so that they can be ignored in the capacity analysis. Especially under high degrees of saturation the realism of the lane allocation should be checked.

Figure 8.3 displays capacity estimates for a two-lane roundabout when 50 % or 90 % of circulating traffic is in the outer lane. The entry capacity is expressed as the sum of the capacities of both entry lanes. In practice, capacity should be calculated separately for

both entry lanes. In most cases the demand on the left entry lane is much lower than on the right lane. New research results in Germany indicate that the increase in entry capacity due to a second entry lane is only about about 14 percent.[1]

Figure 8.4 displays capacity, when both circulating and entering traffic have the same lane distribution. If the capacity of lane 1 is C_1, the capacity of lane 2 is C_2, the proportion of traffic on the lane 1 is p, the entry capacity in Figure 8.3 is calculated as $C = C_1 + C_2$ and in Figure 8.4 as $C = \min\left\{p^{-1}C_1, (1-p)^{-1}C_2\right\}$. When arrival rate is higher than C, demand exceeds capacity in one or both entry lanes. The increase in capacity due to an additional entry lane is highest when the lane distribution is even.

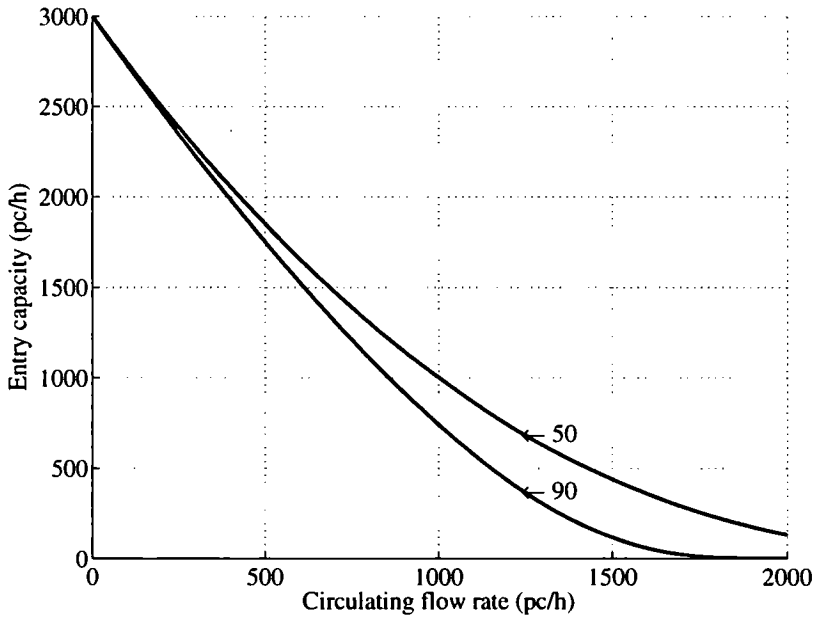

Figure 8.3: Capacity of Finnish two-lane roundabouts with 50 % and 90 % of circulating traffic in the outer lane

A change in the traffic flows at a subject entry may have an effect on the operation of other entries, which again may affect the traffic conditions at the subject entry. This is important especially if the increase of traffic at the subject entry causes oversaturation at another entry, in which case circulating traffic at the subject entry may decrease.

The method presented here addresses only the capacity of entering flow. No data is available on the capacity at exits and weaving sections. The German exit capacity estimate of 1,200 veh/h can be used as a rule of thumb. The effect of crossing pedestrians at entries and exits can be estimated by the procedure presented in Section 3.8. Traffic operation at weaving sections can be analyzed using simulation models.

When the capacity of a roundabout has been calculated, other performance measures can be estimated following the the same procedures as for other unsignalized intersections.

[1] Thorsten Miltner at the German–Dutch–Finnish Seminar on Traffic Engineering at 8–9 June 2004 in Delft. In HBS 2001 (FGSV 2001) adding a second entry lane doubles the capacity.

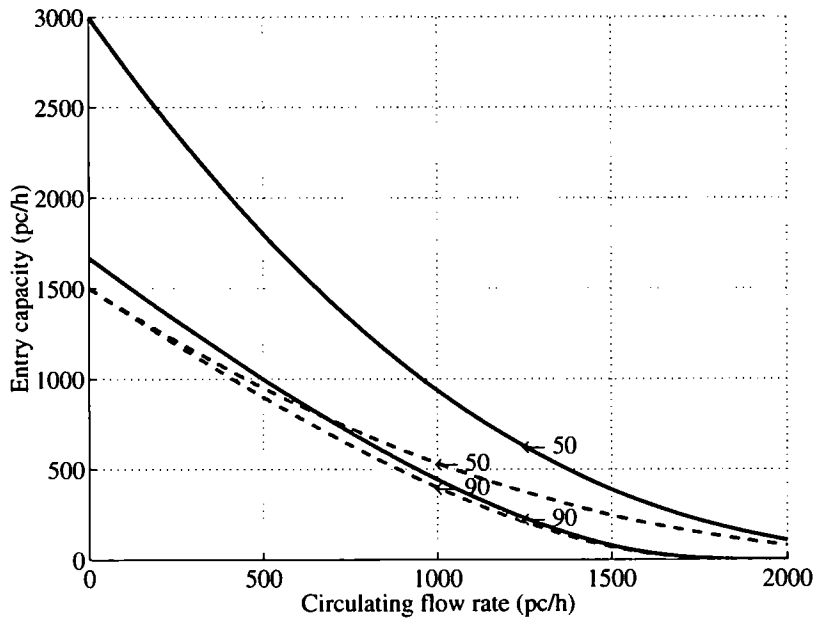

Figure 8.4: Capacity of Finnish two-lane roundabouts with 50 % and 90 % of circulating and entering traffic in the outer lane (solid curves) and with a one-lane entry (dashed curves)

8.4 Level of service

Current level-of-service criteria in Finland (Table 5.14) follow the 1985 HCM (Transportation Research Board 1985). Reserve capacity is used as a service measure. In HCM2000 (Transportation Research Board 2000) and in the German HBS 2001 (FGSV 2001) level of service is based on control delay (Table 5.1). Because delay is a measure experienced directly by road users it should be preferred as a service measure over the more engineering-oriented reserve capacity.

Table 8.1 displays the current thresholds for reserve capacity with a respective delay estimate (4.68). The new level-of-service criteria for control delay have been obtained from HCM2000. Table 8.1 shows that the delay thresholds derived from the reserve capacity and the suggested new criteria are similar. Setting LOS C threshold to 20 s would make it closer to current criterion, but that would make the range of traffic conditions described by LOS C very limited. The German manual (HBS 2001) has an even higher (30 s) threshold. Thus, the control delays in column "New criteria" of Table 8.1 are suggested as the new level-of-service criteria in Finland.

8.5 Further research

This research was started assuming that only a short theoretical description and a few field measurements to adjust current estimates of critical gaps and follow-up times and to calibrate the parameters of HUTSIM were required to make a suggestion for new analysis procedures. It appeared, as it often does, that reality was more complicated. The research revealed some answers, but raised even more questions. Some of these questions are described here as items for further research.

Field studies were used to calibrate HUTSIM parameters. The estimation of critical gaps and follow-up times, however, requires more field studies at highly saturated conditions.

Table 8.1: Current and new level-of-service criteria with approximate delays at reserve-capacity thresholds

LOS	Current criteria		New criteria
	Reserve capacity (veh/h)	Delay (s)	Delay (s)
A	≥ 400	≤ 9	≤ 10
B	≥ 300	≤ 12	≤ 15
C	≥ 200	≤ 18	≤ 25
D	≥ 100	≤ 36	≤ 35
E	≥ 0	> 36	≤ 50
F	$\rho > 1$	$\rho > 1$	> 50

Besides adjusting the base values the studies should consider

1. The correlation of critical gaps and follow-up times
2. Possible flow dependency of critical gaps and follow-up times
3. The effects of intersection and roundabout geometry.

The maximum likelihood method can be suggested as the statistical estimation method. Field studies are also required to further calibrate and validate the Rank 3 and Rank 4 capacity analysis procedures.

In order to evaluate the impedance effect of pedestrians, a description of pedestrian-vehicle interactions and pedestrian flow dynamics at intersections is needed. This requires new field studies.

At two-lane roundabouts field studies are required to estimate the lane allocation. This information is needed in the capacity analysis.

The movement capacity equations for Rank 3 and Rank 4 steams were presented assuming Poisson arrivals. Extension of these models to Cowan's M3 distribution would give additional flexibility and realism.

The simulation experiments revealed some problems in the simulation software. The most important problem is the lack of anticipation of vehicle acceleration and deceleration in the gap acceptance process. Other, mostly minor, details have been reported to the software developer.

REFERENCES

AAGAARD, P. 1998. Danish capacity models. In *NORDKAP—NORDiskt KAPacitetssamarbete* [NORDKAP—Nordic capacity cooperation] (University of Lund 1998). Sammandrag av seminarium på Grand Hotel i Lund, Sverige 2–3 juni 1997.

AAGAARD, P. E. 1995. Recent research into capacity in Danish roundabouts. Paper No. 950080, Transportation Research Board 74th Annual Meeting Preprint.

AAKRE, A. 1998. Norwegian methods for calculation of capacity and level of service at intersections. In *NORDKAP—NORDiskt KAPacitetssamarbete* [NORDKAP—Nordic capacity cooperation] (University of Lund 1998). Sammandrag av seminarium på Grand Hotel i Lund, Sverige 2–3 juni 1997.

ADAMS, W. F. 1936. Road traffic considered as a random series. *Journal of the Institution of Civil Engineers*, vol. 4, no. 1, p. 121–130.

AKÇELIK, R. 1994*a*. Gap-acceptance modelling by traffic signal analogy. *Traffic Engineering and Control*, vol. 35, no. 9, p. 498–506.

AKÇELIK, R. 1997. Analysis of roundabout performance by modeling approach-flow interactions. In Kyte (1997). P. 15–25.

AKÇELIK, R. 1998. *Roundabouts: Capacity and Performance Analysis.* (Research Report ARR–321). Vermont South, Victoria: ARRB Transport Research.

AKÇELIK, R. & CHUNG, E. 1994. Calibration of the bunched exponential distribution of arrival headways. *Road & Transport Research*, vol. 3, no. 1, p. 42–59.

AKÇELIK, R. (ed.) 1994*b*. *Second International Symposium on Highway Capacity.* Australian Road Research Board, Transportation Research Board, Sydney.

AKÇELIK, R. & TROUTBECK, R. 1991. Implementation of the Australian roundabout analysis method in SIDRA. In Brannolte (1991), p. 17–34.

ALLAN, R. R. 1968. On the highway crossing problem. In *ARRB Proceedings*, Vol. 4. Victoria: Australian Road Research Board. P. 529–548.

ANVEDEN, J. 1988. Swedish research on unsignalized intersections. In Brilon (1988*b*), p. 80–102.

ARMITAGE, D. J. & MCDONALD, M. 1974. Roundabout capacity. *Traffic Engineering and Control*, vol. 15, no. 10, p. 812–815.

ASHWORTH, R. 1969. The capacity of priority-type intersections with a non-uniform distribution of critical acceptance gaps. *Transportation Research*, vol. 3, p. 273–278.

ASHWORTH, R. & FIELD, J. C. 1973. The capacity of rotary intersections. *Journal of the Institution of Highway Engineers*, vol. 20, no. 3, p. 14–21.

ASHWORTH, R. & LAURENCE, C. J. D. 1978. A new procedure for capacity calculation at conventional roundabouts. *Proceedings of the Institution of Civil Engineers*, Part 2, vol. 65, p. 1–16.

AUSTROADS 1988. *Intersections at Grade.* (Guide to Traffic Engineering Practice—Part 5). Sydney.

AUSTROADS 1993. *Roundabouts.* (Guide to Traffic Engineering Practice—Part 6). Sydney.

BAASS, K. G. 1987. The potential capacity of unsignalized intersections. *ITE Journal*, vol. 57, no. 10, p. 43–46.

BECKMANN, M., MCGUIRE, C. B. & WINSTEN, C. B. 1956. *Studies in the Economics of Transportation.* New Haven: Yale University Press.

BERGH, T. 1991. Intersections without traffic signals—Swedish experience on capacity and traffic safety. In Brilon (1991), p. 192–213.

BLACKMORE, F. C. 1963. Priority at roundabouts. *Traffic Engineering and Control*, vol. 4, no. 6, p. 104–106.

BLACKMORE, F. C. 1970. *Capacity of single-level intersections.* (RRL Report LR 356). Crowthorne: Road Research Laboratory.

BONNESON, J. A. & FITTS, J. W. 1997. Delay to major-street through vehicles at two-way stop-controlled intersections. In Kyte (1997), p. 45–54.

BONNESON, J. A. & FITTS, J. W. 1999. Delay to major street through vehicles at two-way stop-controlled intersections. *Transportation Research*, vol. 33A, no. 3/4, p. 237–253.

BRANNOLTE, U. (ed.) 1991. *Highway Capacity and Level of Service.* Rotterdam: Balkema.

BRANSTON, D. 1976. Models of single lane time headway distributions. *Transportation Science*, vol. 10, no. 2, p. 125–148.

BRATLEY, P., FOX, B. L. & SCHRAGE, L. E. 1987. *A Guide to Simulation.* Second ed. New York: Springer Verlag.

BREIMAN, L. 1963. The Poisson tendency in traffic distribution. *The Annals of Mathematical Statistics*, vol. 32, p. 308–311.

BRENNAN, M. J. & FITZGERALD, M. P. 1979. A new look at Tanner's formula for the capacity of a minor road at an uncontrolled intersection. *Traffic Engineering and Control*, vol. 20, no. 4, p. 220.

BRIGGS, T. 1977. Time headways on crossing the stop-line after queueing at traffic lights. *Traffic Engineering and Control*, vol. 18, no. 5, p. 264–265.

BRILON, W. 1988*a*. Recent developments in calculation methods for unsignalized intersections in West Germany. In *Intersections without Traffic Signals* (Brilon 1988*b*), p. 111–153.

BRILON, W. (ed.) 1988*b*. *Intersections without Traffic Signals.* Berlin: Springer Verlag.

BRILON, W. (ed.) 1991. *Intersections without Traffic Signals II.* Berlin: Springer Verlag.

BRILON, W. (ed.) 2000. *Fourth International Symposium on Highway Capacity Proceedings.* (Transportation Research Circular E-C018). Washington, D.C.: Transportation Research Board.

BRILON, W. & GROSSMANN, M. 1991. The new German guideline for capacity of unsignalized intersections. In Brannolte (1991), p. 63–73.

BRILON, W., GROSSMANN, M. & BLANKE, H. 1994. *Verfahren für die Berechnung der Leistungsfähigkeit und Qualität des Verkehrsablaufes auf Straßen* [Calculation methods for capacity and quality of traffic flow on roads]. (Forschung Straßenbau und Straßenverkehrstechnik 669). Bonn: Bundesministerium für Verkehr.

BRILON, W., KOENIG, R. & TROUTBECK, R. J. 1997. Useful estimation procedures for critical gaps. In Kyte (1997), p. 71–87.

BRILON, W. & MILTNER, T. 2002. *Verkehrsqualität unterschiedlicher Verkehrsteilnehmerarten an Knotenpunkten ohne Lichtsignalanlage* [Quality of traffic for different modes of travel at unsignalized intersections]. (Slussbericht). Bochum: Ruhr-Universität Bochum, Lehrstuhl für Verkehrswesen. Forschungsauftrag FE-Nr.: 77.434/1999/ des Bundesministeriums für Verkehr, Bau- und Wohnungswesen.

BRILON, W. & STUWE, B. 1993. Capacity and design of traffic circles in Germany. In *Traffic Flow and Highway Capacity.* (Transportation Research Record 1398). Washington, D.C.: Transportation Research Board. P. 61–67.

BRILON, W. & WU, N. 1999. Capacity at unsignalized two-stage priority intersection. *Transportation Research*, vol. 33A, no. 3/4, p. 275–289.

BRILON, W. & WU, N. 2001. Capacity at unsignalized intersections derived by conflict technique. In *Traffic Flow and Highway Capacity 2001.* (Transportation Research Record 1776). Washington, D.C.: Transportation Research Board. P. 82–90.

BRILON, W. & WU, N. 2002. Unsignalized intersections—a third method for analysis. In Taylor (2002), p. 157–178.

BRILON, W., WU, N. & BONDZIO, L. 1997. Unsignalized intersections in Germany—a state of the art 1997. In Kyte (1997), p. 61–70.

BRILON, W., WU, N. & LEMKE, K. 1996. Capacity at unsignalized two-stage priority intersection. In *Highway Capacity Analysis for Interrupted and Uninterrupted Flow Facilities.* (Transportation Research Record 1555). Washington, D.C.: Transportation Research Board. P. 74–82.

BROWN, M. 1995. *The Design of Roundabouts.* London: HMSO.

BUCKLEY, D. J. 1962. Road traffic headway distributions. In *Proceedings*, Vol. 1, part 1. Victoria: Australian Road Research Board. P. 153–187.

BUCKLEY, D. J. 1968. A semi-Poisson model of traffic flow. *Transportation Science*, vol. 2, no. 2, p. 107–133.

BUNKER, J. & TROUTBECK, R. 1994*a*. *The Theory of Limited Priority Merging.* (Research Report 94-4). Brisbane: Physical Infrastructure Centre, Queensland University of Technology.

BUNKER, J. & TROUTBECK, R. J. 1994*b*. *Analysis of Limited Priority Theoretical Equations.* (Research Report 94-07). Brisbane: Physical Infrastructure Centre, Queensland University of Technology.

BUREAU OF PUBLIC ROADS 1950. *Highway Capacity Manual.* Washington, D.C.: U.S. Department of Commerce.

CATCHPOLE, E. A. & PLANK, A. W. 1986. The capacity of a priority intersection. *Transportation Research*, vol. 20B, no. 6, p. 441–456.

CATLING, I. 1977. A time-dependent approach to junction delays. *Traffic Engineering and Control*, vol. 18, no. 11, p. 520–523, 526.

ÇINLAR, E. 1972. Superposition of stochastic processes. In P. A. W. LEWIS (ed.), *Stochastic Point Processes: Statistical Analysis, Theory, and Applications.* New York: Wiley-Interscience. P. 549–606.

CLAYTON, A. J. H. 1941. Road traffic calculations. *Journal of the Institution of Civil Engineers*, vol. 16, no. 7, p. 247–284. With discussion and correspondence in no. 8, pp. 588–594.

CLAYTON, A. J. H. 1945. The capacity of roundabouts at road intersections. *Journal of the Institution of Civil Engineers*, vol. 23, no. 3, p. 149–154.

CLAYTON, A. J. H. 1955. Working capacity of roads. *Proceedings of the Institution of Civil Engineers*, Part 2, vol. 4, no. 3, p. 652–696. With discussion.

COHEN, J., DEARNALEY, E. J. & HANSEL, C. E. M. 1955. The risk taken in crossing a road. *Operations Research Quarterly*, vol. 6, p. 120–128.

COOPER, R. B. 1981. *Introduction to Queueing Theory.* Second ed. London: Edward Arnold (Publishers) Limited.

COWAN, R. 1987. An extension of Tanner's result on uncontrolled intersections. *Queueing Systems*, vol. 1, p. 249–263.

COWAN, R. J. 1975. Useful headway models. *Transportation Research*, vol. 9, no. 6, p. 371–375.

COWAN, R. J. 1984. Adams' formula revised. *Traffic Engineering and Control*, vol. 25, no. 5, p. 272–274.

COX, D. R. & ISHAM, V. 1980. *Point Processes.* London: Chapman and Hall Ltd.

COX, D. R. & MILLER, H. D. 1965. *The Theory of Stochastic Processes.* London: Chapman and Hall.

COX, D. R. & SMITH, W. L. 1954. On the superposition of renewal processes. *Biometrika*, vol. 41, p. 91–99.

CROWDER, M. J., KIMBER, A. C., SMITH, R. L. & SWEETING, T. J. 1991. *Statistical Analysis of Reliability Data*. London: Chapman and Hall Ltd.

DAGANZO, C. F. 1977. Traffic delay at unsignalized intersections: Clarification of some issues. *Transportation Science*, vol. 11, no. 2, p. 180–189.

DAGANZO, C. F. 1997. *Fundamentals of Transportation and Traffic Operations*. Oxford: Pergamon.

DARZENTAS, J. 1981. Gap acceptance: Myth and reality. In V. F. HURDLE, E. HAUER & G. N. STEUART (ed.), *Proceedings of the Eighth International Symposium on Transportation and Traffic Theory*. Toronto: University of Toronto Press. P. 175–192.

DAWSON, R. F. & CHIMINI, L. A. 1968. The hyperlang probability distribution—A generalized traffic headway model. In *Characteristics of Traffic Flow*. (Highway Research Record 230). Washington, D.C.: Highway Research Board. P. 1–14.

DE SMIT, J. H. A. 1971. The transient behaviour of the queue at a fixed cycle traffic light. *Transportation Research*, vol. 5, no. 1, p. 1–14.

DREW, D. R. 1967. Gap acceptance characteristics for ramp-freeway surveillance and control. In *Freeway Traffic Characteristics and Control*. (Highway Research Record 157). Washington, D.C.: Highway Research Board. P. 108–143. With discussion.

DREW, D. R. 1968. *Traffic Flow Theory and Control*. New York: McGraw-Hill.

DUFF, J. T. 1968. Traffic management. In E. DAVIES (ed.), *Traffic Engineering Practice*. Second ed. London: E. & F. N. Spon Ltd. Chapter 5, p. 102–128.

DUNNE, M. C. & BUCKLEY, D. J. 1972. Delays and capacities at unsignalized intersections. In *ARRB Proceedings*, Vol. 6. Victoria: Australian Road Research Board. P. 345–362.

EDWARDS, A. W. F. 1974. The history of likelihood. *International Statistical Review*, vol. 42, p. 9–15.

EDWARDS, A. W. F. 1992. *Likelihood*. Expanded ed. Baltimore: The Johns Hopkins University Press.

ERLANG, A. K. 1909. Sandsynlighedsregning og telefonsamtaler [The theory of probabilities and telephone conversations]. *Nyt Tidskrift Matematik B*, vol. 20, p. 33–39.

ERLANG, A. K. 1917*a*. Løsning af nogle problemer fra sandsynlighedsregningen af betydning for de automatiske telefoncentraler [Solution of some problems in the theory of probabilities of significance in automatic telephone exchanges]. *Elektroteknikeren*, vol. 13, no. 1, p. 5–13. Also in English (Erlang 1917*b*).

ERLANG, A. K. 1917*b*. Solution of some problems in the theory of probabilities of significance in automatic telephone exchanges. *The Post Office Electrical Engineers' Journal*, vol. 10, p. 189–197.

EVANS, D. H., HERMAN, R. & WEISS, G. H. 1964. The highway merging and queuing problem. *Operations Research*, vol. 12, no. 6, p. 832–857.

FELLER, W. 1957. *An Introduction to Probability Theory and Its Applications*. Vol. 1. Second ed. New York: John Wiley & Sons.

FELLER, W. 1966. *An Introduction to Probability Theory and Its Applications*. Vol. 2. New York: John Wiley & Sons.

FGS 1972. *Berechnung der Leistungsfähigkeit von Knotenpunkten ohne Lichtsignalanlagen* [Capacity calculation for unsignalized intersections]. Köln: Forschungsgesellschaft für das Straßenwesen.

FGSV 2001. *Handbuch für die Bemessung von Straßenverkehrsanlagen* [Handbook for assessing road traffic facilities]. Köln: Forschungsgesellschaft für Straßen- und Verkehrswesen. HBS 2001.

FISHER, R. B. 1960. A preliminary study of acceptance distributions for merging traffic. M. Tech. Thesis. Sydney: School of Traffic Engineering, University of N.S.W.

FISK, C. S. 1989. Priority intersection capacity: A generalization of Tanner's formula. *Transportation Research*, vol. 23B, no. 4, p. 281–286.

FISK, C. S. & TAN, H. H. 1989. Delay analysis for priority intersections. *Transportation Research*, vol. 23B, no. 6, p. 453–469.

GANI, J. 1969. Recent advances in storage and flooding theory. *Advances in Applied Probability*, vol. 1, p. 90–110.

GARTNER, N. H. & MESSER, C. J. (ed.) 1997. *Monograph on Traffic Flow Theory*. Federal Highway Administration, http://www.tfhrc.gov/its/tft/tft.htm, 08/03/2001.

GARWOOD, F. 1940. An application of the theory of probability to the operation of vehicular-controlled traffic signals. *Journal of the Royal Statistical Society*, vol. 7, no. 1, p. 65–77.

GAZIS, D. C., NEWELL, G. F., WARREN, P. & WEISS, G. H. 1967. The delay problem for crossing an *n* lane highway. In L. C. EDIE, R. HERMAN & R. ROTHERY (ed.), *Vehicular Traffic Science*. (Proceedings of the Third International Symposium on the Theory of Traffic Flow, New York, June 1965). New York: Elsevier. P. 267–279.

GAZIS, D. C. & POTTS, R. B. 1965. The over-saturated intersection. In J. ALMOND (ed.), *Proceedings of The Second International Symposium on The Theory of Road Traffic Flow*. Paris: The Organisation for Economic Co-operation and Development. P. 221–237.

GIPPS, P. G. 1982. Some modified gap acceptance formulae. In *Traffic Engineering*. (Proceedings, Vol. 11, Part 4). Melbourne: Australian Road Research Board. P. 71–75.

GLYNN, P. W. 1990. Diffusion approximations. In D. P. HEYMAN & M. J. SOBEL (ed.), *Stochastic Models*. Vol. 2 of *Handbooks in Operations Research and Management Science*. Amsterdam: North Holland. Chapter 4, p. 145–198.

GNEDENKO, B. V. 1962. *The Theory of Probability*. New York: Chelsea Publishing Company. Translated from the Russian by B. D. Seckler.

GNEDENKO, B. V. 1967. *The Theory of Probability*. Fourth ed. New York: Chelsea Publishing Company. Translated from the Russian by B. D. Seckler.

GOODMAN, R. 1988. *Introduction to Stochastic Models*. Menlo Park, Ca.: The Benjamin/Cummings Publishing Company, Inc.

GRABE, W. 1954. *Leistungsermittlung von nicht lichtsignalsteuerten Knotenpunkten des Straßenverkehrs* [Capacity calculation of unsignalized intersections in road traffic]. (Forschungsarbeiten aus dem Strassenwesen, Neue Folge 11). Bielefeld: Kirschbaum Verlag.

GREENSHIELDS, B. D., SHAPIRO, D. & ERICKSEN, E. L. 1947. *Traffic Performance at Urban Street Intersections*. (Technical Report 1). New Haven, Connecticut: Yale Bureau of Highway Traffic.

GREENSHIELDS, B. D. & WEIDA, F. M. 1952. *Statistics with Applications to Highway Traffic Analyses*. Saugatuck, Connecticut: The Eno Foundation for Highway Traffic Control.

GRIMMETT, G. & WELSH, D. 1986. *Probability: An Introduction*. Oxford: Clarendon Press.

GRIMMETT, G. R. & STIRZAKER, D. R. 2001. *Probability and Random Processes*. Oxford: Oxford University Press.

GROSS, D. & HARRIS, C. M. 1974. *Fundamentals of Queueing Theory*. New York: John Wiley & Sons.

GROSS, D. & HARRIS, C. M. 1998. *Fundamentals of Queueing Theory*. Third ed. New York: John Wiley & Sons.

GROSSMANN, M. 1991. *Aktualisiertes Berechnungsverfahren für Knotenpunkte ohne Lichtsignalanlagen* [Updated calculation procedure for intersections without traffic signals]. (Strassenbau und Strassenverkehrstechnik 596). Bonn: Bundesminister für Verkehr.

GUICHET, B. 1997. Roundabouts in France: Development, safety, design, and capacity. In Kyte (1997), p. 100–105.

HAGRING, O. 1996*a*. *Roundabout Entry Capacity*. (Bulletin 135). Lund: Tekniska Högskolan i Lund, Institutionen för Trafikteknik.

HAGRING, O. 1996*b*. The use of the Cowan M3 distribution for modelling roundabout flow. *Traffic Engineering and Control*, vol. 37, no. 5, p. 328–332.

HAGRING, O. 1997. Capcal2—A new version of the SNRA capacity, delay, and VOC software. In Kyte (1997), p. 115–123.

HAGRING, O. 1998*a*. A further generalization of Tanner's formula. *Transportation Research*, vol. 32B, no. 6, p. 423–429.

HAGRING, O. 1998*b*. *Vehicle-vehicle Interactions at Roundabouts and their Implications for the Entry Capacity: A Methodological Study with Applications to Two-lane Roundabouts*. (Bulletin 159). Lund: Department of Traffic Planning and Engineering, Lund Institute of Technology.

HAGRING, O. 2000. Effect of OD flows on roundabout entry capacity. In Brilon (2000), p. 434–445.

HAGRING, O. 2001. Derivation of capacity equation for roundabout entry with mixed circulating and exiting flows. In *Traffic Flow and Highway Capacity 2001*. (Transportation Research Record 1776). Washington, D.C.: Transportation Research Board. P. 91–99.

HAGRING, O. & NIITTYMÄKI, J. 1997. A modelling of roundabout entry operations. VTIs och KFBs Forskardagar. Linköping, Sweden, January 8–9, 1997. Unpublished.

HAGRING, O., ROUPHAIL, N. M. & SØRENSEN, H. A. 2003. Comparison of capacity models for two-lane roundabouts. In *82nd Annual Meeting Compendium of Papers CD-ROM*. Transportation Research Board. Washington, D.C.

HAIGHT, F. A. 1963. *Mathematical Theories of Traffic Flow*. New York: Academic Press.

HAIGHT, F. A., BISBEE, E. F. & WOJCIK, C. 1962. Some mathematical aspects of the problem of merging. In *Theory of Traffic Flow*. (Bulletin 356). Washington, D.C.: Highway Research Board. P. 1–14.

HAIGHT, F. A. & BREUER, M. A. 1960. The Borel-Tanner distribution. *Biometrika*, vol. 47, no. 1 and 2, p. 143–150.

HAKKERT, A. S., MAHALEL, D. & ASANTE, S. A. 1991. A comparative study of roundabout capacity procedures. In Brilon (1991), p. 93–106.

HÄKLI, O. 1971. Liikenteenvälityskyky [Traffic capacity]. In *Tekniikan käsikirja 6*. Eighth ed. Jyväskylä: K.J. Gummerus Oy.

HAMMOND, H. F. & SORENSON, L. J. (ed.) 1941. *Traffic Engineering Handbook*. New York: Institute of Traffic Engineers and National Conservation Bureau.

HANSON, A. 1978. Swedish Capacity Manual: Part 2. Capacity of unsignalized intersections. In *Highway Capacity, Measures of Effectiveness, and Flow Theory*. (Transportation Research Record 667). Washington, D.C.: Transportation Research Board. P. 4–11.

HARDERS, J. 1968. *Die Leistungsfähigkeit nicht signalregelter städtischer Verkshrsknoten* [Capacity of unsignalized urban intersections]. (Strassenbau und Strassenverkehrstechnik 76). Bonn: Bundesminister für Verkehr.

HAWKES, A. G. 1966. Delay at traffic intersections. *Journal of the Royal Statistical Society*, vol. 28B, p. 202–212.

HAWKES, A. G. 1968. Gap-acceptance in road traffic. *Journal of Applied Probability*, vol. 5, p. 84–92.

HEIDEMANN, D. 1991. Queue length and waiting-time distributions at priority intersections. *Transportation Research*, vol. 25B, no. 4, p. 163–174.

HEIDEMANN, D. 2002. Mathematical analysis of non-stationary queues in traffic flow with particular consideration of the coordinate transformation technique. In Taylor (2002), p. 675–695.

HERMAN, R. & WEISS, G. 1961. Comments on the highway-crossing problem. *Operations Research*, vol. 9, no. 6, p. 828–840.

HEWITT, R. H. 1985. A comparison between some methods of measuring critical gap. *Traffic Engineering and Control*, vol. 26, no. 1, p. 13–21.

HIGHWAY RESEARCH BOARD 1965. *Highway Capacity Manual.* (Special Report 87). Washington, D.C.: National Research Council.

HOBBS, F. D. 1974. *Traffic Planning and Engineering.* Oxford: Pergamon Press.

HØYLAND, A. & RAUSAND, M. 1994. *Systems Reliability Theory: Models and Statistical Methods.* New York: John Wiley & Sons.

HURDLE, V. F. 1984. Signalized intersection delay model—A primer for the uninitiated. In *Traffic Capacity and Characteristics.* (Transportation Research Record 971). Washington, D.C.: Transportation Research Board. P. 96–105.

JAISWAL, N. K. 1968. *Priority Queues.* New York: Academic Press.

JESSEN, G.-D. 1968. Ein Richtlinienvorschlag für die Behandlung der Leistungsfähigkeit von Knotenpunkten ohne Signalreglerung [A guideline proposal for estimating capacity of unsignalized intersections]. *Straßenverkehrstechnik*, vol. 12, no. 7/8, p. 101–105.

JORMALAINEN, S. 1991. *Kiertoliittymät ja niiden välityskyky* [Roundabouts and their capacity]. (Tielaitoksen selvityksiä 23/1991). Helsinki: Tielaitos. TIEL 3200022.

KARLIN, S. & TAYLOR, H. M. 1975. *A First Course in Stochastic Processes.* Second ed. New York: Academic Press.

KARLIN, S. & TAYLOR, H. M. 1981. *A Second Course in Stochastic Processes.* Orlando: Academic Press.

KEHITTÄMISKESKUS 1991. *CAPCAL-mikroversion käyttöohje* [CAPCAL micro version user's manual]. Helsinki: Tiehallitus.

KEHITTÄMISKESKUS 1996. *Kaksikaistaiset kiertoliittymät* [Two-lane roundabouts]. (Tielaitoksen selvityksiä 47/1996). Helsinki: Tielaitos. TIEL 3200415.

KENDALL, D. G. 1951. Some problems in the theory of queues. *Journal of the Royal Statistical Society*, vol. 13, no. 2, p. 151–185. With discussion.

KENDALL, D. G. 1953. Stochastic processes occurring in the theory of queues and their analysis by the method of the imbedded Markov chain. *The Annals of Mathematical Statistics*, vol. 24, p. 338–354. With discussion.

KHINTCHINE, A. Y. 1960. *Mathematical Methods in the Theory of Queueing.* London: Charles Griffin Ltd. Translated by D. M. Andrews and M. H. Quenouille.

KIMBER, R. M. 1980. *The traffic capacity of roundabouts.* (TRRL Laboratory Report 942). Crowthorne: Transport and Road Research Laboratory.

KIMBER, R. M. 1989. Gap-acceptance and empiricism in capacity prediction. *Transportation Science*, vol. 23, no. 2, p. 100–111.

KIMBER, R. M. & COOMBE, R. D. 1980. *The traffic capacity of major/minor priority junctions.* (TRRL Supplementary Report 582). Crowthorne: Transport and Road Research Laboratory.

KIMBER, R. M. & HOLLIS, E. M. 1978. Peak-period traffic delays at road junctions and other bottlenecks. *Traffic Engineering and Control*, vol. 19, no. 10, p. 442–446.

KIMBER, R. M. & HOLLIS, E. M. 1979. *Traffic queues and delays at road junctions.* (TRRL Laboratory Report 909). Crowthorne: Transport and Road Research Laboratory.

KIMBER, R. M., MARLOW, M. & HOLLIS, E. M. 1977. Flow/delay relationships for major/minor priority junctions. *Traffic Engineering and Control*, vol. 18, no. 11, p. 516–519.

KIMBER, R. M., SUMMERSGILL, I. & BURROW, I. J. 1986. Delay processes at unsignalised junctions: The interrelation between geometric and queuing delay. *Transportation Research*, vol. 20B, no. 6, p. 457–476.

KING, G. F. & WILKINSON, M. 1976. Relationship of signal design to discharge headway, approach capacity, and delay. In *Capacity and Measurement of Effectiveness.* (Transportation Research Record 615). Washington, D.C.: Transportation Research Board. P. 37–44.

KLEIJNEN, J. P. C. 1987. *Statistical Tools for Simulation Practitioners.* New York: Marcel Dekker, Inc.

KLEINROCK, L. 1975. *Queueing Systems. Volume I: Theory.* New York: John Wiley & Sons.

KLEINROCK, L. 1976. *Queueing Systems. Volume II: Computer Applications.* New York: John Wiley & Sons.

KOIVISTO, N. 1999. Valo-ohjaamattomien tasoliittymien liikennevirta ja liikenteen simulointi [Traffic flow of unsignalized at-grade intersections and traffic simulation]. Master's thesis. Espoo: Helsinki University of Technology.

KOSHI, M. (ed.) 1990. *Transportation and Traffic Theory.* (Proceedings of the Eleventh International Symposium on Transportation and Traffic Theory, held July 18–20, 1990, in Yokohama, Japan). New York: Elsevier.

KOSONEN, I. 1996. *HUTSIM—Simulation Tool for Traffic Signal Control Planning.* (Transportation Engineering Publication 89). Otaniemi: Helsinki University of Technology.

KOSONEN, I. 1999. *HUTSIM—Urban Traffic Simulation and Control Model: Principles and Applications.* (Transportation Engineering Publication 100). Espoo: Helsinki University of Technology.

KREMSER, H. 1962. Ein zusammengesetztes Wartezeitproblem bei Poissonschen verkehrsströmen [A complex waiting-time problem under Poisson-distributed traffic flows]. *Österreichisches Ingenieur-Archiv*, vol. 16, no. 3, p. 231–252.

KREMSER, H. 1964. Wartezeiten und Warteschlangen bei Einfädelung eines Poissonprozesses in einen anderen solchen Prozeß [Delays and queues with one Poisson process merging into another one]. *Österreichisches Ingenieur-Archiv*, vol. 18, no. 3–4, p. 269–274.

KYTE, M., DIXON, M. & BASAVARAJU, P. M. 2003. Why field measurements are different than model estimates—an analysis framework for capacity and level of service analysis of unsignalized intersections. In *82nd Annual Meeting Compendium of Papers CD-ROM.* Transportation Research Board. Washington, D.C.

KYTE, M. (ed.) 1997. *Proceedings of the Third International Symposium on Intersections Without Traffic Signals.* Transportation Research Board, Federal Highway Association, National Center for Advanced Transportation Technology, University of Idaho, Transportation Northwest, University of Washington, Portland, Oregon U.S.A.

KYTE, M., TIAN, Z., MIR, Z., HAMEEDMANSOOR, Z., KITTELSON, W., VANDEHEY, M., ROBINSON, B., BRILON, W., BONDZIO, L., WU, N. & TROUTBECK, R. 1996. *Capacity and Level of Service at Unsignalized Intersections: Two-Way Stop-Controlled Intersections.* (NCHRP Web Document 5). Washington, D.C.: Transportation Research Board. Project 3-46, Contractor's Final Report, Vol. 1.

KYTE, M., ZEGEER, J. & LALL, K. B. 1991. Empirical models for estimating capacity and delay at stop-controlled intersections in the United States. In Brilon (1991), p. 335–361.

LAPIERRE, R. & STEIERWALD, G. (ed.) 1987. *Verkehsleittechnik für den Straßenverkehr* [Traffic control engineering for road traffic]. Vol. 1. Berlin: Springer-Verlag.

LERTWORAWANICH, P. & ELEFTERIADOU, L. 2003. Determination of storage lengths of left-turn lanes at unsignalized intersections using M/G2/1 queuing. In *82nd Annual Meeting Compendium of Papers CD-ROM*. Transportation Research Board. Washington, D.C.

LEUTZBACH, W. & KÖHLER, U. 1974. Definitions and relationships for three different time intervals for delayed vehicles. In D. J. BUCKLEY (ed.), *Transportation and Traffic Theory*. (Proceedings of the Sixth International Symposium on Transportation and Traffic Theory. University of New South Wales, Sydney, Australia, 26–28 August 1974). New York: Elsevier. P. 87–103.

LIIMATAINEN, A. 1997. Kiertoliittymät Suomessa [Roundabouts in Finland]. In *Tie- ja liikennetekniikan teemapäivät 26.-27.11.1997*. Tielaitos, tie- ja liikennetekniikka. Helsinki. Unpublished.

LITTLE, J. D. C. 1961. A proof of the queuing formula $L = \lambda W$. *Operations Research*, vol. 9, no. 3, p. 383–387.

LI, W., WANG, W. & JIANG, D. 2003. Unsignalized intersection capacity with mixed vehicle flows. In *82nd Annual Meeting Compendium of Papers CD-ROM*. Transportation Research Board. Washington, D.C.

LOUAH, G. 1986. *La capacite des carrefours sans feux: Méthodes et modelès* [Capacity of unsignalized intersections: Methods and models]. Bagneux Cedex: Service de d'Etudes Techniques des Routes et Autoroutes.

LOUAH, G. 1988. Recent French studies on capacity and waiting times at rural unsignalized intersections. In Brilon (1988*b*), p. 248–262.

LUTTINEN, R. T. 1990. *Johdatus aikavälijakaumien teoriaan* [Introduction to the theory of headway distributions]. (Julkaisu 71). Otaniemi: Teknillinen korkeakoulu, Liikennetekniikka.

LUTTINEN, R. T. 1991. Testing goodness of fit for 3-parameter gamma distribution. In *Proceedings of the Fourth IMSL User Group Europe Conference*. IMSL and CRPE-CNET/CNRS. Paris. P. B10/1–13.

LUTTINEN, R. T. 1994. Identification and estimation of headway distributions. In Akçelik (1994*b*), p. 427–446.

LUTTINEN, R. T. 1996. *Statistical Analysis of Vehicle Time Headways*. (Transportation Engineering Publication 87). Otaniemi: Helsinki University of Technology.

LUTTINEN, R. T. 1998. *Laajennetun T-liittymän välityskyky* [Capacity at a two-stage T-intersection]. (Tielaitoksen sisäisiä julkaisuja 2/1998). Helsinki: Tielaitos.

LUTTINEN, R. T. 1999. Properties of Cowan's M3 headway distribution. In *Highway Capacity, Quality of Service, and Traffic Flow and Characteristics*. (Transportation Research Record 1678). Washington, D.C.: Transportation Research Board. P. 189–196.

LUTTINEN, R. T. 2001. *Capacity and Level of Service on Finnish Two-Lane Highways*. (Finnra Reports 18/2001). Helsinki: Finnish Road Administration.

LUTTINEN, R. T. 2003. *Capacity at Unsignalized Intersections*. (TL Research Report 3). Lahti: TL Consulting Engineers, Ltd.

LUTTINEN, R. T. 2004*a*. Capacity of unsignalized intersections under random arrivals. Paper presented at German-Dutch-Finnish Seminar on Traffic Engineering, Delft, June 8- 9, 2004.

LUTTINEN, R. T. 2004*b*. Movement capacity at two-way stop-controlled intersections. In *83rd Annual Meeting Compendium of Papers CD-ROM*. Transportation Research Board. Washington, D.C.

LUTTINEN, R. T. & NEVALA, R. 2002. *Capacity and Level of Service of Finnish Signalized Intersections.* (Finnra Reports 25/2002). Helsinki: Finnish Road Administration.

LYLY, S. (ed.) 1988. *Liikenne ja väylät* [Transportation Planning and Facilities]. (In two volumes: RIL 165-I and RIL 165-II). Helsinki: Suomen Rakennusinsinöörien Liitto.

MADANAT, S. M., CASSIDY, M. J. & WANG, M.-H. 1994. Probabilistic delay model at stop-controlled intersection. *Journal of Transportation Engineering*, vol. 120, no. 1, p. 21–36.

MAJOR, N. G. & BUCKLEY, D. J. 1962. Entry to a traffic stream. In *ARRB Proceedings*, Vol. 1. Victoria: Australian Road Research Board.

MATLOFF, N. S. 1988. *Probability Modeling and Computer Simulation.* Boston: PWS-KENT Publishing Company.

MAY, A. D. & KELLER, H. E. M. 1967. A deterministic queueing model. *Transportation Research*, vol. 1, no. 2, p. 117–128.

MAYNE, A. J. 1954. Some further results in the theory of pedestrians and road traffic. *Biometrika*, vol. 41, p. 375–389.

MCDONALD, M. & ARMITAGE, D. J. 1978. The capacity of roundabouts. *Traffic Engineering and Control*, vol. 19, no. 10, p. 447–450.

MCDONALD, M., HOUNSELL, N. B. & KIMBER, R. M. 1984. *Deometric delay at non-signalised intersections.* (TRRL Supplementary Report 810). Crowthorne: Transport and Road Research Laboratory.

MCLEAN, J. R. 1989. *Two-Lane Highway Traffic Operations: Theory and Practice.* New York: Gordon and Breach Science Publishers.

MCNEIL, D. R. & WEISS, G. H. 1974. Delay problems for isolated intersections. In D. C. GAZIS (ed.), *Traffic Science.* New York: John Wiley & Sons. Chapter 2, p. 109–174.

MILLER, A. J. 1961. A queueing model for road traffic flow. *Journal of the Royal Statistical Society*, vol. 23B, no. 1, p. 64–75.

MILLER, A. J. & PRETTY, R. L. 1968. Overtaking on two-lane rural roads. In *Proceedings of the Fourth Australian Road Research Board Conference.* Victoria: Australian Road Research Board. P. 582–594.

MORSE, P. M. 1958. *Queues, Inventories and Maintenance.* New York: John Wiley & Sons.

NELSON, W. 1982. *Applied Life Data Analysis.* New York: John Wiley & Sons.

NEUBURGER, H. 1971. The economics of heavily congested roads. *Transportation Research*, vol. 5, no. 4, p. 283–293.

NEUTS, M. F. 1989. *Structured Stochastic Matrices of M/G/1 Type and Their Applications.* New York: Marcel Dekker, Inc.

NEWELL, G. F. 1965. Approximation methods for queues with application to the fixed-cycle traffic light. *SIAM Review*, vol. 7, no. 2, p. 223–240.

NEWELL, G. F. 1971. *Applications of Queueing Theory.* London: Chapman and Hall.

NEWELL, G. F. 1982. *Applications of Queueing Theory.* Second ed. London: Chapman and Hall.

NIITTYMÄKI, J. 1993. Calibration of HUTSIM traffic signal simulator. In *Simulering och Trafiksignalstyrning—Seminariet* [Simulation and traffic signal control—Seminar]. TFK. Stockholm.

NIITTYMÄKI, J. 1998. *Isolated Traffic Signals — Vehicle Dynamics and Fuzzy Control.* (Transportation Engineering Publication 94). Otaniemi: Helsinki University of Technology.

NIITTYMÄKI, J. & PURSULA, M. 1994. *Valo-ohjattujen liittymien simulointi ja ajodynamiikka* [Simulation and vehicle dynamics of signalized intersections]. (Julkaisu 81). Otaniemi: Teknillinen korkeakoulu, Liikennetekniikka.

NIITTYMÄKI, J. & PURSULA, M. 1997. Saturation flows at signal-group-controlled traffic signals. In *Highway Capacity Issues and Analysis*. (Transportation Research Record 1572). Washington, D.C.: Transportation Research Board. P. 24–32.

NIITTYMÄKI, J. & UUSIHEIMALA, M. 1996. Kritiska tidsavstånd i korsningar utan signalreglering [Critical gaps at unsignalized intersections]. In *VTI & KFB Forskardagar*. (KFB & VTI forskning/research 18, part 5). KFB & VTI. Linköping. P. 167–177.

NORDQVIST, S. 1958. *Gators och vägars kapacitet* [Capacity of streets and highways]. (Meddelande nr 39). Stocholm: IVA:s Transportforskningskommission.

NORDQVIST, S., BÅNG, K.-L. & HANSSON, A. 1973. *Kapacitetsutredning: Literaturstudier och analys* [An inquiry on capacity: Literature studies and analyses]. Np.: Statens Vägverk. TV 118.

OECD ROAD RESEARCH GROUP 1974. *Capacity of At-Grade Junctions*. (Road Research). Paris: Organisation for Economic Co-operation and Development.

O'FLAHERTY, C. A. 1997. Intersection design and capacity. In C. A. O'FLAHERTY (ed.), *Transport Planning and Traffic Engineering*. London: Arnold. Chapter 20, p. 356–399.

OLIVER, R. M. 1961. A traffic counting distribution. *Operations Research*, vol. 9, no. 6, p. 802–810.

PALM, C. 1943. *Intensitätsschwankungen im Fernsprechverkehr* [Intensity fluctuations in telephone traffic]. (Ericsson Technics 44). Stockholm: Telefonaktiebolaget L M Ericsson.

PARZEN, E. 1962. *Stochastic Processes*. New York: Holden-Day.

PASANEN, E. 1991. *Ajonopeudet ja jalankulkijan turvallisuus* [Driving speeds and pedestrian safety]. (Julkaisu 72). Otaniemi: Teknillinen korkeakoulu, Liikennetekniikka.

PÉCHEUX, K. K., PIETRUCHA, M. T. & JOVANIS, P. P. 2000. User perception of level of service at signalized intersections: Methodological issues. In Brilon (2000), p. 322–335.

PHILBRICK, M. J. 1977. *In search of a new capacity formula for conventional roundabouts*. (TRRL Laboratory Report 773). Crowthorne: Transport and Road Research Laboratory.

PLANK, A. W. 1982. The capacity of a priority intersection—two approaches. *Traffic Engineering and Control*, vol. 23, no. 2, p. 88–92.

PLANK, A. W. & CATCHPOLE, E. A. 1984. A general capacity formula for an uncontrolled intersection. *Traffic Engineering and Control*, vol. 25, no. 6, p. 327–329.

POLLACZEK, F. 1930. Über eine Aufgabe der Wahrscheinlichkeitstheorie I–II [Concerning a question in probability theory]. *Mathematische Zeitschrift*, vol. 32, p. 64–100, 729–750.

PÖSCHL, F. J. 1983. Die nicht signalgesteuerte nebenstraßenzufahrt als verallgemeinertes M/G/1-warteschlangensystem [The unsignalized minor street entry as a generalized M/G/1 queuing system]. *Zeitschrift für Operations Research*, vol. 27, p. B91–B111.

PRABHU, N. U. 1965. *Queues and Inventories: A Study of Their Basic Stochastic Processes*. New York: John Wiley & Sons.

PREVEDOUROS, P. D. 1988. A model of unsignalized intersection capacity based on Erlang-3 gap distribution. In Brilon (1988*b*). P. 165–179.

PURSULA, M., HAGRING, O. & NIITTYMÄKI, J. 1997. Simulation and capacity calculation of intersections without traffic signals—a discussion and a roundabout case study. In Kyte (1997), p. 208–216.

PURSULA, M. & PELTOLA, V. 1997. Capacity analysis and design practice for unsignalized at-grade intersections in Finland. In Kyte (1997), p. 197–207.

PURSULA, M. & PELTOLA, V. 1998. Finska beräkningsmetoder för korsningarnas kapacitet och fördröjningar [Finnish calculation methods for capacity and delays of intersections]. In *NORDKAP—NORDiskt KAPacitetssamarbete* [NORDKAP—Nordic capacity cooperation] (University of Lund 1998). Sammandrag av seminarium på Grand Hotel i Lund, Sverige 2–3 juni 1997.

PURSULA, M. & RISTIKARTANO, J. 1988. Liikennevirta ja välityskyky [Traffic flow and capacity]. In Lyly (1988). Chapter B4, p. 131–177.

RAFF, M. S. 1950. *A Volume Warrant For Urban Stop Signs*. Saugatuck, Connecticut: The Eno Foundation for Highway Traffic Control.

ROAD RESEARCH LABORATORY 1965. *Research on Road Traffic*. London: Her Majesty's Stationery Office.

ROBERTSON, D. I. 1969. *TRANSYT: A Traffic Network Study Tool*. (RRL Report LR 253). Crowthorne, Berkshire: Road Research Laboratory.

ROSS, S. 2002. *A First Course in Probability*. Sixth ed. Upper Saddle River: Prentice-Hall.

ROSS, S. M. 1996. *Stochastic Processes*. Second ed. New York: John Wiley & Sons.

ROUPHAIL, N. M. & AKÇELIK, R. 1992. Oversaturation delay estimates with consideration of peaking. In *Highway Capacity and Traffic Flow*. (Transportation Research Record 1365). Washington, D.C.: Transportation Research Board. P. 71–81.

ROUPHAIL, N. M., TARKO, A. & LI, J. 1997. Traffic flow at signalized intersections. In Gartner & Messer (1997). Chapter 9.

SCHNABEL, W. & LOHSE, D. 1997. *Grundlagen der Straßenverkehrstechnik und der Verkehrsplanung* [Fundamentals of traffic engineering and transportation planning]. Vol. 1. Second ed. Berlin: Verlag für Bauwesen.

SEMMENS, M. C. 1988. The capacity of non-signalised road junctions with high-speed controlling flows. *Traffic Engineering and Control*, vol. 29, no. 5, p. 280–283.

SHROPE, E. B. 1952. Testing a traffic circle for possible capacity. *Proceedings of the Highway Research Board*, vol. 31, p. 415–424.

SIEGLOCH, W. 1973. *Die Leistungsermittlung an Knotenpunkten ohne Lichtsignalsteuerung* [Capacity calculations at unsignalized intersections]. (Strassenbau und Strassenverkehrstechnik 154). Bonn: Bundesminister für Verkehr.

SIMON, M. J. 1991. Roundabouts in Switzerland. In Brilon (1991), p. 41–52.

SNRA 1995*a*. *CAPCAL 2: Model description of Intersection with signalcontrol*. Borlänge: Swedish National Road Administration. Publication 1995:008E.

SNRA 1995*b*. *CAPCAL 2: Model description of Intersection without signalcontrol*. Borlänge: Swedish National Road Administration. Publication 1995:007E.

SNRA 1995*c*. *CAPCAL 2: Model description of Roundabouts*. Borlänge: Swedish National Road Administration. Publication 1995:009E.

SONG, L., DUNNE, M. C. & BLACK, J. A. 1993. Models of delay and accident risk to pedestrians. In C. F. DAGANZO (ed.), *Transportation and Traffic Theory*. (Proceedings of the 12th International Symposium on Transportation and Traffic Theory, Berkeley, California, USA, 21–23 July, 1993). Amsterdam: Elsevier. P. 295–312.

SPANIER, J. & OLDHAM, K. B. 1987. *An Atlas of Functions*. New York: Hemisphere Publishing Corporation.

STATENS VÄGVERK 1977. *Beräkning av kapacitet, kölängd, fördröjning i vägtrafikanläggningar* [Calculation of capacity, queue length, delay in road traffic facilities]. Stockholm. TV 131.

STATENS VEGVESEN 1985. *Kapasitet i kryss* [Capacity at an intersection]. Oslo. Håndbok–127.

STUWE, B. 1991. Capacity and safety of roundabouts—German results. In Brilon (1991), p. 1–12.

SULLIVAN, D. P. & TROUTBECK, R. J. 1994. The use of Cowan's M3 headway distribution for modelling urban traffic flow. *Traffic Engineering and Control*, vol. 35, no. 7/8, p. 445–450.

SYYRAKKI, V., LYLY, S. & GRANBERG, T. 1975. Liikennevirta ja liikenteenvälityskyky [Traffic flow and capacity]. In S. LYLY (ed.), *Liikenne ja väylät* [Transportation Planning and Facilities]. Helsinki: Suomen Rakennusinsinöörien Liitto. Chapter 3, p. 65–94.

TANNER, J. C. 1951. The delay to pedestrians crossing a road. *Biometrika*, vol. 38, p. 383–392.

TANNER, J. C. 1953. A problem of interference between two queues. *Biometrika*, vol. 40, p. 58–69.

TANNER, J. C. 1961*a*. Delays on a two-lane road. *Journal of the Royal Statistical Society*, vol. 23B, no. 1, p. 38–63.

TANNER, J. C. 1961*b*. A derivation of the Borel distribution. *Biometrika*, vol. 48, p. 222–224.

TANNER, J. C. 1962. A theoretical analysis of delays at an uncontrolled intersection. *Biometrika*, vol. 49, no. 1 and 2, p. 163–170.

TANNER, J. C. 1967. The capacity of an uncontrolled intersection. *Biometrika*, vol. 54, no. 3 and 4, p. 657–658.

TANYEL, S. & YAYLA, N. 2003. A discussion on the parameters of Cowan M3 distribution for Turkey. *Transportation Research*, vol. 37A, no. 2, p. 129–143.

TAYLOR, M. A. P. (ed.) 2002. *Transportation and Traffic Theory in the 21st Century*. (Proceedings of the 15th International Symposium on Transportation and Traffic Theory, Adelaide, Australia, 16–18 July 2002). Amsterdam: Pergamon.

TEPLY, S. & JONES, A. M. 1991. Saturation flow: Do we speak the same language? In *Freeway Operations, Highway Capacity, and Traffic Flow*. (Transportation Research Record 1320). Washington, D.C.: Transportation Research Board. P. 144–153.

THEDÉEN, T. 1964. A note on the Poisson tendency in traffic distribution. *The Annals of Mathematical Statistics*, vol. 35, no. 4, p. 1823–1824.

THOMPSON, W. A. 1988. *Point Process Models with Applications to Safety and Reliability*. London: Chapman and Hall Ltd.

TIAN, Z. Z., TROUTBECK, R., KYTE, M., BRILON, W., VANDEHEY, M., KITTELSON, W. & ROBINSON, B. 2000. A further investigation on critical gap and follow-up time. In Brilon (2000), p. 397–408.

TIEHALLITUS 1992. *Kiertoliittymät: Suunnitteluohje* [Roundabouts: Design guidelines]. Helsinki: Tielaitos. TIEL 2130010.

TIE- JA LIIKENNETEKNIIKKA 2001. *Tasoliittymät: Suunnitteluvaiheen ohjaus* [At-grade intersections: Design guide]. Helsinki: Tiehallinto. TIEH 2100001-01.

TIENSUUNNITTELUTOIMISTO 1978. *Valo-ohjaamattoman tasoliittymän välityskyky: Laskenta-ohje* [Capacity of an unsignalized intersection: Calculation guidelines]. Helsinki: Tie- ja vesirakennushallitus. TVH 722306.

TIENSUUNNITTELUTOIMISTO 1987. *CAPCAL-tietokoneohjelman käyttöohje 2* [CAPCAL user's manual 2]. Helsinki: Tie- ja vesirakennushallitus. TVH 723860.

TIJMS, H. C. 2003. *A First Course in Stochastic Models*. Chichester: John Wiley & Sons.

TRACZ, M., CHODUR, J. & GONDEK, S. 1990. The use of reserve capacity and delay as the complementary measures of junction effectiveness. In Koshi (1990), p. 497–516.

TRANSPORTATION RESEARCH BOARD 1985. *Highway Capacity Manual*. (Special Report 209). Washington, D.C.: National Research Council.

TRANSPORTATION RESEARCH BOARD 1994. *Highway Capacity Manual*. (Special Report 209). Third ed. Washington, D.C.: National Research Council. Updated October 1994.

TRANSPORTATION RESEARCH BOARD 1997. *Review of International Practices Used To Evaluate Unsignalized Intersections*. (Transportation Research Circular 468). Washington, D.C.: National Research Council.

TRANSPORTATION RESEARCH BOARD 2000. *Highway Capacity Manual.* Washington, D.C.: National Research Council. HCM2000, metric units.

TRB COMMITTEE A3A10, HIGHWAY CAPACITY AND QUALITY OF SERVICE 2003. *Approved Corrections and Changes for the Highway Capacity Manual 2000.* http://www.a3a10.gati.org/public/errata-2003-01-29.pdf, 2003-01-29.

TROUTBECK, R. 1992. *Estimating the Critical Acceptance Gap from Traffic Movements.* (Research Report 92-5). Brisbane: Physical Infrastructure Centre, Queensland University of Technology.

TROUTBECK, R. 1995. *The Capacity of a Limited Priority Merge.* (Research Report 95-8). Brisbane: Physical Infrastructure Centre, Queensland University of Technology.

TROUTBECK, R. J. 1986. Average delay at an unsignalized intersection with two major streams each having a dichotomized headway distribution. *Transportation Science*, vol. 20, no. 4, p. 272–286.

TROUTBECK, R. J. 1988. Current and future Australian practices for the design of unsignalized intersections. In Brilon (1988*b*), p. 1–19.

TROUTBECK, R. J. 1990. Roundabout capacity and the associated delay. In Koshi (1990), p. 39–57.

TROUTBECK, R. J. 1991. Recent Australian unsignalized intersection research and practices. In Brilon (1991), p. 238–257.

TROUTBECK, R. J. 1993. Capacity and design of traffic circles in Australia. In *Traffic Flow and Highway Capacity.* (Transportation Research Record 1398). Washington, D.C.: Transportation Research Board. P. 68–74.

TROUTBECK, R. J. 1997*a*. *The Analysis of the Performance of Roundabouts.* (Research Report 97-8). Brisbane: Physical Infrastructure Centre, Queensland University of Technology.

TROUTBECK, R. J. 1997*b*. A review on the process to estimate the Cowan M3 headway distribution parameters. *Traffic Engineering and Control*, vol. 38, no. 11, p. 600–603.

TROUTBECK, R. J. 1999. Capacity of limited-priority merge. In *Highway Capacity, Quality of Service, and Traffic Flow and Characteristics.* (Transportation Research Record 1678). Washington, D.C.: Transportation Research Board. P. 269–276.

TROUTBECK, R. J. 2000. Modeling of signalized and unsignalized junctions. In D. A. HENSHER & K. J. BUTTON (ed.), *Handbook of Transport Modelling.* (Handbooks in Transport 1). Amsterdam: Pergamon. P. 375–391.

TROUTBECK, R. J. 2002. The performance of uncontrolled merges using a limited priority process. In Taylor (2002), p. 463–482.

TROUTBECK, R. J. & BRILON, W. 1997. Unsignalized intersection theory. In Gartner & Messer (1997), p. 8:1–8:47.

TROUTBECK, R. J. & KAKO, S. 1997. Limited priority merge at unsignalized intersections. In Kyte (1997), p. 294–302.

TROUTBECK, R. J. & KAKO, S. 1999. Limited priority merge at unsignalized intersections. *Transportation Research*, vol. 33A, no. 3/4, p. 291–304.

TROUTBECK, R. J. & WALSH, D. J. 1994. The differences between queueing theory and gap acceptance theory. In Akçelik (1994*b*), p. 617–635.

UNIVERSITY OF LUND 1998. *NORDKAP—NORDiskt KAPacitetssamarbete* [NORDKAP—Nordic capacity cooperation]. (Bulletin 156). Lund. Sammandrag av seminarium på Grand Hotel i Lund, Sverige 2–3 juni 1997.

UUSIHEIMALA, M. 1995. *Kriittisen aikavälin tarkastelu* [A study of critical gaps]. (Special assignment). Otaniemi: Teknillinen korkeakoulu, liikennelaboratorio.

VEJDIREKTORATET 1999*a*. *Kapacitet og serviceniveau: Baggrund og dokumentation* [Capacity and level of service: Background and documentation]. Draft.

VEJDIREKTORATET 1999*b*. *Kapacitet og serviceniveau* [Capacity and level of service]. Draft.

VOIGT, W. 1973. Modificationen des zeitlückenverfahrens [Modifications of Time Headway Process]. *Die Strasse*, vol. 13, no. 6, p. 224–227.

WANG, Z. 2000. Critical gap and traffic volume—re-examining the relationship. *Traffic Engineering and Control*, vol. 41, no. 7, p. 275–278.

WARDROP, J. G. 1957. The traffic capacity of weaving sections of roundabouts. In M. DAVIES, R. T. EDDISON & T. PAGE (ed.), *Proceedings of the First International Conference on Operational Research*. Baltimore: Operations Research Society of America. P. 266–281. With discussion.

WATSON, H. 1933. *Street Traffic Flow*. London: Chapman and Hall Ltd.

WEBSTER, F. V. 1958. *Traffic Signal Settings*. (Road Research Technical Paper No. 39). London: Her Majesty's Stationery Office.

WEBSTER, F. V. 1960. Greenford roundabout experiment. *Traffic Engineering and Control*, vol. 2, no. 5, p. 266–271.

WEGMANN, H. 1991. A general capacity formula for unsignalized intersections. In Brilon (1991), p. 177–191.

WEISS, G. 1963. A note on highway transparency. *Operations Research*, vol. 11, p. 460–461. Letter to the Editor.

WEISS, G. & HERMAN, R. 1962. Statistical properties of low-density traffic. *Quarterly of Applied Mathematics*, vol. 20, p. 121–130.

WEISS, G. H. & MARADUDIN, A. A. 1962. Some problems in traffic delay. *Operations Research*, vol. 10, p. 74–104.

WOLFF, R. W. 1989. *Stochastic Modeling and the Theory of Queues*. Englewood Cliffs: Prentice-Hall International, Inc.

WU, N. 1994. An approximation for the distribution of queue lengths at unsignalized intersections. In Akçelik (1994*b*), p. 717–736.

YAGAR, S. 1977. Minimizing delays for transient demands with application to signalized road junctions. *Transportation Research*, vol. 11, no. 1, p. 53–62.

YEO, G. F. 1962. Single server queues with modified service mechanisms. *Journal of the Australian Mathematical Society*, vol. 2, p. 499–507.

YEO, G. F. & WEESAKUL, B. 1964. Delays to road traffic at an intersection. *Journal of Applied Probability*, vol. 1, p. 291–310.

APPENDICES

A CRITICAL GAP ESTIMATES

Table A.1: Critical gap estimates for major-road left-turn movements at unsignalized intersections with major-road speed limit 50 km/h

	Maximum likelihood				Raff's	
	Noncensored		Censored		method	
Location	N	$\hat{t}_c$	N	$\hat{t}_c$	N	$\hat{t}_c$
Postitie	16	5.0	11	3.7	16	4.9
Seutula	274	5.6	165	5.2	274	5.6
Seutula	169	5.8	90	5.3	169	5.7
Kuitinmäki	90	5.9	29	4.4	90	5.6
Vihti	89	6.0	27	4.6	89	5.5
Vanha Turuntie-Jorvi	31	7.2	11	6.5	31	7.6
Vanha Turuntie-Jorvi	16	8.2	6	5.4	16	7.5
Sturel	22	10.1	2	4.6	22	10.3
Average		6.6		4.9		6.4
Weighted average		6.0		5.1		5.9

Table A.2: Critical gap estimates for minor-road right-turn movements at yield-controlled intersections with major-road speed limit 50 km/h

	Maximum likelihood				Raff's	
	Noncensored		Censored		method	
Location	N	$\hat{t}_c$	N	$\hat{t}_c$	N	$\hat{t}_c$
Seutula	161	5.6	90	5.0	161	5.2
Seutula	167	6.3	79	5.7	167	6.3
Vanha Turuntie-Jorvi	26	8.8	4	5.6	26	8.2
Vanha Turuntie-Jorvi	29	9.0	3	7.0	29	8.6
Average		7.3		5.8		6.9
Weighted average		6.4		5.4		6.1

Table A.3: Critical gap estimates for minor-road left-turn movements at yield-controlled intersections with major-road speed limit 50 km/h

	Maximum likelihood				Raff's	
	Noncensored		Censored		method	
Location	N	$\hat{t}_c$	N	$\hat{t}_c$	N	$\hat{t}_c$
Rajatorppa	113	5.0	87	4.8	113	4.9
Kuitinmäki	156	6.3	86	5.5	156	6.2
Otaniemi	47	6.7	25	5.2	47	6.5
Malminkartano	57	6.9	23	6.3	57	6.6
Vanha Turuntie-Jorvi	94	7.1	49	6.2	94	6.9
Vanha Turuntie-Jorvi	114	7.6	40	6.5	114	6.9
Vanha Turuntie-Jorvi	58	7.6	18	6.2	58	7.0
Pukinmäki	41	8.4	9	6.1	41	7.8
Average		6.9		5.8		6.6
Weighted average		6.7		5.6		6.4

Table A.4: Critical gap estimates for major-road left-turn movements at unsignalized intersections with major-road speed limit 60 km/h

	Maximum likelihood				Raff's	
	Noncensored		Censored		method	
Location	N	$\hat{t}_c$	N	$\hat{t}_c$	N	$\hat{t}_c$
Leppävaara	38	5.3	16	4.5	38	4.7
Leppävaara	115	5.6	54	5.1	115	5.5
Karak2	33	6.2	12	5.1	33	5.7
Leppävaara	97	6.5	34	4.8	97	5.7
Seurasaari	25	6.7	6	4.1	25	5.5
Saukkola	24	7.4	5	4.4	24	6.7
Saukkola	24	8.0	6	7.7	24	7.8
Porintie	52	7.2	21	5.6	52	6.6
Average		6.6		5.2		6.0
Weighted average		6.4		5.1		5.8

Table A.5: Critical gap estimates for minor-road right-turn movements at unsignalized intersections with major-road speed limit 60 km/h

		Maximum likelihood				Raff's	
		Noncensored		Censored		method	
Location	Control	N	$\hat{t}_c$	N	$\hat{t}_c$	N	$\hat{t}_c$
Leppävaara	Yield	89	5.8	41	4.8	89	5.4
Leppävaara	Yield	140	6.2	69	5.2	140	5.7
Saukkola	Yield	9	6.8	7	6.8	9	6.8
Porintie	Stop	180	8.9	53	6.8	180	8.6
Average			6.9		5.9		6.0
Weighted average			6.4		5.7		6.9

Table A.6: Critical gap estimate for minor-road left-turn movements at a yield-controlled intersection with major-road speed limit 60 km/h

	Maximum likelihood				Raff's	
	Noncensored		Censored		method	
Location	N	$\hat{t}_c$	N	$\hat{t}_c$	N	$\hat{t}_c$
Saukkola	32	8.3	11	6.3	32	8.0

Table A.7: Critical gap estimates for minor-road right-turn movements at yield-controlled intersections with major-road speed limit 80 km/h

	Maximum likelihood				Raff's	
	Noncensored		Censored		method	
Location	N	$\hat{t}_c$	N	$\hat{t}_c$	N	$\hat{t}_c$
Numpjl	80	7.9	59	7.1	80	7.5
Myllylampi	20	7.8	16	7.3	20	7.4
Hanko-Hyvinkää-Nummela	44	10.7	25	10.0	44	10.4
Average		8.8		8.1		8.4
Weighted average		8.7		7.9		8.4

Table A.8: Critical gap estimates for minor-road left-turn movements at unsignalized intersections with major-road speed limit 80 km/h

	Maximum likelihood				Raff's	
	Noncensored		Censored		method	
Location	N	$\hat{t}_c$	N	$\hat{t}_c$	N	$\hat{t}_c$
Jorvaksentie-Sundsberg	69	6.6	62	6.5	69	6.7
Jorvaksentie-Sundsberg	96	6.6	84	6.5	96	6.7
Vihdintie-Lahnus	41	8.9	31	8.9	41	9.5
Hanko-Hyvinkää-Nummela	28	8.6	26	8.3	28	8.9
Hanko-Hyvinkää-Nummela	25	8.8	13	7.8	25	8.2
Numet2	25	10.0	13	9.3	25	10.4
Average		8.3		7.9		8.4
Weighted average		7.6		7.3		7.8

Table A.9: Critical gap estimates for roundabouts

	Central island	Maximum likelihood				Raff's	
	diameter	Noncensored		Censored		method	
Location	(m)	N	$\hat{t}_c$	N	$\hat{t}_c$	N	$\hat{t}_c$
Nummela 1	8.0	50	4.9	18	4.8	50	5.1
Nummela 2	8.0	69	5.1	14	4.1	69	4.4
Tapanila	11.0	20	6.1	5	2.6	20	4.7
Pukinmäki	12.5	42	2.9	27	2.4	42	2.5
Kitee	17.0	53	4.2	39	3.9	53	4.2
Veikkola	25.0	41	4.3	38	4.2	41	4.3
Katinen	26.0	13	5.2	3	3.7	13	4.0
Katuma	38.0	61	4.6	21	3.9	61	4.9
Hyrylä	55.0	302	4.5	204	4.1	302	4.3
Lappeenranta		140	5.5	53	4.6	140	5.0
Average			4.6		3.7		4.3
Weighted average			4.7		4.0		4.4

B HUTSIM INITIALIZATION FILE

A typical HUTSIM initialization file, which shows the most important parameters, is displayed below.

```
1151   HUTSIM 5.373I/TPMA Initialization File
101          *.*;              Input File Mask
102         Test.trf;          Input File
103         Test.out;          Output File
104         Test.rep;          Report File
105          ;              Default Directory
111          4              Input Mode      Traf-file
112          4              Output Mode     Delay file
113          1              Report Mode     BasicReport
121          0              TimeHour (0-60)
122         60              TimeMin  (0-60)
123         10              NoRepINT (minutes)
124          0              NoGenINT (minutes)
125         60              RepINT (minutes)
131          0              VCOL (vehicle color coding)
132          0              DWIN (downer window mode)
133          0              PLOT (plotter mode)
134          0              PIPE (pipes visible)
135          1              ANIM (animation mode)
136          1              TIME (time update mode)
201          1              Real Time Connection
202         10              Time Step Unit (1/100 s)
203          0              Extra Load (ms)
204       2.00              Low Frequency Warning (Hz)
205          1              Screen Update Interval (sec)
211          3              Graph Time Scale (pixels/second)
212          3              Graph Speed Scale (pixels/unit)
213        300              Graph Display Area (pixels)
221          1              Sound Effects
251      41952              Seed Number (0-63999)
252       1.00              Traffic Scale Factor
253       0.50              Minimum Arrival Time Headway (s)
261          2              Max. Group Number
262          0              Max. Report Number
263          1              Stop Criteria (Level number)
264       0.50              Option-Zone Weight (n=1)
265       1.00              Option-Zone Weight (n>1)
266          ,;             Column Delimiter
267          6              Column Spacing
271      0.026              Delay Cost (1/sec)
272      0.180              Stop Cost (1/stop)
273      2.000              Option-Zone Cost (1/veh)
274     10.000              Queue Criteria (dist/m)
301       2.50              Unit Speed Value (km/h)
302       1.20              Following Time Headway (s)
303       0.20              Stable Area Width (s)
304       1.20              Stop Distance (m)
305       0.05              Acceleration Adjustment
308  0.005000               Speed Limit Coefficient
321        300              Max Obstacle Sight (m)
322        300              Max. Vehicle Sight (m)
323       1.00              Average Reaction Time (s)
325          1              Reaction Mode (0=No Reaction Delay)
326          2              Creeping Mode (0=No Creeping)
327       0.05              Creeping Unstability Factor
351       0.90              Left Changing Treshold
352       0.05              Right Changing Treshold
353       0.80              Forced Lnc Gap Back Left
354       0.80              Forced Lnc Gap Front Left
373       0.50              Forced Lnc Gap Back Right
374       0.50              Forced Lnc Gap Front Right
361       0.20              Maximum Gap Decrease \% (Forced Lane Change)
362         20              Forced Lane Change Gap Decreasing Time
363       0.70              Polite Drivers %
355      10.00              Minimum Time in Lane (s)
356          1              Lane Switch Allowed
357          0              Left Handed Traffic
358       1.10              Voluntary Lnc Gap Back Left
359       1.10              Voluntary Lnc Gap Front Left
378       1.10              Voluntary Lnc Gap Back Right
379       1.10              Voluntary Lnc Gap Front Right
360       7.50              Speed Loss Threshold (km/h)
701       0.70              AICC Following Gap
702       1.00              AICC Stopping Distance
721          0              Route Guidance Mode
722          0              Route Guided Vehs (%)
723       0.90              Route Choice Threshold
724       0.20              Travel Time Averaging
400         10              Number of Vehicle Types
100    Normal Deceleration Rates
401    1.9    1.6    1.2    1.7    1.7    1.5    1.3    5.0    1.9    1.9
100    High Deceleration Rates
402    3.2    3.0    2.0    2.8    2.8    2.6    2.4    6.0    3.2    3.2
100    Normal Acceleration Rates
403    1.6    0.7    1.0    0.5    0.6    0.4    0.2    5.0    1.6    1.6
100    High Acceleration Rates
404    2.4    1.0    1.4    0.7    0.8    0.6    0.3    6.0    2.4    2.4
100    Vehicle Lengths
405    4.0    7.0   12.0   18.0   24.0   24.0   24.0   40.0    4.0    4.0
```

```
100    Vehicle Type Distributions
501     88      4      2      2      2      1      1      0      0      0
502    100      0      0      0      0      0      0      0      0      0
503     85      4     11      0      0      0      0      0      0      0
504     57     21      4     18      0      0      0      0      0      0
505     87      4      9      0      0      0      0      0      0      0
506    100      0      0      0      0      0      0      0      0      0
507      0      0    100      0      0      0      0      0      0      0
508      0      0      0      0    100      0      0      0      0      0
509     50      0     50      0      0      0      0      0      0      0
100    Car-following Gap Distributions 0.1-5.0s
800          0           Default Distr No (0=Not Used)
801     0   0   0   0   0   0   0   0   0   0 100   0   0   0   0   0   0   0   0   0   0   0   0   0   0   0
0   0   0   0   0   0   0   0   0   0   0   0   0   0   0   0   0   0   0   0   0   0
802     0   0   0   0   0   0   0   0   0  10  20  40  20  10   0   0   0   0   0   0   0   0   0   0   0   0
0   0   0   0   0   0   0   0   0   0   0   0   0   0   0   0   0   0   0   0   0   0
803     0   0   0   0   0   0  10  10  10  10  10  20  10  10  10  10   0   0   0   0   0   0   0   0   0   0
0   0   0   0   0   0   0   0   0   0   0   0   0   0   0   0   0   0   0   0   0   0
804     0   0   0   0   0  10  10  10  10  10  10  10  10  10  10  10   0   0   0   0   0   0   0   0   0   0
0   0   0   0   0   0   0   0   0   0   0   0   0   0   0   0   0   0   0   0   0   0
805     0   0   0   0   0  10  10  10  10  10  20  10  10  10  10   0   0   0   0   0   0   0   0   0   0   0
0   0   0   0   0   0   0   0   0   0   0   0   0   0   0   0   0   0   0   0   0   0
806     0   0   0   0   0  10  10  10  10  10  20  10  10  10  10   0   0   0   0   0   0   0   0   0   0   0
0   0   0   0   0   0   0   0   0   0   0   0   0   0   0   0   0   0   0   0   0   0
807     0   0   0   0   0  10  10  10  10  10  20  10  10  10  10   0   0   0   0   0   0   0   0   0   0   0
0   0   0   0   0   0   0   0   0   0   0   0   0   0   0   0   0   0   0   0   0   0
808     0   0   0   0   0  10  10  10  10  10  20  10  10  10  10   0   0   0   0   0   0   0   0   0   0   0
0   0   0   0   0   0   0   0   0   0   0   0   0   0   0   0   0   0   0   0   0   0
809     0   0   0   0   0  10  10  10  10  10  20  10  10  10  10   0   0   0   0   0   0   0   0   0   0   0
0   0   0   0   0   0   0   0   0   0   0   0   0   0   0   0   0   0   0   0   0   0
100    Desired Speed Level Distributions
900          0           Default Distr No (0=Not Used)
901     0   0   0 100   0   0   0   0   0   0   0   0   0   0   0   0   0   0   0   0   0   0   0   0   0   0
0   0   0   0   0   0   0   0   0   0   0   0   0   0   0   0   0   0   0   0   0   0
902     0   0   0   0   0   0   0 100   0   0   0   0   0   0   0   0   0   0   0   0   0   0   0   0   0   0
0   0   0   0   0   0   0   0   0   0   0   0   0   0   0   0   0   0   0   0   0   0
903     0   0   0   0   0   0   0   0   0   0 100   0   0   0   0   0   0   0   0   0   0   0   0   0   0   0
0   0   0   0   0   0   0   0   0   0   0   0   0   0   0   0   0   0   0   0   0   0
904     0   0   0   0   0   0   0   0   0   0   0   0   0   0 100   0   0   0   0   0   0   0   0   0   0   0
0   0   0   0   0   0   0   0   0   0   0   0   0   0   0   0   0   0   0   0   0   0
905     0   0   0   0   0   0   0   0   0   0   0   0   0   0   0   0   0   0 100   0   0   0   0   0   0   0
0   0   0   0   0   0   0   0   0   0   0   0   0   0   0   0   0   0   0   0   0   0
906     0   0   0   0   0   0   0   0   0   0   0   0   0   0   0   0   0   0   0   0   0 100   0   0   0   0
0   0   0   0   0   0   0   0   0   0   0   0   0   0   0   0   0   0   0   0   0   0
907     0   0   0   0   0   0   0   0   0   0   0   0   0   0   0   0   0   0   0   0   0   0   0   0   0   0
100   0   0   0   0   0   0   0   0   0   0   0   0   0   0   0   0   0   0   0   0   0   0   0   0   0   0
908     0   0   0   0   0   0   0   0   0   0   0   0   0   0   0   0   0   0   0   0   0   0   0   0   0   0
0   0   0   0 100   0   0   0   0   0   0   0   0   0   0   0   0   0   0   0   0   0
909     0   0   0   0   0   0   0   0   0   0   0   0   0   0   0   0   0   0   0   0   0   0   0   0   0   0
0   0   0   0   0   0   0   0 100   0   0   0   0   0   0   0   0   0   0   0   0   0
910     0   0   0   0   0   0   0   0   0   0   0   0   0   0   0   0   0   0   0   0   0   0   0   0   0   0
0   0   0   0   0   0   0   0   0   0   0   0 100   0   0   0   0   0   0   0   0   0
911     0   0   0   0   0   0   0   0   0   0   0   0   0   0   0   0   0   0   0   0   0   0   0   0   0   0
0   0   0   0   0   0   0   0   0   0   0   0   0   0   0   0 100   0   0   0   0   0
912     0   0   0   0   0   0   0   0   0   0   0   0   0   0   0   0   0   0   0   0   0   0   0   0   0   0
0   0   0   0   0   0   0   0   0   0   0   0   0   0   0   0   0   0   0   0 100   0   0
913     0   0   0   0   0   0   0   0   0   0   0   0   0   0   0   0   0   0   0   0   0   0   0   0   0   0
0   0   0   0   0   0   0   0   0   0   0   0   0   0   0   0   0   0   0   0   0   0
914     0   0   0   0   0   0   0   0   0   0   0   0   0   0   0   0   0   0   0   0   0   0   0   0   0   0
0   0   0   0   0   0   0   0   0   0   0   0   0   0   0   0   0   0   0   0   0   0
915     0   0   0   0   0   0   0   0   0   0   0   0   0   0   0   0   0   0   0   0   0   0   0   0   0   0
0   0   0   0   0   0   0   0   0   0   0   0   0   0   0   0   0   0   0   0   0   0
916     0   0   0   0   0   0   0   0   0   0   0   0   0   0   0   0   0   0   0   0   0   0   0   0   0   0
0   0   0   0   0   0   0   0   0   0   0   0   0   0   0   0   0   0   0   0   0   0
917     0   0   0   0   0   0   0   0   0   0   0   0   0   0   0   0   0   0   0   0   0   0   0   0   0   0
0   0   0   0   0   0   0   0   0   0   0   0   0   0   0   0   0   0   0   0   0   0
918     0   0   0   0   0   0   0   0   0   0   0   0   0   0   0   0   0   0   0   0   0   0   0   0   0   0
0   0   0   0   0   0   0   0   0   0   0   0   0   0   0   0   0   0   0   0   0   0
919     0   0   0   0   0   0   0   0   0   0   0   0   0   0   0   0   0   0   0   0   0   0   0   0   0   0
0   0   0   0   0   0   0   0   0   0   0   0   0   0   0   0   0   0   0   0   0   0
1000   End of Initialization File
```

ISBN 951-803-180-0
ISSN 1457-9871
TIEH 3200849E